INFORMATION TO USERS

This manuscript has been reproduced from the microfilm master. UMI films the text directly from the original or copy submitted. Thus, some thesis and dissertation copies are in typewriter face, while others may be from any type of computer printer.

The quality of this reproduction is dependent upon the quality of the copy submitted. Broken or indistinct print, colored or poor quality illustrations and photographs, print bleedthrough, substandard margins, and improper alignment can adversely affect reproduction.

In the unlikely event that the author did not send UMI a complete manuscript and there are missing pages, these will be noted. Also, if unauthorized copyright material had to be removed, a note will indicate the deletion.

Oversize materials (e.g., maps, drawings, charts) are reproduced by sectioning the original, beginning at the upper left-hand corner and continuing from left to right in equal sections with small overlaps. Each original is also photographed in one exposure and is included in reduced form at the back of the book.

Photographs included in the original manuscript have been reproduced xerographically in this copy. Higher quality 6" x 9" black and white photographic prints are available for any photographs or illustrations appearing in this copy for an additional charge. Contact UMI directly to order.

UMI

A Bell & Howell Information Company
300 North Zeeb Road, Ann Arbor MI 48106-1346 USA
313/761-4700 800/521-0600

MACROPHAGE INTERACTIONS WITH BIOMATERIAL SURFACES AND THEIR EFFECTS ON ENDOTHELIAL CELL ACTIVATION

by

ANN E. SCHMIERER

A dissertation submitted in partial fulfillment of the requirements for the degree of

DOCTOR OF PHILOSOPHY

University of Washington

1998

Approved by _____
Chairperson of Supervisory Committee

Program Authorized to Offer Degree Bioengineering

Date 6/12/98

UMI Number: 9836243

UMI Microform 9836243
Copyright 1998, by UMI Company. All rights reserved.

This microform edition is protected against unauthorized copying under Title 17, United States Code.

UMI
300 North Zeeb Road
Ann Arbor, MI 48103

Doctoral Dissertation

In presenting this dissertation in partial fulfillment of the requirements for the Doctoral degree at the University of Washington, I agree that the Library shall make its copies freely available for inspection. I further agree that extensive copying of this dissertation is allowable only for scholarly purposes, consistent with "fair use" as prescribed in the U.S. Copyright Law. Requests for copying or reproduction of this dissertation may be referred to University Microfilms, 1490 Eisenhower Place, P.O. Box 975, Ann Arbor, MI 48106, to whom the author has granted "the right to reproduce and sell (a) copies of the manuscript in microform and/or (b) printed copies of the manuscript made from microform."

Signature _____

Date 6/12/98

University of Washington

Abstract

MACROPHAGE INTERACTIONS WITH BIOMATERIAL SURFACES AND THEIR EFFECTS ON ENDOTHELIAL CELL ACTIVATION

by ANN E. SCHMIERER

Chairperson of the Supervisory Committee: Professor Buddy D. Ratner
Department of Bioengineering

This research project focused on the development of *in vitro* models to study cell reactions with material surfaces and how materials exert their influence on cell-cell interactions. Macrophage inflammatory cytokine release was shown to be affected by surface chemistry, topography and extracellular matrix (ECM) coating. Material characteristics could affect endothelial cell (EC) activation through material-induced macrophage cytokine signaling. The degree of EC activation depended upon the material the macrophages contacted.

Surface chemistry affected the number of human monocytes that initially adhered to the different polymers. The materials studied were mixed esters of cellulose (MEC), and the fluoropolymers polytetrafluoroethylene (PTFE) and expanded PTFE (ePTFE). Materials varied in porosity, but not surface chemistry. The fluoropolymers had significantly lower monocyte adhesion compared to the MEC, but adhesion could be improved with fibronectin (FN) pre-coating.

Monocytes seeded on the different polymer surfaces were activated to varying degrees, determined by measuring inflammatory cytokine release. Macrophages contacting MEC showed low levels of interleukin-1ß (IL-1ß) and tumor necrosis factor-α (TNFα)

secretion. The fluoropolymers showed significantly higher levels of secretion of IL-1ß and TNFα. Cytokine release increased with increasing fibril length in the fluoropolymer series. All cytokine data was normalized to cell number.

FN pre-coating had varied effects, depending on the surface chemistry and fibril length of the ePTFE materials. FN did not significantly influence cytokine production on the MECs, whereas significant decreases in IL-1ß and TNFα release from macrophages contacting 10μ and 30μ ePTFE were seen. Pre-coating 60μ ePTFE did not lower IL-1ß or TNFα secretion.

EC activation by macrophage-derived products was determined by monitoring neutrophil adherence to EC after being incubated in macrophage conditioned medium. There was a direct correlation between EC activation and material-induced macrophage cytokine production.

These results support the hypothesis that macrophage activation can be influenced by surface properties, such as surface chemistry, porosity or fibril length, and ECM coatings. Also, material-induced macrophage activation can cause activation of ECs, having profound implications for macrophage interactions with materials *in vivo*. Several material characteristics were identified that could aid in the development of more biocompatible medical implants.

TABLE OF CONTENTS

LIST OF FIGURES vi
LIST OF TABLES ix
Chapter 1: Introduction 1
1.1 Introduction 1
1.2 Notes to Chapter 1 6
Chapter 2: Literature Review 7
2.1 Review of Literature 7
2.2 Notes to Chapter 2.1 22
Chapter 3: Materials and Methods 31
3.1 Materials 31
3.1.1 Polymer Sample Preparation 32
3.2 Surface Analysis 35
3.2.1 Electron Spectroscopy for Chemical Analysis (ESCA) 35
3.2.2 Scanning Electron Microscopy (SEM) 35
3.2.3 Atomic Force Microscopy (AFM) 36
3.2.4 Time-of-Flight Secondary Ion Mass Spectroscopy (TOF-SIMS) 37
3.3 Fibronectin Adsorption 37
3.3.1 Fibronectin Adsorption for Cell Culture Experiements 37
3.3.2 Fibronectin Adsorption for Experiments in Chapter 5 37
3.4 Isolation and Culture of Human Cells 39
3.4.1 Human Umbilical Vein Endothelial Cells (HUVECs) 39
3.4.2 Human Blood Monocytes 41
3.4.2.1 Monocyte Isolation Using Percoll® Density Gradients 41
3.4.2.2 Monocyte Isolation by Adherence to Tissue Culture Plastic 43
3.4.2.3 Monocyte Isolation by Direct Adherence to Materials 45
3.5 Cell Surface Staining of Endothelial Cells for E-selectin 46
3.6 Interleukin-1ß (IL-1ß), Tumor Necrosis Factor α (TNFα) and Interleukin-8 (IL-8) Enzyme-linked Immunosorbent Assays (ELISAs) 47
3.7 RNA Isolation and Northern Blot Analysis 47

3.7.1 Messenger RNA Isolation....47
3.7.2 Detection of E-selectin mRNA....48
3.8 Neutrophil Adhesion Assays....49
3.8.1 Radio-labeling Method....49
3.8.2 Neutral Red Labeling Method....50
3.9 Cell Number Determination by Lactate Dehydrogenase (LDH) Activity....51
3.10 Endotoxin Assays for Biomaterial Surfaces....53
3.11 Notes for Chapter 3....55
Chapter 4: Surface Analysis of Materials....56
4.1 Introduction....56
4.2 Surface Analysis of Mixed Esters of Cellulose (MEC) Membranes....56
4.2.1 Scanning Electron Microscopy of MEC Membranes....56
4.2.2 ESCA Analysis of MEC Membranes....58
4.3 Surface Analysis of Nylon 6....61
4.4 Surface Analysis of Poly(tetrafluoroethylene) (PTFE) and Expanded PTFE (ePTFE)....63
4.4.1 SEM of PTFE and ePTFE....63
4.4.2 ESCA of PTFE and ePTFEs....66
4.4.3 TOF-SIMS of 30μ ePTFE....69
4.5 Notes for Chapter 4....71
Chapter 5: Fibronectin Adsorption to Radiofrequency Plasma-deposited Films: Scatchard Analysis and Cell Growth Characteristics....72
5.1 Abstract....72
5.2 Introduction....72
5.3 Materials and Methods....75
5.3.1 Scatchard Analysis....75
5.3.2 Clonal Cell Growth on Polymers....76
5.4 Results....77
5.4.1 Surface Chemistry Characterization....77
5.4.2 Scatchard Analysis of Protein Adsorption Isotherms....80
5.4.3 Cell Growth Assays....90
5.5 Discussion....94
5.6 Conclusions....101

5.7 Acknowledgments 101
5.8 Notes for Chapter 5 102
Chapter 6: Monocyte-derived Macrophage Interactions with Biomaterial Surfaces 105
6.1 Introduction 105
6.2 Isolation of Monocyts 106
6.2.1 Background 106
6.2.2 Effect of Monocyte Isolation on Cellular Activity 106
6.3 Monocyte-Macrophage Adhesion to Biomaterial Surfaces 109
6.3.1 Backgound 109
6.3.2 Materials and Methods 109
6.3.3 Results and Discussion 110
6.4 IL-1ß Production by Macrophages Cultured on Silicone Implant Materials 120
6.4.1 Background 120
6.4.2 Introduction 121
6.4.3 Materials and Methods 122
6.4.3.1 Sample Preparation 122
6.4.3.2 Isolation of Monocytes from Blood 123
6.4.3.3 Interleukin-1ß Enzyme-linked Immunosorbent Assay (ELISA) 123
6.4.4 Results and Discussion 124
6.5 IL-1ß, TNFα, and IL-8 Cytokine Release from Macrophages Contacting Material Surfaces 135
6.5.1 Background 135
6.5.2 Materials and Methods 136
6.5.3 IL-1ß ELISA Results 136
6.5.4 TNFα ELISA Results 143
6.5.5 IL-8 ELISA Results 148
6.5.6 Conclusions 153
6.6 Notes for Chapter 6 155
Chapter 7: Activation of Endothelial Cells by Macrophage Interactions with Biomaterial Surfaces 157
7.1 Introduction 157
7.2 Materials and Methods 158

7.3 Results and Discussion 159
7.4 Conclusions 169
7.5 Notes for Chapter 7 170
Chapter 8: Material Effects on Macrophage, Endothelial Cell and Smooth Muscle Cell Interactions: Cell Co-cultures with Biomaterials 171
8.1 Background 171
8.2 Objectives 171
8.3 Material and Methods 172
8.3.1 Materials 172
8.3.2 Macrophage Purification 172
8.3.3 Cell Number Determination 172
8.3.4 Co-culture Studies 173
8.3.5 Cell Supernatant Effect on Responding Cell Growth 174
8.3.6 Statistical Analysis 174
8.4 Results and Discussion 175
8.4.1 HUVEC and Macrophage Co-cultures 175
8.4.2 HUVEC Response to Macrophage Supernatants 176
8.4.3 Macrophage and SMC Co-cultures 180
8.4.4 HUVEC Growth in Response to SMCs on Materials 181
8.4.5 SMC Growth in Response to HUVECs on Materials 182
8.4.6 Heat-treated Supernatants 183
8.5 Conclusions 184
Chapter 9: Endothelial Cell Interactions with Biomaterial Surfaces 187
9.1 Introduction 187
9.2 Objective 187
9.3 Materials 188
9.4 Results and Discussion 188
9.4.1 Cell Surface Staining for E-selectin 188
9.4.2 Northern Blot Analysis for the Detection of E-selectin Gene Expression . 192
9.4.3 Effect of Protein Adsorption on E-selectin Expression 194
9.4.4 Effects of Surface Chemistry on E-selectin Expression 195
9.4.5 Neutrophil Adhesion Assays 196
9.5 Conclusions 198

9.6 Notes for Chapter 9 199
Chapter 10: Conclusions and Future Work 200
10.1 Conclusions 200
10.2 Future Work 205
10.3 Notes for Chapter 10 209
Bibliography 210
Appendix A: Cell Culture Materials and Reagents 224
Appendix B: Messenger RNA Isolation from Whole Cell Lysates 225
Appendix C: IL-1ß Production by Human Monocytes Cultured on Silicone Implant Materials 227
Appendix D: Macrophage IL-1ß, TNFα, and IL-8 Production: By Donor 231

LIST OF FIGURES

Number *Page*

Figure 3.1 The composite LDH standard curve for all monocyte preparations 52
Figure 4.1 SEM of 0.22μ MEC with a few macrophages attached to the surface.....57
Figure 4.2 SEM of 5μ MEC with a few macrophages attached to the surface.....57
Figure 4.3 ESCA survey scans of the MEC membranes. 58
Figure 4.4 Stack plot of high-resolution C1s ESCA spectra for MEC membranes.....60
Figure 4.5 High resolution C1s ESCA spectrum of 0.22μ MEC showing peak fitting....60
Figure 4.6 ESCA survey spectrum showing the elemental of Nylon 6 62
Figure 4.7 High-resolution C1s spectrum for Nylon 6 showing peak fits 62
Figure 4.8 SEM of PTFE (non-porous) 64
Figure 4.9 SEM of 10μ ePTFE.....64
Figure 4.10 SEM of 30μ ePTFE 65
Figure 4.11 SEM of 60μ ePTFE 65
Figure 4.12 SEM of 100μ ePTFE.....66
Figure 4.13 ESCA survey spectra for PTFE/ePTFE showing elemental composition.....67
Figure 4.14 High-resolution C1s spectra for the PTFE/ePTFE fluoropolymers.....68
Figure 4.15 Detail of the high-resolution C1s spectra for the ePTFEs only.....68
Figure 4.16: TOF-SIMS false-color image of 30μ ePTFE 69
Figure 4.17 TOF-SIMS spectra of 30μ ePTFE.....70
Figure 5.1 Nitrogen content of plasma films.....79
Figure 5.2 Oxygen content of plasma films.....80
Figure 5.3 a) Acetone/20% N_2 FN adsorption isotherm and b) Scatchard plot.....81
Figure 5.4 a) Acetone/30% N_2 FN adsorption isotherm and b) Scatchard plot.....82
Figure 5.5 The apparent K_a initially versus % N.....85
Figure 5.6 The total B_{max} values with increasing N content 86
Figure 5.7 A K_a's for the acetone-oxygen and acrylic acid plasma-deposited films 89
Figure 5.8 B_{max} for the acetone-O_2 and acrylic acid plasma films.....90
Figure 5.9 McCoy and EaHY 926 clonal cell growth per cm^2 92
Figure 5.10 McCoy and EaHY 926 data from Figure 5.9.....93

Figure 6.1: Total cell number on each material for Donor #1 110
Figure 6.2: Total cell number on each material for Donor #2 111
Figure 6.3: Total cell number on each material for Donor #3 112
Figure 6.4: Total cell number on each material for Donor #4 113
Figure 6.5: Total cell number on each material for Donor #6. 114
Figure 6.6: Total cell number on each material for Donor #7. 115
Figure 6.7: Total cell number on each material for Donor #8. 116
Figure 6.8: Total cell number on each material for Donor #9 117
Figure 6.9: Total cell number on each material for Donor #10..... 118
Figure 6.10: IL-1ß production by macrophages after 3 days in culture on materials..... 125
Figure 6.11: IL-1ß production by macrophages after 7 days in culture on materials..... 125
Figure 6.12: IL-1ß production by macrophages after 14 days in culture on materials ... 126
Figure 6.13: IL-1ß production by macrophages after 21 days in culture on materials ... 126
Figure 6.14: IL-1ß production by macrophages after 28 days in culture on materials.. . 127
Figure 6.15: IL-1ß production by macrophages after 35 days in culture on materials.. . 127
Figure 6.16: Normalized IL-1ß production for all donors..... 129
Figure 6.17 Macrophage IL-1ß release from contact with TCPS or glass ring..... 137
Figure 6.18 IL-1ß production from macrophages contacting 0.22μ MEC. 138
Figure 6.19 IL-1ß production from macrophages contacting 5μ MEC. 138
Figure 6.20 IL-1ß production from macrophages contacting 8μ MEC..... 139
Figure 6.21 IL-1ß production from macrophages contacting Nylon 6..... 139
Figure 6.22 IL-1ß production from macrophages contacting PTFE..... 141
Figure 6.23 IL-1ß production from macrophages contacting 10μ ePTFE..... 141
Figure 6.24 IL-1ß production from macrophages contacting 30μ ePTFE..... 142
Figure 6.25 IL-1ß production from macrophages contacting 60μ ePTFE..... 142
Figure 6.26 Macrophage TNFα release from contact with TCPS or a glass ring..... 143
Figure 6.27 TNFα production from macrophages contacting 0.22μ MEC..... 144
Figure 6.28 TNFα production from macrophages contacting 5μ MEC..... 144
Figure 6.29 TNFα production from macrophages contacting 8μ MEC..... 145
Figure 6.30 TNFα production from macrophages contacting Nylon 6..... 145
Figure 6.31 TNFα production from macrophages contacting PTFE..... 146
Figure 6.32 TNFα production from macrophages contacting 10μ ePTFE..... 147
Figure 6.33 TNFα production from macrophages contacting 30μ ePTFE..... 147

Figure 6.34 TNFα production from macrophages contacting 60μ ePTFE.. 148
Figure 6.35 Macrophage IL-8 release from contact with TCPS or glass ring..... 149
Figure 6.36 IL-8 production from macrophages contacting 0.22μ MEC..... 149
Figure 6.37 IL-8 production from macrophages contacting 5μ MEC..... 150
Figure 6.38 IL-8 production from macrophages contacting 8μ MEC..... 150
Figure 6.39 IL-8 production from macrophages contacting Nylon 6 151
Figure 6.40 IL-8 production from macrophages contacting PTFE..... 151
Figure 6.41 IL-8 production from macrophages contacting 10μ ePTFE 152
Figure 6.42 IL-8 production from macrophages contacting 30μ ePTFE 152
Figure 6.43 IL-8 production from macrophages contacting 60μ ePTFE 153
Figure 7.1 HL-60 assay of HUVECs stimulated with varying amounts of IL-1ß..... 159
Figure 7.2 HL-60 assay of Donor #1: 0.22μ MEC, 5μ MEC and Nylon 6.. 161
Figure 7.3 HL-60 assay of Donor #2: 0.22μ MEC, 5μ MEC and Nylon 6. 162
Figure 7.4 HL-60 assay of Donor #9: 8μ MEC (+/- FN).. 162
Figure 7.5 HL-60 assay of Donor #3: Nylon 6 and PTFE.. 165
Figure 7.6 HL-60 assay of Donor #4: PTFE, ePTFEs and Nylon 6.. 166
Figure 7.7 HL-60 assay of Donor #7: PTFE, ePTFEs (10μ and 30μ) and Nylon 6.... 166
Figure 7.8 HL-60 assay of Donor #8: PTFE, 60μ ePTFE and 8μ MEC.. 167
Figure 7.9 HL-60 assay of Donor #10: PTFE, 10μ, 30μ and 60μ ePTFE (+/- FN).... 167
Figure 8.1 Cell Co-culture system..... 174
Figure 8.2 HUVEC proliferation in response to macrophages seeded on materials..... 175
Figure 8.3 HUVEC growth in response to macrophage supernatants 177
Figure 8.4 A, B, and C HUVEC growth in response to macrophage supernatants..... 179
Figure 8.5 SMC growth in response to co-culture with macrophages on materials..... 180
Figure 8.6 SMC growth from SMC/mø co-culture supernatants..... 181
Figure 8.7 HUVEC proliferative response to SMCs seeded on different materials 182
Figure 8.8 SMC proliferation in response to HUVECs seeded on materials..... 183
Figure 8.9 Heat treatment of mø supernatants reduces HUVEC proliferation 184
Figure 9.1 Phosphorimage data of Northern blot..... 194

LIST OF TABLES

Number *Page*

Table 3.1: Plasma Treatments....33

Table 3.2: HUVEC Culture Medium....40

Table 3.3: TNFα Results: Testing for Endotoxin Contamination....53

Table 4.1: Elemental Composition of MEC Membranes....59

Table 4.2: Percent of Molecular Species from the MEC C1s High-resolution Spectra....61

Table 4.3: Summary of High-resolution C1s Peak Fitting Results for Nylon 6....63

Table 4.4: Elemental Composition of PTFE and ePTFE....66

Table 5.1: Surface Composition Summary from ESCA Data....78

Table 5.2: Summary of Apparent K_a (aK_a) and B_{max} Values....83

Table 5.3: Surface Roughness and Total FN Adsorption....88

Table 7.1: HL-60 Adherence Associated with Macrophage IL-1ß and TNFα Production: Hydrophilic Polymers....163

Table 7.2: HL-60 Adherence Associated with Macrophage IL-1ß and TNFα Production: PTFE and ePTFE Polymers....168

Table 9.1: Key to Number Designations for E-selectin Staining....189

Table 9.2: E-selectin Staining Results....190

Table 9.3: Troubleshooting the Staining Protocol....191

Table 9.4: Amounts of RNA Loaded Per Lane in Agarose Gel....193

Table 9.5: Fibronectin Adsorption Conditions and Northern Blot Analysis Results....195

Table 9.6: Plasma-deposited Film Coatings and Northern Blot Analysis Results....196

Table 9.7: HL-60 Adherence to HUVEC Monolayers....197

ACKNOWLEDGMENTS

I have come to believe that it takes a lot of hard work, persistence, and a bit of ingenuity to succeed in finishing a doctorate. It has been a long seven year journey, and it would be untrue if I said I did it all on my own. There have been a number of people that have helped along the way, which I would like to acknowledge.

First, would like to thank my advisor, Prof. Buddy D. Ratner, and the members of my Supervisory Committee, Dr. Timothy Pohlman, Prof. Tom Horbett, and Prof. Patrick Stayton for their help, support and encouragement in my studies.

Being a member of the Biomaterials Group, I would like to acknowledge the support of all my fellow students that have helped during group discussions or in the lab. I would like to give special thanks to Dr. Pohlman's laboratory staff, past and present, who have helped me with my research over the years. Specifically, I would like to acknowledge Colette-Norby Slycord for technical assistance and Ellen Collins for her endothelial cell cultures. I would like to thank all of my blood donors that participated in my studies. I did a quick calculation and found that I processed almost 10 liters of blood, which is a large contribution and sacrifice to my research.

I have received financial support from a variety of governments, federal agencies, private foundations, and companies during the last 7 years. I would like to acknowledge and thank the following funding sources: Whitaker Foundation, National Institutes of Health, National Science Foundation, the Chateaubriand Fellowship from the French Government, the Mentor Corporation, and the Johnson & Johnson Focused Giving Grant.

There are a few individuals that have been particularly helpful, and I would like to give them due recognition. Winston Ciridon was instrumental in fabricating a number of

the material surfaces that were used in my research. James Bain provided help and constructive criticism during the early stages of my work, especially with my Qualifying and General Exams, for which I would like to thank him. Deborah-Leach Scampavia helped me immensely with my surface analysis work, especially towards the end. Deborah has taught me much of what I know about data interpretation of surface analyses, and I am grateful that she was a patient teacher. Laura Martinson has been invaluable as a co-investigator on the Johnson & Johnson Focused Giving Grant. Laura's understanding of biology and medical implants helped guided me over a number of hurdles in my research, which I doubt that I could have succeeded without her intuitive sense. Caren Tidwell has been my office mate, daily advisor in the practical matters of my dissertation and research, an inspiration, and a friend. I will always be indebted to Caren for providing the much needed encouragement and confidence during the more difficult times, of which there were (unfortunately) many.

I would like to acknowledge the support of my parents and my brothers for their only female child/sibling. The paths I have taken in life have not been conventional, and they have encouraged me in all of my pursuits. My biggest regret is that my brother, Kurt, is not here to share this moment with me. He was my closest friend, a mentor, and an inspiration to me. He presence is greatly missed.

Lastly, I would like to extend my heart-felt thanks to my husband-to-be, W. Craig Jones, for the past 3.5 years of unwavering daily support in a number of ways. Craig selflessly provided an environment for me to focus on my work, giving encouragement and strength at those critical moments. Behind this successful woman is a hard working, dedicated, loving man. I don't know if I could ever adequately express my appreciation, but I'll have a lifetime to try.

In loving memory of my brother

Kurt E. Schmierer

1956-1994

Chapter 1

Introduction

1.1 Introduction

In cardiovascular medicine, artificial vascular grafts have been effective in saving lives and restoring circulation in humans, usually to replace large diameter vessels. There is an urgent need for replacements of smaller vessels of the extremities, particularly for people suffering from circulation problems brought on by diseases such as diabetes. However, small diameter grafts continue to be fraught with problems, mainly graft occlusion (Benton et al., 1993).

A number of research groups are attempting to improve the biocompatibility of vascular grafts by incorporation of a biological component. This has been done by the seeding of endothelial cells, the cells that line our vasculature, on the interior (lumen) of the graft. The rationale is that by lining the lumen of the graft with endothelial cells, a biologically compatible interface is produced to prevent a number of unwanted reactions from occurring, such as blood coagulation that leads to graft occlusion. This type of modification to vascular grafts has been attempted for approximately 20 years, with only isolated reports of success. To date, this hybrid graft is not routinely used clinically.

Explanted grafts have shown the presence of white blood cells that attach from the blood stream to seeded or unseeded grafts (Emerick et al., 1987; Margiotta et al., 1992). These cells are typically monocytes and neutrophils, both of which participate in the body's defense against foreign materials. The interaction of monocytes, neutrophils and endothelial cells are important for initiation and propagation of an inflammatory response. Monocytes can activate endothelial cells through secretion of inflammatory cytokines; likewise activated endothelial cells recruit monocytes and neutrophils from the blood

stream to sites of inflammation via cell adhesion molecule expression. Activation of one cell type *in vivo* would elicit a response from the other cell types.

The inflammatory reaction is a natural response to injury or insult. A foreign object such as a bacterium, a splinter, or a medical implant may initiate this response. Normally, the initial inflammatory reaction slowly abates giving way to wound healing and tissue reconstruction. Unfortunately, this normal healing response does not occur around medical implants, and it is thought the aberrant healing is caused by an excessive inflammatory response to these implants. The typical reaction to an implanted material is what has been termed as the "foreign body reaction" or implant encapsulation. In this type of reaction, the implant is walled-off from the rest of the body by the formation of a dense collagenous capsule, varying in thickness depending upon the type of implant material and the site of implantation.

Since the implant process is initiated by creation of a wound, improvement of implant design has focused on modifying the wound healing process to encourage incorporation of an implant into the surrounding tissues, thus minimizing or eliminating the formation of the unwanted fibrous capsule. One key cell, the monocyte-derived macrophage, is involved in orchestrating not only the inflammatory response, but also healing and tissue remodeling. Macrophages are implicated in extreme inflammatory reactions due to the myriad of inflammatory cell products they produce and the subsequent actions they have on other cells at the wound site. My investigations focus around the production of inflammatory cytokines from macrophages contacting different material surfaces, and what effect these cytokines have on endothelial cell activation and function.

Every implanted medical device must contend with inflammation. The reaction of macrophages to materials has implications specifically to vascular grafts, and medical implants in general. Since macrophages are seen to adhere and invade bare grafts or endothelial cell-seeded grafts, their presence will have an effect on endothelial cells at the

anastomoses of the graft, the endothelial cells seeded on the lumen of the graft, and the tissues contacting the exterior of the graft. Thus, knowing what type of reaction can be expected from monocyte-derived macrophages to different materials or material coatings, and how these reactions influence endothelial activation have profound significance to the medical implant community. My research encompasses macrophage cytokine expression in response to material surfaces, as well as the interpretation of those signals by endothelial cells in the context of their inflammatory cell adhesion molecules expression.

The hypotheses that define my work are four-fold. I hypothesized that macrophage cytokine gene expression is influenced by:

1) the surface chemistry of the material,

2) the topography or porosity of the material, and

3) extracellular matrix protein coating of the material.

In addition:

4) endothelial cells that are exposed to the products secreted by macrophages contacting materials may be activated depending upon the types and quantities of cytokines produced. If activation occurs, a functional change in the endothelial cell will ensue.

These hypotheses were constructed within the frame work of modeling cellular interactions with vascular prosthesis materials, as well as other materials that are of interest due to their ability to heal more naturally than other materials.

The choice of materials for my research emphasizes materials that are used clinically or for which there existed some *in vivo* data to integrate my findings into what has been previously observed by others. It is my contention that a systematic approach to using materials that have a long history of use in the body can give some insight into how to best interpret my *in vitro* findings. In particular, expanded poly(tetrafluoroethylene)

(ePTFE), a porous form of Teflon®, has been used for many years in a variety of medical implants, primarily in vascular applications. I also used a series of mixed ester cellulose membranes (MEC) in collaboration with Laura Martinson, who has extensive knowledge of the performance of these materials implanted into animals. The 5μ and 8μ pore size MEC membranes have demonstrated a dramatically different healing response, showing better integration into tissues through the formation of capillaries in direct apposition to the material surface and into the pores. These two materials present a diverse set of properties such as surface chemistry, wettability, pore size and pore shape.

Particular attention was given to polymer cleaning and preparation. The two cell types used, human monocytes and human umbilical vein endothelial cells, are exquisitely sensitive to a common contaminant, bacterial endotoxin. The origin of endotoxin is primarily from impure water contacting the materials. The presence of endotoxin can profoundly influence cellular mechanisms, causing extreme inflammatory responses. Since my studies focus around understanding the inflammatory responses of these cell types on the materials, monitoring endotoxin was vital.

To make this research as clinically relevant as possible, I chose to use only human cells, most of them primary cultures isolated from human blood or tissues. In comparison to using established cell lines or cells from other species, the difficulty of culturing human cells and obtaining sufficient cell numbers introduces added challenges. Once a cell is removed from its natural setting in the body, a variety of changes occur. The longer a cell is cultured *in vitro*, the more likely it will display an unnatural phenotype. Every effort was made to use monocyte-derived macrophages directly isolated from blood or endothelial cells of low passage number. The argument is well taken that *in vitro* evaluations of cell-material interactions have limitations, but if adequate attention to species differences, cell types, culture conditions, isolation procedures and cell age in culture are carefully monitored, I feel there is useful information that can be generated

from these types of studies. Often, the complexity of *in vivo* experiments makes it difficult to investigate many of the intricate mechanisms of cells contacting a material surface. Also, the differences in species often produce results that can not be extrapolated to human biology. Thus reductionism is indicated for this type of research, tempered with cautious interpretation of the results.

When I arrived to begin my graduate studies, the extent of biomaterials evaluation in our group was limited to determining cell growth on the different polymer surfaces produced "in house." My goal was to incorporate more information-rich techniques into my research to probe a cell's biology and function upon contact with biomaterial surfaces. This is the first thesis in our group to investigate cytokine production and changes in gene expression in cells contacting materials. And, being the first to travel down this path, there were several challenges to contend with. A number of techniques are often used in cell biology to investigate protein and gene expression. These techniques work well for cells cultured in the standard tissue culture "plastic", but do not lend themselves to cells cultured on other materials, especially porous materials. Simple tasks, such as cell enumeration, become extremely difficult when cells are contacting opaque, porous materials with widely varying surface properties. A number of techniques used in this dissertation had to be adapted to the special conditions presented by these materials.

The trials that presented themselves provided a number of valuable lessons. By "pushing" to implement new techniques and assays, I have a greater appreciation for the complexities of biomaterials research. The contribution of this research comes not only from the successes, but also the paths taken and subsequently retreated from. I feel that the understanding of how a foreign material interacts with cells in the body is still in its infancy. My hope is that this research takes us forward in the journey to understanding the body's interplay with implanted materials, and provides useful insights in the design or modification of future medical implants.

1.2 Notes to Chapter 1

Benton, L. D., Khan, M., and Greco, R. S. (1993). Integrins, Adhesion Molecules and Surgical Research. Surg. Gyn, Obstet. *177*, 311-327.

Emerick, S., Herring, M., Arnold, M., Baughman, S., Reilly, K., and Glover, J. (1987). Leukocyte depletion enhances cultured endothelial retention on vascular prostheses. J. Vasc. Surg. *5*, 342-347.

Margiotta, M. S., Robertson, F. S., and Greco, R. S. (1992). The Adherence of Endothelial Cells to Dacron Induces the Expression of the Intercellular Adhesion Molecule (ICAM-1). Ann. Surgery *216*, 600-604.

Chapter 2

Literature Review

2.1 Review of the Literature

Autogenous tissue, such as saphenous vein, provides the best arterial replacement for all applications in humans and is far superior to synthetic materials (Graham and Bergan, 1982). However, healthy saphenous vein is not always available. In these circumstances, synthetic vascular grafts must be used.

In cardiovascular medicine, artificial vascular grafts have been effective in saving lives and restoring circulation in humans when used in certain applications. The primary materials used clinically for vascular grafts are Dacron (poly(ethylene terephthalate)) and expanded polytetrafluoroethylene (ePTFE) (Frazier et al., 1994). The characteristics necessary for a successful vascular graft are 1) maximum graft porosity to promote ingrowth of blood vessels, but at the same time limit blood loss through the graft material, 2) high strength, 3) ease of handling for the surgeon, and 4) low biological activity (Snyder and Botzko, 1982). But ultimately, artificial vascular grafts are assessed on their clinical performance, not only for early graft function, but for long-term patency of grafts (Reichle, 1982).

Sauvage et al. demonstrated increased early thrombogenicity for ePTFE grafts compared to Dacron, so there is an effect of material type on graft patency (Sauvage et al., 1979). Larger diameter vascular replacements, grafts having diameters larger than 6mm, show similar patency rates for the two different materials, between 60% and 70% over 2 years (Reichle, 1982). Grafts implanted below the inguinal ligament fail at a much higher rate (47-65%) after 2 years compared to those implanted more proximal (5-35%) (Graham and Bergan, 1982). For femoropoliteal and femorotibial grafts, some investigators report patency rates as low as 24% for ePTFE grafts after 2 years, in contrast to 84% patency for

autogenous saphenous vein (Graham and Bergan, 1982). The patency rates for all types of vascular grafts decrease with time, making these prostheses temporary replacements at best. The failure rates, especially at extended times, demonstrate the need for improvement of vascular graft performance.

Thrombosis and intimal hyperplasia are the primary modes of graft failure, especially for medium to small diameter grafts (Herring et al., 1982) (Benton et al., 1993). Short-term failure is mainly due to graft occlusion from thrombus formation on the interior of the graft. The reason for late occlusions is not always clear, although intimal hyperplasia and the lack of an established endothelial cell layer on the interior of the graft most likely contribute to late-stage graft failure (Graham and Bergan, 1982; Kaplan, 1994). At these longer time points, the graft surface remains thrombogenic and unstable due to the lack of an endothelial cell lining. Human endothelial cells (ECs) have a much lower capacity to reproduce themselves when contacting synthetic materials than other mammalian species (Kaplan, 1994). Vascular grafts implanted in dogs, pigs, sheep and non-human primates endothelialize relatively well within weeks to a few months after implantation (Callow, 1988). Due to the frequent and early failure rates of vascular grafts, it is suggested that the establishment of an EC layer on the graft interior is essential to reduce the magnitude of biological reaction to these synthetic prostheses.

The resurfacing of vascular grafts with ECs, in theory, would limit thrombus formation by providing a natural covering to the synthetic graft (Williams et al., 1991). Deactivation of thrombin and suppression of platelet activation through prostacyclin secretion by endothelial cells would reduce thrombosis (Herring, 1991). Also, it is suggested that providing an EC covering early may reduce the amount of intimal hyperplasia by reducing the exposure of smooth muscle cells and fibroblasts to thrombin which causes these cells to become more sensitive to growth factors (Herring, 1991). If

ECs could be made to grow and cover the luminal surface of the graft, in theory, a non-thrombogenic surface could be made.

The sources of ECs are typically from enzymatic digestion of fat tissue, which contains large numbers of microvascular ECs (Jarrell et al., 1987; Williams et al., 1992; Williams et al., 1989; Williams et al., 1991), or the interior lining of veins (Greisler et al., 1989; Jarrell et al., 1987). Early reports of endothelial cell seeding on grafts *in vitro* showed modest cell retention on the bare graft surface under flow conditions (Kempczinski et al., 1987). EC retention could be improved by first pre-coating the graft with a variety of proteins such as fibronectin (Greisler et al., 1989; Jarrell et al., 1988; Jarrell et al., 1987; Kempczinski et al., 1987), fibrin (Herring et al., 1982), collagen (Herring et al., 1982; Li et al., 1992), and other extracellular matrix proteins (Bujan et al., 1998; Matsuda et al., 1988; Mazzucotelli et al., 1991; Schneider et al., 1997; Schneider et al., 1992). The adsorbed proteins permitted strong attachment of seeded endothelial cell layers, with very high cell retention, even for perfusion rates that exceed physiologic flow rates (Greisler et al., 1989). These early studies were encouraging, showing that viable, confluent layers of ECs could be established on the interior of vascular grafts.

Data from numerous non-human animal studies showed some encouraging results (Williams and Jarrell, 1996; Williams et al., 1994; Williams et al., 1994), but human clinical trials demonstrated modest improvements in vascular graft patency, if any improvement was seen at all (Fasol et al., 1989; Herring et al., 1987; Herring, 1991; Herring et al., 1987; Jarrell and Williams, 1991). Upon further analysis of explanted grafts, retention of seeded ECs was shown to be very low in human and non-human animal models (Herring et al., 1987; Hussain et al., 1989). An explanation for the success of the non-human (mostly canine) models is that these animal have a high degree of spontaneous endothelialization of vascular grafts, and that with even low seeded EC

retention, it provided some advantage over the bare graft controls. For humans, however, this was not the case.

Another observation from these studies is that large numbers of leukocytes (neutrophils and monocytes) were seen to adhere to the seeded ECs from the bloodstream (Emerick et al., 1987; Herring et al., 1987). In some cases, accumulation of macrophages is pronounced on seeded grafts, whereas unseeded or bare patches on seeded grafts had lower macrophage attachment (Burkel et al., 1982). In another study, EC retention on grafts in dogs was very low, reporting only 3.2% of seeded cell remained after 24 hours (Emerick et al., 1987). The loss of cells was not attributed to mechanical failure of attachment, but the interaction of neutrophils with the seeded cells. Emerick et al. elegantly demonstrated this by comparing implants in normal dogs to those in neutropenic (without neutrophil) dogs. The neutropenic dogs had almost complete retention of seeded cells after 30 minutes, compared to 60% for the normal animals. Other investigators showed similar results demonstrating the importance of cellular interactions for EC-seeded grafts (Herring et al., 1987; Margiotta et al., 1992).

Interaction of ECs with circulating neutrophils and monocyte-derived macrophages suggests the seeded ECs may be activated, responding in a manner similar to an inflammatory response. Although the recruitment of blood monocytes by endothelial cells seeded on vascular grafts is appreciated, little is known about the mechanisms involved and what part they play in the long-term patency of these grafts (Nerem, 1988). The preponderance of evidence showing neutrophil and monocyte adhesion to seeded ECs strongly indicates that inflammatory neutrophils and monocytes profoundly affect the performance of EC-seeded vascular grafts (Libby et al., 1987). Although EC seeding of vascular grafts had promising results in non-human animal models, there has been no clinical success with this technique to date (Eskin et al., 1987; Graham et al., 1991).

Monocytes, the precursor cells to macrophages, are considered to be the single most important cell type in directing the course of the inflammatory reactions to synthetic materials *in vivo* (Bhardwaj et al., 1997; Brauker et al., 1995; Zhao et al., 1992). Macrophages persist at implant sites for long periods of time compared to neutrophils which are no longer found in association with implants after about one week (Shankar and Greisler, 1994). For this reason, the following discussion will focus on monocyte/macrophage interactions with materials. Monocytes are capable of adhesion to a variety of substrates such as implanted materials, extracellular matrix (ECM) proteins and endothelial cells via specific cellular receptors (Lundahl et al., 1996). However, the role of adhesion molecules and integrins in the human response to implanted materials is not well understood.

Monocytes appear to activate specific genes depending on the substrate to which they attach (Sastry and Horwitz, 1993). As has been shown by years of investigation, monocytes are profoundly affected by adhesion. Adhesion can initiate a variety of cellular responses, such as differentiation, inflammatory cytokine gene expression, cytoskeletal assembly, and migration (Jones et al., 1993; Luna and Hitt, 1992; Margiotta et al., 1992; Menconi et al., 1992). The group of receptors that is responsible for the interaction of macrophages and neutrophils with extracellular matrix proteins is the integrins. The integrin external receptor is associated directly with internal cytoskeletal proteins through its transmembrane and cytoplasmic domains (Albelda and Buck, 1990). Some of the proteins capable of phosphorylative activity on cytoskeletal elements have been identified and are thought to be responsible for adhesion-initiated gene expression by cytoplasmic signaling to the nucleus (Sastry and Horwitz, 1993). The dramatic changes in phosphorylation of tyrosine and protein kinases, intracellular calcium concentrations and cytoplasmic pH upon adhesion or binding of receptor ligands influence the expression of

genes through phosphorylation of second messengers (Gimond and Aumailley, 1992; Watson, 1991).

Integrins are composed of 2 subunits, α and ß. The $ß_1$ integrins, sharing a common ß subunit but varying in the α subunit, are receptors for extracellular matrix proteins such as vitronectin and fibronectin (Hynes, 1992). Adhesion of unstimulated monocytes to fibronectin-coated surfaces *in vitro* is rapid, with high levels of monocyte attachment (80%) occurring in 15 minutes (Lundahl et al., 1996). This level of adhesion in monocytes was not affected by chemotactic factors such as RANTES or IL-8.

The monocyte CD11b/CD18 (Mac-1) integrin receptor is a member of the $ß_2$ integrins, participating in a number of adhesion processes via a wide array of ligands (Lundahl et al., 1996). Macrophages adherent to ECM are substantially mediated by CD11b/CD18 (Davis, 1992; Owen et al., 1992). It has also been suggested that this integrin complex recognizes denatured protein sequences and binds to them (Lundahl et al., 1996). CD11b-mediated adhesion to plastic culture dishes has long been utilized for the isolation of monocytes (Lundahl et al., 1996). This appears to be a nonspecific reaction to material surfaces, and may be an influence of leukocyte purification schemes on CD11b expression (Macey et al., 1995). Recent reports show up-regulation in expression of CD11b for monocytes contacting vascular graft materials. Benton et al. showed significant increase in CD11b expression in leukocytes exposed to ePTFE (Benton et al., 1996). Another study showed similar results for ePTFE and Dacron graft materials (Swartbol et al., 1996). This implies vascular graft materials are capable of initiating monocyte adhesion and activation by contact alone. Other cell adhesion molecules, such as macrophage expression of ICAM-1, are being investigated as well (Bernatchez et al., 1997). CD11b/CD18-mediated adhesion of monocytes may be a primary mechanism of monocyte/macrophage adhesion to vascular graft materials *in vivo*.

In general, upon binding to adhesion receptors, profound changes in functional properties of cells are seen. It is conceivable that by forcing a cell to adhere in a certain way will also influence gene expression. One mechanism that may be involved with changes in cell function in response to biomaterials is an altering of the cell's shape upon attachment to an artificial surface, such as to a fiber (Bernatchez et al., 1996). The cell's shape may transmit signals to the nucleus via the arrangement of cytoskeletal elements within the cell (Blum and Wicha, 1988; Lafrenie and Yamada, 1996; Lelievre et al., 1996; Maniotis et al., 1997). The Whitesides group has reported that when hepatocytes were confined to a very small area for attachment, they functioned normally by producing albumin (Singhvi et al., 1994). However, when cells were given a larger area to become fully spread, they ceased producing albumin. The shape of the cell seemed to dictate the function of the cell in this system. The more rounded the cell, the more closely it appeared to function as it would *in vivo*. Similar findings have been reported by Brauker et al. concerning the shape of pores and how they affect angiogenesis and wound healing around implanted materials (Brauker et al., 1995). These findings have stimulated investigations into the effects that the 3-dimensional environment of porous materials have on cell and tissue reactions.

As mentioned before, the adhesion of macrophages to different ECM proteins affects not only migration of cells, but other processes important to generating an inflammatory response from these cells, namely activation and cytokine expression (Eierman et al., 1989; Webb et al., 1990). Induction of inflammatory cytokine production in monocytes and macrophages after adhesion or integrin engagement has been shown by a number of investigators (Beezhold and Personius, 1992; Cahalon et al., 1994; Eierman et al., 1989; Fuhlbrigge et al., 1987; Rosales and Juliano, 1995; Webb et al., 1990). Adhesion induces the expression of a large number of genes associated with the inflammatory response. The study by Benton et. al, where increases in CD11b were seen

in leukocytes attached to ePTFE, ties in with their earlier studies. Macrophages exposed to ePTFE and other materials caused an increase in inflammatory cytokine expression, suggesting that integrin engagement can lead to macrophage activation and cytokine release (Benton et al., 1996; Krause et al., 1990). But it appears that the expression of specific genes requires more than just integrin binding; other required events are receptor crosslinking, cell adhesion, and cytoskeletal reorganization (Rosales and Juliano, 1995).

The degree of macrophage activation can be monitored by measuring released inflammatory cytokines. Two cytokines, interleukin-1ß (IL-1ß) and tumor necrosis factor-α (TNFα) are the most common inflammatory cytokines, and have a long history of initiating and sustaining inflammatory reactions. Another inflammatory cytokine, interleukin-8 (IL-8) is also a potent inflammatory agent, but little research has been directed towards its involvement in the host response to implanted materials. These cytokines are expressed together during inflammation, since expression of one cytokine will induce the expression of the others.

IL-1ß is produced during inflammation, tissue damage, wound healing, and a variety of disease states, such as rheumatoid arthritis and septic shock (Dinarello, 1991). IL-1ß affects a large number of cell types, such as fibroblasts, endothelial cells, neutrophils, B- and T-cells, and other cell types involved in inflammation and cellular interactions with implanted materials (Dinarello, 1990; Furth, 1988; Miller and Anderson, 1988; Ziats et al., 1988). Being a potent cytokine, IL-1ß is responsible for the recruitment of inflammatory and immune cells to implant sites. IL-1ß stimulates B- and T-cells, increases B-cell production of immunoglobulin, and stimulates T-cells to produce IL-2, IL-4, and GM-CSF (Dinarello, 1991). It also contributes to tissue breakdown, causes fibroblast proliferation and increases collagen production leading to fibrosis (Dinarello, 1991). Because IL-1ß is soluble, it is not limited to local effects. Monocytes and

macrophages produce IL-1ß in response to lipopolysaccharide (from bacteria), foreign particles, implanted materials (Bonfield and Anderson, 1993; Cardona et al., 1992; Krause et al., 1990), and immune complexes (Nathan, 1987; Oppenheim et al., 1986). Macrophages are also capable of autocrine production of IL-1ß, and other cytokines such as TNFα and IL-6 that participate in the inflammatory response. Autocrine stimulation is an effective method for amplifying the inflammatory response.

Activated macrophages also produce TNFα, also known as cachectin. TNFα was originally found to kill certain types of tumor cells, thus its name (Dinarello, 1988). TNFα is commonly referred to as an inflammatory cytokine (although it has pleiotropic activities), which emphasizes its role in initiation the cascade of other soluble factors that comprise a host's reaction to trauma and infection. Having almost identical biological functions as IL-1ß, TNFα and IL-1ß often act synergistically, and stimulate the production of each other (Dinarello, 1988). TNFα is able to activate a number of signal transduction pathways and induce or suppress a vast number of genes. These include genes for growth factors, cytokines, transcription factors, receptors, inflammatory mediators, and acute phase proteins (Aggarwal and Vilcek, 1992). TNFα is produced by neutrophils monocyte/macrophages, activated lymphocytes, endothelial cells, smooth muscle cells, and others (Dinarello, 1988). TNFα is a membrane-bound cytokine containing both hydrophilic and hydrophobic domains. The soluble 17 kDa form of TNFα is cleaved from the extracellular domain (Perez et al., 1990). The membrane-bound form on macrophages and monocytes not only serves as a reservoir for release of soluble TNFα, but also has cytotoxic activity and may participate in intercellular

communication (Macchia et al., 1993). Over production of TNFα, as is the case with septic shock, can cause considerable damage to the host. Other pathological conditions resulting from excessive TNFα production are cachexia (progressive wasting), and autoimmune disorders (Beutler et al., 1985; Pujol-Borrell et al., 1987).

IL-8 belongs to a superfamily of small (8-10 kDa), inducible pro-inflammatory chemotactic cytokines called chemokines. IL-8 is a member of the a subfamily, also referred to as the C-X-C subfamily, which is responsible for neutrophil chemoattraction and activation (Ben-Baruch et al., 1995). The ß subfamily of chemokines are chemoattractant for monocytes and lymphocytes. A number of cell types such as monocytes, macrophages, endothelial cells, neutrophils, fibroblasts, and others produce IL-8 constitutively or in an inducible manner in response to pro-inflammatory signals IL-1ß, TNFα, and LPS (Ben-Baruch et al., 1995; Kunkel et al., 1995). Besides being a potent chemotactic and activating factor for neutrophils, IL-8 has a number of other pro-inflammatory actions. IL-8 causes degranulation of neutrophil specific granules, increases the expression of CD11/CD18 cell adhesion molecules, and augments the adherence of neutrophils to endothelial cells and ECM proteins (Furie and Randolph, 1995). IL-8 has also been reported to possess angiogenic activity *in vivo* and *in vitro* (Yue et al., 1994). Red blood cells are capable of binding IL-8 with high affinity, and once bound it is inactive to neutrophils (Furie and Randolph, 1995). This suggests a mechanism by which circulating IL-8 and other chemokines are cleared from the body, and may be a method of controlling inflammation. From the activities outlined above and from examination of a number of inflammatory disease states, it is indicated that IL-8 plays a significant role in inflammatory responses. To date, however, there is no information on IL-8's role in inflammatory reactions to implanted materials.

The primary functions of neutrophils and monocytes occur for the most part in association with surfaces *in vitro* or *in vivo* (Henson et al., 1981). An example is the relative quiescence of these cell types in the bloodstream. It is only when they become attached to endothelium or synthetic surfaces do they express a whole host of inflammatory mediators. In this fashion, one can see the importance of neutrophils and monocytes to the field of medical implants. Either through direct attachment to materials or to the adsorbed proteins on the material surface, these cell types have well developed mechanisms of activation when exposed to surfaces in the body.

It is well accepted in the field of biomaterials that monocytes and macrophages play a large role in inflammatory reactions to implanted materials (Kaplan, 1994; Ziats et al., 1988). Also, cytokines released from monocytes and macrophages have long been associated with medical implants. A number of investigators, primarily in collaboration with J.M. Anderson, have demonstrated monocyte activation and/or subsequent IL-1ß or TNFα secretion from macrophages contacting a wide variety of material surfaces (Bernatchez et al., 1996; Bonfield and Anderson, 1993; Bonfield et al., 1992; Cardona et al., 1992; Das et al., 1992; Davies et al., 1981; DeFife et al., 1995; Hunt et al., 1997; Krause et al., 1990; Miller and Anderson, 1988; Miller and Anderson, 1989; Miller et al., 1989; Petillo et al., 1994; Rhodes et al., 1997; Yun et al., 1995; Zhao et al., 1992). Also, these studies have shown it is the nature of the surface that dictates the level of cytokine release from macrophages. Surface characteristics that were tested in the above studies include differences in material composition or surface chemistry, surface topography or fibril length, and adsorbed proteins to materials. The results of individual studies will not be reviewed here due to the large number of studies cited. Difficulties arise in comparing one study to the next due to differences in the types of polymers used in each study, the tissue or species origin of monocytes/macrophages used, exogenous stimulation with

LPS, and different monocyte isolation procedures employed, to list just a few of the concerns. The literature citations should be used as a guide for those interested in this topic.

When reviewing this body of literature, several criticisms warrant mentioning which affect the interpretation of the data contained in these reports. Almost all of the Anderson publications cultured monocytes with materials in the presence of LPS, which may mask the effect of material characteristics on cytokine production. Since LPS stimulates the autocrine production of IL-1ß, TNFα, IL-8 and numerous other macrophage products, the influence of LPS stimulation could subvert any contributions of the material to macrophage activation and cytokine production. None of the cytokine data reported in any of the reports was normalized to cell number. This could have a profound effect on the quantitative values reported. Also, these reports do not indicate any testing for endotoxin contamination on the materials. Endotoxin is a common contaminant in water, and is a potent activator of monocytes and macrophages (as demonstrated in the LPS-stimulation used in the Anderson studies), as well as a number of other cell types. For these reasons several aspects of the cited studies should be interpreted cautiously. Finally, almost none of the reports demonstrated biological activity on another target cell population. There are a few exceptions, but none of these studies discuss the effects of cytokine production on endothelial cell function as it pertains to seeded vascular grafts.

Since cytokines work in concert, the measurement of a single cytokine released may only give part of their function as inflammatory stimuli and how they affect other cells. As discussed in Chapter 7, cell-based assays to determine the cumulative effect of inflammatory cytokine release is suggested. One method for determining the effect of inflammatory cytokines is to monitor cell adhesion molecules on EC surfaces. The expression of cell adhesion molecules could explain the recruitment of neutrophils and

monocytes to ECs adhered on the graft surface, since cell adhesion molecule expression is the cellular mechanism for initiation of an inflammatory response via inflammatory cell recruitment.

Cell adhesion molecules are responsible for the recruitment of many cell types involved in inflammation, and may be key to understanding how biomaterials influence cell behavior *in vivo*. E-selectin, a cell adhesion molecule of the selectin family, is expressed on activated ECs and is under transcriptional control (Ghosh and Baltimore, 1990; Montgomery et al., 1991). It plays a vital role in the initial attachment of neutrophils and monocytes to activated endothelium (Hession et al., 1990). Known activators are TNFα, IL-1ß, and endotoxin (lipopolysaccharide, LPS) (Pober and Cotran, 1990; Pober and Cotran, 1991). The E-selectin gene is regulated through a second messenger, NFkB, which translocates to the nucleus to initiate transcription after phosphorylation of its inhibitor, IkB (Baeuerle and Baltimore, 1988; Ghosh and Baltimore, 1990; Montgomery et al., 1991). Protein kinase C is suspected to be involved in the phosphorylation of IkB, but other kinases may also be involved (Baeuerle and Baltimore, 1988). E-selectin expression peaks at 4-6 hours, and is transient (Bevilacqua et al., 1989). E-selectin binds the tetrasaccharide sialyl-Lewis^{x} found on the surface of neutrophils and monocytes (Foxall et al., 1992; Lasky, 1992; Polley et al., 1991).

Vascular cell adhesion molecule, VCAM-1, is another cell adhesion molecule expressed on activated endothelial cells. The tissue distribution of VCAM-1 is activated endothelial cells, and macrophage-like (or dendritic cells) in lymph nodes, skin, or synovium (Harlan and Liu, 1992). Under normal conditions, VCAM-1 is not constitutively expressed, and is only seen on endothelial cells at sites of inflammation or tissue damage (Pober and Cotran, 1990). VCAM-1 is primarily expressed on endothelial cells in response to cytokines (TNF, IL-1ß), and endotoxin (LPS) (Pober and Cotran,

1990), and is the primary element responsible for the recruitment of monocytes (Harlan and Liu, 1992). Activation of endothelial cells with these substances does not give a selective expression of VCAM-1, as a variety of cell adhesion molecules are expressed given the same stimuli, namely E-selectin and ICAM-1 (Weller et al., 1991). The integrin α4ß1 (VLA-4) on monocytes can bind both VCAM-1 and fibronectin (Smyth et al., 1993). Selective stimulation of VCAM-1 in endothelial cells can be attained with IL-4, which is secreted by lymphocytes (Schleimer et al., 1992). This selective stimulation gives endothelial cells the ability to regulate neutrophil infiltration (seen early in inflammation), switching from neutrophil-rich to mononuclear leukocyte/lymphocyte-rich infiltrates. During the evolution of the inflammatory process, infiltration of monocytes, lymphocytes and eosinophils to a wound site is seen at later time points (Pober and Cotran, 1991). VCAM-1 expression is first detectable 2 hours after stimulation, is maximal at 10-24 hours, and will be maintained with constant (chronic) stimulation (Pober and Cotran, 1991). VCAM-1 expression seems to be involved in allergies, graft rejection, and atherosclerosis (Benton et al., 1993; Heemann et al., 1994).

A combination of cell adhesive mechanisms may explain the in vivo results seen with endothelial cell seeding of vascular prostheses. Direct interaction of neutrophils and monocytes with the graft surface is possible through leukocyte adhesion molecules of the CD11/CD18 family. These adhesive events are enhanced in the presence of adsorbed extracellular matrix proteins, such as fibronectin, that can adsorb to implant surfaces from circulating blood. Upon adhesion, neutrophils and monocytes are known to become activated and subsequently inflammatory cytokines such as IL-1ß, TNFα, or IL-8 can be secreted. Expression of cell adhesion molecules on endothelial cells could be through direct interaction with the graft surface or through induction by IL-1ß or TNFα release from neutrophils and monocytes that attach to the graft. Once cell adhesion molecules are

expressed on endothelium, more leukocytes are recruited from the bloodstream, initiating a full inflammatory reaction. This vicious circle of leukocyte attachment, activation, endothelial cell activation, and active recruitment of more leukocytes may set up a host reaction that eventually leads to loss of seeded endothelium. This scenario could be an explanation for the in vivo "desquamation" of ECs (Herring et al., 1987), and the lack of improvement in vascular graft performance using the EC seeding technique. The challenge of the biomaterialist is to first understand the biological mechanisms at play, and then to engineer materials that better suit the host's biology. It may be possible in the future to design a graft material that would reduce/eliminate leukocyte adhesion, provide a compatible surface for endothelial cell attachment and function, and be incorporated into the surrounding host tissues without inducing intimal hyperplasia. Having a firm grasp of the potential initiators of an inflammatory reaction to a medical implant is critical. Only when all of these factors are addressed will EC seeding of vascular grafts be a viable technique for improving vascular graft performance.

2.2 Notes to Chapter 2

Aggarwal, B. B., and Vilcek, J. (1992). Tumor necrosis factors: structure, function and mechanism of action (New York: M. Dekker).

Albelda, S. M., and Buck, C. A. (1990). Integrins and other cell adhesion molecules. FASEB *4*, 2868-2880.

Baeuerle, P. A., and Baltimore, D. (1988). IkB: A Specific Inhibitor of the NF-kB Transcription Factor. Science *242*, 540-546.

Beezhold, D. H., and Personius, C. (1992). Fibronectin fragments stimulate tumor necrosis factor secretion by human monocytes. J. Leukocyte Biol. *51*, 59-64.

Ben-Baruch, A., Michiel, D. F., and Oppenheim, J. J. (1995). Signals and Receptors Involved in Recruitment of Inflammatory Cells. J. Biol. Chem. *270*, 11703-11706.

Benton, L. D., Khan, M., and Greco, R. S. (1993). Integrins, Adhesion Molecules and Surgical Research. Surg. Gyn, Obstet. *177*, 311-327.

Benton, L. D., Purohit, U., Khan, M., and Greco, R. S. (1996). The Biologic Role of B_2 Integrins in the Host Response to Expanded Polytetrafluoroethylene. J. Surg. Res. *64*, 116-119.

Bernatchez, S., Atkinson, M. R., and Parks, P. J. (1997). Expression of intercellular adhesion molecule-1 on macrophages *in vitro* as a marker of activation. Biomaterials *18*, 1371-1378.

Bernatchez, S., Parks, P. J., and Gibbons, D. F. (1996). Interactions of macrophages with fibrous materials *in vitro*. Biomaterials *17*, 2077-2086.

Beutler, B., Greenwald, D., Hulmes, J. D., Chang, M., Pan, Y.-C., Mathison, J., Ulevitch, R., and Cerami, A. (1985). Identity of tumor necrosis factor and the macrophage-secreated factor cachectin. Nature *316*, 552-554.

Bevilacqua, M. P., Stengelin, S., Gimbrone, M. A., and Seed, B. (1989). Endothelial Leukocyte Adhesion Molecule 1: An Inducible Receptor for Neutrophils Related to Complement Regulatory Proteins and Lectins. Science *243*, 1160-1165.

Bhardwaj, R. S., Henze, U., Klein, B., Zwadlo-Klarwasser, G., Klinge, U., Mittermayer, C., and Klosterhalfen, B. (1997). Monocyte-biomaterial interaction inducing phenotypic dynamics of monocytes: a possible role of monocyte subsets in biocompatibility. J. Mater. Sci.: Mater. Med. *8*, 737-742.

Blum, J. L., and Wicha, M. S. (1988). Role of the Cytoskelton in Laminin Induced Mammary Gene
Expression. J. Cell. Physiol. *135*, 13-22.

Bonfield, T. L., and Anderson, J. M. (1993). Functional versus quantitative comparison of IL-1b from monocytes/macrophages on biomedical polymers. J. Biomed. Mat. Res. *27*, 1195-1199.

Bonfield, T. L., Colton, E., Marchant, R. E., and Anderson, J. M. (1992). Cytokine and growth factor production by monocytes/macrophages on protein preadsorbed polymers. J. Biomed. Mater. Res. *26*, 837-850.

Brauker, J. H., Carr-Brendel, V. E., Martinson, L. A., Crudele, J., Johnston, W. D., and Johnson, R. C. (1995). Neovascularization of synthetic membranes directed by membrane architecture. J. Biomed. Mater. Res. *29*, 1517-1524.

Bujan, J., Garcia-Honduvilla, N., Contreras, L., Gimeno, M. J., Escudero, C., Bellon, J. M., and San-Roman, J. (1998). Coating PTFE vascular prostheses with a fibroblastic matrix improves cell retention when subjected to blood flow. J. Biomed. Mater. Res. *39*, 32-39.

Burkel, W. E., Ford, J. W., Vinter, D. W., Kahn, R. H., Graham, L. M., and Stanley, J. C. (1982). Endothelial Seeding of Enzymatically Derived and Cultured Cells on Prosthetic Grafts. In Biologic and Synthetic Vascular Grafts, J. C. Stanley, ed. (New York: Grune & Stratton), pp. 631-651.

Cahalon, L., Hershkoviz, R., Gilat, D., Miller, A., Akiyama, S. K., Yamada, K. M., and Lider, O. (1994). Functional Interactions of Fibronectin and TNFα: A Paradigm of Physiological Linkage Between Cytokines and Extracellualr Matrix Moieties. Cell Adh. Comm. *2*, 269-273.

Callow, A. D. (1988). Problems in the Construction of a Small Diameter Graft. International Angiology *7*, 246-253.

Cardona, M. A., Simmons, R. L., and Kaplan, S. S. (1992). TNF and IL-1 generation by human monocytes in response to biomaterials. J. Biomed. Mater. Res. *26*, 851-859.

Das, S. K., Johnson, M., Ellsaesser, C., Brantley, S. K., Kanosky, M. G., and Johnson, S. G. (1992). Macrophage Interleukin 1 Response to Injected Silicone in a Rat Model. Ann. Plast. Surg. *28*, 535-537.

Davies, P., Bonney, R. J., Humes, J. L., and F.A. Kuehl, J. (1981). Secretory functions of macrophages participating in inflammatory responses. In Cellular Interactions, J. T. Dingle and J. L. Gordon, eds. (New York: Elsevier), pp. 33-42.

Davis, G. E. (1992). The Mac-1 and p150, 95ß2 integrins bind denatured proteins to mediate leukocyte cell-substrate adhesion. Exp. Cell Res. *200*, 242-252.

DeFife, K. M., Yun, J. K., Azeez, A., Stack, S., Ishihara, K., Nakabayashi, N., Colton, E., and Anderson, J. M. (1995). Adhesion and cytokine production by monocytes on poly(2-methacryloyloxyethyl phosphorylcholine-co-alkyl methacrylate)-coated polymers. J. Biomed. Mater. Res. *29*, 431-439.

Dinarello, C. A. (1990). Cytokines and Biocompatibility. Blood Purif. *8*, 208-213.

Dinarello, C. A. (1988). Cytokines: Interleukin-1 and Tumor Necrosis Factor (Cachectin). In Inflammation: Basic Principles and Clinical Correlates, J. I. Gallin, I. M. Goldstein and R. Snyderman, eds. (New York: Raven Press), pp. 195-208.

Dinarello, C. A. (1991). Interleukin-1 and Interleukin-1 Antagonism. Blood *77*, 1627-1652.

Eierman, D. F., Johnson, C. E., and Haskill, J. S. (1989). Human Monocyte Inflammatory Mediator Gene Expression is Selectively Regulated By Adherence Substrates. J. Immunol. *142*, 1970-1976.

Emerick, S., Herring, M., Arnold, M., Baughman, S., Reilly, K., and Glover, J. (1987). Leukocyte depletion enhances cultured endothelial retention on vascular prostheses. J. Vasc. Surg. *5*, 342-347.

Eskin, S. G., Navarro, L. T., Zamora, J. L., Ives, C. L., Anderson, J. M., Weilbaecher, D. G., Gao, Z. R., and Noon, G. P. (1987). Preliminary Studies on Autologous versus Homologous Endothelial Cell Seeding of Ateriovenous Grafts. In Endothelial Seeding in Vascular Surgery, M. Herring and J. L. Glover, eds. (New York: Grune & Stratton), pp. 155-163.

Fasol, R., Zilla, P., Deutsch, M., Grimm, M., and Fischlein, T. (1989). Human endothelial cell seeding: Evaluation of its effectiveness by platelet parameters after one year. J. Vasc. Surg. *9*, 432-436.

Foxall, C., Watson, S. R., Dowbenko, D., Fennie, C., Lasky, L. A., Kiso, M., Hasegawa, A., Asa, D., and Brandley, B. K. (1992). The three members of the selectin receptor family recognize a common carbohydrate epitope, the sialyl Lewis-x oligosaccharide. J. Cell Biol. *117*, 895-902.

Frazier, O. H., Kadipasaoglu, K. A., Parnis, S. M., and Radovancevic, B. (1994). Biomaterials Used in Cardiac Surgery. In Implantation Biology: The Host Response and Biomedical Devices, R. S. Greco, ed. (Boca Raton: CRC Press), pp. 165-178.

Fuhlbrigge, R. C., Chaplin, D. D., Kiely, J.-M., and Unanue, E. R. (1987). Regulation of Interleukin 1 Gene Expression by Adherence and Lipopolysaccharide. J. Immunol. *138*, 3799-3802.

Furie, M. B., and Randolph, G. J. (1995). Chemokines and Tissue Injury. Am. J. Path. *146*, 1287-1301.

Furth, R. v. (1988). Inflammation: Basic Principles and Clinical Correlates, J. I. Gallin, ed. (New York: Raven Press).

Ghosh, S., and Baltimore, D. (1990). Activation in vitro of NF-kB by phosphorylation of its inhibitor IkB. Nature *344*, 678-682.

Gimond, C., and Aumailley, M. (1992). Cellular Interactions with the Extracellular Matrix Are Coupled to Diverse Transmembrane Signalling Pathways. Exp. Cell Res. *203*, 365-373.

Graham, L. M., and Bergan, J. J. (1982). Expanded Polytetrafluoroethylene Vascular Grafts: Clinical and Experimental Observations. In Biologic and Synthetic Vascular Grafts, J. C. Stanley, ed. (New York: Grune & Stratton), pp. 563-585.

Graham, L. M., Brothers, T. E., Vincent, C. K., Burkel, W. E., and Stanley, J. C. (1991). The role of an endothelial cell lining in limiting distal anastomotic intimal hyperplasia of 4-mm-I.D. Dacron grafts in a canine model. J. Biomed. Mater. Res. *25*, 525-533.

Greisler, H. P., Endean, E. D., Klosak, J. J., Ellinger, J., Henderson, S. C., Pham, S. M., Durham, S. J., Showalter, D. P., Levine, J., and Borovetz, H. S. (1989). Hemodynamic Effects on Endothelial Cell Monolayer Detachment From Vascular Prostheses. Arch. Surg. *124*, 429-433.

Harlan, J. M., and Liu, D. Y. (1992). Adhesion: Its Role in Inflammatory Disease (New York: W. H. Freeman and Co.).

Heemann, U. W., Tullius, S. G., Azuma, H., Kupiec-Weglinsky, J., and Tilney, N. L. (1994). Adhesion Molecules and Transplantation. Ann. of Surgery *219*, 4-12.

Henson, P. M., Webster, R. O., and Henson, J. E. (1981). Neutrophil and monocyte activation and secretion: role of surfaces in inflammatory reactions and *in vitro*. In Cellular Interactions, J. T. Dingle and J. L. Gordon, eds. (New York: Elsevier), pp. 43-56.

Herring, M., Arnold, M., Emerick, S., Ashworth, E., Hoagland, W., and Glover, J. (1987). Suppressing Endothelial Desquamation From Vascular Prostheses. In Endothelial Seeding in Vascular Surgery, M. Herring and J. L. Glover, eds. (New York: Grune & Stratton), pp. 119-138.

Herring, M. B. (1991). Endothelial Cell Seeding. J. Vasc. Surg. *13*, 731-732.

Herring, M. B., Compton, R. S., LeGrand, D. R., Gardner, A. L., Madison, D. L., and Glover, J. L. (1987). Endothelial seeding of polytetrafluoroethylene popliteal bypasses. J. Vasc. Surg. *6*, 114-118.

Herring, M. B., Dilley, R., Gardner, A. L., and Glover, J. (1982). Seeding of Mechanically Derived Endothelium on Arterial Prostheses. In Biologic and Synthetic Vascular Grafts, J. C. Stanley, ed. (New York: Grune & Stratton), pp. 621-629.

Hession, C., Osborn, L., Goff, D., Chi-Rosso, G., Vassallo, C., Pasek, M., Pittack, C., Tizard, R., Goelz, S., McCarthy, K., Hopple, S., and Lobb, R. (1990). Endothelial leukocyte adhesion molecule 1: Direct expression cloning and functional interactions. Proc. Natl. Acad. Sci. USA *87*, 1673-1677.

Hunt, J. A., Meijs, G., and Williams, D. F. (1997). Hydrophilicity of polymers and soft tissue responses: A quantitative analysis. J. Biomed. Mater. Res. *36*, 542-549.

Hussain, S., Glover, J. L., Augelli, N., Bendick, P. J., Maupin, D., and McKain, M. (1989). Host response to autologous endothelial seeding. J. Vasc. Surg. *9*, 656-664.

Hynes, R. O. (1992). Integrins: versatility, modulation and signalling in cell adhesion. Cell *69*, 11-25.

Jarrell, B., Williams, S., Park, P., Carter, T., Carabasi, A., and Rose, D. (1988). Human Endothelial Cell Interactions With Vascular Grafts. In Tissue engineering: Proceedings of a workshop, held at Granlibakken, Lake Tahoe, California, February 26-29, 1988, R. Skalak and C. F. Fox, eds. (New York: Liss), pp. 11-15.

Jarrell, B. E., and Williams, S. K. (1991). Microvessel Derived Endothelial Cell Isolation, Adherence, and Monolayer Formation for Vascular Grafts. J. Vasc. Surg. *13*, 733-734.

Jarrell, B. E., Williams, S. K., Carabasi, R. A., and Hubbard, F. A. (1987). Immediate Vascular Graft Monolayers Using Microvessel Endothelial Cells. In Endothelial Seeding in Vascular Surgery, M. Herring and J. L. Glover, eds. (New York: Grune & Stratton), pp. 37-55.

Jones, P. L., Schmidhauser, C., and Bissell, M. J. (1993). Regulation of Gene Expression and Cell Function by Extracellular Matrix. Crit. Rew. Euk. Gene Exp. *3*, 137-154.

Kaplan, S. (1994). Biomaterial-host interactions: consequences, determined by implant retrieval analysis. Medical Progress through Technology *20*, 209-230.

Kempczinski, R. F., Douville, E. C., Ramalanjaona, G., Ogle, J. D., and Silberstein, E. B. (1987). Endothelial Cell Seeding on a Fibronectin-Coated Substrate. In Endothelial Seeding in Vascular Surgery, M. Herring and J. L. Glover, eds. (New York: Grune & Stratton), pp. 57-77.

Krause, T. J., Robertson, F. M., Liesch, J. B., Wasserman, A. J., and Greco, R. S. (1990). Differential Production of Interleukin 1 on the Surface of Biomaterials. Arch. Surg. *125*, 1158-1160.

Kunkel, S. L., Lukacs, N., and Strieter, R. M. (1995). Expression and biology of neutrophil and endothelial cell-derived chemokines. Cell Biol. *6*, 327-336.

Lafrenie, R. M., and Yamada, K. M. (1996). Integrin-Dependent Signal Transduction. J. Cell. Biochem. *61*, 543-553.

Lasky, L. A. (1992). Selectins: Interpreters of Cell-Specific Carbohydrate Information During Inflammation. Science *258*, 964-969.

Lelievre, S., Weaver, V. M., and Bissell, M. J. (1996). Extracellular Matrix Signalling from the Cellular Membrane Skeleton to the Nuclear Skeleton: A Model of Gene Regulation. Recent Prog. Hormone Res. *51*, 417-432.

Li, J., Menconi, M. J., Wheeler, H. B., Rohrer, M. J., Klassen, V. A., Ansell, J. E., and Appel, M. C. (1992). Precoating expanded polytetrafluoroethylene grafts alters production of endothelial cell-derived thrombomodulators. J. Vasc. Surg. *15*, 1010-1017.

Libby, P., Birinyi, L. K., and Callow, A. D. (1987). Functions of Endothelial Cells Related to Seeding of Vascular Prostheses: The Unanswered Questions. In Endothelial Seeding in Vascular Surgery, M. Herring and J. L. Glover, eds. (New York: Grune & Stratton), pp. 17-35.

Luna, E. J., and Hitt, A. L. (1992). Cytoskeleton-Plasma Membrane Interactions. Science *258*, 955-964.

Lundahl, J., Sköld, C. M., Halldén, G., Hallgren, M., and Eklund, A. (1996). Monocyte and Neutrophil Adhesion to Matrix Proteins is Selectively Enhanced in the Presence of Inflammatory Mediators. Scand. J. Immunol. *44*, 143-149.

Macchia, D., Almerigogna, F., Parronchi, P., Ravina, A., Maggi, E., and Romagnani, S. (1993). Membrane Tumor Necrosis Factor-a is Involved in the Polyclonal B-Cell Activation Induced by HIV-infected T Cells. Nature *363*, 464-466.

Macey, M. G., McCarthy, D. A., Vordermeier, S., Newland, A. C., and Brown, K. A. (1995). Effects of cell purification methods on CD11b and L-selectin expression as well as the adherence and activation of leukocytes. J. Immunological Meth. *181*, 211-219.

Maniotis, A. J., Chen, C. S., and Ingber, D. E. (1997). Demonstration of mechanical connections between integrins, cytoskeletal filaments, and nucleoplasm that stabilize nuclear structure. Proc. Natl. Acad. Sci. USA *94*, 849-854.

Margiotta, M. S., Robertson, F. S., and Greco, R. S. (1992). The Adherence of Endothelial Cells to Dacron Induces the Expression of the Intercellular Adhesion Molecule (ICAM-1). Ann. Surgery *216*, 600-604.

Matsuda, T., Kitamura, T., Iwata, H., Takano, H., and Akutsu, T. (1988). A Hybrid Artificial Vascular Graft Based upon an Organ Reconstruction Model. Trans. Am. Soc. Artif. Intern. Organs *34*, 640-643.

Mazzucotelli, J.-P., Klein-Soyer, C., Beretz, A., Brisson, C., Archipoff, G., and Cazenave, J.-P. (1991). Endothelial cell seeding: coating Dacron and expanded polytetrafluoroethylene vascular grafts with a biological glue allows adhesion and growth of human saphenous vein endothelial cells. International J. of Artif. Organs *14*, 482-490.

Menconi, M. J., Owen, T., Dasse, K. A., Stein, G., and Lian, J. B. (1992). Molecular Approaches to the Characterization of Cell and Blood/Biomaterial Interactions. J. Cardiac Surg. *7*, 177-187.

Miller, K. M., and Anderson, J. M. (1988). Human monocyte/macrophage activation and interleukin 1 generation by biomedical polymers. J. Biomedical Materials Research *22*, 713-731.

Miller, K. M., and Anderson, J. M. (1989). *In vitro* stimulation of fibroblast activity by factors generated from human monocytes activated by biomedical polymers. J. Biomed. Mater. Res. *23*, 911-930.

Miller, K. M., Rose-Caprara, V., and Anderson, J. M. (1989). Generation of IL1-like activity in response to biomedical polymer implants: A comparison of in vitro and in vivo models. J. Biomedical Materials Research *23*, 1007-1026.

Montgomery, K. F., Osborn, L., Hession, C., Tizard, R., Goff, D., Vassallo, C., Tarr, P. I., Bomsztyk, K., Lobb, R., Harlan, J. M., and Pohlman, T. H. (1991). Activation of endothelial-leukocyte adhesion molecule 1 (ELAM-1) gene transcription. Proc. Natl. Acad. Sci. USA *88*, 6523-6527.

Nathan, C. F. (1987). Secretory Products of Macrophages. J. Clinical Investigation *79*, 319-326.

Nerem, R. M. (1988). Endothelial Cell Responses to Shear Stress: Implications in the Development of Endothelialized Synthetic Vascular Grafts. In Tissue engineering: Proceedings of a workshop, held at Granlibakken, Lake Tahoe, Califonia, February 26-29, 1988, R. Skalak and C. F. Fox, eds. (New York: Liss), pp. 5-10.

Oppenheim, J. J., Kovacs, E. J., Matsushima, K., and Durum, S. K. (1986). There is more than one interleukin 1. Immunology Today *7*, 45-56.

Owen, C. A., Campbell, E. J., and Stockley, R. A. (1992). Monocyte adherence to fibronectin: role of CD11b/CD18 integrins and relationship to other monocyte functions. J. Leukocyte Biol. *51*, 400-408.

Perez, C., Albert, I., DeFay, K., Zachariades, N., Gooding, L., and Kriegler, M. (1990). A nonsecretable cell surface mutant of tumor necrosis factor (TNF) kills by cell-to-cell contact. Cell *63*, 251-258.

Petillo, O., Peluso, G., Ambrosio, L., Nicolais, L., Kao, W. J., and Anderson, J. M. (1994). *In vivo* induction of macrophage Ia antigen (MHC class II) expression by biomedical polymers in the cage implant system. J. Biomed. Mater. Res. *28*, 635-646.

Pober, J. S., and Cotran, R. S. (1990). Cytokines and Endothelial Cell Biology. Physiological Reviews *70*, 427-451.

Pober, J. S., and Cotran, R. S. (1991). What Can Be Learned From the Expression of Endothelial Adhesion Molecules in Tissues? Lab. Invest. *64*, 301-305.

Polley, M. J., Phillips, M. L., Wayner, E., Nudelman, E., Singhal, A. K., Hakomori, S.-I., and Paulson, J. C. (1991). CD62 and endothelial cell-leukocyte adhesion molecule 1 (ELAM-1) recognize the same carbohydrate ligand, sialyl-Lewis x. Proc. Natl. Acad. Sci. USA *88*, 6224-6228.

Pujol-Borrell, R., Todd, I., Doshi, M., Bottazzo, G. F., Sutton, R., Gray, D., Adolf, G. R., and Feldmann, M. (1987). HLA class II induction in human islet cells by interferon-gamma plus tumor necrosis factor of lymphotoxin. Nature *326*, 304-306.

Reichle, F. A. (1982). Function and Biologic Fate of Woven Dacron Grafts Compared to Other Materials in Femoropopliteal Arterial Bypass Procedures. In Biologic and Synthetic Vascular Prostheses, J. C. Stanley, ed. (New York: Grune & Stratton), pp. 495-508.

Rhodes, N. P., Hunt, J. A., and Williams, D. F. (1997). Macrophage subpopulation differentiation by stimulation with biomaterials. J. Biomed. Mater. Res. *37*, 481-488.

Rosales, C., and Juliano, R. L. (1995). Signal transduction by cell adhesion receptors in leukocytes. J. Leukocyte Biol. *57*, 189-198.

Sastry, S. K., and Horwitz, A. F. (1993). Integrin cytoplasmic domains: mediators of cytoskeletal linkages and extra- and intercellular initiated transmembrane signaling. Current Opinion in Cell Biology *5*, 819-831.

Sauvage, L. R., Walker, M. W., Berger, K., Robel, S. B., Lischko, M. M., Yates, S. G., and Logan, G. A. (1979). Current arterial prostheses: Experimental evaluation by implantation in the carotid and circumflex coronary arteries of the dog. Arch. Surg. *114*, 687-691.

Schleimer, R. P., Sterbinsky, S. A., Kaiser, J., Bickel, C. A., Klunk, D. A., Tomioka, K., Newman, W., Luscinskas, F. W., Michael A. Gimbrone, J., McIntyre, B. W., and Bochner, B. S. (1992). IL-4 Induces Adherence of Human Eosinophils and Basophils but not Neutrophils to Endothelium. J. Immunol. *148*, 1086-1092.

Schneider, A., Chandra, M., Lazarovici, G., Vlodavsky, I., Merin, G., Uretzky, G., Borman, J. B., and Schwalb, H. (1997). Naturally produced extracellular matrix is an excellent substrate for canine endothelial cell proliferation and resistance to shear stress on PTFE vascular grafts. Thromb. Haemost. *78*, 1392-1398.

Schneider, A., Melmed, R. N., Schwalb, H., Karck, M., Vlodavsky, I., and Uretzky, G. (1992). An improved method for endothelial cell seeding on polytetrafluoroethylene small caliber vascular grafts. J. Vasc. Surg. *15*, 649-656.

Shankar, R., and Greisler, H. P. (1994). Inflammation and Biomaterials. In Implantation Biology: The Host Response and Biomedical Devices, R. S. Greco, ed. (Boca Raton: CRC Press), pp. 67-80.

Singhvi, R., Kumar, A., Lopez, G. P., Stephanopoulos, G. N., Wang, D. I. C., Whitesides, G. M., and Ingber, D. E. (1994). Engineering Cell Shape and Function. Science *264*, 696-698.

Smyth, S. S., Joneckis, C. C., and Parise, L. V. (1993). Regulation of Vascular Integrins. Blood *81*, 2827-2843.

Snyder, R. W., and Botzko, K. M. (1982). Woven, Knitted, and Externally Supported Dacron Vascular Grafts. In Biologic and Synthetic Vascular Prostheses, J. C. Stanley, ed. (New Yord: Grune & Stratton), pp. 485-494.

Swartbol, P., Truedsson, L., Parsson, H., and Norgren, L. (1996). Surface adhesion molecule expression on human blood cells induced by vascular graft materials *in vitro*. J. Biomed. Mater. Res. *32*, 669-676.

Watson, P. A. (1991). Function follows form: generation of intracellular signals by cell deformation. FASEB *5*, 2013-2019.

Webb, D. S. A., Shimizu, Y., Seventer, G. A. V., Shaw, S., and Gerrard, T. L. (1990). LFA-3, CD44, and CD45: Physiologic Triggers of Human Monocyte TNF and IL-1 Release. Science *249*, 1295-1297.

Weller, P. F., Rand, T. H., Goelz, S. E., Chi-Rosso, G., and Lobb, R. R. (1991). Human eosinophil adherence to vasculr endothelium mediated by binding to vascular cell adhesion molecule 1 and endothelial leukocyte adhesion molecule 1. Proc. Natl. Acad. Sci. USA *88*, 7430-7433.

Williams, S. K., Carter, T., Park, P. K., Rose, D. G., Schneider, T., and Jarrell, B. E. (1992). Formation of a multilayer cellular lining on a polyurethane vascular graft following endothelial cell sodding. J. Biomed. Mater. Res. *26*, 103-117.

Williams, S. K., and Jarrell, B. E. (1996). Tissue-engineered vascular grafts. Nature Medicine *2*, 32-34.

Williams, S. K., Jarrell, B. E., and Kleinert, L. B. (1994). Endothelial cell transplantation onto polymeric ateriovenous grafts evaluated using a canine model. J. Invest. Surg. *7*, 503-517.

Williams, S. K., Jarrell, B. E., Rose, D. G., Pontell, J., Kapelan, B. A., Park, P. K., and Carter, T. L. (1989). Human Microvessel Endothelial Cell Isolation and Vascular Graft Sodding in the Operating Room. Ann. Vasc. Surg. *3*, 146-152.

Williams, S. K., Rose, D. G., and Jarrell, B. E. (1994). Microvascular endothelial cell sodding of ePTFE vascular grafts: Improved patency and stability of the cellular lining. J. Biomed. Mater. Res. *28*, 203-212.

Williams, S. K., Schneider, T., Kapelan, B., and Jarrell, B. E. (1991). Formation of a Functional Endothelium on Vascular Grafts. J. Electron Microscopy Tech. *19*, 439-451.

Yue, T.-L., Wang, X., Sung, C.-P., Olson, B., McKenna, P. J., Gu, J.-L., and Feuerstein, G. Z. (1994). Interleukin-8: A Mitogen and Chemoattractant for Vascular Smooth Muscle Cells. Circulation Res. *75*, 1-7.

Yun, J. K., DeFife, D., Colton, E., Stack, S., Azeez, A., Cahalan, L., Verhoeven, M., Cahalan, P., and Anderson, J. M. (1995). Human monocyte/macrophage adhesion and cytokine production on surface-modified poly(tetrafluoroethylene/hexafluoropropylene) polymers with and without protein adsorption. J. Biomed. Mater. Res. *29*, 257-268.

Zhao, Q. H., Anderson, J. M., Hiltner, A., Lodoen, G. A., and Payet, C. R. (1992). Theoretical analysis on cell size distribution and kinetics of foreign-body giant cell formation *in vivo* on polyurethane elastomers. J. Biomed. Mater. Res. *26*, 1019-1038.

Ziats, N. P., Miller, K. M., and Anderson, J. M. (1988). In vitro and in vivo interaction of cells with biomaterials. Biomaterials *9*, 5-13.

Chapter 3

Materials and Methods

3.1 Materials

A variety of materials are used in the studies described in the following chapters. Materials were chosen for either interesting surface chemistries (plasma-deposited films) or for interesting surface topographies (expanded poly(tetrafluoroethylene)). These two material characteristics, surface chemistry or topography, were investigated to determine their influence on subsequent protein or cell interactions with the material surfaces, and creates the basis for this thesis.

The acetone plasmas have been shown to support cell growth to a degree similar to tissue culture polystyrene (TCPS) (Ertel et al., 1991; Ertel et al., 1990). These plasma films were used to compare endothelial cell function on polymers possessing similar cell growth characteristics, with the same surface morphology. These acetone plasma films were shown to possess dissimilar FN adsorption characteristics (see Chapter 5). The TFE plasma film is similar to a fluoropolymer surface, and has distinctly different protein adsorption characteristics to the acetone plasmas.

The PTFE and ePTFE materials were used as a series of polymers that vary only in surface microtexture, but not surface chemistry (see ESCA results in Chapter 4.2). All materials were analyzed by ESCA and were found to have identical surface chemistry. The samples vary in surface texture by increasing fibril length of the expanded regions ranging from unexpanded (PTFE sheeting) to 100μ.

A polyurethane, Biospan®, was included in some but not all experiments. Polyurethanes are of interest for vascular prostheses due to their compliance and ease of processing.

The mixed esters of cellulose (MEC) are commercially available filter membranes. The 5μ and 8μ pore MEC membranes have been reported to exhibit a modified healing response in an animal model (Brauker et al., 1995). In this *in vivo* model, implanted 0.22μ MEC membranes demonstrated the standard foreign body response, whereas the 5μ showed better integration and formation of capillaries in close apposition to the surface. Here we wanted to investigate the response of cells *in vitro* to these materials to understand the potential cell signaling events that differ between the two porous surfaces and which lead to a marked difference in the *in vivo* response to these materials. The three porosities used were of identical surface composition, only differing in surface topography.

The control surfaces used were commercially available tissue culture-treated poly(ethylene terephthalate) (Thermanox®) and tissue culture treated polystyrene (TCPS, Falcon). The Thermanox® control surface was used for the fibronectin adsorption experiments outlined in Chapter 5. TCPS was used as a control for essentially all other experiments.

3.1.1 Polymer Sample Preparation

The plasma-deposited films listed in Table 3.1 were produced in our laboratories by Winston Ciridon. Plasma-deposited films were prepared by radio-frequency (RF)-plasma treatment on Lux Thermanox® PET 15 mm round coverslips. These films and the plasma-deposition apparatus have been previously described (Ertel et al., 1991; Ertel et al., 1990). All samples were etched with an argon plasma prior to plasma gas deposition. Thermanox® argon-etched (AE) and non-etched samples were included as controls. Plasma-treated samples were removed from the reactor in a sterile manner and stored sealed in a clean hood. The plasma process sterilizes the samples, possibly by the ultra-violet radiation produced from the plasma gas.

Table 3.1: Plasma Treatments

Composition of Plasma Feed	Treatment Conditions *
Thermanox®	No plasma treatment
Argon-Etched Thermanox®	AE, open/40/5
Methanol (100%)	AE, 250/30/20; Flow = 1 sccm
Acetone (100%)	AE, 250/30/20; Flow = 2 sccm
Acetone (90%)-N_2 (10%)	AE, open/50/20; Flow = 2 sccm
Acetone (80%)-N_2 (20%)	AE, open/50/20; Flow = 2 sccm
Acetone (70%)-N_2 (30%)	AE, open/50/20; Flow = 2 sccm
Acetone (60%)-N_2 (40%)	AE, open/50/20; Flow = 2 sccm
Allylamine (100%)	AE, 250/30/10; Flow = 44.3 sccm
Acetone (80%)-O_2 (20%)	AE, open/5/10; Flow = 1 sccm
Acetone (60%)-O_2 (40%)	AE, open/5/10; Flow = 1 sccm
Acrylic Acid (100%)	AE, 250/30/10; Flow, 1 sccm

*Samples were argon-etched (AE) prior to deposition where indicated. Plasma conditions are reported as pressure (millitorr)/power level (watts)/ time (minutes). Gas flow is reported as standard cubic cm/min. (sccm) at standard temperature and pressure.

Poly(tetrafluoroethylene) (PTFE) sheeting was purchased from Berghof/America, Concord, CA. Expanded PTFE (ePTFE) materials used varied in fibril length of the porous regions between solid nodes in the material. Fibril lengths used were 10μ, 30μ, 60μ and 100μ. These materials were provided by W.L. Gore and Associates, Flagstaff, AZ. The PTFE and ePTFE used required no special preparation; the materials were used as formed by the manufacturer. Materials were cut (if necessary) using a solvent-washed punch or scalpel blade. PTFE and ePTFE materials were cleaned by sonication with 3 changes of 100% ethanol. The materials were dried in a laminar flow hood and considered sterile. Polymers were dried and fitted into 12-well plates with baked Pyrex® (Corning) washers to weigh-down the samples.

Biospan® polyurethane was obtained from Polymer Technology Group, Berkeley, CA. Biospan® was precipitated 2 times and then spin-cast twice on polystyrene dishes as a 4% solution in n-pyrollidone. The Biospan®-coated polystyrene dishes were covered and sealed after drying in a laminar flow hood, and considered sterile.

Mixed esters of cellulose (MEC) membranes in three different porosities were purchased from Millipore, Bedford, MA. The porosities used were: 0.22μ (GSWP 02400), 5μ (SMWP 02400), and 8μ MEC (SCWP 02500). The mixed esters of cellulose (MEC) membranes were cut to appropriate sizes using a solvent washed punch and scalpel. The membranes were soaked in 95% ethanol for approximately 1 hour. They were then immersed in 70% ethanol for approximately 1 hour for sterilization. The membranes were then washed with 3-4 changes of USP sterile water, waiting at least 30 minutes between changes. Finally, the membranes were soaked in sterile PBS for at least one hour prior to use, changing the buffer once.

Nylon 6 (polyamide) film was purchased from Goodfellow, Cambridge, England, as 0.25mm thick sheets. Twenty millimeter discs were cut with a punch and cleaned using the following procedure: 1) soak in 0.1M NaOH (diluted in endotoxin-free water) for one hour, 2) sonicate in 100% ethanol for 20 minutes, 3) sonicate in 70% ethanol for 20 minutes, and 4) soak in sterile, endotoxin-free water prior to use.

A tissue-culture treated poly(ethylene terephthalate) (PET) under the trade name of Thermanox® was purchased as 15mm discs from Nunc. Thermanox® disks were purchased in the sizes needed (15 mm) from the manufacturer. Samples were sterilized by soaking in 70% ethanol for at least 15 minutes, and then dried in a laminar flow hood.

Tissue culture polystyrene (TCPS), a material commonly used for cell culture, was purchased from Falcon. A variety of dish sizes and welled-plate configurations were used in these studies. All TCPS plates used were provided sterile by the manufacturer, and were used without further cleaning or processing.

Many of the materials needed to be weighed down to secure them to the bottom of tissue culture wells. Approximately 1.5 cm sections were cut from thick-walled Pyrex® glass tubes (22 mm OD, 18 mm ID, Corning), and polished by Bob Morley in the Physics Glass Shop. Special care was given to cleaning these rings to remove any endotoxin contamination. Rings were first cleaned with detergent, rinsed thoroughly with distilled deionized H_20 (ddH_20), and then soaked in 0.1M NaOH for 1 hour. The rings were rinsed thoroughly with ddH_2O, with the last wash done with endotoxin-free water. The rings were then sonicated in 100% ethanol, and rinsed again with endotoxin-free water. The rings were autoclaved and then baked overnight at 180°C.

3.2 Surface Analysis

3.2.1 Electron Spectroscopy for Chemical Analysis (ESCA)

Material samples were analyzed on a Surface Science Instruments (SSI) X-Probe ESCA instrument. This instrument contains an aluminum $K_\alpha 1,2$ monochromatized X-ray source for the generation of photoelectrons from a sample surface. The SSI data analysis software was used to determine the elemental composition and to perform peak fitting in the high resolution spectra. The samples were analyzed at a take-angle of 55° with respect to the surface. This angle allows for analysis of the outermost 100 Å of the sample. High resolution C1s spectra were collected and analyzed for each sample.

3.2.2 Scanning Electron Microscopy (SEM)

All of the PTFE, Berghof ePTFE membranes, Gore ePTFE, and MEC materials, were analyzed using SEM. The surfaces were cleaned, mounted on SEM studs using a non-aqueous conducting cement, and sputter coated using a Au/Pd source. The materials were then analyzed using a JEOL SEM at 15 eV. By placing a small amount of the

conducting cement in contact with the surface of the material down to the stud (before sputtering), surface charging was eliminated. Images were captured on Polaroid film.

The PTFE surface was non porous, but had definite surface striations, which can also be seen by close examination by eye. These striations were probably formed during processing of the PTFE sheeting.

The Berghof ePTFE membranes did not have the characteristic fibril/node structure expected of an ePTFE. The surface had an irregular, pitted, globlular surface which varied with the manufacturer's "pore size". These ePTFE membranes have an unusual surface topography and were not considered useful for studying cell interactions due to the high irregularity of their surfaces.

The Gore ePTFE materials had the characteristic fibril/node structure, and agreed well with the manufacturer's reported fibril lengths. There exists a range of fibril lengths in these materials, with the reported fibril length as an average. The actual deviation from the reported fibril length was typically +/- 5μ. The surface topography of these materials was highly regular with nodes separating the fibrous, stretched portions of the material.

The MEC membranes had a finely textured porous surface. The pore appeared to be small and spherical in nature, not fibrous like the ePTFE materials.

3.2.3 Atomic Force Microscopy (AFM)

Analyses were performed by Stefan Domino, University of Washington. The surface roughness of the radio-frequency plasma-deposited films was determined using AFM. A Nanoscope II AFM (Digital Instruments, Santa Barbara, CA) was used with a 10,000 nm^2 scan size for each material. Roughness is expressed as the variation in the Z-direction in nm, and the standard deviation as the error. The results are found in Chapter 4.1.

3.2.4 Time-of-flight Secondary Ion Mass Spectroscopy (TOF-SIMS)

Analyses were performed by Dr. Anna Belu, University of Washington, on a Model 7200 Physical Electronics PHI instrument. Secondary ions were generated using a Cs+ source and captured in the time-of-flight analyzer. This analysis was performed on only one sample, the 30μ ePTFE. See Chapter 4.2 for experimental rationale and a discussion of the data obtained.

3.3 Fibronectin Adsorption

3.3.1 Fibronectin Adsorption for Cell Culture Experiments

Human fibronectin (FN, Chemicon, Temecula, CA) adsorption was performed on cell culture surfaces or materials where noted. FN was diluted to 20 μg/mL in phosphate buffered saline (PBS) and allowed to adsorbed to surfaces for 1.5-2 hours at 37°C. One mL was added to non-porous materials secured in 12-well plates, 1.5 mL for porous materials. These FN-coated materials were rinsed once with PBS to remove any unbound FN prior to seeding with cells.

3.3.2 Fibronectin Adsorption for Experiments in Chapter 5

For this set of experiments it was necessary to radio-label FN. The Bolton-Hunter method for radioiodination was used. ^{125}I-Bolton-Hunter reagent in dry benzene was purchased from Amersham France SA (Les Ulis, France) with a specific activity of 5 mCi. Human FN (Chemicon) was dissolved at a high concentration (1-5 mg/mL) in 0.1 M borate buffer (pH 8.5) and stored on ice before using. Two hundred microliters of the ^{125}I-Bolton Hunter reagent was added to a small glass test tube (0.75 cm x 4 cm). The benzene was evaporated by gently blowing a stream of nitrogen gas over the liquid. The concentrated FN solution (20-30 μL, 100-200 μg) was added to the bottom of the tube, mixed well, and put on ice. The reaction was allowed to continue at 4°C for 15 minutes

with frequent agitation, and was stopped by adding 100 μL of 0.1M borate/0.2 M glycine buffer (pH 8.5). The FN solution was then placed in a Sephadex G-25 column (Pharmacia, Piscataway, NJ) previously equilibrated with ice cold 0.05 M sodium phosphate buffer (pH 7.5). The protein was eluted with cold phosphate buffer, 0.5 mL per fraction; 40 fractions were collected. Five microliter samples of each fraction were counted on a gamma counter to determine the peak fractions. Typically, two fractions were pooled and placed on a second pre-equilibrated column for further purification, collecting and counting the fractions as before. The peak fractions were pooled, aliquoted and stored at -20°C. This ^{125}I-labeled FN was used within 2 weeks.

FN adsorption isotherms were generated using the following procedure. The adsorption buffer used for these experiments was composed of 0.01 M sodium citrate, 0.01 M dibasic sodium phosphate, 0.11 M sodium chloride, 0.01 M sodium iodide, 0.02% sodium azide (final pH adjusted to 7.4). This buffer was used due to the inhibitory effects of citrate on protease activity and passivation of iodide-specific binding sites by free ("cold") iodide (Lopez et al., 1993). All polymer samples were cut in half, placed in tubes, and were incubated overnight in adsorption buffer at 4°C. Samples were equilibrated to room temperature prior to adsorption. No evidence of delamination of the films was seen.

All dilutions and washes were done with adsorption buffer. A stock solution of 100 μg/mL FN spiked with 2-5 x 10^6 cpm/mg of ^{125}I-labeled FN was prepared immediately prior to adsorption. All other FN dilutions were made from this spiked FN solution; stock solutions were prepared at twice the desired final concentration. The final concentrations used were 5, 10, 20, or 50 μg/mL. Prior to the addition of the FN solutions, 0.5 mL of fresh, degassed buffer was added to the presoaked polymer samples. An equal volume of the desired spiked FN solution (0.5 mL) was added to each polymer sample, resulting in a twofold dilution. Adsorptions were performed as duplicates for

each FN concentration due to the limited number of polymer samples. Static adsorption was allowed to proceed for 2 hours at 37°C. The samples were then displacement washed with 80-100 mL of buffer and transferred to new tubes containing 1 mL of buffer for gamma counting. To determine the cpm/μg FN in each dilution used, 50 μL samples of each stock FN solution were counted. Results and discussion of these FN adsorption experiments are found in Chapter 5.

3.4 Isolation and Culture of Human Cells

Because endothelial cells and monocyte-derived macrophages are very sensitive to endotoxin contamination, every effort was made to eliminate all sources of endotoxin from the tissue-culture reagents. When ordering cell culture media and serum, lots containing the lowest levels of endotoxin were requested. Most cell culture material and reagent product numbers are found in Appendix A.

3.4.1 Human Umbilical Vein Endothelial Cells (HUVECs)

HUVECs are isolated by collagenase treatment of post-natal human umbilical veins and cultured for at least 2 passages before use. Tissue culture surfaces or material samples must be coated with 2% gelatin (G-1393, Sigma, St. Louis, MO) or preadsorbed with FN to facilitate cell attachment to the polymer substrates. HUVECs were maintained in 0.22μ-filtered culture medium containing the materials in the table below. The recipe, outlined in Table 3.2, is for a total volume of 100 mL, using RPMI 1640 medium to dilute the other components to 100 mL.

Table 3.2: HUVEC Culture Medium

Reagent	Quantity	Final Concentration
RPMI 1640 with glutamine	74.5 mL	Dilute other ingredients to 100 mL with RPMI
Adult Bovine Serum (ABS)	20 mL	20% v/v
Nonessential Amino Acids	1 mL	1% v/v
Sodium Pyruvate	1 mL (1 mM)	1% v/v
Penicillin/Streptomycin	1 mL (50 units/mL/50 μg/mL)	1% v/v
Heparin	100 μL of a 90 mg/mL stock solution	90 mg/liter
Endothelial Cell Growth Supplement (ECGS)	2.5 mL of a 1 mg/mL stock solution	25 μg/mL

Cells were removed from culture surfaces by washing twice with PBS and then EDTA/trypsin treatment (0.05% trypsin/ 0.53 mM EDTA). Inactivation of the trypsin was done by adding serum-containing medium and centrifugation of cells before plating. Cells were typically split 1:3 or 1:4 3-5 days prior to their use. Cells were fed once in this time period by removing all of the culture medium and replacing it with fresh medium. HUVECs were never used after passage 5.

Lipopolysaccharide (LPS)-stimulated HUVECs were treated with 100 ng/mL of either *Escherichia coli* or *Salmonella typhimurium* LPS (Sigma). Some cells were stimulated with 100-200 pg/mL human interleukin-1ß (IL-1ß, R&D Systems, Minneapolis, MN) where noted.

3.4.2 Human Blood Monocytes

Blood was drawn asepticly into 10 or 15 mL heparinized Vacutainer® tubes by members of the Laboratory Medicine department at the University of Washington Medical Center. To collect serum only, 4-5 10 mL "red top" (without anticoaguiant) 15 mL Vacutainer® tubes were drawn. Typical volumes of whole blood obtained were 150-200 mL. All University of Washington guidelines were followed for the recruitment of human subjects, as well as the proper handling and disposal of human blood. The donors were asked not to take any anti-inflammatory drugs 24 hours prior to the blood draw.

The blood was diluted approximately 2-fold with phosphate buffered saline (PBS), pH 7.4, containing 60 units of heparin/mL and 1 mM EDTA to avoid coagulation and loss of monocytes due to adhesion during the separation process. All cell counts were done using Turk's and trypan blue stains.

Tubes drawn for serum recovery were allowed to clot at room temperature and then refrigerated for at least 1 hour to cause the clots to contract. The serum was removed by pipetting into centrifuge tubes and centrifuged at 2000 rpm for 10 minutes. The serum was collected, filtered, and stored refrigerated. This adult human serum (AHS) was used as a media supplement in some experiments where noted.

3.4.2.1 Monocyte Isolation Using Percoll® Density Gradients

Diluted blood (see above) was centrifuged in 50 mL polystyrene tubes using a refrigerated, swinging-bucket centrifuge at 2000 rpm for 15 minutes, 20°C, and no brake. This produced a white blood cell-rich layer, or "buffy coat", which was collected with a pipette. These cells were diluted with the above PBS solution to an approximate volume of 200 mL.

An isotonic stock solution was previously made, 9 parts Percoll® (Pharmacia), density 1.130 g/mL, 1 part 1.5 M NaCl, with a final density 1.124 g/mL (Pertoft et al.,

1980). All Percoll® gradients were made from this stock solution by diluting with PBS. A solution of density 1.075 g/mL (a 60% dilution of the stock solution) was used for the first separation step, placing 12-15 mL per 50 mL polystyrene conical tube (Pertoft et al., 1980). Approximately 35 mL of diluted, buffy-coated blood was carefully layered over the Percoll®, avoiding mixing at the interface. The tubes were centrifuged at 800 x g (2500 rpm) for 30 minutes at 20°C with no brake. A band of cells was resolved and collected at the serum-Percoll® interface. This band was composed of mostly monocytes and lymphocytes.

After 2 washes with PBS containing 1 mM EDTA, the separation procedure was repeated once more using a 1.064 g/mL gradient (a 50% dilution of the isotonic stock solution) (Pertoft et al., 1980). Approximately 7 mL of cell suspension were layered over 5 mL of the diluted Percoll® and centrifuged at 800 x g (2500 rpm) for 60 minutes at 4°C. The monocytes were found in the low density fraction at the PBS-Percoll® interface. Efforts were made to keep the cells near 4°C during all subsequent steps to avoid forming cell aggregates and to discourage monocyte adherence to the polystyrene tubes.

The cells were washed 3 times, counted, and plated onto the samples at a density of 2×10^5 cells/well in a volume of 220 μL. The culture medium, RPMI with glutamine, containing 10% fetal calf serum (JRH), 1% MEM nonessential amino acids, 1% sodium pyruvate, and 1% penicillin/streptomycin/Fungizone® antibiotic/antifungal solution (Gibco/BRL), was sterile filtered (0.22 micron, Corning) before use. The RPMI and fetal calf serum were specifically requested from the manufacturers to be of the lowest endotoxin levels available. Some cells were stimulated with lipopolysaccharide (LPS) at 50 ng/well, strain *Salmonella typhimurium* (Sigma). A sample of cells was seeded into a flask to monitor monocyte differentiation to macrophages, the degree of lymphocyte contamination, and the general health of the isolated cells over several weeks. All plates were incubated at 37°C, 5% CO_2 in air, in a humidified chamber. The plates were also

enclosed in a plastic box with a loose-fitting lid containing a small amount of water to decrease evaporation from the plates and minimize the chance of contamination. The loose-fitting lid insured adequate gas exchange.

On days 3, 7, 14, 21, 28, and 35 days, 125 μL was removed from each well, placed in labeled Eppendorf tubes, and stored at -20°C until assayed for IL-1ß. Pipette tips were changed between each well to avoid "carry-over" effects of neighboring wells. The volume removed was replaced with fresh culture medium. To the TCPS + LPS wells, one half of the original amount of LPS (25 ng/well) was added after the fresh medium was introduced.

3.4.2.2 Macrophage Isolation by Adherence to Tissue Culture Plastic

The protocol outline in this section was used only for experiments in Chapter 8. A method of macrophage isolation by adherence to tissue culture plastic was developed by Laura Martinson, Department of Bioengineering, University of Washington. Using this procedure, approximately 10-15 million monocytes can be isolated from 100-150 mL whole blood.

Room temperature Histopaque 1077 (Ficoll-Hypaque, 1.077 mg/L, Sigma # H8889) solution was placed into 50 mL centrifuge tubes. 30-35 mL diluted whole blood (see 3.4.2 above) was loaded on top of the Histopaque solution, avoiding mixing at the interface. The tubes were centrifuged at 1600 rpm, no brake, room temperature for 20 minutes. This enriches for peripheral blood mononuclear cells (PBMC's), and removes red blood cells and granulocytes. PBMC's migrate to the Histopaque/plasma interface where they are collected using a pipette.

All the following steps are done @ 4° C, using chilled buffer solutions. The cells from the interface were transferred into new 50 mL tubes, placing approximately 20-30 mL of cell suspension in each tube and diluted with PBS containing 1mM EDTA

(PBS/EDTA). The PBMC population is then washed extensively to remove platelets. The cells were centrifuged at 4°C, 1000 rpm, for 10 minutes. The cells were resuspended and the wash was repeated twice more to remove more of the platelets. The pellets were resuspended in approximately 6 mL PBS/EDTA and layered over 6 mL cold heat-inactivated fetal bovine serum in 15 mL tubes (3 mL of cells per tube), avoiding any mixing at the interface. The cells were centrifuged at 800-900 rpm for 10 minutes, at 4°C with no brake. This was repeated once more. The cells were then resuspended in approximately 5 mL of serum-free RPMI containing 1% nonessential amino acids, 1% sodium pyruvate, and 1% penicillin/streptomycin (referred to as "RPMI complete"). The cells were then counted using Turk's and trypan blue stains.

After the number of cells was determined, the cells were diluted to 3-6 x 10^6 cells/mL in RPMI complete + 20% FBS, and 10 mL of cells suspension added to a T75 flask. The cells were incubated for 1-1.5 hours 37° C, 5% CO_2. After incubation, non adherent cell were mixed well, washing the bottom surface of the flask well, and transferred to a new T75 flask and incubated as before. The adherent cells in the original flasks were washed twice using the serum-free RPMI complete medium, discarding the washes. To these flasks, 10 mL RPMI complete + 5-10% FBS was place in each flask and placed in the incubator. After the 1 hour incubation, the second set of flasks was washed and medium added as to the first set of flasks. The remaining non adherent population from the second set was discarded.

After incubation overnight in 5-10% serum-containing medium, many of the previously adherent cells had released from the flasks. These flasks were placed on ice for approximately 10 minutes to encourage more cells to release. The cells were collected into 50 mL centrifuge tubes and the flasks washed extensively using serum-free RPMI complete. It can be anticipated that 60-80% of the cells will release from the flasks. The cells were then centrifuged at 1000 rpm for 10 minutes to pellet cells. They were then

resuspended in RPMI complete + 15% autologous human serum (AHS). The cells were counted with trypan blue, and diluted to the desired cell concentration. The cells were seeded onto materials at 2 x 10^5 cells/well in a 12 well plate, and allowed to adhere in the AHS medium for at least 2 hours. The medium is carefully removed to avoid removing significant numbers of cells, and RPMI complete + 10% FBS. All further manipulations of the cells are done using the 10% FBS medium.

LPS-stimulated monocyte/macrophages were treated with 10-20 μg/mL of *Escherichia coli* LPS (Sigma, L-4391) at designated time points.

3.4.2.3 Isolation of Monocyte-Derived Macrophages by Direct Adherence To Materials

A monocyte-rich fraction was obtained using the identical protocol outline in 3.4.2.2 above through the Histopaque fractionation and layering over fetal bovine serum to remove platelets. At the point of resuspending the cells in culture medium, RPMI complete medium containing 15% autologous human serum was used to resuspend the cells to a density of approximately 2 x 10^6 cells/mL. This cell suspension was added directly to wells containing the materials to be tested and allowed to incubate in at 37° C in a 5% CO_2 humidified incubator to promote adhesion of the monocytes to the materials. After 2 hours the wells were washed one to two times using serum-free medium, gently agitating the wells to remove any non-adherent cells. RPMI complete medium containing 15% AHS was added to each well. Some wells were stimulated with 5-10 ug/mL LPS as in section 3.4.2.2. Cell supernatants were removed after 1, 3, and 7 days. The supernatants were centrifuged at 12000 rpm for 5 minutes to remove cells and cell debris. The supernatants were aliquoted into sterile tubes and frozen at -70°C. The cell pellet and the empty wells were retained for cell number determination using the LDH assay (see section 3.9).

3.5 Cell Surface Staining of Endothelial Cells for E-selectin

Reagents

Primary antibody: Mouse-anti-human E-selectin monoclonal antibody H18/7; Becton Dickinson, San Jose, CA

Secondary Antibody: FITC-labeled goat-anti-mouse IgG (heavy and light chains), Zymed, South San Francisco, CA

Wash Buffer: 0.4% Bovine Serum Albumin (BSA, Sigma, St. Louis, MO) in Dulbecco's phosphate buffered saline (PBS, Sigma). The BSA solution was 0.22μ filtered, adding 0.2% sodium azide to discourage bacterial and fungal growth, and stored at 4°C. 5% goat serum (Zymed) was added on the day of the experiment as an additional non-specific binding blocking agent.

Procedure

- Materials were placed in the wells of a 96-well plate. The materials were precoated with human fibronectin diluted to 20 μg/mL in PBS for 1.5-2 hours.
- HUVECs were seeded onto materials at 2×10^4 cells/well in a 96-well plate. They were then incubated overnight at 37°C, 5% CO_2.
- Cells were lightly fixed for 90 min. in 0.01% glutaraldehyde in 0.1 M cacodylate buffer (pH 7.4), then washed with wash buffer.
- The primary antibody, a mouse monoclonal antibody directed against human E-selectin, was diluted 1:500 in wash buffer and incubated with the HUVECs for 45 minutes at 37°C. The wells were then washed 5 times with wash buffer.
- The second antibody, a goat-anti-mouse-IgG-FITC was diluted 1:50 in wash buffer and incubated with the HUVECs for 45 minutes at 37°C. The wells were then washed 5 times with wash buffer.

- The cells were then fixed with 2% paraformaldehyde, dried, and mounted between microscope slides.
- Samples were viewed under a 20X objective and 485 nm light using and inverted epifluorescence Nikon Diaphot microscope equipped with appropriate filters. Cells on the materials were photographed with 1600 ASA film using a Nikon camera equipped with time exposure control. Exposure times usually ranged from 2-8 seconds. On occasion, images were captured using a high-resolution CCD camera (Photometrics), and viewed using METAMORPH software (Universal Imaging).

3.6 Interleukin-1β (IL-1β), Tumor Necrosis Factor α (TNFα) and Interleukin-8 (IL-8) Enzyme-Linked Immunosorbent Assays (ELISAs)

After the completion of the time series, the culture supernatants were assayed using the IL-1ß, TNFα and IL-8 ELISAs from R & D Systems (Minneapolis, MN) or Genzyme (Cambridge, MA).

The standard curves gave very good regression analyses. yielding R values in excess of 0.99. There was little plate-to-plate variability. The data is expressed in picograms of human IL-1ß, TNFα or IL-8 per milliliter. Samples which had been assayed and found to have high levels of activity such that they were over the limit of detection by the ELISA plate reader were re-assayed at greater dilutions. All long-term storage of samples was done at -70°C.

3.7 RNA Isolation and Northern Blot Analysis

3.7.1 Messenger RNA Isolation

The complete protocol is found in Appendix 2. Briefly, the initial steps are to isolate cytoplasmic mRNA from proteins and the nuclear fraction (DNA) from lysed HUVECs (Chomczynski and Sacchi, 1987). The whole-cell lysates contain many

enzymes that degrade polynucleic acids (e.g. ribonucleases (RNAases)); these are inactivated during lysis and removed in subsequent steps. Measures must be taken to avoid reintroduction of ubiquitous RNAase from hands, glassware, buffers, and chemical solutions. RNAase inhibitors can be used, but if care is taken to avoid introduction of RNAase it is not necessary. RNAase inhibitors are undesirable due to their toxicity. The amount of mRNA was measured at 260 nm and 280 nm on a spectrophotometer (Maniatis et al., 1982). An optical density (OD) of one at 260 nm is equal to 40 μg/mL RNA. The purity of the mRNA can be estimated by determining the ratio of the readings taken at OD_{260nm} and OD_{280nm}. A OD_{260nm}/OD_{280nm} equaling 2.0 is considered a pure mRNA preparation (Maniatis et al., 1982). E-selectin expression was compared to unstimulated TCPS-cultured HUVECs (negative control), and interleukin-1ß (IL-1ß)-stimulated (1 unit/mL) or lipopolysaccharide-stimulated (100 ng/mL, *S. typhimurium*) HUVECs (positive control)(Montgomery et al., 1991).

3.7.2 Detection of E-selectin mRNA

Agarose gel electrophoresis was used to separate mRNAs; 10 μg loaded per lane has been shown to be sufficient for detection of E-selectin transcripts (Montgomery et al., 1991). mRNA electrophoresed in a denaturing 1% agarose/formaldehyde gel was transferred to a nitrocellulose membrane using the Northern blotting technique (Maniatis et al., 1982). ^{32}P-labeled, E-selectin cDNA fragments was hybridized to the mRNA-blotted nitrocellulose as described (Maniatis et al., 1982; Montgomery et al., 1991). The detection of E-selectin transcripts was performed using autoradiography (Maniatis et al., 1982). E-selectin expression was compared to ß-actin mRNA expression to verify equal amounts of RNA were loaded into each well. Autoradiography for ß-actin expression was usually 24 hours at -70°C.

3.8 Neutrophil Adhesion Assays

The neutrophil adhesion protocol is used in the laboratory of Professor Timothy Pohlman. Minor modifications were made to adapt this assay for use with cells seeded on biomaterial surfaces. This assay uses the neutrophil cell line HL-60 as a method to detect E-selectin expressed on the surface of activated endothelial cells. Isolated blood neutrophils can also be used in this protocol in place of HL-60s. The assay is designed for use with HUVECs seeded in 12 or 24 well plates.

3.8.1 Radio-labeling Method

HUVECs were seeded on materials approximately 20-24 hours prior to the neutrophil adhesion assay. Results using this method are found in Chapter 9. IL-1ß-stimulated HUVECs were used as a positive control, which were stimulated for 3-4 hours prior to the addition of the labeled HL-60s.

- HL-60s are removed from culture flask and washed with room temperature phosphate buffered saline (RT-PBS). Resuspend in 5 mL RT-PBS.
- 100-150 μL of ^{51}-chromium (Amersham sodium chromate; CJSIV, 1 mCi) is added to HL-60s.
- Incubate at 37°C in a shaking water bath for 1 hour.
- Centrifuge cells at 1000 rpm for 8 minutes to pellet cells. Wash cells 3 times with 10 mL RT-PBS.
- Resuspend pelleted cells in warm RPMI + 1% FBS. Count cells and dilute to 1.67 x 10^6 cells/mL. This is for a 12-well plate configuration. Use 5 x 10^5 cells/mL for a 48 well plate.
- Add 300 μL of labeled cells to four counting tubes as a control to determine the total counts added to each HUVEC well.
- Wash the HUVEC wells twice with PBS + 5% FBS.

- Add 300 μL of labeled HL-60s in each HUVEC well and material only control wells.
- Incubate for 30 minutes at 37°C in a 5% CO_2 incubator.
- Wash each well gently twice with 500 μL of PBS + 5% FBS.
- Aspirate all PBS from wells and add 500 μL of 1N NH_4OH.
- Leave for 3 hours or overnight to allow cells to lyse completely.
- Transfer contents from each well to a counting tube. Count on a gamma counter.
- The percent adherence is calculated as the (test well cpms)/(total counts cpms)

3.8.2 Neutral Red Labeling Method

An alternative method was developed to label the HL-60s without the need for using radioisotopes. Some level of sensitivity was lost compared to the ^{51}-chromium method, but is safer and more convenient than working with radioisotopes. Results using this method are found in Chapter 7.

Endothelial cell monolayers were prepare 24 hours prior to the assay by plating at near-confluence in 24 well plates. The endothelial cells were stimulated by adding 150μL of macrophage supernatant to 300μL of culture medium, for a final dilution of the supernatants of 1:3 (150μL diluted to a final volume of 450 μL). The same supernatant was used in duplicate wells. IL-1ß-stimulated HUVECs were used as a positive control, which were stimulated for 3-4 hours prior to the addition of the labeled HL-60s.

The HL-60s were resuspended in RPMI containing 1% bovine serum albumin (BSA) and 1% fetal bovine serum (FBS). Neutral red stain, obtained as a 3.3g/L in PBS solution (N-2889, Sigma), was added at 1/10 the volume of the cell suspension. The cells were incubated for 1 hour at 37°C, 5% CO_2 in air, in a humidified chamber. The cells were then washed extensively in RPMI containing 10% FBS; washes were repeated approximately 6 times, with the final wash done in PBS containing 1% BSA to check the amount of red color remaining in the wash. If the level of Neutral Red was negligible, the

cells were resuspended in RPMI containing 10% FBS, counted and suspended at 1-1.7 x 10^6 cells/mL. Labeled HL-60s were added to wells containing macrophage supernatant-treated HUVECs in 24-well plates at 3-5 x 10^5 HL-60s per well (300 μL of cell suspension). After a 20 minute incubation with the HUVECs, the wells were gently washed once with 1 mL RPMI containing 10% FBS. The cells were lysed by adding 200-300 μL of 0.05M HCl in ethanol, releasing the neutral red from the HL-60 cells that remained in each well. The optical density (OD) of the lysates was determined by transferring 100μL from each well to a 96-well microtiter plate. The OD was read at 560 nm less the OD at 650 nm on a plate reader.

3.9 Cell Number Determination by Lactose Dehydrogenase (LDH) Activity

The wells and pelleted cells from section 3.4.5 were assayed for their LDH activity, which directly correlates with total cell number. The cells in the wells were lysed using a "lysis buffer" solution consisting of 2% Triton X-100 (Sigma) in PBS. One mL of lysis buffer was added per well. The plate was sealed with Parafilm® and sonicated for at least 20 minutes to disrupt any cells in the porous materials. Similarly, the pelleted cells were lysed using 1 mL of the lysis buffer and vigorous vortexing. One hundred μL of each cell lysate was transferred to wells in a 96-well plate. A catalyst/dye solution of diaphorase/NAD+ mixture, iodotetrazolium chloride and sodium lactate was prepared from the LDH Cytotoxicity Detection Kit (cat. #1-644-793, Boehringer Mannheim, Indianapolis, IN) as per instruction by the manufacturer. To each well in the 96-well plate, 100 μL of the catalyst/dye solution was added. The optical density was measured at 5 minute intervals for 15-20 minutes.

To generate a standard curve for each monocyte preparation, monocytes were isolated using the Martinson adherence protocol. The recovered monocytes were counted and plated at known densities in a 24-well plate in 500 μL. To each well 500 μL of lysis

buffer was added, and the plate allowed to sit for at least 20 minutes. Each well was triturated to break-up the cells prior to removal of 100 μL to a 96 well plate. The LDH activity was determined as describe above. A standard curve was generated for each monocyte preparation, from which cell numbers were calculated for cells contacting the different material substrates. Regressions for the individual monocyte preparations standard curves yielded R values of at least 0.998. A composite standard curve from all monocyte preparations is illustrated below in Figure 3.1. There was surprisingly little variation in monocyte-derived macrophage LDH activity between donors, especially at low cell densities.

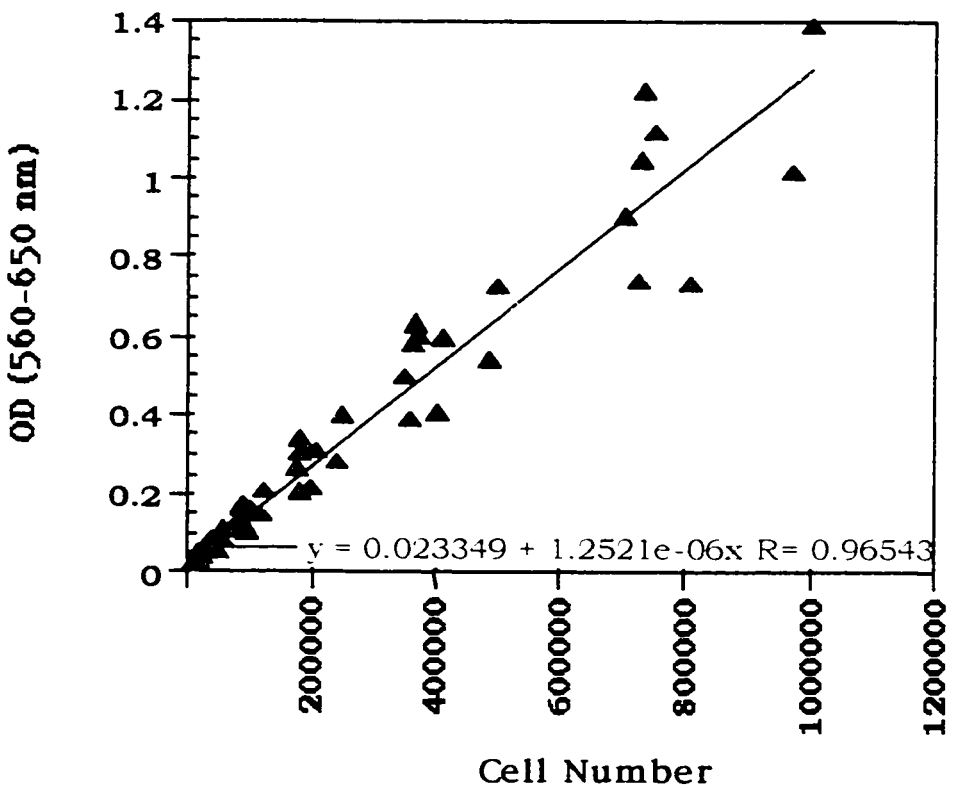

Figure 3.1 The composite LDH standard curve for all monocyte-derived macrophages preparations.

3.10 Endotoxin Assays for Biomaterial Surfaces

The Limulus amebocyte assay (LAL) was used by Laura Martinson for the determination of endotoxin on some material surfaces. This assay is based on the ability of amebocyte lysate from the horseshoe crab (*Limulus polyphemus)* to coagulate in the presence of endotoxin. Ms. Martinson did not find any evidence of endotoxin contamination on any of the MEC materials, Nylon 6 or PTFE.

An alternative method was used to evaluate endotoxin contamination on the ePTFE materials (Poole et al., 1987). Monocytes isolated using the adherence protocol developed by Ms. Martinson in section 3.4.4 were found to be exquisitely sensitive to the presence of endotoxin contamination on material surfaces. The monocytes produce significant levels of TNFα in response to endotoxin. To test for endotoxin, monocytes isolated using the 3.4.4 protocol were plated onto the ePTFE materials at a density of 4 x 10^5 cells/well in a 12-well plate. After 1 day in culture, supernatants were removed, centrifuged to remove any cells, aliquoted and stored at -80°C. The supernatants were then tested for TNFα activity using an ELISA, as described in section 3.6. LPS-stimulated monocytes were included as a positive control. The results are given in Table 3.3.

Table 3.3: TNFα Results: Testing for Endotoxin Contamination

Material	TNFα (pg/mL)	Standard Deviation
Glass Ring Controls	0.4	0.3
PTFE	2.4	0.9
10μ ePTFE	3.3	0.8
30μ ePTFE	4.2	1.3
60μ ePTFE	1.4	0.4
LPS	2155	85

All of the materials tested showed low levels of TNFα production from monocytes seed on the different materials. PTFE had been previously tested in the LAL assay and shown to be negative for endotoxin contamination. Compared to PTFE, none of the materials showed any indication of endotoxin contamination. This was further supported by the endothelial cell seeding on these material surfaces in Chapter 9, which never showed indication of endothelial cell activation, a common response to endotoxin. If endotoxin was present, either of these cell types would be extremely sensitive its presence. All of the materials used in the macrophage and endothelial cells studies were considered endotoxin-free.

3.11 Notes for Chapter 3

Brauker, J. H., Carr-Brendel, V. E., Martinson, L. A., Crudele, J., Johnston, W. D., and Johnson, R. C. (1995). Neovascularization of synthetic membranes directed by membrane architecture. J. Biomed. Mater. Res. 29, 1517-1524.

Chomczynski, P., and Sacchi, N. (1987). Single-step method of RNA isolation by acid guanidinium thiocyante-phenol-chloroform extraction. Anal. Biochem. 162, 156-159.

Ertel, S. I., Chilkoti, A., Horbett, T. A., and Ratner, B. D. (1991). Endothelial cell growth on oxygen-containing films deposited by radio-frequency plasmas: the role of surface carbonyl groups. J. Biomater. Sci. Polymer Edn. 3, 163-183.

Ertel, S. I., Ratner, B. D., and Horbett, T. A. (1990). Radiofrequency plasma deposition of oxygen-containing films on polystyrene and poly(ethylene terephthalate) substrates improves endothelial cell growth. J. Biomed. Mater. Res. 24, 1637-1659.

Maniatis, T., Fritsch, E. F., and Sambrock, J. (1982). Molecular Cloning: A Laboratory Manual (Cold Spring Harbor, NY: Cold Spring Harbor Laboratory).

Montgomery, K. F., Osborn, L., Hession, C., Tizard, R., Goff, D., Vassallo, C., Tarr, P. I., Bomsztyk, K., Lobb, R., Harlan, J. M., and Pohlman, T. H. (1991). Activation of endothelial-leukocyte adhesion molecule 1 (ELAM-1) gene transcription. Proc. Natl. Acad. Sci. USA 88, 6523-6527.

Pertoft, H., Johnsson, A., Wärmegård, B., and Seljelid, R. (1980). Separation of Human Monocytes on Density Gradients of Percoll®. J. Immunological Methods 33, 221-229.

Poole, S., Thorpe, R., Meager, A., and Gearing, A. J. H. (1987). Assay of Pyrogenic Contamination in Pharmaceuticals by Cytokine Release From Monocytes. In Developments in Biological Standardization, A. J. H. Gearing and W. Hennessen, eds. (New York: Karger), pp. 121-123.

Chapter 4

Surface Analysis of Materials

4.1 Introduction

Only a select group of polymers will be discussed in this chapter. The materials most relevant to Chapters 6, 7, 8 and 9 are focused on: the MEC, Nylon 6 and PTFE/ePTFE materials. A detailed discussion of the plasma-deposited films can be found in Chapter 5.

To isolate the effects of material topography on macrophage activation, the types of materials needed were those of identical surface chemistry with variations only in pore size or fibril length within a polymer series. The MEC and PTFE/ePTFE polymer series fit these criteria very well. For each polymer, the surface chemistry was determined using electron spectroscopy for chemical analysis (ESCA). The surfaces within each polymer group had identical chemical characteristics, while varying widely in surface topographies. Only in this fashion can the effects of surface topography be separated from surface chemistry effects.

4.2 Surface Analysis of Mixed Esters of Cellulose (MEC) Membranes

4.2.1 Scanning Electron Microscopy of MEC Membranes

The 0.22μ and 5μ MEC membranes were seeded with macrophages prior to viewing under SEM. The materials were critical point dried, mounted on SEM studs, and sputter coated with platinum and gold. SEM of the 8μ MEC membrane was not performed.

The 0.22μ MEC has a fine grain structure to its surface (Figure 4.1). The porosity is determined by the size of particles it allows to pass through the material, not by the actual physical dimensions of the pores as found in track-etched membranes. The 5μ

MEC surface does not have the fine structure seen with the 0.22μ (Figure 4.2). This surface shows more defined pits, about 10μ across.

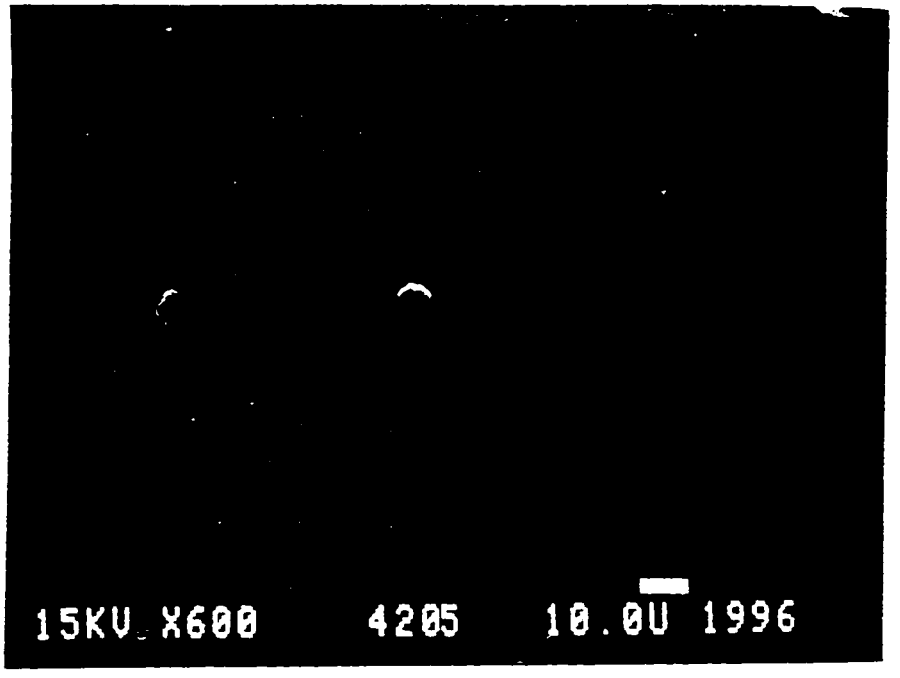

Figure 4.1 SEM of 0.22μ MEC with a few macrophages attached to the surface.

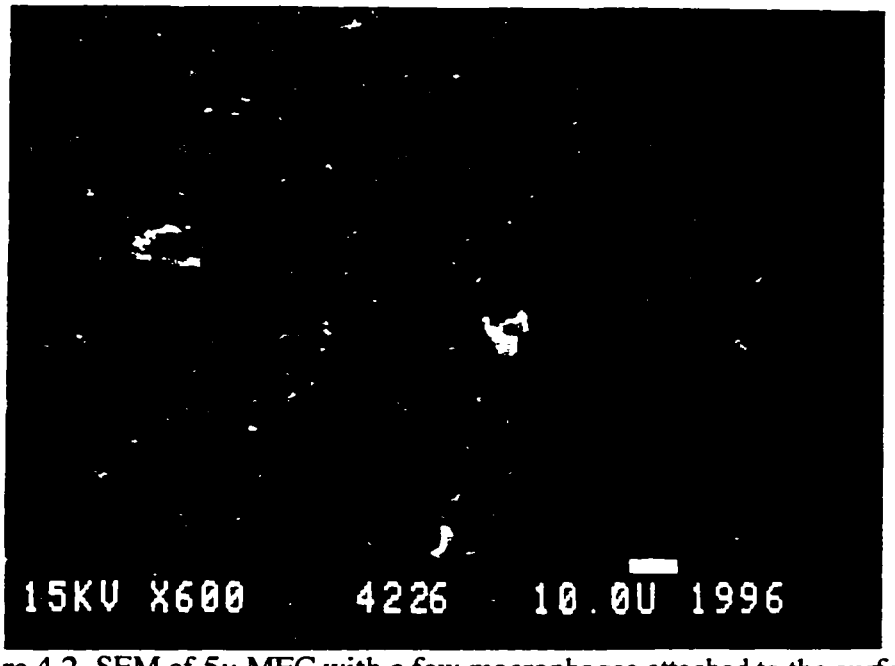

Figure 4.2 SEM of 5μ MEC with a few macrophages attached to the surface.

4.2.2 ESCA Analysis of MEC Membranes

The survey scan of the 0.22μ, 5μ and 8μ MEC membranes show the expected oxygen and carbon species, but also a significant amount of nitrogen which was not expected (Figure 4.3). The MEC membranes are manufactured by Millipore, and their exact chemical composition is considered proprietary information. The presence of nitrogen may be due to the "mixed ester" chemistry (if it contains amines, amides, etc.) or to a post-manufacturing surface modification performed on the membranes. Frequently filter membrane manufacturers modify the filter surfaces with hydrophilic functional groups to improve wetting, which may be the case here.

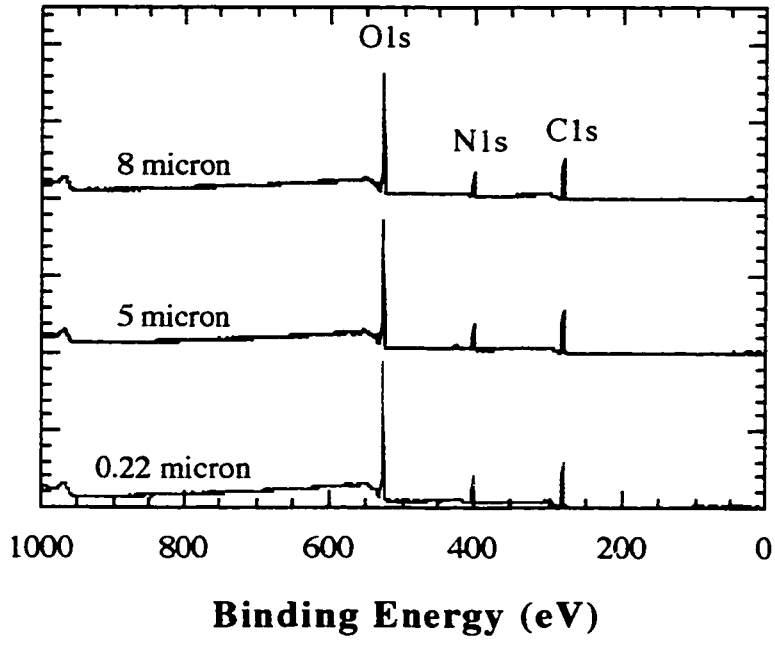

Figure 4.3 ESCA survey scans of the MEC membranes.

In Table 4.1, the chemical composition data is summarized. All of the membranes have almost identical chemical profiles, varying less than 1% in elemental composition.

There was a small amount of silicon contamination on the 8μ MEC, but this amount is considered minimal.

Table 4.1: Elemental Composition of MEC Membranes

Material	**% C (1s)**	**% O (1s)**	**% N (1s)**	**% Si (2p)**
0.22μ MEC	36.82	51.14	12.05	---
5μ MEC	37.36	51.04	11.61	---
8μ MEC	36.89	51.14	11.34	0.63

By stacking the high resolution C1s spectra, shown in Figure 4.4, further evidence of the similarity of surface composition of the MEC membranes is given by the similar peak shapes. Peak fitting of the C1s spectrum of 0.22μ MEC was performed (Figure 4.5), and the resulting peak fit data is reported in Table 4.2. The following binding energies were assigned to the carbon functional groups: 286.7 eV for hydrocarbon (C-H), 286.7 eV for alcohol (C-O), 287.9 eV for O-C-O, and 289.0 eV for ester (O=C-O). No peak fitting was done for any nitrogen species due to the overlap in binding energies with the oxide functional groups. It should be noted, however, that amine (BE 286.0 eV) and amide (BE 288.2 eV) groups may be present. There was a fair amount of hydrocarbon contamination on these membranes as shown in the C-H peak, comprising approximately 3-4% on all the membranes, which is common for cellulose membranes (Beamson and Briggs, 1992). There is a relatively low level of ester content in these membranes, at approximately 3%. These membranes have almost identical surface chemistry even though pore size and topography vary significantly.

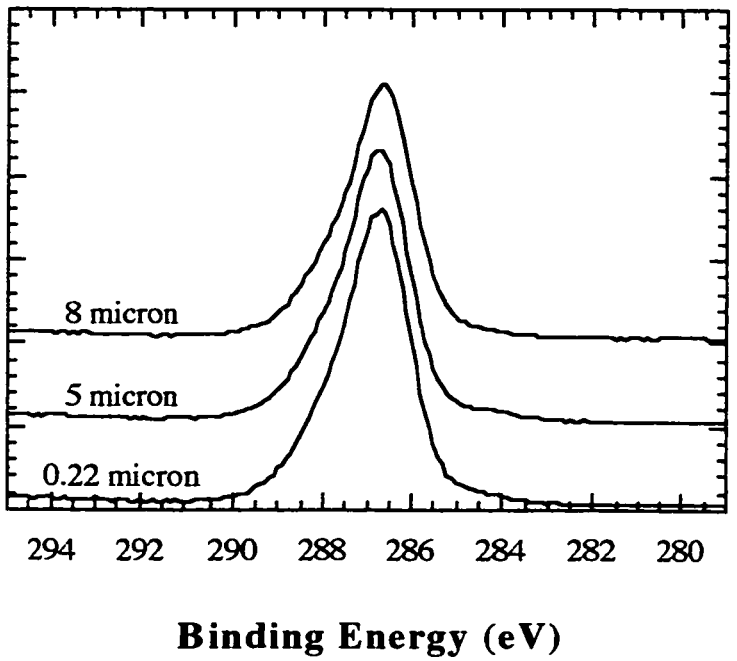

Figure 4.4 Stack plot of the high resolution C1s ESCA spectra for the MEC membranes.

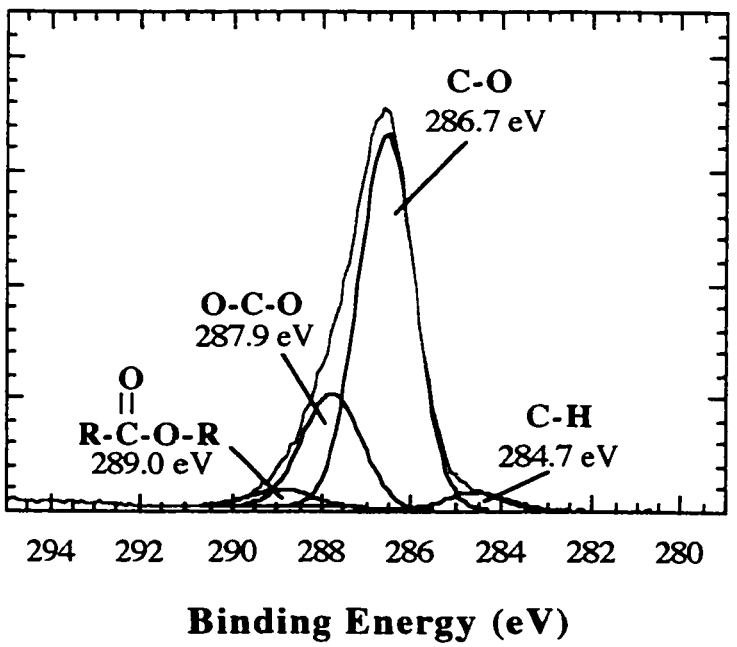

Figure 4.5 High resolution C1s ESCA spectrum of 0.22μ MEC showing peak fitting.

Table 4.2: Percent of Molecular Species from the MEC C1s High-resolution Spectra

Material	**C-H**	**C-O**	**O-C-O**	**O=C-O**
0.22μ MEC	3.45	70.79	22.38	3.38
5μ MEC	4.41	72.02	21.13	2.44
8μ MEC	4.06	73.03	20.10	2.81

4.3 Surface Analysis of Nylon 6

The Nylon 6 used in Chapters 6.3, 6.5 and 7 was commercially produced. The Nylon 6 used in Chapter 6.4 was made "in-house" and had very different characteristics, being more opaque and porous than the commercially available product. Since no surface analysis or endotoxin data is available for the "in-house" product, it will not be discussed here. Also, comparison of the two types of Nylon 6 should not be made. The Nylon 6 used for Chapters 6.3, 6.5 and 7 is well characterized, as shown below.

The Nylon 6 elemental composition is given in Figure 4.6, showing the expected oxygen, nitrogen and carbon elements (Beamson and Briggs, 1992). The high-resolution C1s spectrum in Figure 4.7 demonstrates the distinctive hydrocarbon (C-H), amine (C-N), and amide peaks (O=C-N) with the expected ratio of 4:1:1 respectively (also refer to Table 4.3).

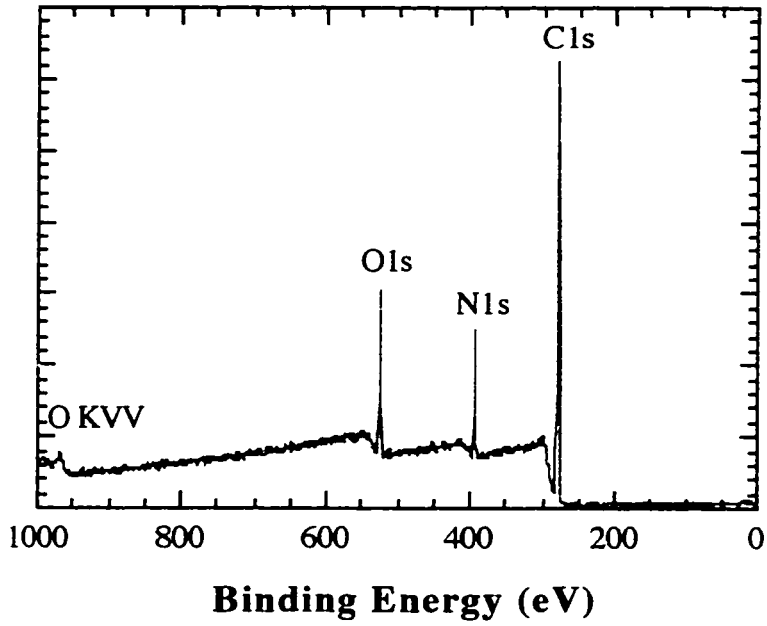

Figure 4.6 ESCA survey spectrum showing the elemental of Nylon 6.

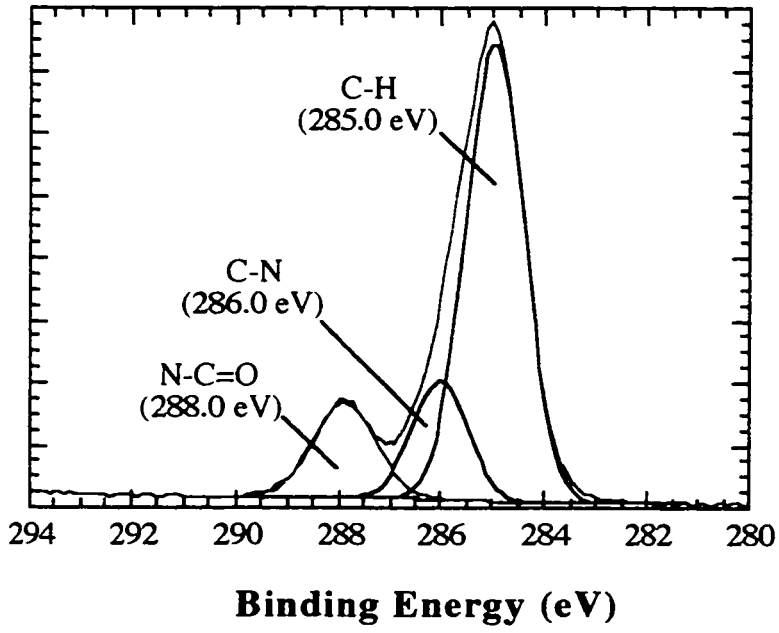

Figure 4.7 High-resolution C1s spectrum for Nylon 6 showing peak fits.

Table 4.3: Summary of the High-resolution C1s Peak Fitting Results for Nylon 6: Percent of Each Functional Group

Material	C-H	C-N	N-C=O
Nylon 6: rough side	67.99	16.75	15.26
Nylon 6: smooth side	67.39	17.01	15.6
Published values	67	17	16

There was a slight variation visually on each side of the Nylon 6 sheets purchased. One side was smoother than the other, the "rough" side having more striations, presumably from polymer processing. The rough side was always used as the macrophage-contacting surface for all of the studies in Chapters 6.3, 6.5 and 7. There was very little difference chemically for the individual sides as shown in Table 4.3.

4.4 Surface Analysis of Poly(tetrafluoroethylene) (PTFE) and Expanded PTFE (ePTFE)

4.4.1 SEM of the PTFE and ePTFE Fluoropolymers

Expanded PTFE materials with 10μ, 30μ, 60μ, and 100μ nominal fibril lengths were compared to non-expanded PTFE.

All PTFE and ePTFE samples were analyzed using SEM. The materials were mounted on SEM studs, and sputter coated with platinum and gold. The ePTFE fiber lengths observed by SEM fell into the ranges reported by the manufacturer. The surface of the non-porous PTFE was by no means smooth, as seen in Figure 4.8. The fibril length increases as expected, shown in Figures 4.9-4.12. The characteristic "node and fibril" structures of ePTFE is evident.

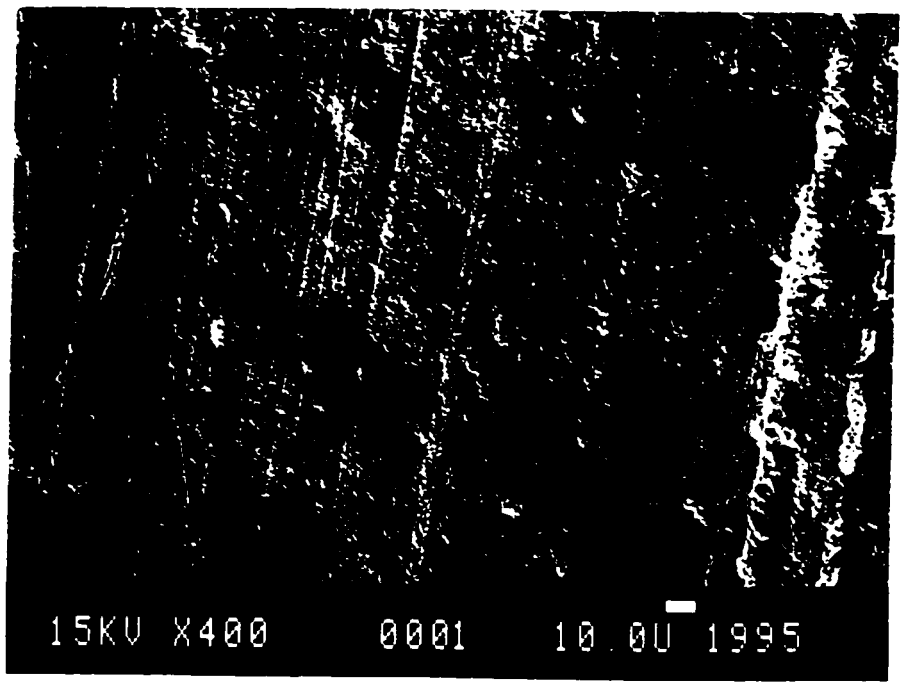

Figure 4.8 SEM of PTFE (non-porous).

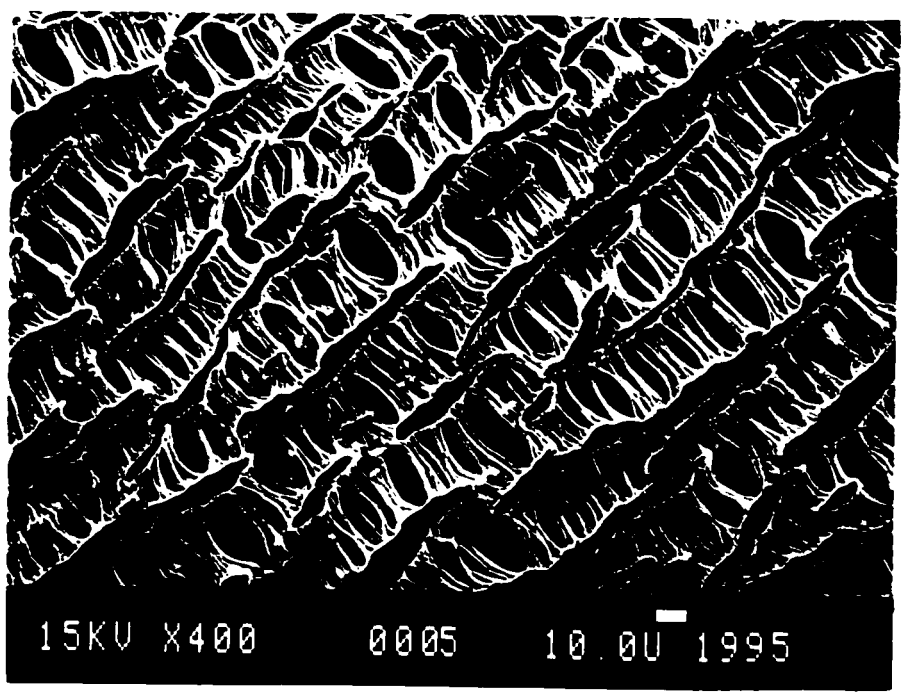

Figure 4.9 SEM of 10μ ePTFE.

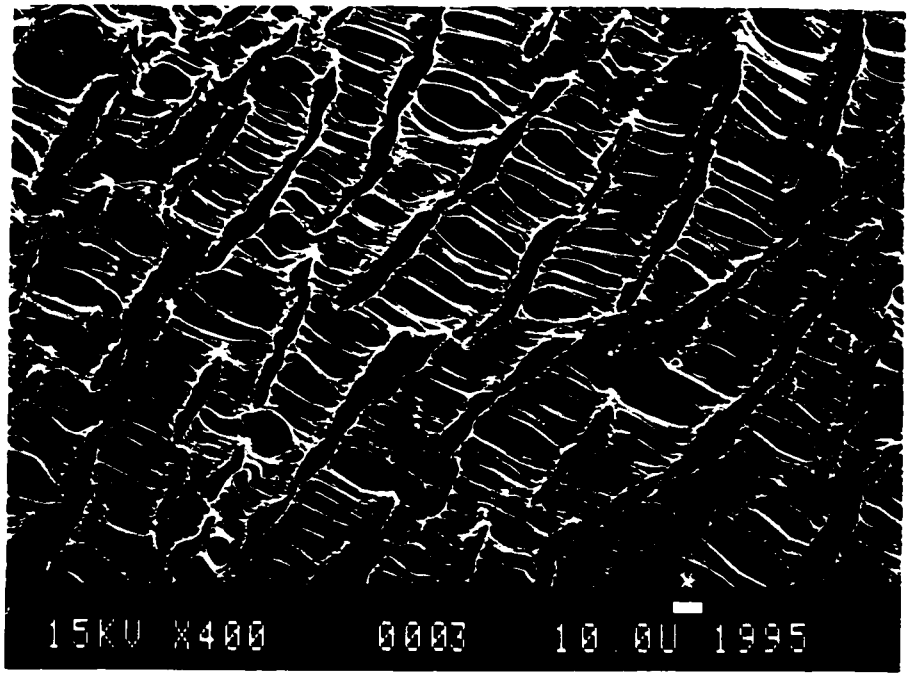

Figure 4.10 SEM of 30μ ePTFE.

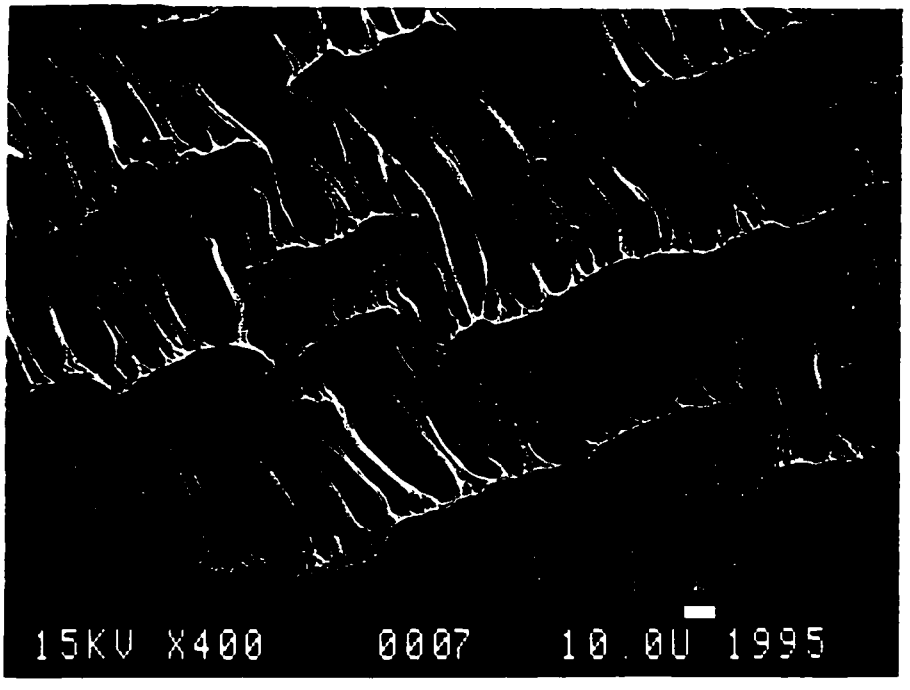

Figure 4.11 SEM of 60μ ePTFE.

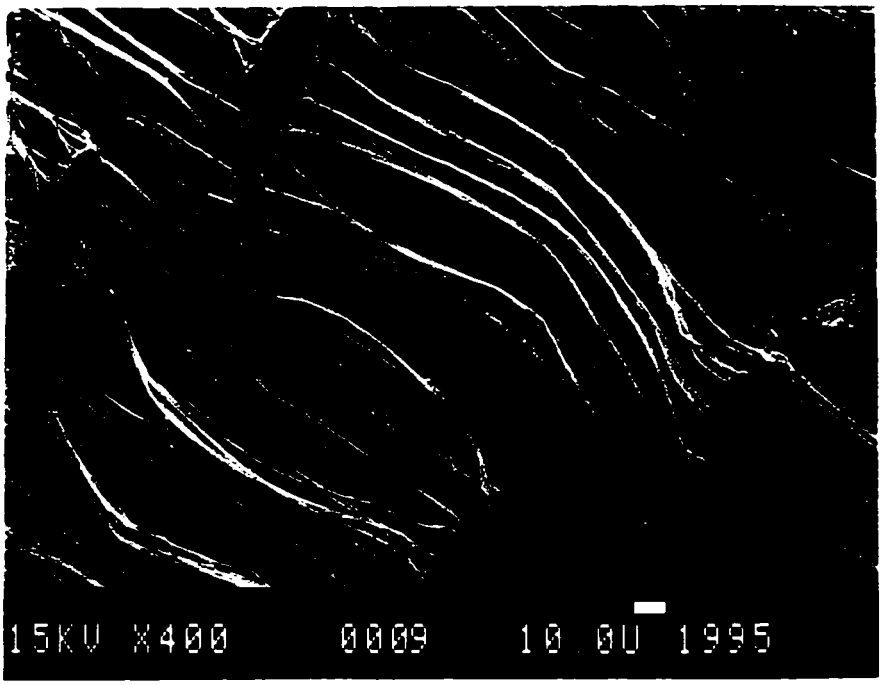

Figure 4.12 SEM of 100μ ePTFE.

4.4.2 ESCA of PTFE and ePTFEs

All samples were analyzed using ESCA to obtain the surface chemical composition. The results are summarized below in Table 4.4 and Figure 4.13. As expected, all of the ePTFE samples had identical surface composition as the non-porous PTFE due to the -(-CF_2-)- repeats within the polymer (Beamson and Briggs, 1992). All samples had the theoretical C:F ratio of 1:2.

Table 4.4: Elemental Composition of PTFE and ePTFE

Sample	**% Carbon**	**% Fluorine**	**C:F ratio**
PTFE, non-porous	32.29	67.71	1:2.09
ePTFE, 10 μ	33.11	66.89	1:2.02
ePTFE, 30 μ	33.77	66.23	1:1.96
ePTFE, 60 μ	33.88	66.12	1:1.95
ePTFE, 100 μ	33.50	66.50	1:1.99

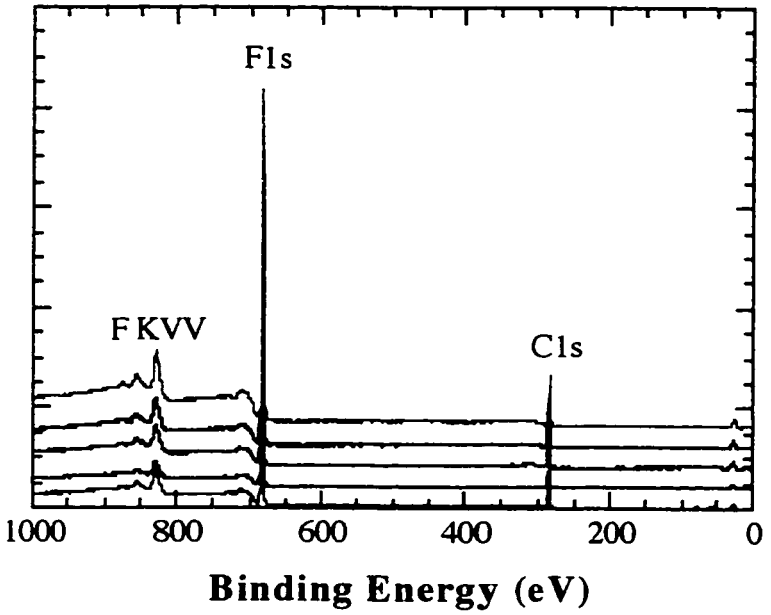

Figure 4.13 ESCA survey spectra for PTFE/ePTFE showing elemental composition.

The high-resolution C1s spectra for all of the fluoropolymers are shown in Figures 4.14 and 4.15. The single peak for the -(C-F_2)- monomer is seen in these figures, also showing no hydrocarbon contamination. These data verify the cleaning protocol was effective in removing hydrocarbon contamination (less than 1% remained) from the material surfaces. These data are important for subsequent biological evaluations to ensure that all materials are identical in surface chemistry and only differ in surface topography.

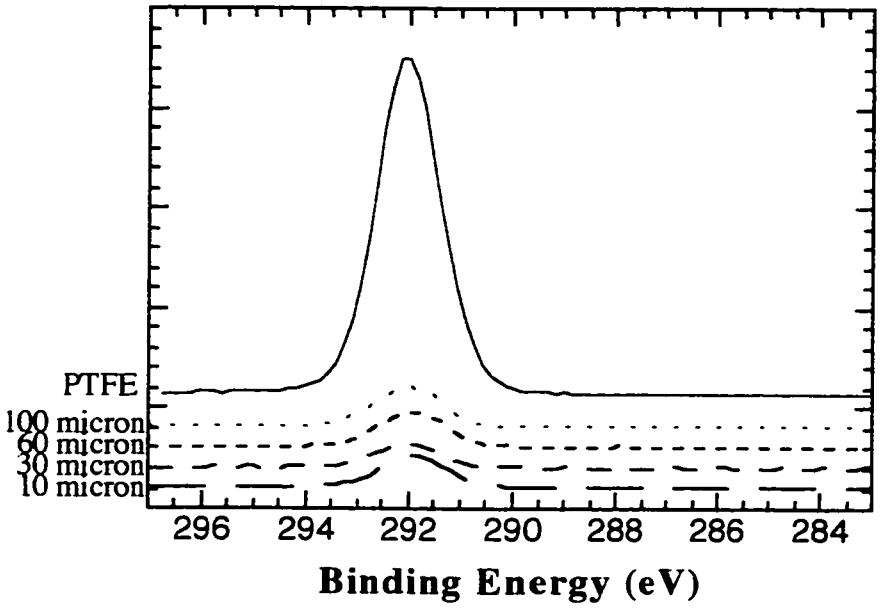

Figure 4.14 High-resolution C1s spectra for the PTFE/ePTFE fluoropolymers.

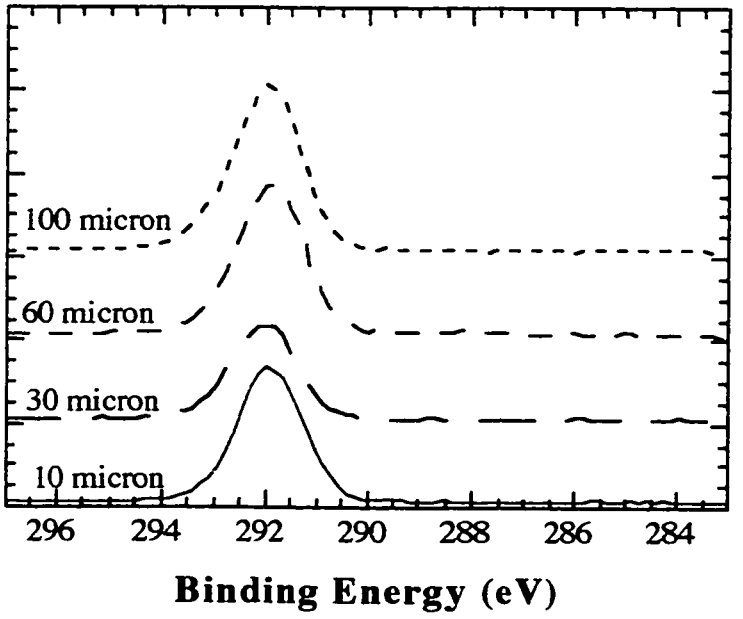

Figure 4.15 Detail of the high-resolution C1s spectra for the ePTFE fluoropolymers only.

4.4.3 TOF-SIMS of 30μ ePTFE

Analyses were performed by Anna Belu, Ph.D., University of Washington. ESCA analysis uses a fairly large spot size (approximately 1000μ), which could make the determination of the existence of domains within a polymer difficult by the averaging of the chemical composition over the spot size area. Although the PTFE and ePTFE surfaces appeared to have the same surface chemistry by ESCA, we questioned whether the fibrous regions of ePTFE had the same chemistry as the intervening nodes or non-stretched, solid areas. We performed TOF-SIMS to determine if there were any subtle differences between the fibrous and non-fibrous regions. TOF-SIMS can image a much smaller region, approximately 200μ in the x-axis for Figure 4.16, and a shallower sampling depth of 10 Å than ESCA (100Å), making it much more surface sensitive in depth and lateral resolution. A 30μ ePTFE sample was imaged by rastering across the sample, summing all of the ions generated, and producing a false-color "chemical picture" of the surface.

Figure 4.16: TOF-SIMS false-color image of 30μ ePTFE. The image clearly identifies the expanded regions (red), and solid nodes (yellow), characteristic of this material. X-axis is approximately 200μ.

A full SIMS spectra exists for each pixel which can be accessed to compare the spectra of any two pixels in the image. The image identified the regions of interest, and by comparing the SIMS profile of pixels in the expanded (red) and non-expanded solid (yellow) regions we determined that the molecular fragments that are generated from each region were identical, only differing in intensity (Figure 4.17). The non-expanded region generated approximately 2.5 times the counts/pixel of the expanded areas. Differences in signal intensity are expected due to the different average mass densities of the regions. For each ePTFE domain, identical molecular ions were produced. These data show there are no differences in surface chemistry between the fibrous and node regions that are produced from stretching or other processing of the polymer.

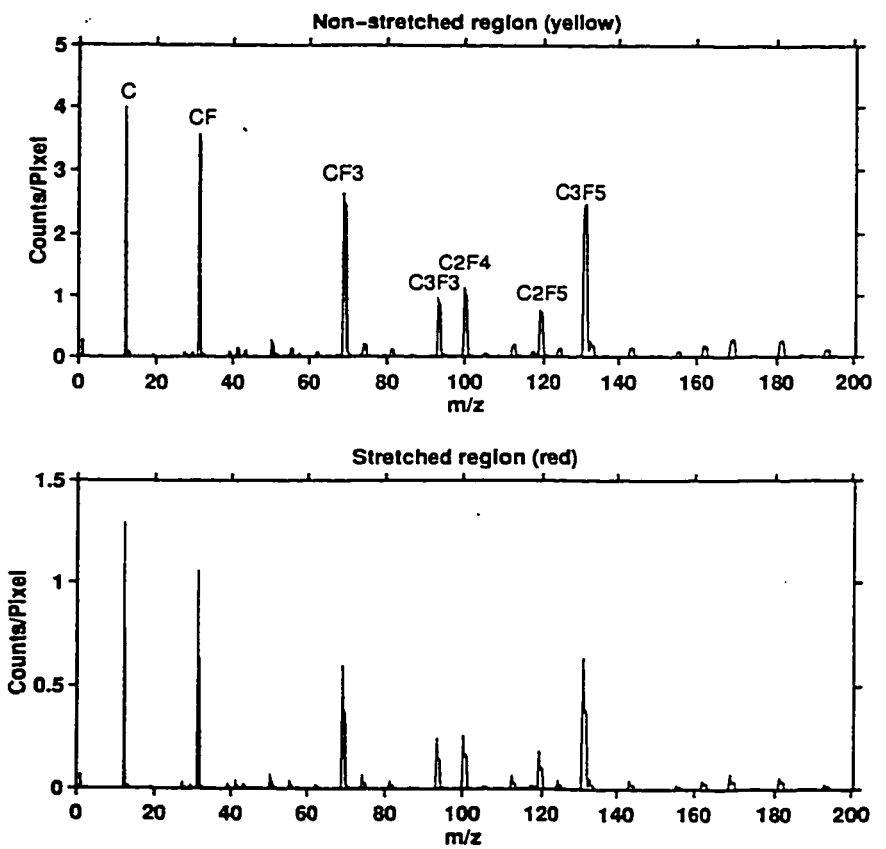

Figure 4.17 TOF-SIMS spectra of 30μ ePTFE. Two areas, expanded and non-expanded regions, were identified from Figure 4.16. The SIMS spectrum for each region is reported here.

4.5 Notes for Chapter 4

Beamson, G., and Briggs, D. (1992). High Resolution XPS of Organic Polymers (New York: John Wiley & Sons).

Chapter 5

Fibronectin Adsorption to Radiofrequency Plasma-deposited Films: Scatchard Analysis and Cell Growth Characteristics

5.1 Abstract

Proteins adsorb in response to the presence of specific functional groups on the material surface. We propose that this is analogous to ligands binding to specific sites, such as receptors, on a cell surface. Scatchard analysis is used to determine the affinity of a ligand for it's binding site and the number of binding sites present. Using protein adsorption isotherms, Scatchard analysis was used to model fibronectin (FN) adsorption to radiofrequency plasma-deposited films with differing surface chemistries. Electron spectroscopy for chemical analysis (ESCA) was used to characterize the surface chemistry of each material. Marked differences in protein binding characteristics were observed including: the complexity of binding (high affinity vs. high and low affinity binding), differences in apparent FN affinity, and the amount of protein bound to each polymer film surface. The differences in FN affinity are attributed to the types and distribution of the functional groups on these surfaces. High levels of oxygen- and nitrogen-containing species showed complex binding phenomena compared to the other materials studied. Scatchard analysis provides a useful method for measuring protein affinity for surfaces. No other established technique has been identified that can do this.

5.2 Introduction

The adsorption of proteins to material surfaces has been implicated in phenomena as diverse as the performance of medical implants, the adhesion of marine organisms, the

failure of biosensors, the fouling of heat exchangers in food processing, the accuracy of ELISAs and the growth of cells in culture. The protein parameters that influence these phenomena are the specific proteins adsorbed from complex, multi-protein solutions, the degree of denaturation of the protein at the surface and the tightness of binding of the protein. These three considerations are not independent--for example, the tightness of binding will influence the mixture of proteins that adsorb to a surface and the ability of a surface to denature the proteins. Quantitative methods to study protein binding and surface affinity of proteins are valuable, but relatively few methods to measure protein interaction strength and affinity exist (Horbett et al., 1977; Wojciechowski and Brash, 1993). As a result, little is known about the mechanisms involved in protein and cell interactions with biomaterials. The importance for studying cell interactions with biomaterials stems from the clinical applications of materials where promotion of cell growth is critical for the performance of the material *in vivo*. These clinical applications include endothelialization of vascular grafts and the promotion of epithelial cell growth on corneal implants: in essence, to "promote healing" or incorporation of the biomaterial into the host tissues.

This study used Scatchard analysis to model protein adsorption to polymer surfaces. Scatchard analysis has been widely used in cell-receptor biology to calculate the affinity of a ligand for its receptor, and to determine the number of receptors on cells (Limbird, 1986). It is assumed that polymers have specific binding sites (functional groups) and the protein's affinity for these sites can be measured from the Scatchard plot of the adsorption isotherms. The affinity of the protein will vary with the surface chemical composition, the number of binding sites, and the distribution of the sites on the surface. Proteins may interact with more than one type of site, so the affinity will be expressed as the "apparent" affinity constant (termed "apparent K_a") to differentiate it from a receptor-ligand interaction where only one ligand interacts with a receptor on a cell surface.

Another quantity determined from the Scatchard analysis is the total number of binding sites or the maximal amount of bound species (B_{max}). The methods for determining both the apparent K_a and B_{max} are discussed in a later section.

Traditionally, the Scatchard analysis is a linear transformation of ligand binding isotherm data. Here we use the data obtained from the protein adsorption isotherms. We make a number of assumptions for the application the Scatchard analysis to protein adsorption phenomena. First, we assume protein adsorption to a surface demonstrates a simple, reversible interaction that follows the mass action law [P] + [S] <--> [PS], were [P], [S], and [PS] are the concentrations of protein, "binding sites" on the material surface, and the protein/surface complex, respectively. This is consistent with the ligand/receptor scheme typically used. Second, the time at which measurements are taken must represent an equilibrium state. Thus, we assumed that after two hours of adsorption at 37°C, the events of adsorption are essentially completed.

Interpretation of the shape of the Scatchard plots is critical for this analysis, especially when nonlinear plots are observed. A linear Scatchard plot indicates that the surface to which the protein is bound possesses one type of binding site that binds the protein with one apparent affinity. A nonlinear Scatchard plot suggests that there are two types of binding occurring to the surface, one of high affinity, the other low affinity. This type of plot indicates a heterogeneous surface where there are multiple independent binding sites with differing protein affinities, or that there exists multiple affinity binding states of one type of binding site (Adamson, 1982; Limbird, 1986).

A set of radiofrequency-deposited (RF) plasma films were used here to probe the changes in fibronectin (FN) adsorption with varying surface chemistry. Plasma deposits made by blending nitrogen gas into the oxygen-containing plasma have been shown to have a high affinity for FN, the amount of FN bound increasing with nitrogen content in the deposited films (Ertel et al., 1990). This observation led to this study applying the

Scatchard analysis method in order to gain insight into not only the amount of FN adsorbed, but its state of adsorption. Cell growth has been shown to depend on the amount of oxygen content of plasma films deposited from oxygen-containing volatile organics (Ertel et al., 1990). However, in our study, no significant differences in endothelial cell growth was observed when the materials were precoated with FN prior to cell seeding. This suggests that FN preadsorbed from pure solution has little affect on cell growth, in contrast to competitive adsorption from complex cell growth medium.

5.3 Materials and Methods

All of the plasma-deposited films used in this chapter were prepared as discussed in Chapter 3.1. Atomic force microscopy (AFM) was performed, as described in Chapter 3.2. Fibronectin radiolabelling and adsorption isotherm protocols are found in Chapter 3.3.

5.3.1 Scatchard Analysis

The amount of FN adsorbed is expressed in molar units, necessary for Scatchard analysis. The adsorption volume used was 1 mL; all molar quantities are calculated from this volume. The molecular weight used for FN was 450,000 grams/mole (Furcht, 1983). The data are not normalized to surface area; all samples were assumed to have approximately the same surface area.

Scatchard analysis was performed as described (Limbird, 1986), plotting the bound FN divided by free FN versus the bound FN. From the Scatchard analysis, apparent affinity constants ("apparent K_a's") and the maximum amount of bound FN that can bind to the surface, B_{max}, were determined for each polymer. The apparent K_a is determined by the slope of the Scatchard plot. The B_{max} is calculated from the x-intercept of the Scatchard plot. To calculate theoretical values of B for generating the curve fits, the

equations below were used (Limbird, 1986). The Type 1 equation is used for linear Scatchard plots which suggests that only one type of binding is present in the system. The Type 2 equation is used for biphasic Scatchard plots which indicates two types of binding are occurring, high affinity and low affinity binding.

Type 1 Binding:

$$B_{theory} = \frac{(K_a)(B_{max})(F)}{1 + (K_a)(F)}$$

Type 2 Binding:

$$B_{theory} = \frac{(K_{a1})(B_{max1})(F)}{1 + (K_{a1})(F)} + \frac{(K_{a2})(B_{max2})(F)}{1 + (K_{a2})(F)}$$

where:

$K_{a(1)}$ = high-affinity K_a
K_{a2} = low-affinity K_a
$B_{max(1)}$ = B_{max} for high-affinity binding
B_{max2} = B_{max} for low-affinity binding
F = Free FN concentration

5.3.2 Clonal Cell Growth on Polymers

A clonal, or low-cell-density, growth assay was performed with 2 cell lines: McCoy cells, a transformed human fibroblast cell line, and EaHY 926, a transformed human endothelial cell line. McCoy cells were maintained in Dulbecco's modified Eagle's medium (DMEM) containing 10% fetal bovine serum, 100 units/mL penicillin, 100 μg/mL streptomycin, and 0.3 mg/mL L-glutamine. The EaHY 926 cells were cultured in DMEM supplemented with 7.5% fetal bovine serum, 100 units/mL penicillin, 100 μg/mL streptomycin, 0.3 mg/mL L-glutamine, and HAT selection solution (0.1 mM hypoxanthine, 0.4 mM aminopterin, and 16 μM thymidine; Sera-lab, Sussex, England). The cells were incubated in 5% CO_2 at 37°C. Cells were removed from culture surfaces by a light trypsin/EDTA treatment (0.05% trypsin, 0.53 mM EDTA, GIBCO/BRL).

To maintain cell growth at very low densities for this assay it was necessary to add conditioned medium to the cells. Conditioned medium contains various nutrients and growth factors produced by the cells which enhance cell growth. Conditioned medium was prepared by seeding cells at subconfluence (20-30%), collecting, filtering, and freezing the medium after 4-5 days in culture.

The polymer samples were placed in 24 well plates and presoaked in PBS overnight at 37°C. Prior to cell seeding, the polymers were precoated with 500 μl/well of 20 μg/mL human FN in PBS for 2 hours at 37°C. The samples were then washed 3 times to remove any unbound FN. Conditioned medium (0.5 mL) was added to each well followed by 0.5 mL of cell suspension. The McCoy cells were seeded at 20 cells/well, and the EaHY 926 at 100 cells/well. After 4 days the cells were fixed with cold 95% EtOH and Giemsa stained. The cells were counted visually under a microscope. Triplicate samples were averaged.

5.4 Results

5.4.1 Surface Chemistry Characterization

Column 1 of Table 5.1 references the number designations given to the surfaces. The surface composition of the plasma treated discs is given in Table 5.1, showing the atomic composition of the chemical species found from the ESCA spectra and the percentage of carbon-containing functional groups as determined from the high-resolution C(1s) spectra (Dilks, 1981; Ratner and McElroy, 1986).

Table 5.1: Surface Composition Summary from ESCA Data: Surface Composition in Atomic Percent and Percent Functional Groups

#	Sample	C	N	O	Hydro-carbon	Amine/ether/ ester/ hydroxyl	Cabonyl / amide	Carboxyl/ ester
1	Thermanox®	70.4	1.8	27.7	58.8	19.0	4.6	15.9
2	AE Thermanox®	71.5	4.3	24.2	58.3	22.0	6.6	13.1
3	Methanol Plasma	72.1	3.5	24.3	66.6	14.8	7.7	10.9
4	Acetone Plasma	91.4	1.6	7.0	91.6	4.8	2.4	1.1
5	Acetone-10% N_2	83.9	3.6	12.5	79.2	12.5	4.7	3.5
6	Acetone-20% N_2	83.1	5.2	11.7	81.4	11.9	4.1	2.6
7	Acetone-30% N_2	77.9	10.0	12.1	69.5	21.0	7.2	2.2
8	Acetone-40% N_2	79.5	8.4	12.0	64.1	23.9	8.1	3.9
9	Allylamine	68.7	14.3	15.5	55.6	18.4	8.9	17.0
10	Acetone-20% O_2	83.4	1.7	14.9	75.2	14.4	5.7	4.7
11	Acetone-40% O_2	74.7	1.5	23.7	63.0	19.6	8.6	8.8
12	Acrylic Acid	80.4	--	19.6	64.1	19.9	5.3	10.7

As can be seen in Figure 5.1 and Table 5.1, the fraction of nitrogen-containing functional groups generally increases with increasing nitrogen (N) in the feed plasma. A broadening of the carbon peak in the C(1s) high-resolution spectra was seen with increasing N, suggesting an increase in amine, amide, or other nitrogenous functional groups. A precise determination of the percentage of these groups is not possible from the C(1s) spectra due to the small chemical shifts (less than 1 eV and overlapping) of amine,

amide and carbon-oxygen functional groups. Reference values used for peak fitting are as follows: hydrocarbon 285.0 eV, amine/ether/ester/hydroxyl 285.7-286.5 eV, carbonyl/amide 288.0-288.2 eV, carboxyl/ester 288.8 eV (Ratner and McElroy, 1986). However, by looking at the ratios of the functional group peaks, some indication of changes in a particular type of functional group relative to another polymer sample can be made. A broad N(1s) peak was observed, supporting the C(1s) data suggesting a variety of nitrogen-containing groups.

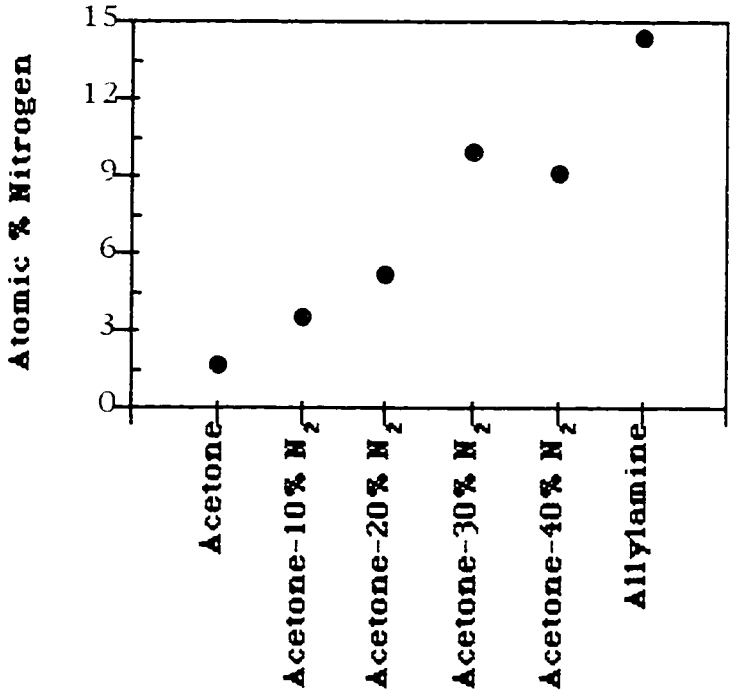

Figure 5.1 Nitrogen content of plasma films for each of the plasma feed gas mixtures, as determined by ESCA.

Similarly, with an increasing fraction of oxygen (O) in the plasma feed, an increase in surface O content was seen on the acetone-oxygen plasmas (Figure 5.2). A broadening of the C(1s) peak was observed, suggesting a variety of oxygen-containing functional groups such as carbonyl, carboxyl, ester, ether, and hydroxyl groups. The acrylic acid

plasma also has a variety of functional groups present, similar to the acetone-oxygen plasmas.

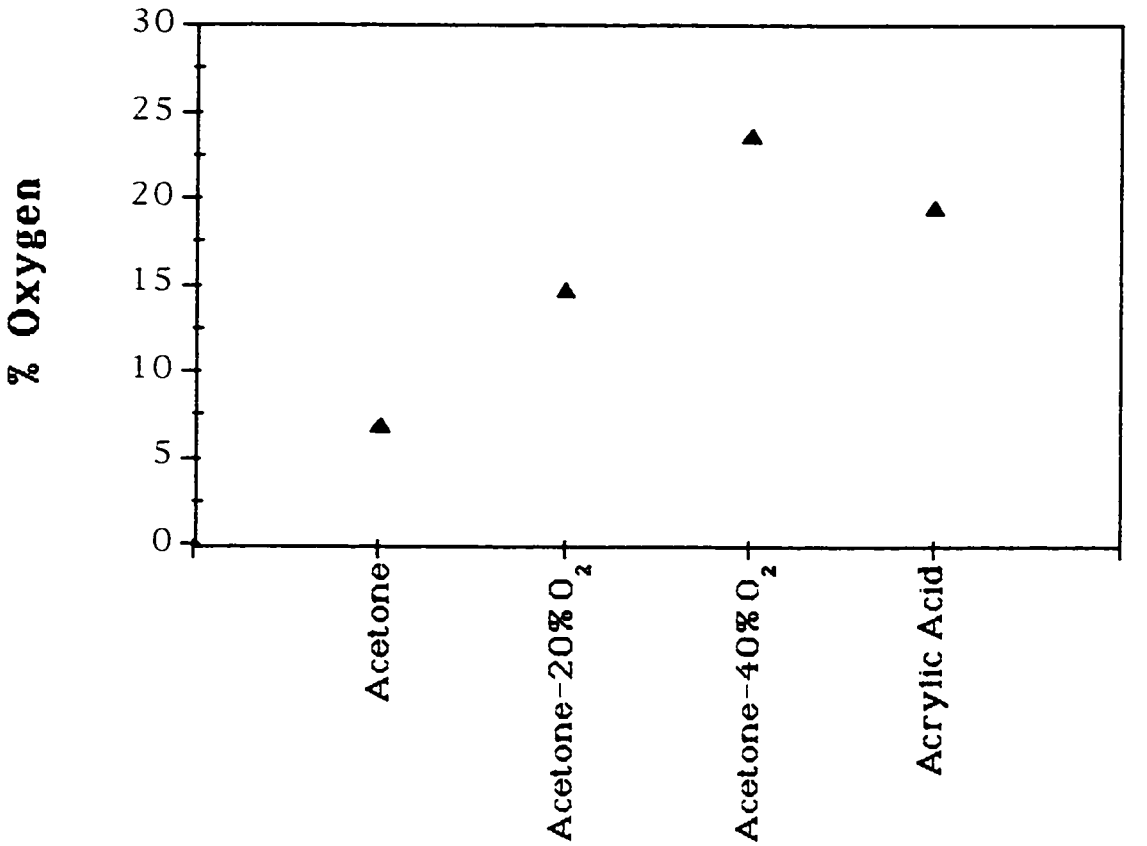

Figure 5.2 Oxygen content of plasma films for each of the plasma feed gas mixtures, as determined by ESCA.

5.4.2 Scatchard Analysis of Protein Adsorption Isotherms

Table 5.2 summarizes the apparent K_a and B_{max} values calculated from the Scatchard plots for each polymer. The curve fits for all isotherm and Scatchard plots were determined from the apparent K_a and B_{max} values.

Type 1 binding is determined from a linear Scatchard plot; a linear plot suggests only one type of binding occurred with apparent K_a and B_{max} values determined from the

slope of the line and the x-intercept respectively. An example of this type of adsorption isotherm and Scatchard plot are shown in Figure 5.3 a and b.

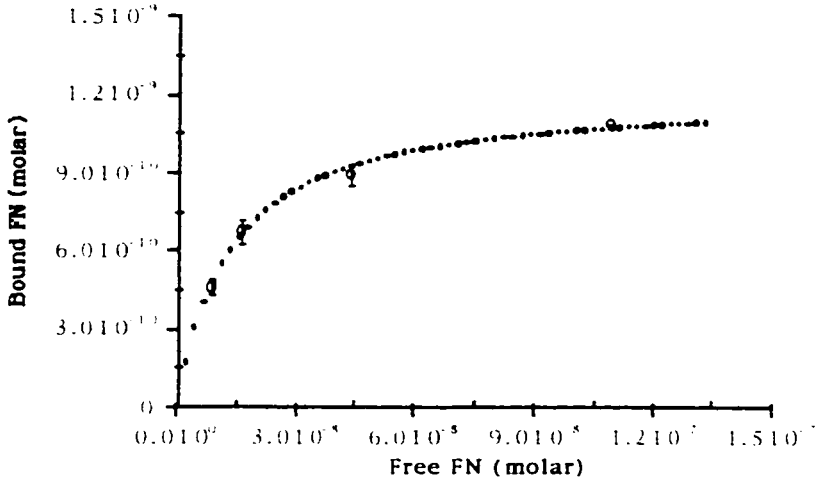

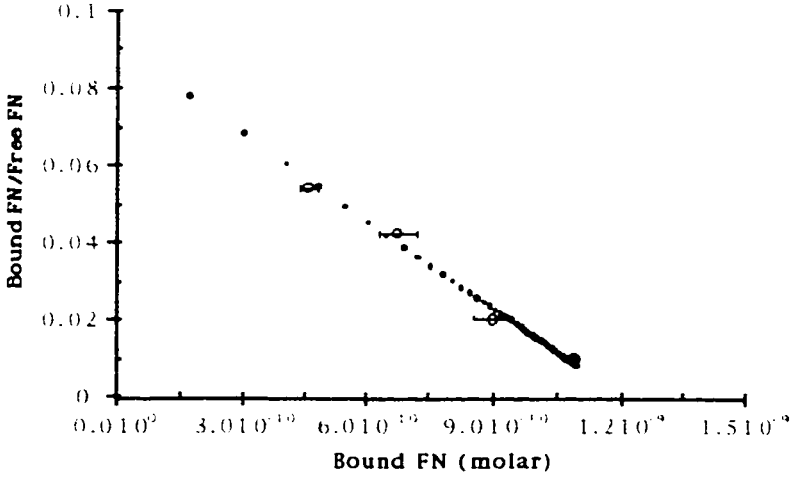

Figures 5.3 a (top) and b (bottom): a) Acetone/20% N_2 fibronectin adsorption isotherm and b) Scatchard plot.

Type 2 binding is indicated by a biphasic Scatchard plot (e.g. Acetone/30% N_2 in Figure 5.4 a and b); this shows that at least two types of binding occurred; one of high

affinity (apparent K_{a1}) and one of low affinity (apparent K_{a2}). Contributions of each binding type must be considered for the proper curve fit by selecting tangents to the initial and final slope for the high and low affinity apparent K_a's. This provides the two x-intercepts, designated B_{max1} for the number of high affinity binding sites (initial slope), and B_{max2} for the low affinity binding sites (final slope). As can be seen in Figures 5.3 and 5.4, the values of apparent K_a and B_{max} values calculated for each polymer generated good fits to the experimental points.

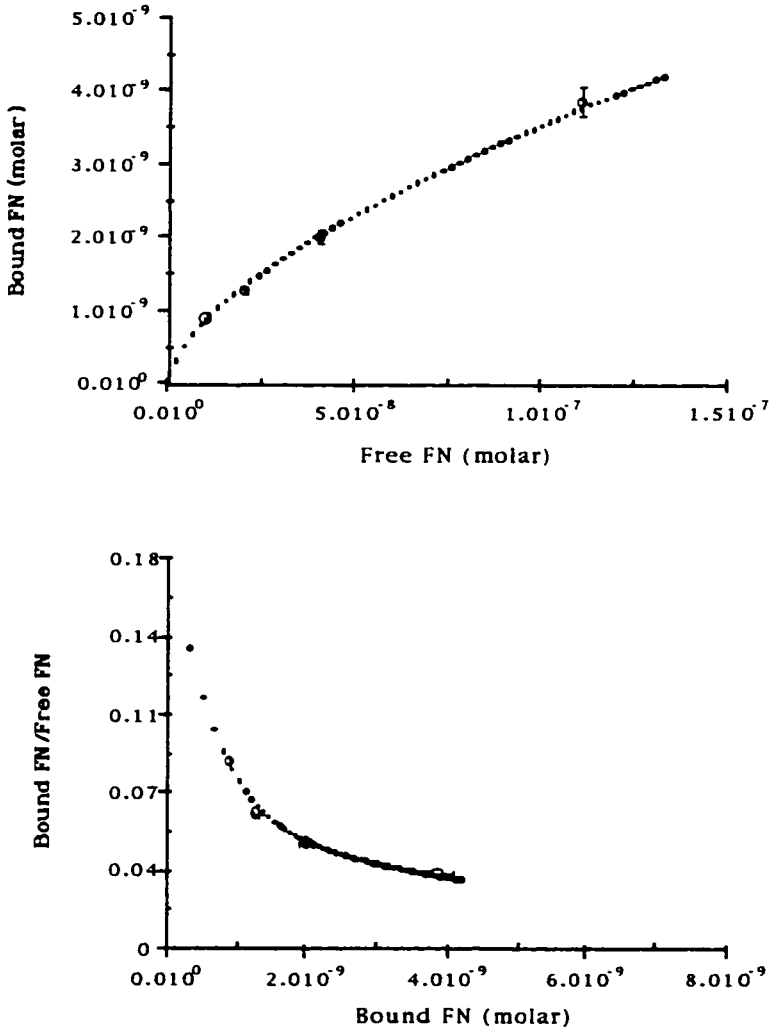

Figure 5.4 a (top) and b (bottom): a) Acetone/30% N_2 fibronectin adsorption isotherm and b) Scatchard plot.

Table 5.2: Summary of Apparent K_a (aK_a) and B_{max} Values

#	Plasma Feed Composition	High aK_a (x 10^8 M^{-1})	Low aK_a (x 10^8 M^{-1})	B_{max1} (x 10^{-10} M)	B_{max2} (x10^{-10} M)
1	Thermanox®	2.3	--	7.4	--
2	AE-Thermanox®	2.5	0.03	2.4	12
3	Methanol-100%	1.4	--	4.9	--
4	Acetone-100%	2.6	--	6.8	--
5	Acetone-10% N_2	1.8	--	8.1	--
6	Acetone-20% N_2	0.76	--	12.1	--
7	Acetone-30% N_2	1.8	0.03	8.0	120
8	Acetone-40% N_2	1.0	0.03	11.0	130
9	Allylamine	2.5	0.05	7.5	80
10	Acetone-20% O_2	1.8	--	8.5	--
11	Acetone-40% O_2	1.8	.02	5.7	23
12	Acrylic Acid	2.0	0.03	9.2	50

The Thermanox control, methanol, acetone, acetone-10 and 20% N_2, and acetone-20% O_2 plasmas exhibit the classic Langmuir isotherm characteristic as suggested by the defined plateau on the isotherm plots. The Scatchard analysis indicates that these polymers have only one type of binding site, based on the shape of the Scatchard plot (linear). The apparent K_a values also indicate that the binding is in the high-affinity range. For cell-receptor/ligand interactions, values near 10^8 M^{-1} are considered high affinity (Limbird, 1986). All polymers of this set, except the acetone-20% N_2, have apparent

affinity constants in excess of 1 x 10^8 M^{-1}. These data suggest the surfaces are homogeneous in their binding behavior; one type of high-affinity adsorption occurs for FN on these surfaces.

Argon-etched Thermanox, acetone-30% and 40% N_2, acetone-40% O_2, allylamine and acrylic acid plasmas all show the characteristic biphasic Scatchard plot, indicative of two types of binding: one fraction binding with a higher affinity, and then a low-affinity fraction. All polymers in this group have high affinity apparent K_a's (K_{a1}) in excess of 1 x 10^8 M^{-1} much like those found in the type 1 binding group. The low affinity sites have apparent K_a's (K_{a2}) nearly two orders of magnitude less than the high affinity sites. All the apparent K_a's for the low affinity sites are of the same order of magnitude, 10^6 M^{-1}. For cell-receptor/ligand interactions, K_a's in this range are considered low-affinity and non-specific in nature (Limbird, 1986). This indicates that the non-specific type of binding is similar for all of these polymers. These polymers clearly exhibit characteristics suggestive of specific and nonspecific binding of FN to the surface.

Within the acetone-nitrogen series, acetone-0-40% N_2, increasing N content in the feed plasma shows a drop in the affinity constants from 2.6 x 10^8 M^{-1} to 0.8 x 10^8 M^{-1} (Figure 5.5). Also, the change from a one-site, high-affinity surface to type 2 binding is seen with increasing N_2 content in the plasma feed. This suggests that the surface changes from a highly specific surface for FN in its binding characteristics, to a less homogeneous, less specific surface that binds much of the FN with a lower apparent affinity. A minimum in the apparent high affinity constants appears between 5-9% N surface content.

The allylamine surface (included in Figure 5.5) had a very high N content and apparent K_{a1}, displaying a low-affinity fraction as well. Its FN binding characteristics were similar to those of the acetone-30% and -40% N_2 feed plasmas. This suggests a functional group is present on this surface with binding characteristics similar to the

acetone-N_2 plasma films. Unfortunately, the high-resolution N(1s) ESCA spectrum displayed a broad peak, which makes it difficult to determine the dominance of one type of nitrogen-containing functional group that is associated with each type of binding characteristic seen in this polymer series.

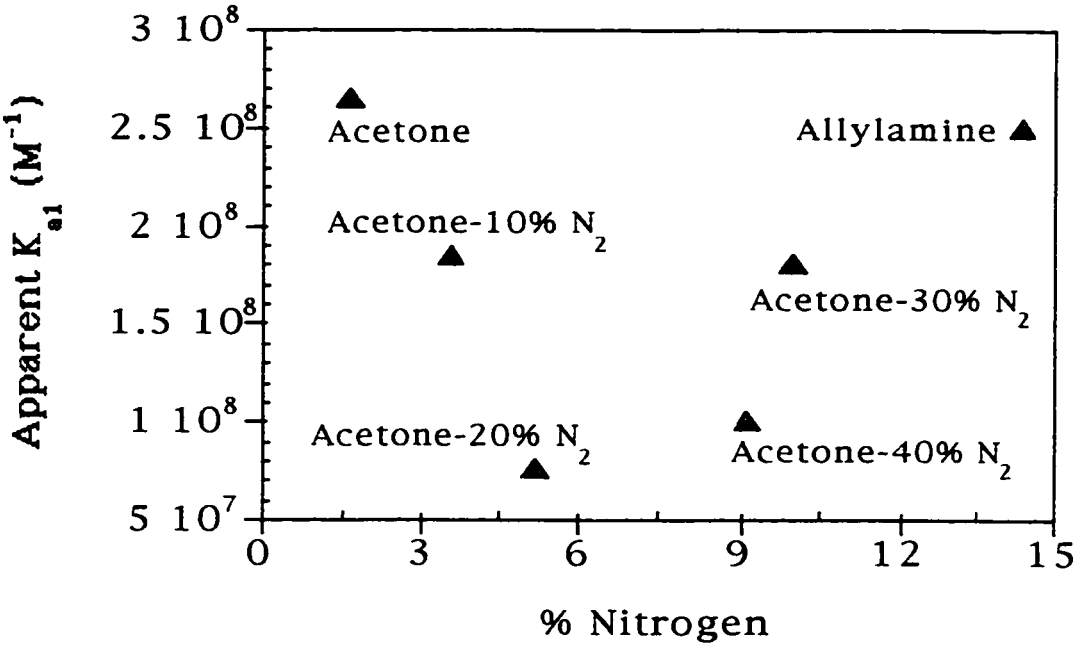

Figure 5.5 The apparent K_a initially versus % N.

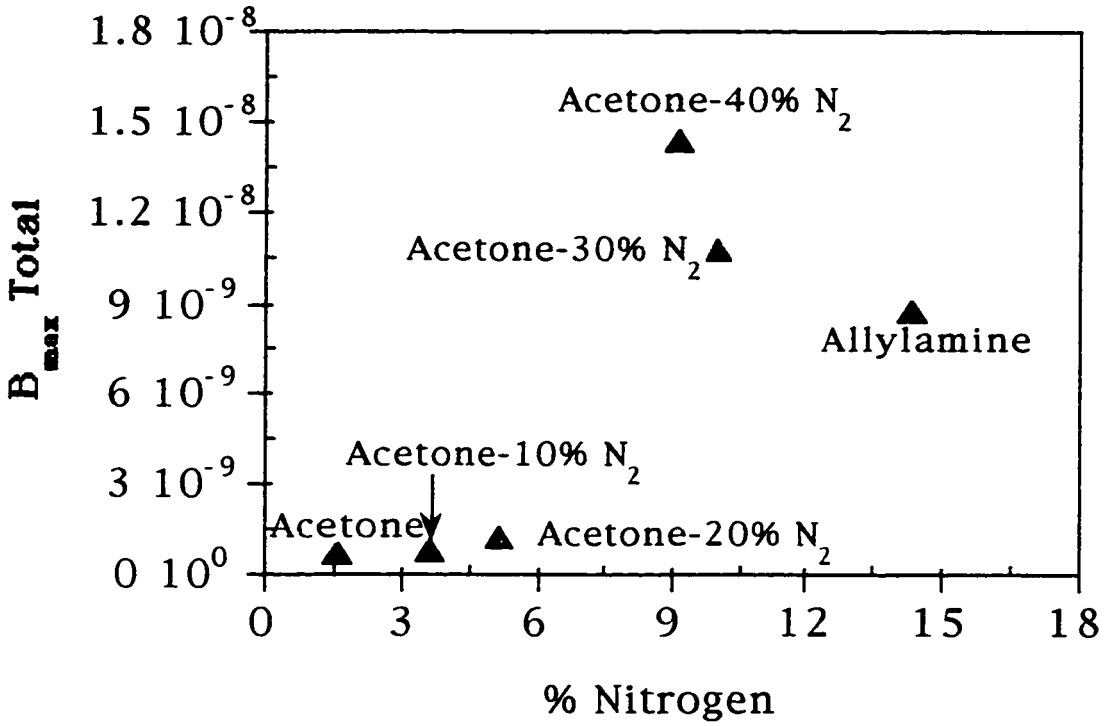

Figure 5.6 The total B_{max} values (B_{max1} + B_{max2}) increase with increasing N content reaching a maximum at 9% N surface content. At higher N surface content, the total amount of protein bound decreases. The high values of B_{max} for the acetone-30%, acetone-40%, and the allylamine feed plasmas are primarily due to the contribution from the low-affinity fraction of FN.

Concurrent with the drop in K_a is a rise in the B_{max} values with increasing N content in the plasma feed (Figure 5.6). An increase in B_{max} indicates there is an increase in the total amount of bound FN, with a large contribution from B_{max2} for the higher N content plasma films (above 6% N). This could suggest a possible increase in the total surface area, caused by etching, increased roughness, or uneven deposition on the surface during the plasma process. However, as is shown in Table 3, there is no clear indication that increases in surface roughness, determined by AFM, contribute to the increase in FN

binding to the surface. Also given in Table 3 are the total B_{max} (B_{max1} + B_{max2}), and the theoretical maximum of bound FN in ng/cm^2 converted from the total B_{max} values. Those values above 1000 ng/cm^2 indicate multilayer formation, and we speculate this is due to association of the outer FN layers with a tightly bound fraction directly contacting the surface. It must be noted, however, that these B_{max} values were not experimentally determined, but high levels of FN did adsorb on the type 2 materials (approximately 1000-1200 ng/cm^2 at the 50 μg/mL adsorption solution concentration). This phenomenon is clearly seen in the N series, where the acetone-30% and -40% N_2 plasma feeds are smoother than the 0-20% N samples, but they have large amounts of FN adsorbed to the surface.

Table 5.3: Surface Roughness and Total FN Adsorption

Plasma Feed	Roughness (nm)	B_{max} Total (10^{-10} M)	B_{max} Total (ng/cm^2)*
Thermanox®	28.56 +/- 1.46	7.4	188.0
AE-Thermanox®	25.57 +/- 3.08	14.4	365.8
Methanol-100%	231.12 +/- 14.21	4.9	124.5
Acetone-100%	29.41 +/- 3.94	6.8	172.7
Acetone-10% N_2	173.28 +/- 23.66	8.1	205.7
Acetone-20% N_2	277.39 +/- 32.12	12.1	307.3
Acetone-30% N_2	93.70 +/- 10.80	128.0	3251.2
Acetone-40% N_2	76.90 +/- 9.81	141.0	3581.4
Allylamine	376.30 +/- 24.05	87.5	2222.5
Acetone-20% O_2	77.21 +/- 9.41	8.5	215.9
Acetone-40% O_2	275.89 +/- 35.02	28.7	729.0
Acrylic Acid	87.27 +/- 6.43	59.2	1503.7

*These values were converted from molarity units in the previous column assuming the molecular weight of FN is 450,000 g/mole in a 1 mL adsorption volume. These values, calculated from the Scatchard plots for each isotherm, represent the theoretical maximum of bound FN.

The acetone-oxygen series exhibits the same trends seen in the nitrogen series (Figure 5.7). The difference between apparent K_a values is much less however, ranging from 2.6x 10^8 M^{-1} to 1.8 x 10^8 M^{-1} for 0% and 40% oxygen in the feed plasma films. The rise in the B_{max} values seen in Figure 8 is also less marked than seen in the acetone-nitrogen series, but there are still some interesting differences. The acrylic acid plasma should have similar functional groups to the acetone-oxygen series. The apparent K_{a1}

was consistent with the acetone-oxygen series, and had similar binding characteristics to the acetone-40% oxygen plasma (type 2 binding, increased B_{max}), which is consistent with the similar surface oxygen content of these two surfaces (Table 5.1). Once again, the low affinity fraction of FN accounts for the large increases in the total B_{max}.

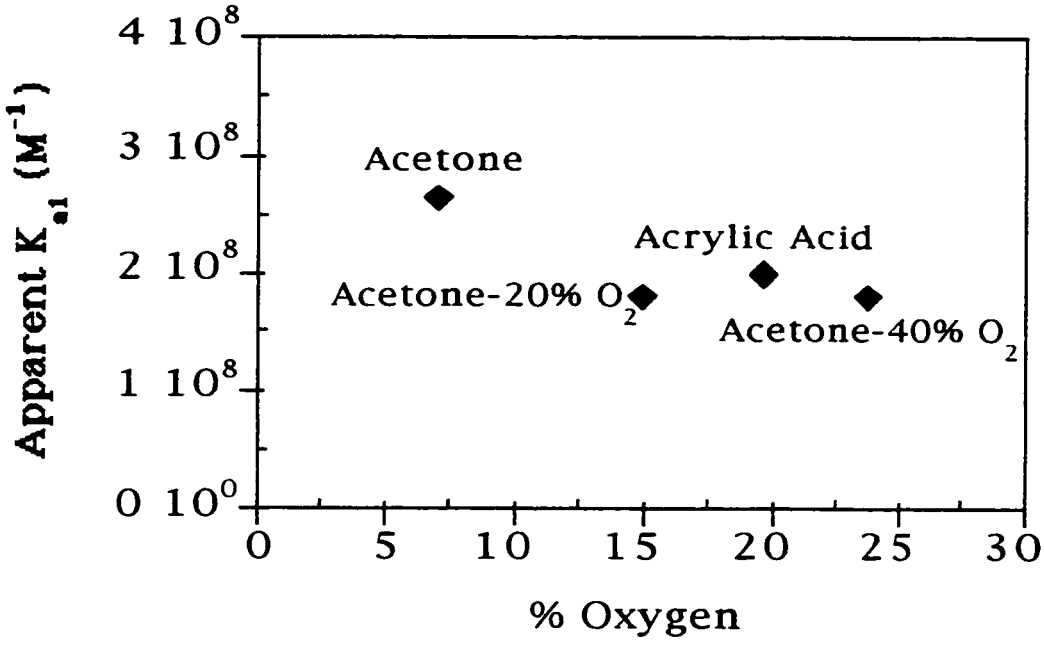

Figure 5.7 Little change is observed in the apparent K_a's for the acetone-oxygen and acrylic acid plasma-deposited films.

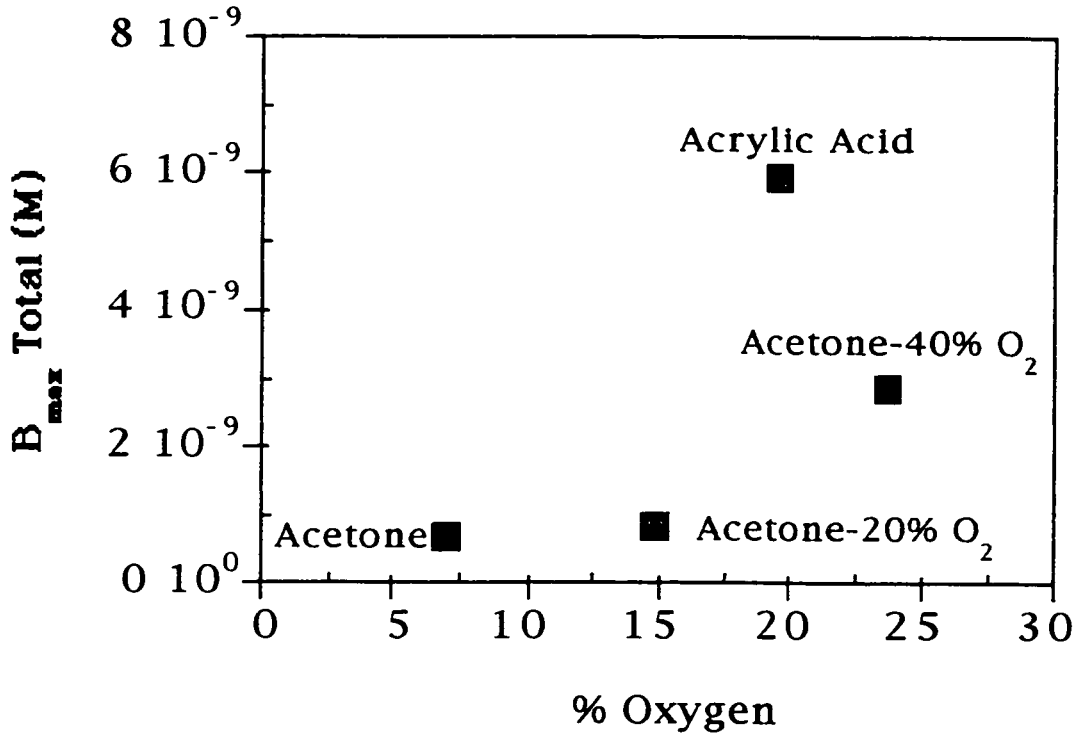

Figure 5.8 A marked rise in the B_{max} is noted for the acetone-40% O_2 and acrylic acid plasma films, primarily due to the low-affinity fraction (B_{max2}).

Another interesting comparison is between the clean Thermanox® and the argon-etched coverslips. The apparent K_a's are similar, but a switch from type 1 to type 2 FN binding is observed. Because there is no difference in the surface roughness of these samples, the surface composition must be dictating the FN binding to these surfaces.

5.4.3 Cell Growth Assays

The McCoy cell assay showed little difference in cell growth on the different substrates (Figure 5.9). Only the acetone-30% N_2 surface was significantly different ($p=0.003$) compared to the fibronectin-coated tissue culture polystyrene (TCPS + FN) control, showing a decrease in cell growth on this surface. Although several of the

materials showed growth in excess of the TCPS control, none of them were significantly greater.

The EaHY 926 cells responded differntly than the McCoy cells, showing some interesting trends in cell proliferation. For the nitrogen-containing surfaces adsorbing large amounts of FN (such as for the acetone-30% N_2, -40% N_2 and the allylamine surfaces), there is a significant decrease in cell growth compared to the control ($p<0.01$), unlike the acetone-20% N_2 surface. The acetone-O_2, acrylic acid and methanol surfaces were good substrates for cell growth, however none of the surfaces showed proliferation in excess of the TCPS + FN control. There appears to be no trend in type 1 or 2 binding and cell growth. Although type 2 members of the nitrogen series showed decreases in cell growth, other type 2 surfaces proved to be good cell growth supports (acetone-40% O_2 and acrylic acid plasmas).

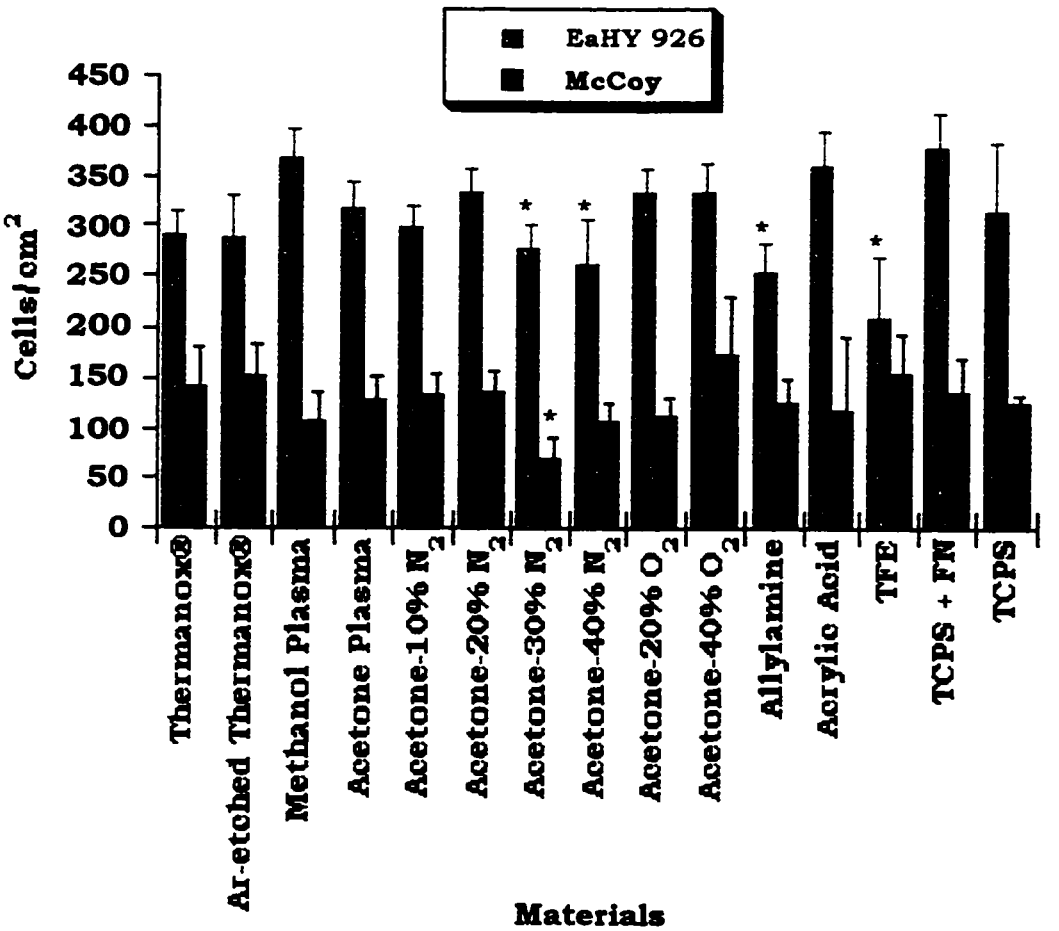

Figure 5.9 McCoy and EaHY 926 clonal cell growth per cm^2. Samples were pre-coated with FN prior to cell seeding. Significance at $p<0.01$ is denoted by *.

If the data are normalized to the theoretical amount of FN bound, significant differences can be seen. The clonal growth data presented in Figure 10 are the cells/cm^2 divided by the theoretical FN bound per cm2 at the 20 ug/mL adsorption concentration, determined from the adsorption isotherms for each material. Since the TCPS surface was not analyzed for amount of FN bound, Thermanox® is used as the control surface here.

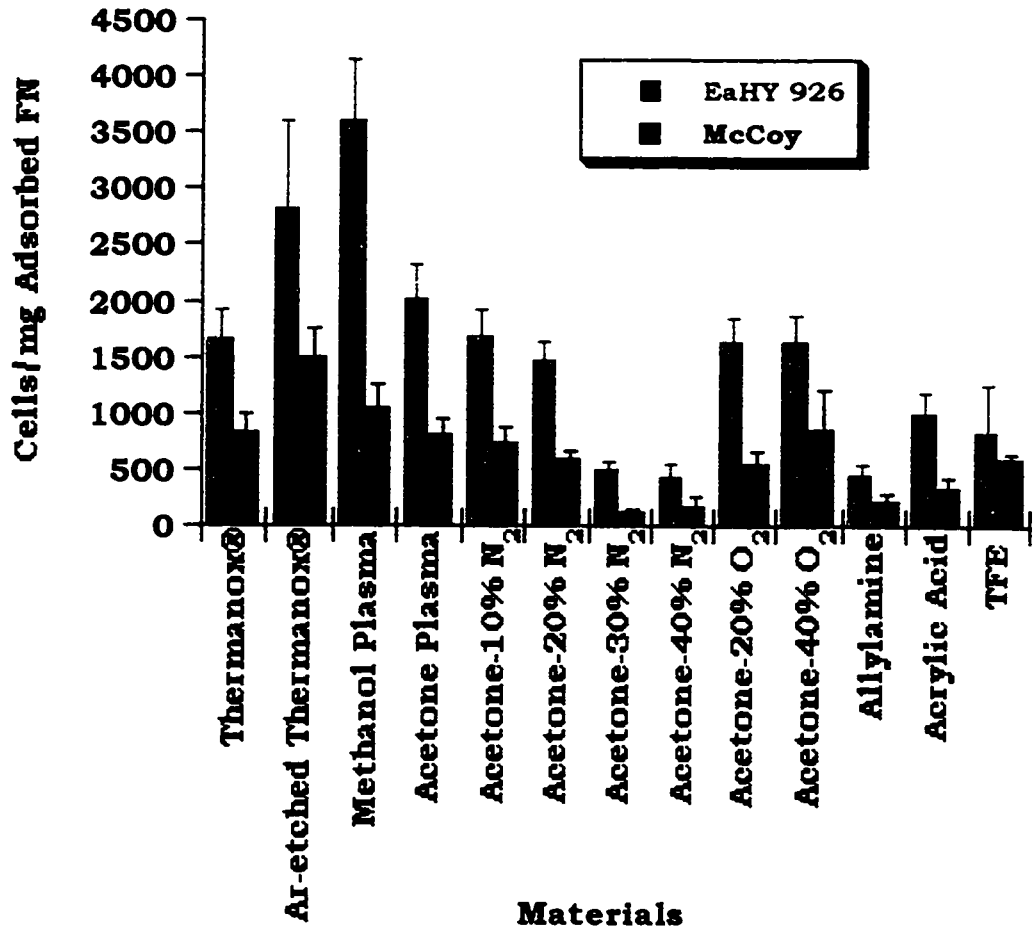

Figure 5.10 McCoy and EaHY 926 data from Figure 5.9 were normalized to the amount of FN bound to each surface at the adsorption concentration of 20 μg/mL determined from the adsorption isotherms.

The data in Figure 5.10 suggest that having more adsorbed FN does not necessarily enhance cell growth. Those surfaces adsorbing large quantities of FN show no advantage in cell growth over those that bind considerably lesser amounts of FN (e.g. methanol vs. acrylic acid plasmas). We suggest those surfaces exhibiting type 2 binding

have a low affinity, loosely-bound layer of FN contacting the cells which does not appear to influence how well cells attach to the surface (nitrogen-containing plasmas), but not all type 2 materials show this effect.

5.5 Discussion

In plasma-deposited films, a distribution of functional groups is produced due to molecular fragmentation during the plasma process (López and Ratner, 1991; López and Ratner, 1992; López et al., 1993; Winters, 1980; Winters et al., 1985). ESCA is limited in its ability to unambiguously identify certain chemical species due to overlapping binding energies (Dilks, 1981). The ESCA analysis of the C(1s) region of the oxygen-containing plasmas suggests the presence of ether, alcohol, carbonyl, acid and/or ester groups on the surfaces. The acetone/nitrogen surfaces are even more complex: along with the potential for all of the aforementioned oxygen-containing groups, amide and amine functionalities are also present. Within the high resolution C(1s) spectra, peak deconvolution was performed by fitting 4 functionalities for the oxygen-containing surfaces (hydrocarbon, ether/ester/hydroxyl, carbonyl, and carboxyl/ester) based on their predicted binding energy shifts. The same was done for the nitrogen-containing groups, but due to the overlap of amine, ether, ester and hydroxyl group binding energies, these individual peaks were not resolved. Thus these four functional groups were fit as one peak with the assumptions that the oxygen and nitrogen in these surfaces were associated with carbon in some manner, and that all of the groups mentioned were present to some degree. The amide and carbonyl peaks were also fit as one peak for the same reasons. The high-resolution oxygen and nitrogen ESCA spectra showed broad, featureless peaks, indicating a variety of functional groups. As a result, no unambiguous information could be extracted from the high resolution O(1s) and N(1s) spectra.

The ratios of the C(1s) peak components were examined. For the oxygen-containing plasmas, the nitrogen content did not change significantly through the acetone, acetone/O_2, and acrylic acid series, indicating that the changes in the surfaces were due to the increase in the oxygen-content in the films (increase from 7% to 23% O). With increasing oxygen in the acetone plasma feed (20% to 40%), the ether/ester/hydroxyl peak increased by 5%, the carbonyl peak by about 3%, and the carboxyl/ester by 4%. Also seen with these changes in surface composition were changes from type 1 to type 2 binding in the Scatchard analysis. With a surface similar to the acetone/40% O_2 feed in composition and Scatchard analysis, the acrylic acid plasma shows an increase in the ether/ester/hydroxyl and carboxyl/ester content, but a decrease in the carbonyl content. This suggests that the ether/ester/hydroxyl and carboxyl/ester functional groups may be responsible for the changes from a type 1 to type 2 protein binding on these surfaces, not the carbonyl content. Due to the concurrent increase in the ether/ester/hydroxyl and carboxyl/ester content in this polymer series, it suggests an increase in the ester content alone that is contributing to the switch from type 1 to type 2 binding since the ester content of the material will contribute to both of these peaks. Without further determination of the exact functional group composition, however, this is speculation. From the cell growth studies, the acrylic acid surface supported cell growth better than the other surfaces. Previous studies have also shown increased cell growth on acetone/oxygen surfaces with high carboxyl content (Ertel et al., 1991). However, the FN adsorption data contradicts that seen in an earlier study where a decrease in FN adsorption was observed with increasing oxygen content (Ertel et al., 1991). Here we see an increase in FN adsorption.

Numerous studies have reported on the effects of amine groups on cell growth (Chilkoti et al., 1995; Massia and Hubbell, 1992; Steele et al., 1995). The acetone/N_2 films in this study showed a constant ratio of amine to amide groups of approximately 2.75:1 (amine:amide) from the high resolution C(1s) ESCA spectra. The carboxyl/ester

and overall oxygen content remained constant throughout the nitrogen series, with the exception of the allylamine plasma, as seen in Table 1. The allylamine surface has a high oxygen content, which can be attributed to subsequent oxidation of the surface after plasma deposition. In a previous study, the oxygen content increased with aging from 4.5% to approximately 14% after 80 days (Francese, 1989). Here the allylamine surfaces aged for approximately 90 days prior to use. The dramatic increase in the "carboxyl/ester" peak is probably due to urea-like functional groups ($-N_2-C=O$), not carboxylic acid or ester groups. The same effect of amine/ether/ester/hydroxyl content in the films on the type of FN binding (type 1 vs. 2) seen with the oxygen plasmas was demonstrated in the nitrogen-containing surfaces as well. All of the N-containing surfaces with type 2 FN binding had a high amine/ether/ester/hydroxyl content (18-23%) compared to the type 1 binding surfaces (4-14%). This suggests that the FN binding changes are dominated by the effects of increasing amine and amide content with increasing nitrogen in the feed plasmas. These findings are consistent with another study where it was shown that adsorption of FN from serum increased with increasing N-content in acetone-N_2 films (Ertel et al., 1990).

Our results are consistent with an increase in charged species in the form of amine or carboxylic acid groups as being responsible for the change to type 2 FN binding. Interactions between oppositely-charged species on the surface and protein could contribute to protein binding (e.g. negatively-charged carbohydrates on protein with amine groups on surface) or participate in hydrogen bonding. van Wachem et al. showed that charged surfaces (positive and negative) increased cell attachment, and on certain charged surfaces cell proliferation occurred (Wachem, 1987). Another study showed higher levels of FN adsorption on carboxylic acid-terminated self-assembled monolayers (SAMs) compared to methyl ester, hydroxyl, or methyl-terminated SAMs (Tidwell et al., 1997). The increased amount of FN adsorbed to the carboxyl surface may have been responsible

for increased cell growth though the ability of albumin to be displaced from the surface was also correlated with cell growth. In this study, increased cell growth was also seen with the acrylic acid plasma surfaces.

Protein adsorption isotherms are sensitive to true surface area. The changes in protein adsorption are attributed to the surface chemistry, not to changes in surface roughness, with the possible exception of the acetone/O_2 surfaces, as demonstrated in Table 5.3. Since these surfaces are relatively smooth, the change in FN adsorption may be attributed to the density, type, or heterogeneity of functional groups on the surfaces. The effect on protein adsorption of argon-etching is marked. Since there is no alteration in surface roughness between the etched and non-etched Thermanox, the changes in the amount and type of binding of FN to these surfaces must be due to differences in surface chemistry, indicated by an increase in atomic %N by ESCA. However, the method employed only gives variations in the Z direction measurement of peaks and valleys, which is not a true determination of surface area.

Langmuir and Freundlich isotherms have been used to describe proteins adsorbing to surfaces (Horbett et al., 1977; Wojciechowski and Brash, 1993). Unfortunately, these data analysis methods give little insight into the processes involved in protein adsorption, such as why certain proteins are more attracted to certain surfaces and why they may displace other adsorbed proteins. Our use of the Scatchard analysis is an attempt to model the affinity between a protein and a surface. For example, an adsorbate/surface interaction exhibiting a characteristic Langmuir isotherm, by definition, is homogeneous in nature (Adamson, 1982). In these experiments, such adsorption can be described by type 1 binding of FN. In contrast, the Freundlich-type isotherms indicate heterogeneity in the surface, and demonstrate type 2 binding in the Scatchard analysis (Adamson, 1982). As seen in Tables 5.1 and 5.2, increases in the amine/ether/ ester/hydroxyl, carbonyl/amide, and carboxyl/ester peaks correlate with type 2 FN binding, indicating that a more

chemically complex surface allows for high levels of FN binding, presumably due to increases in the number of binding sites, or the types of binding sites. The biphasic Scatchard plots of type 2 surfaces demonstrate the heterogeneity of the material surface, indicative of the availability of both high and low affinity sites binding sites. Surfaces that are less chemically complex demonstrate simple FN binding to high affinity sites only, as shown by a linear Scatchard plot.

To investigate the role of surface chemistry in surface-protein interactions, the methods used here provide a systematic approach to quantitate a protein's affinity for a surface. These results are, in effect, an approximation of affinity, due to the differing nature of receptor-ligand interactions compared to non-specific surface-protein interactions. The primary differences in the cell receptor and surface adsorption systems are: 1) a protein will have several points of contact to the surface, 2) the availability of binding sites will change as surface saturation is approached, and 3) the reversibility of protein adsorption may not be a valid assumption. The number of contacts that a protein makes with the surface will directly affect its affinity for a surface through specific interactions of multiple side chains on the protein with surface functional groups, whether they be hydrophobic or hydrophilic in nature. This is analogous to what occurs when a ligand interacts with a receptor: hydrophobic amino acid residues will find hydrophobic pockets, and charged side chains will interact with residues of complementary charge. In the case of protein adsorption, specific adsorbent/adsorbate interactions are more akin to chemisorption (Langmuir-type isotherms with large K values) than to physisorption (Adamson, 1982). The resulting chemical interaction will affect the reversibility of binding. This was seen in these experiments: after a 24 hr soak in adsorption buffer, little protein was seen to desorb (data not shown). This is not surprising, however, since there was no driving force for the protein to dissociate from the surface, such as addition of a surfactant (SDS) or displacement by other proteins (such as those in serum).

One phenomenon unaccounted for in this model is the potential for formation of protein multilayers. The additional layers of FN could be bound to the first adsorbed layer via the FN binding site in FN which is important for matrix formation *in vivo*. Other models, such as the Brunauer, Emmett, and Teller (BET) model, take into account the possibility of multilayer formation. In the BET model, the adsorption process is akin to phase separation, with the heat of adsorption measured for first layer adsorbed, and heat of condensation for the additional layers (Adamson, 1982). Similarly, one could envision the first layer being chemisorbed and the subsequent layers physisorbed. At higher concentrations of protein one would anticipate multilayer formation as unoccupied sites on the surface become less available. Further analysis, for example with ellipsometry, would be necessary to determine film thickness and to see if this correlates with multilayer formation. Also, this model, in common with the Langmuir and Freundlich calculations, does not consider the effect of lateral interactions of adsorbed FN. Another interaction which may prove important for FN adsorption to surfaces is the presence of a FN binding site within FN which is important for matrix stabilization *in vivo* (Furcht, 1983; Morla and Ruoslahti, 1992).

FN precoated materials used in this study showed little differences in their ability to support McCoy cell growth. However, the EaHY 926 cells were more sensitive to changes in growth substrate. Other studies have shown a correlation between increases in surface oxygen content and cell growth where precoating of materials with extracellular matrix proteins was not done (Ertel et al., 1990). Differences in EAHY 926 cell growth were seen. However, there appears to be no trend in type 1 or 2 binding and cell growth. Although type 2 members of the nitrogen series showed decreases in cell growth (acetone-30% and -40% N_2, allylamine), other type 2 surfaces proved to be good cell growth supports (acetone-40% O_2 and acrylic acid plasmas). Similar results were reported showing that increases in N-content of acetone-N_2 films did not significantly affect cell

growth even though high levels of FN adsorbed to these surfaces (Ertel et al., 1990). This would indicate the protein contacting the cell surface is not bound with a high enough affinity or favorable conformation to enhance cell growth on those surfaces that bind large amounts of FN. For type 2 materials, the low-affinity layer could possibly be easily remodeled or pushed aside by the cell in such a way that the presence of more protein does not adversely affect cell growth on these surfaces. Alternatively, the low-affinity layer of FN may be displaced by proteins of higher affinity found in the serum-containing medium. One of the proteins that may displace FN is vitronectin (VN), a similar adhesive protein commonly found in serum which is also responsible for cell adhesion to surfaces (Steele et al., 1995). In another study, Steele et al. have shown that oxygen and nitrogen plasmas differ in their FN and VN requirements for cell adhesion. For oxygen plasmas, cell attachment occurred primarily due to VN adsorption, with less dependency on FN. Conversely, the nitrogen plasmas could sustain cell attachment with either FN or VN (Steele et al., 1994).

Steele's group has also demonstrated that on TCPS, the half-maximal level of human umbilical vein endothelial cell attachment for FN was about 12 ng/cm^2, where as on a nitrogen-containing surface (Primaria®) it was approximately half that level (Steele et al., 1995). This suggests that the conformation of the protein on the surface (dictated by the surface chemistry) can make the surface more "potent" for cell attachment. Also, the level of adsorbed FN for maximal cell growth on a given surface is far less than what was obtained in this study by precoating from a pure FN solution. For this study, depending on the surface, the adsorbed FN at the 20 μg/mL pure FN solution concentration was in the μg/cm^2 range, in contrast to the ng/cm^2 range seen with adsorptions from serum. We caution that cell attachment studies rarely predict proliferation.

5.6 Conclusions

In conclusion, the group of plasma deposited films studied here exhibits a wide range of protein adsorption characteristics with different surface treatments. The use of Scatchard analysis for protein adsorption provides a useful method for determining differences in binding characteristics of proteins to surfaces, providing more information than just total protein adsorption. Although this use of Scatchard analysis to model protein adsorption is novel (Stanislawski et al., 1993), it is useful for determining the differences in FN affinity for this set of polymers samples. It is widely believed that proteins have different affinities for surfaces (Horbett, 1984; Horbett et al., 1977; Wojciechowski and Brash, 1993), but until this time, no one has developed a systematic method of measuring these affinities. This Scatchard system could be applied to protein adsorption from serum, which would be more relevant than the single protein adsorption studied here. Lastly, this method may be useful to study the effect of surface/protein interactions on cellular responses *in vitro*. Others have studied this phenomenon (Kiaei et al., 1992; Pettit et al., 1992) suggesting protein affinity and binding characteristics may be as important as the protein's conformation for cell growth and migration.

5.7 Acknowledgments

We thank the French Government for their generous support for this work with the Chateaubriand Fellowship for Ann Schmierer. The LRM, Université Paris Nord, provided further support for this work. Winston Ciridon, Deborah Leach-Scampavia, and Stefan Domino at the University of Washington provided technical assistance for sample preparation and surface analysis.

5.8 Notes for Chapter 5

Adamson, A. W. (1982). Physical Chemistry of Surfaces, 4th edition Edition (New York: John Wiley & Sons).

Chilkoti, A., Schmierer, A. E., Perez-Luna, V. H., and Ratner, B. D. (1995). Investigating the Relationship between Surface Chemistry and Endothelial Cell Growth: Partial Least-Squares Regression of the Static Secondary Ion Mass Spectra of Oxygen-Containing Plasma Deposited Films. Anal. Chem. *67*, 2883-2891.

Dilks, A. (1981). Electron Spectroscopy: Theory, Techniques and Applications., Volume 4, A. B. Baker and C. R. Brundle, eds. (London: Academic Press).

Ertel, S. I., Chilkoti, A., Horbett, T. A., and Ratner, B. D. (1991). Endothelial cell growth on oxygen-containing films deposited by radio-frequency plasmas: the role of surface carbonyl groups. J. Biomater. Sci. Polymer Edn. *3*, 163-183.

Ertel, S. I., Ratner, B. D., and Horbett, T. A. (1991). The Adsorption and Elutability of Albumin, IgG, and Fibronectin on Radiofrequency Plasma Deposited Polystyrene. J. Coll. Interface Sci. *147*, 433-442.

Ertel, S. I., Ratner, B. D., and Horbett, T. A. (1990). Radiofrequency plasma deposition of oxygen-containing films on polystyrene and poly(ethylene terephthalate) substrates improves endothelial cell growth. J. Biomed. Mater. Res. *24*, 1637-1659.

Francese, J. (1989). Application of PLS Modeling to ELISA Measurements of Fibrinogen Adsorption to Untreated and RF Plasma Modified Microtiter Wells. In Chemical Engineering (Seattle: University of Washington), pp. 136.

Furcht, L. T. (1983). Structure and Function of the Adhesive Glycoprotein Fibronectin. Modern Cell Biol. *1*, 53-117.

Horbett, T. A. (1984). Mass Action Effects on Competitive Adsorption of Fibrinogen from Hemoglobin Solutions and from Plasma. Thromb. Haemostas. *51*, 174-181.

Horbett, T. A., Weathersby, P. K., and Hoffman, A. S. (1977). The Preferential Adsorption of Hemoglobin to Polyethylene. J. Bioeng. *1*, 61-78.

Kiaei, D., Hoffman, A. S., and Horbett, T. A. (1992). Tight binding of albumin to glow discharge treated polymers. J. Biomater. Sci. Polymer Edn. *4*, 35-44.

Limbird, L. E. (1986). Cell Surface Receptors: A Short Course on Theory and Methods (Boston: Martinus Nijhoff Publishing).

López, G. P., and Ratner, B. D. (1991). Substrate Temperature Effects on Film Chemistry in Plasma Deposition of Organics. 1. Nonpolymerizable Precursors. Langmuir *7*, 766-773.

López, G. P., and Ratner, B. D. (1992). Substrate Temperature Effects on Film Chemistry in Plasma Depositions of Organics. II. Polymerizable Precursors. J. Polym. Sci., Polym. Chem. Ed. *30*, 2415-2425.

López, G. P., Ratner, B. D., Rapoza, R. J., and Horbett, T. A. (1993). Plasma Deposition of Ultrathin Films of Poly(2-hydroxyethyl methacrylate): Surface Analysis and Protein Adsorption Measurements. Macromolecules *26*, 3247.

Massia, S. P., and Hubbell, J. A. (1992). Immobilized Amines and Basic Amino Acids as Mimetic Heparin-binding Domains for Cell Surface Proteoglycan-mediated Adhesion. J. Biol. Chem. *267*, 10133-10141.

Morla, A., and Ruoslahti, E. (1992). A Fibronectin Self-Assembly site Involved in Fibronectin Matrix Assembly: Reconstruction in a Synthetic Peptide. J. Cell Biology *118*, 421-429.

Pettit, D. K., Horbett, T. A., and Hoffman, A. S. (1992). Influence of the substrate binding characteristics of fibronectin on corneal epithilial cell outgrowth. J. Biomed. Mat. Res. *26*, 1259-1275.

Ratner, B. D., and McElroy, B. J. (1986). Electron Spectroscopy for Chemical Analysis: Application in the Biomedical Sciences, R. M. Gendreau, ed. (Boca Raton, Florida: CRC Press).

Stanislawski, L., Serne, H., Stanislawski, M., and Jozefowicz, M. (1993). *Conformational changes in fibronectin induced by polystyrene derivatives with a heparin-like fuction.* J. Biomater. Sci. Polymer Edn. *27*, 619-626.

Steele, J. G., Dalton, B. A., Johnson, G., and Underwood, P. A. (1995). Adsorption of fibronectin and vitronectin onto Primaria and tissue culture polystyrene and relationship to the mechanism of initial attachment of human vein endothelial cells and BHK-21 fibroblasts. Biomaterials *16*.

Steele, J. G., Johnson, G., McFarland, C., Dalton, B. A., Gengenbach, T. R., Chatelier, R. C., Underwood, P. A., and Griesser, H. J. (1994). Roles of serum vitronectin and fibronectin in intial attachment of human vein endothelial cells and dermal fibroblasts on oxygen- and nitrogen-containing surfaces made by radiofrequency plasmas. J. Biomat. Sci. Polym. Edn. *6*, 511-532.

Tidwell, C. D., Ertel, S. I., Ratner, B. D., Tarasevich, B. J., Atre, S., and Allara, D. L. (1997). Endothelial Cell Growth and Protein Adsorption on Terminally Functionalized, Self-Assembled Monolayers of Alkanethiolates on Gold. Langmuir *13*, 3404-3413.

Wachem, v. (1987). Adhesion of cultured human endothelial cells onto methacrylate polymers with varying surface wettability and charge. Biomaterials *8*, 323-328.

Winters, H. F. (1980). Elementary Processes at Solid Surfaces Immersed in Low Pressure Plasmas. Top. Curr. Chem. *94*, 69-125.

Winters, H. F., Chang, R. P. H., Mogab, C. J., Evans, J., Thorton, J. A., and Yasuda, H. (1985). Coatings and Surface Modification Using Low Pressure Non-Equilibrium Plasmas. Mater. Sci. and Eng. *70*, 53-77.

Wojciechowski, P. W., and Brash, J. L. (1993). Fibrinogen and albumin adsorption from human blood plasma and from buffer onto chemically functionalized silica substrates. Colloids and Surfaces B: Biointerfaces *1*, 107-117.

Chapter 6

Monocyte-derived Macrophage Interactions with Biomaterial Surfaces

6.1 Introduction

Soluble cytokines and chemokines are produced during inflammation, tissue damage, wound healing, and a variety of disease states, such as rheumatoid arthritis and septic shock (Dinarello, 1991). A few of the key soluble factors involved in inflammation are interleukin-1ß (IL-1ß), tumor necrosis factor α (TNFα), and interleukin-8 (IL-8) are produced by monocyte-macrophages. IL-1ß and TNFα subsequently affect other cell types, such as fibroblasts, which participate in the foreign body response to implanted materials (Furth, 1988; Miller and Anderson, 1988; Shankar and Greisler, 1994; Ziats et al., 1988). IL-8 has not been investigated previously for its role in implant pathology, but has the potential to influence the inflammatory response to foreign materials. Most importantly, all of these soluble factors are responsible for recruitment of inflammatory cells, such as neutrophils and monocytes, through the activation of endothelial cells (IL-1ß and TNFα) or through chemotactic mechanisms (IL-8).

It is well accepted that monocyte-macrophages play a key role in the inflammatory and foreign body responses around implanted materials. However, the details of these responses are poorly understood, and have profound implications clinically for implant performance. These studies were undertaken to determine monocyte-macrophage activation in response to implanted materials through the use of an *in vitro* assay system. Activation was monitored by IL-1ß, TNFα and IL-8 production. This model was designed to evaluate clinically relevant materials and gain some understanding as to the

role that different material characteristics, such as surface chemistry, topology and extracellular matrix proteins, have on monocyte-macrophage activation.

6.2 Isolation of Monocytes

6.2.1 Background

A variety of monocyte purification schemes were used throughout this thesis. The methods used to isolate monocytes can profoundly influence their actions in culture. The differences in monocyte activity using the different isolation methods will be discussed.

6.2.2 Effect of Monocyte Isolation on Cellular Activity

The three isolation methods are described in Chapter 3.4. The Percoll® method (Chapter 3.4.2.1) was used solely for section 6.4, the Martinson protocol (Chapter 3.4.2.2) for those studies found in Chapter 8, and the adherence method (Chapter 3.4.2.3) for sections 6.3 and 6.5.

This will be an informal discussion of some observations. I am addressing this topic primarily to guide future investigators so that others will not be led down some of the less fruitful paths I had to encounter.

The Percoll® protocol is described in Chapter 3.4.2.1, which utilizes poly(vinylpyrollidone)-coated particles to form gradients of a specified density. Cells can be separated on these gradients on the basis of cell size and cell density. Percoll® gradients performed relatively well, yielding a population of approximately 80-90% monocytes with the "contaminating" cells being lymphocytes and platelets. After isolation, repeated washes were performed to remove residual Percoll® and platelets, however there always remained a significant amount of both. I found it worrisome that Percoll® remained in the cell suspension because it is a particle that is easily engulfed by monocytes. The moderate levels of IL-1ß release from cells cultured on TCPS alone (seen in section 6.4 and

Appendix C) led me to believe that the Percoll® particles were probably "priming" the monocytes by inducing a phagocytic response. We strove to find a more acceptable isolation technique that would not artificially activate the cells to such a great degree.

Laura Martinson devised a purification scheme that took advantage of a monocyte's ability to adhere to TCPS in medium containing a high-serum concentration. Monocytes would adhere to the bottom of TCPS flasks allowing us to wash away any non-adherent lymphocytes. The monocytes were then cultured overnight in low serum medium (5-10% FBS), which caused approximately 60-80% of the monocyte-macrophages to spontaneously release and become non-adherent. This protocol permitted the collection of an essentially pure population of monocytes and allowed us to seed a known number of cells on materials. Maria Werthen provided an additional step that effectively removed platelets by spinning the cell suspension over pure FBS at low centrifuge speeds, separating the heavier monocytes from the platelets.

After using monocytes isolated using the Martinson protocol in a number of studies, it became apparent that these cells were not capable of eliciting an inflammatory response without addition of endotoxin. The monocyte-macrophages were monitored for inflammatory cytokine release, but none was ever detected. This response seemed highly unlikely, because macrophages are always present at implant sites and should participate in at least a short term inflammatory response to materials. This is especially true if the monocytes are adhering to the materials as shown by LDH activity of an adherent population and microscopic observation of materials such as PTFE and Nylon 6. Thinking it might be a cell concentration-to-culture volume problem, I tried seeding the monocyte-macrophages at much higher densities, as high as 8×10^5 cells per well, with only the slightest trace of inflammatory cytokines detected. Due to the low numbers of monocytes that are collected from large volumes of blood, this method did not yield adequate numbers of monocytes to compensate for their low level of activity. These cells

appear to lose their ability to become activated via contact, and only respond to soluble activation factors such as bacterial endotoxin.

An alternative protocol was necessary to isolate monocytes that were not "primed" from Percoll® particles and were contact sensitive. A protocol was developed to directly adhere the monocytes to materials without an intervening adhesion step (Chapter 3.4.2.3). With the development of the LDH assay, it was possible to enumerate cells adhered to materials directly from a lymphocyte/monocyte rich population, which had kept us from using this method before. Briefly, a monocyte/lymphocyte rich population was harvested after a Ficoll- Hypaque gradient (which removes red blood cells and granulocytes) and platelets removed over pure FBS gradients. This population was added directly to the material samples of interest, allowing the monocytes to adhere for 2 hours in serum containing autologous human serum (AHS). The non-adherent lymphocytes were removed by washing with serum-free medium, adding back 15% AHS medium for long-term culture.

This adherence protocol yields low inflammatory cytokine production from monocytes contacting the negative control surfaces TCPS and TCPS wells containing the glass retaining rings used to anchor the materials. The monocyte-macrophages were sensitive to not only stimulation by endotoxin, but showed varying levels of IL-1ß, TNFα and IL-8 in response to contact with materials of differing surface chemistry, porosity and adhesive protein coatings. I believe this to be a superior isolation method over others developed to date for its relative ease and consistent results. The results of using this monocyte isolation protocol are found in sections 6.3 (monocyte adhesion) and 6.5 (cytokine release) of this chapter.

6.3 Monocyte-Macrophage Adhesion to Biomaterial Surfaces

6.3.1 Background

Monocyte-macrophage adhesion to biomaterial surfaces was monitored by measuring lactate dehydrogenase activity in the cells. This technique is advantageous when working with porous biomaterial surfaces, such as the mixed ester cellulose membranes or expanded PTFE. Total cell number on each polymer surface was determined at 3 time points, after 1, 3 and 7 days in culture. Variations between donor and monocyte preparations is evident, but some interesting trends exist.

6.3.2 Materials and Methods

The material substrates used were: PTFE, 10μ ePTFE, 30μ ePTFE, 60μ ePTFE, 0.22μ MEC, 5μ MEC, 8μ MEC and Nylon 6. In some of the experiments, the materials were pre-coated with 20μg/mL human fibronectin for approximately 2 hours and rinsed with PBS to remove any unbound FN from the wells prior to seeding the monocytes. See Chapter 3 for more details on material preparation.

Human monocytes were isolated from human blood as describe in Chapter 3.4.2.3. Isolated monocytes were allowed to adhere directly to the polymer surfaces in autologous serum-containing medium for 2 hours. Non-adherent cells were removed by washing with serum-free medium. Autologous serum-containing medium was added back to the cells adhered to the polymers. At the designated time points, the culture medium was removed, and centrifuged to pellet any cells. The supernatant was aliquotted and retained for cytokine determination and neutrophil adhesion assays. The cells in the culture wells and the pelleted cells were lysed in a detergent solution and the level of LDH determined using an assay kit as described in Chapter 3.9. The total cell number was calculated from a standard curve and represents both the cells that remained in the wells on the materials and a non-adherent fraction that was pelleted.

6.3.3 Results and Discussion

The total monocyte-derived macrophage number was determined for 9 monocyte preparations, each from a different human donor. Figures 6.1-6.9 illustrate the data obtained.

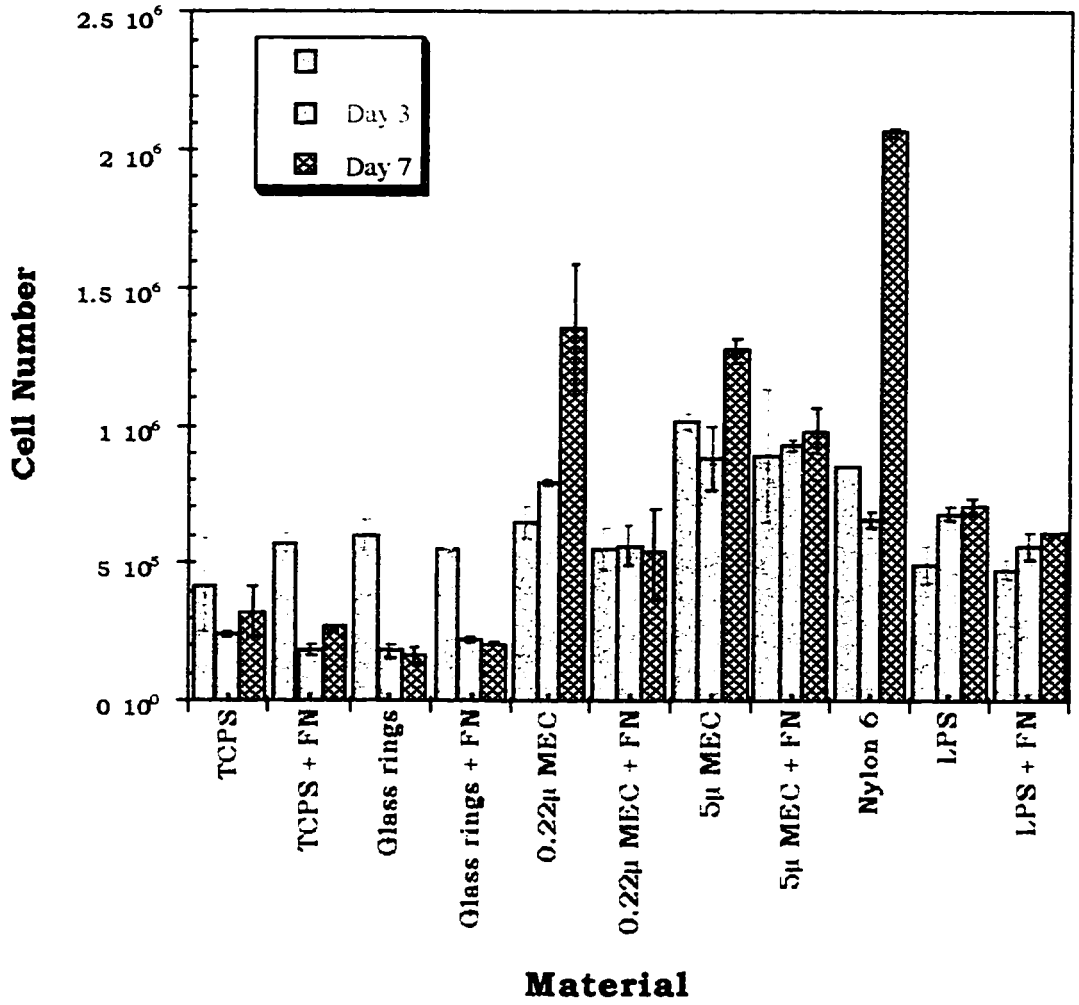

Figure 6.1: Total cell number on each material for Donor #1.

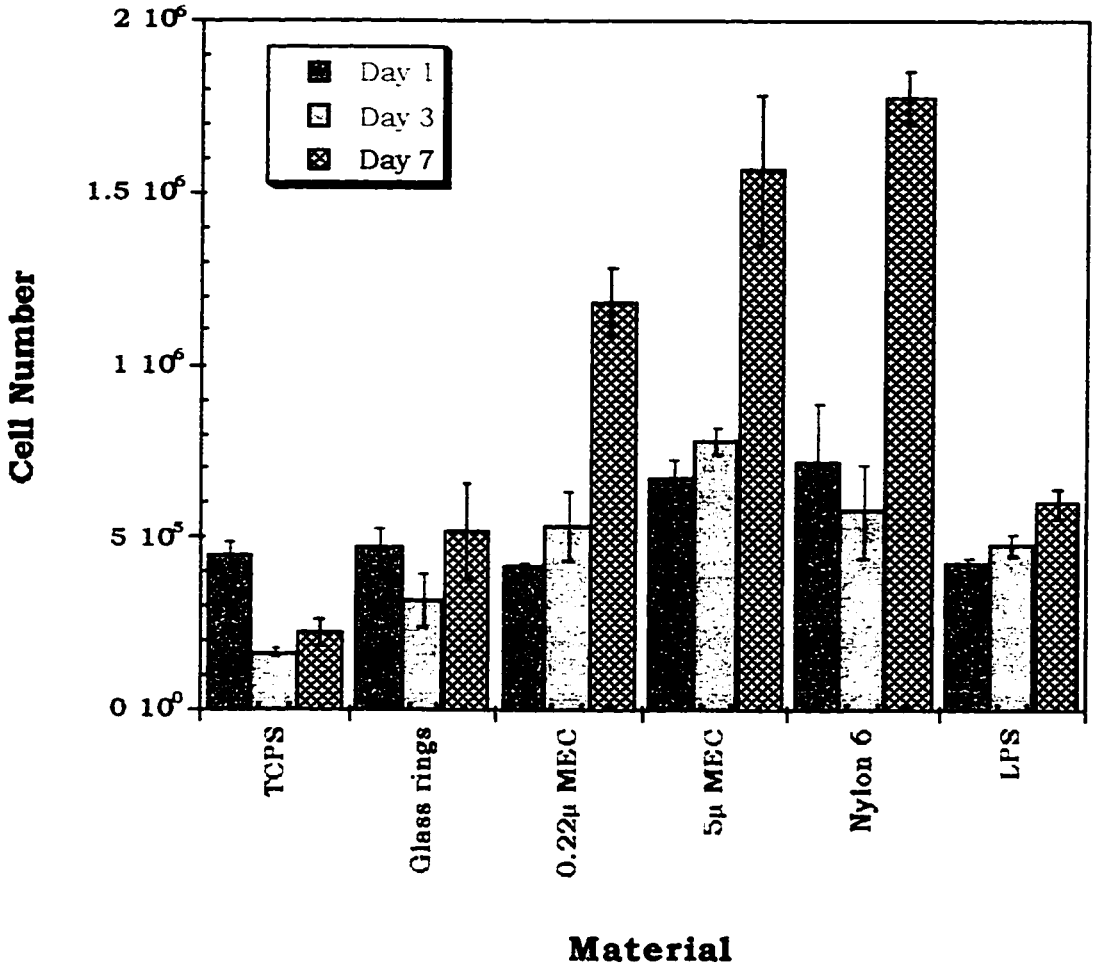

Figure 6.2: Total cell number on each material for Donor #2.

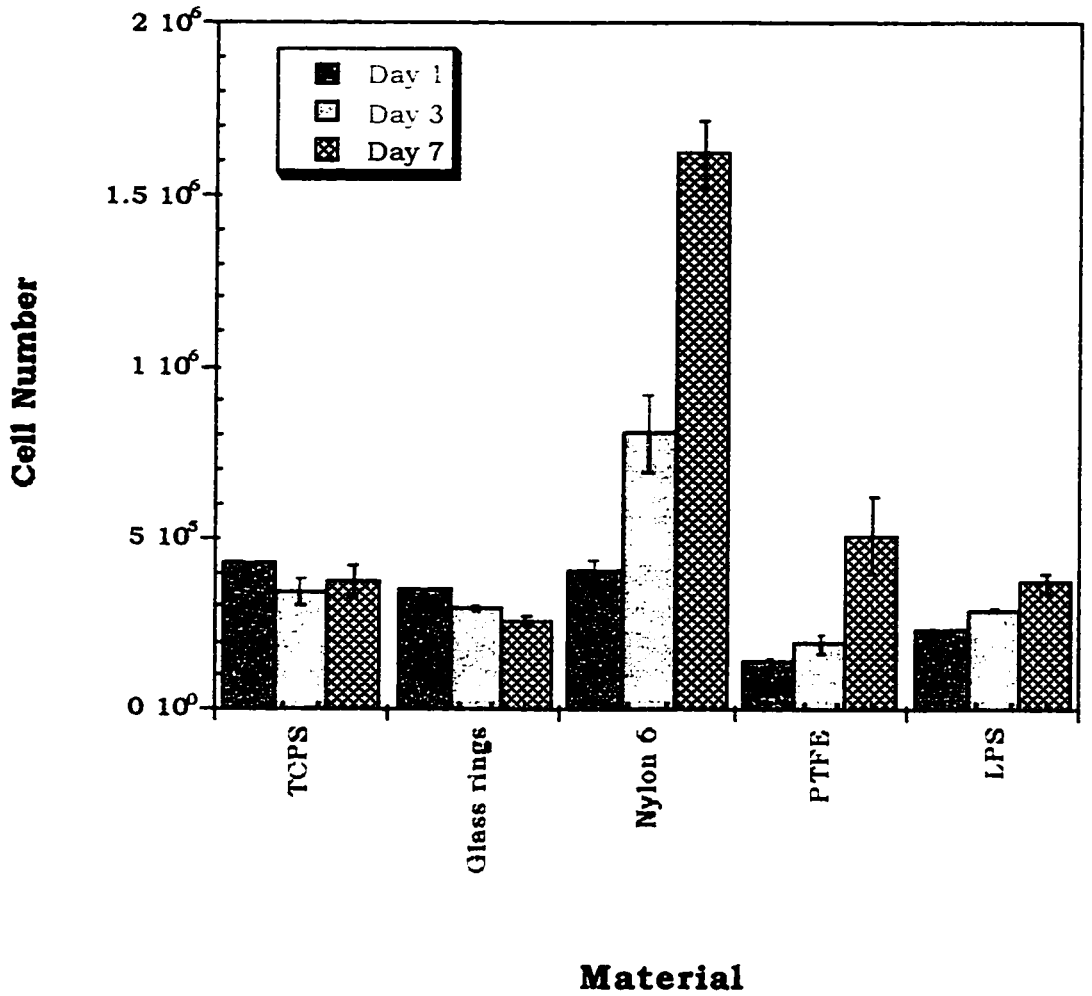

Figure 6.3: Total cell number on each material for Donor #3.

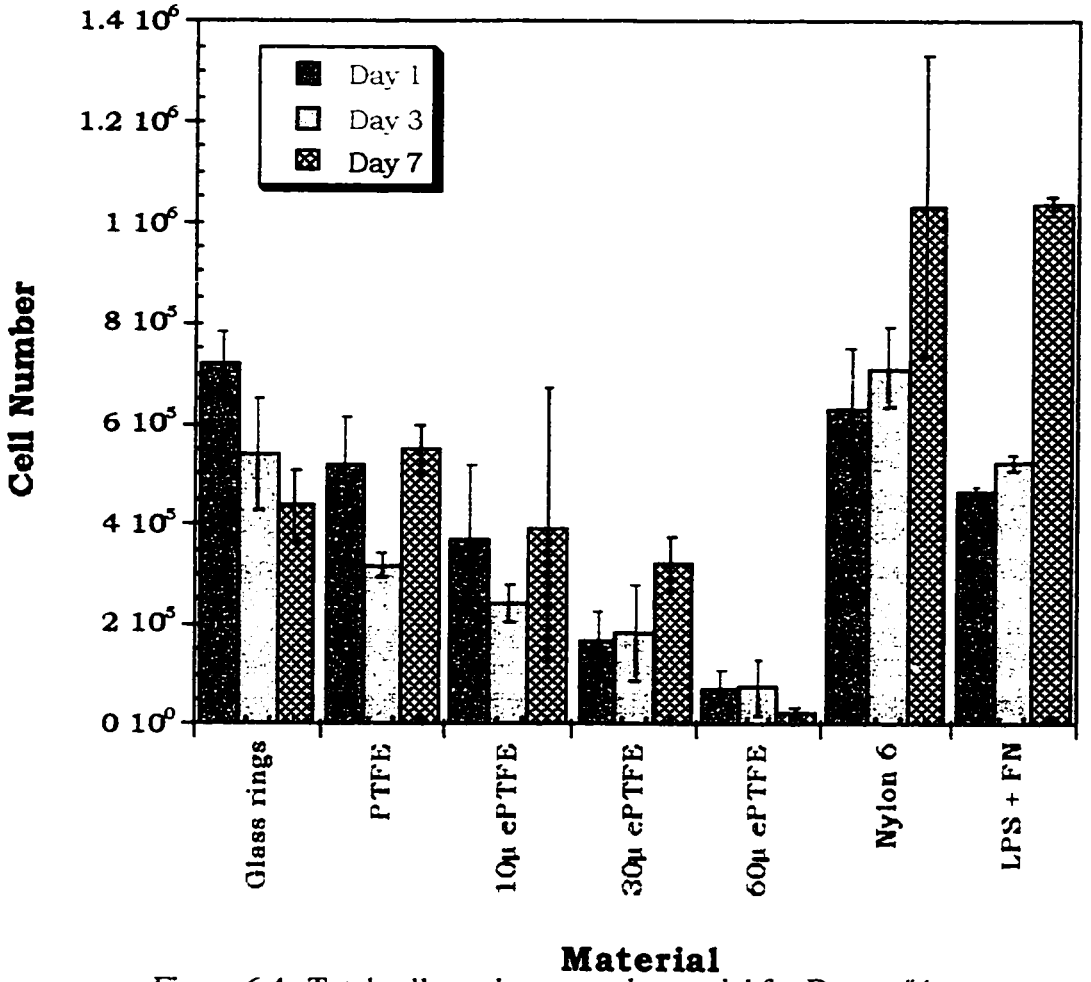

Figure 6.4: Total cell number on each material for Donor #4.

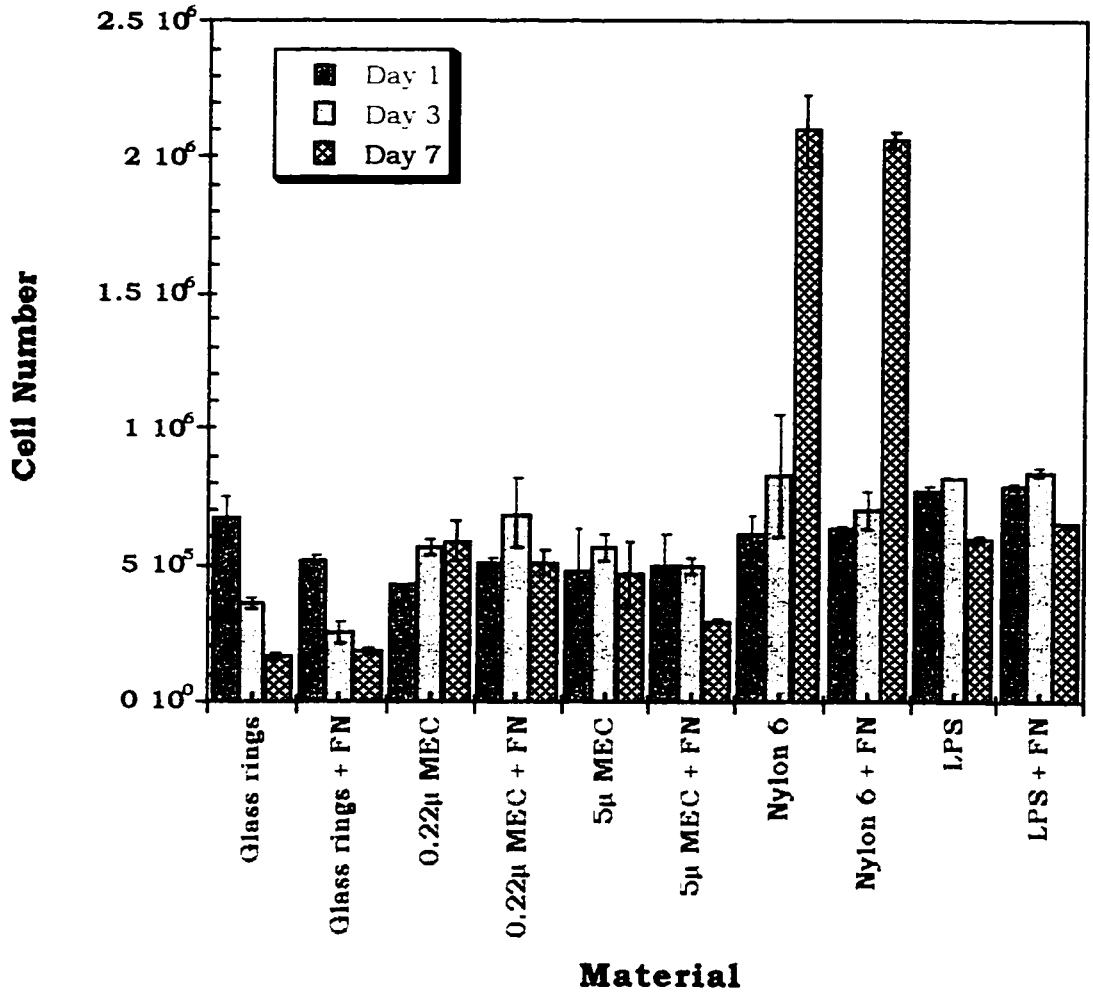

Figure 6.5: Total cell number on each material for Donor #6.

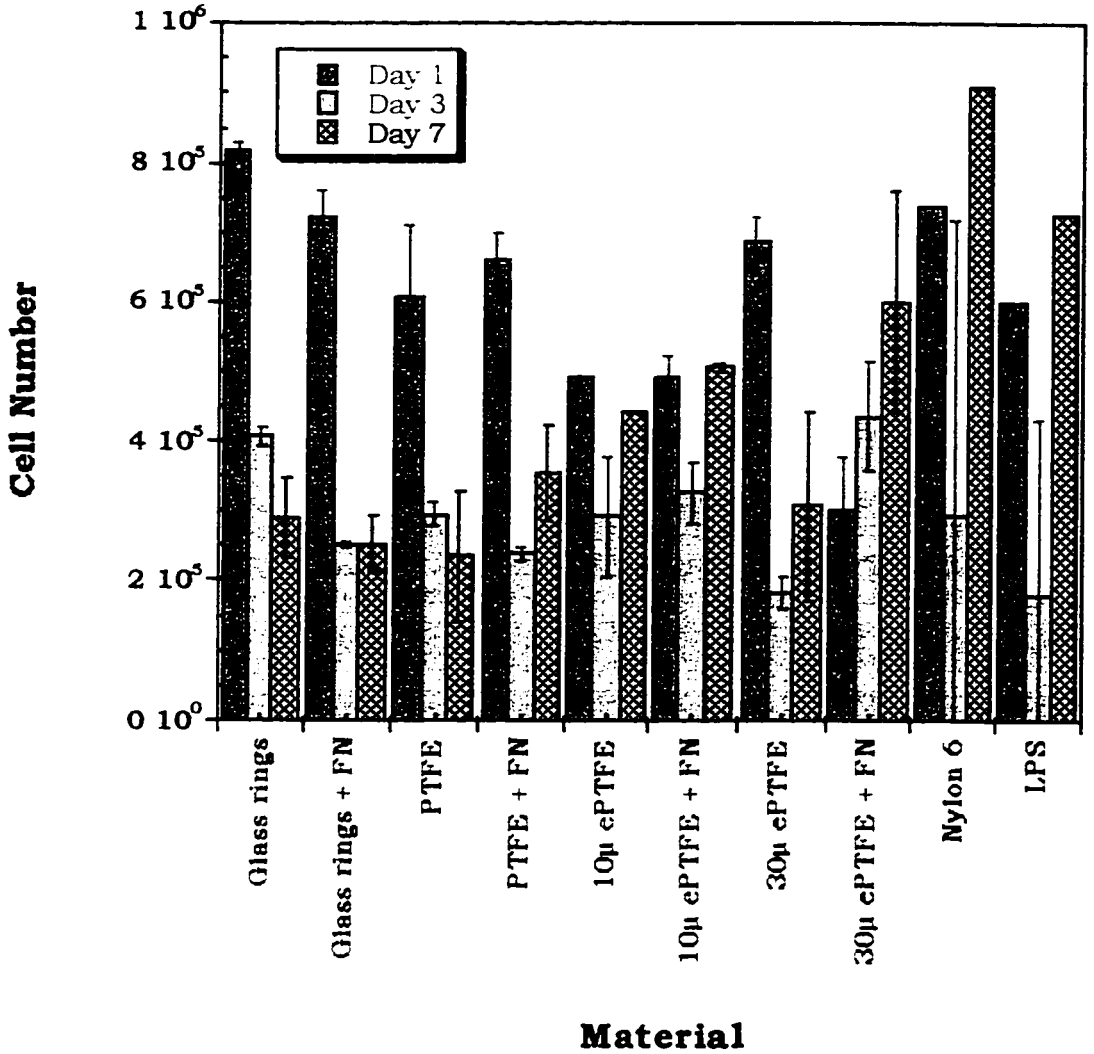

Figure 6.6: Total cell number on each material for Donor #7.

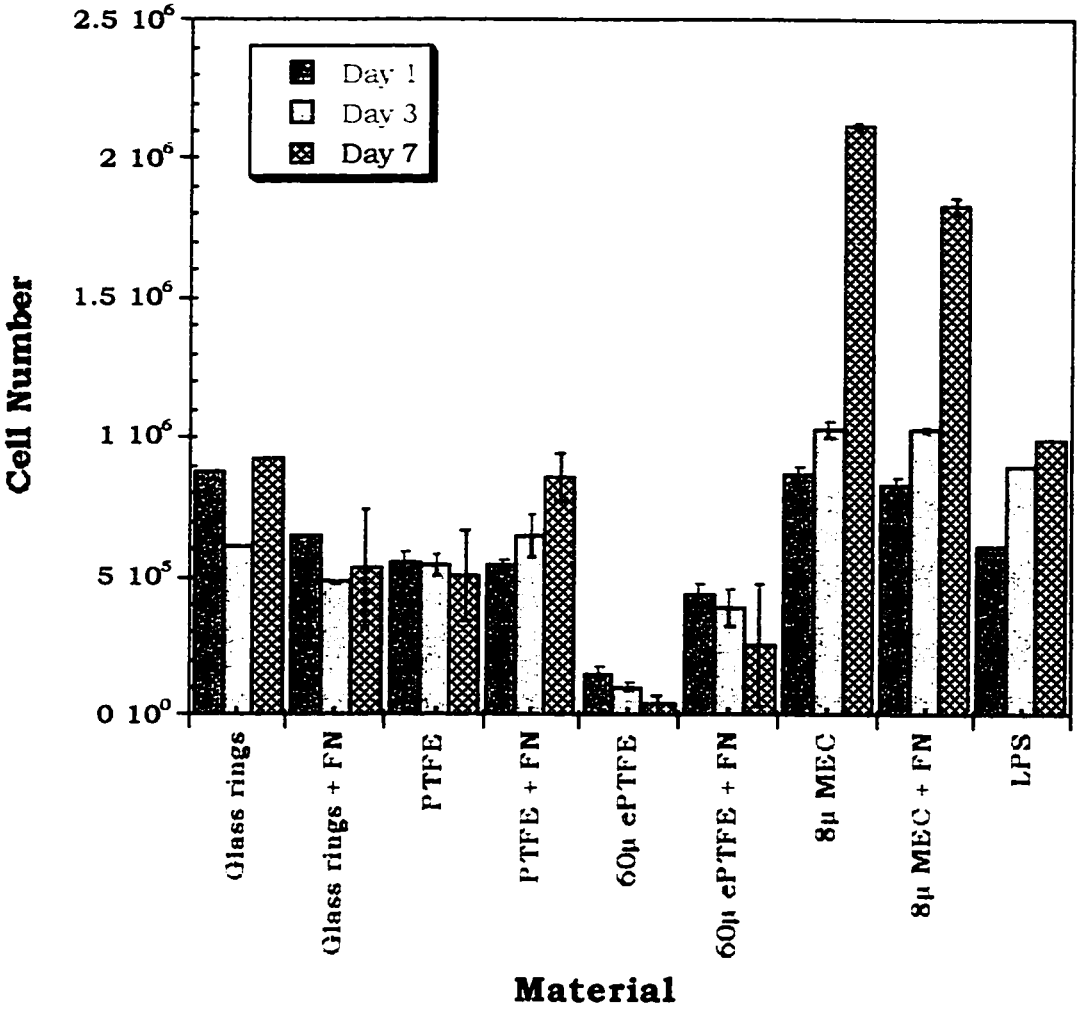

Figure 6.7: Total cell number on each material for Donor #8.

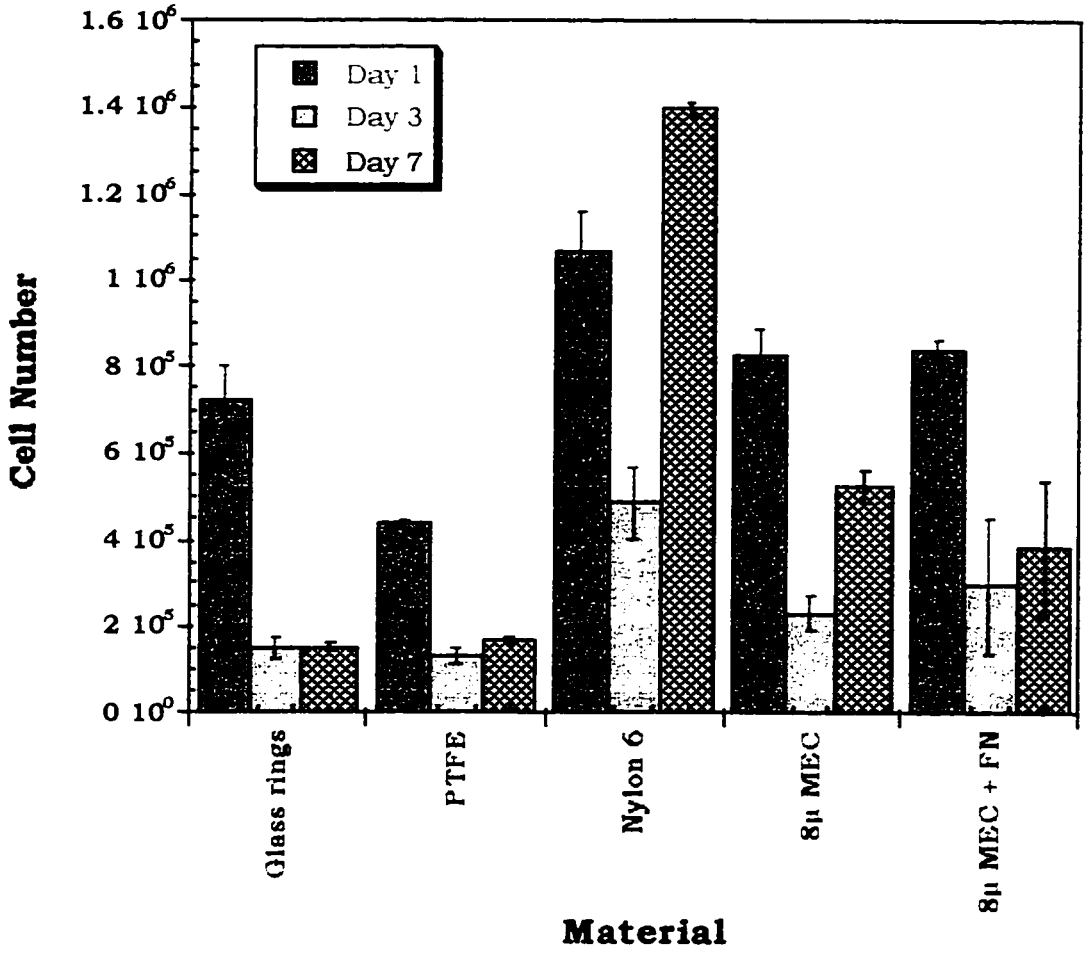

Figure 6.8: Total cell number on each material for Donor #9.

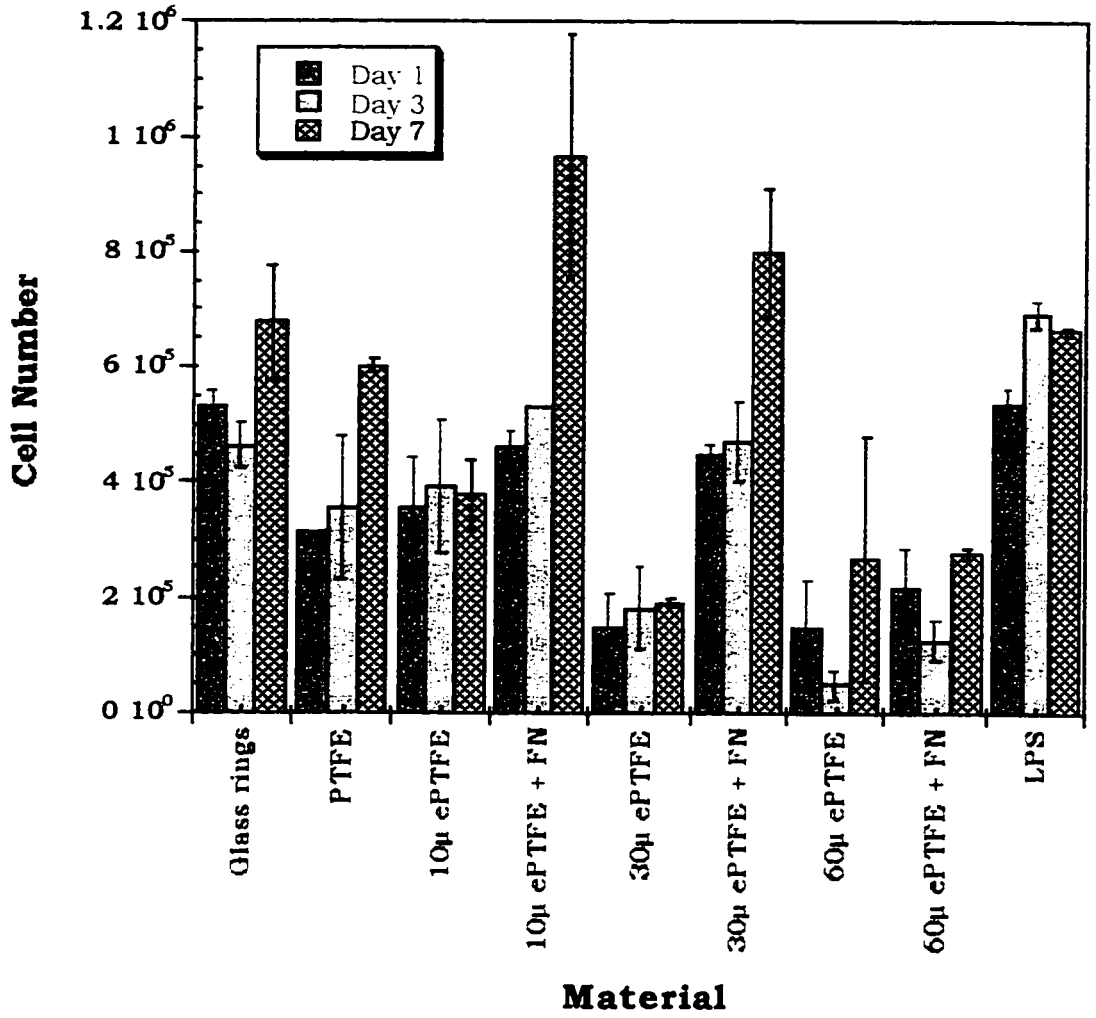

Figure 6.9: Total cell number on each material for Donor #10.

Due to the variability from donor-to-donor and in the monocyte preparations, few definitive conclusions can be made. However, there are some interesting trends that exist between the polymer groups. Although the hydrophilic MEC membranes tended to adhere the same number of monocytes as the TCPS or glass ring control wells after 1 day, they appear to promote cell proliferation, as seen in Figures 6.1 and 6.2. Nylon 6, also a hydrophilic polymer, consistently showed higher cell numbers with increasing time in culture. Fibronectin pre-coating had little or no effect on the hydrophilic polymer group.

The hydrophobic PTFE and ePTFE materials generally showed a trend from highest monocyte adhesion to PTFE, then decreasing as the fibril length increased from 10μ to 60μ. The 60μ ePTFE had the lowest monocyte adhesion of all of the polymers tested. Fibronectin pre-coating on the fluoropolymers had significant effects on monocyte adhesion, especially for the 30 and 60μ ePTFE. The presence of an adhesive protein on the surface of these polymers probably allows for more and or better attachment through integrin binding of the cell to the adsorbed fibronectin, possibly through CD11b/CD18 (however this was not tested).

The TCPS and glass ring controls generally decreased with time in culture, whereas the LPS stimulated cells remained relatively constant for most of the preparations. Visually, the cells on TCPS tend to become less adherent than those seen in the LPS wells. LPS has a marked effect on cell adhesiveness and viability. There was no visually apparent cell proliferation in either the TCPS, glass ring or LPS wells, as is supported by the LDH assays.

There are few reports of monocyte adhesion to polymers in the biomaterials literature. Little is know about the specific events that occur when a monocyte encounters a foreign surface. Most interesting is the apparent ability of monocytes to proliferate. Only in recent years have investigators found instances of monocyte proliferation, which appears to play important roles in atherosclerotic plaque and granuloma formation (Lan et al., 1995). In conjunction with the cytokine studies, the hydrophilic materials adhere and may promote monocyte proliferation while having much lower cytokine release on a per cell basis. These data suggest that there may be two mechanisms that are at work: materials that promote moderate monocyte adhesion and proliferation may promote more normal healing, as seen with the 5μ and 8μ MEC materials *in vivo*. The extreme proliferative response to monocytes contacting Nylon 6 may explain why this material is not tolerated well in the body.

6.4 Interleukin-1β Production by Human Macrophages Cultured on Silicone Implant Materials

6.4.1 Background

This section describes an assay system that was developed to investigate interleukin-1ß release from human monocyte-macrophages contacting biomaterial surfaces. This assay has a distinct advantage over other previous assay systems (Cardona et al., 1992; Miller and Anderson, 1988) in that it extended over 35 days. Although the materials used are unique to this section, it is included as a historical beginning of many of the techniques and ideas developed later. These experiments initiated subsequent studies of other cytokines released from monocyte-macrophages in section 6.5 and Chapter 8, however different monocyte isolation protocols were used for the later studies.

This study spawned the ideas that were followed up on with the aid of a Johnson and Johnson (J & J) Focused Giving Grant. The J & J grant allowed us to develop a variety of techniques which are critical to the interpretation of cytokine data, in particular the influence of monocyte isolation protocols on cytokine release, cell number determination on porous materials, and detection of endotoxin contamination on materials. The cell isolation protocol used in this study was not optimal due to the influence of the isolation medium or other cell types on macrophage secretion of cytokines, as addressed in section 6.2. The need to normalize cytokine data to account for differences in cell numbers on the materials (section 6.5) led to the development of the LDH protocol used in section 6.3 (and other methods). This study, as well as those conducted by Laura Martinson, raised questions about the influence of endotoxin contamination on material surfaces. As it being the "oncogenesis" from which much of the later research evolved, this section is included here.

6.4.2 Introduction

Attention has been focused on silicone implants due to their extensive use for breast reconstruction and augmentation; approximately 1 million women in the United States have received breast implants (Stone, 1993). Numerous other implants are fabricated from silicone materials such as testicular and penile implants, hydrocephalic shunts, and small joint replacements (Peimer et al., 1986; Snow and Kossovsky, 1989). With the wide-spread use of silicone implants, unexplained complications have surfaced which have been attributed to the leakage of the silicone oil encased in the implant or the implant materials themselves. Unfortunately, little is known of the cellular mechanisms of reaction to implants, and how they are manifested in the variety of pathologies described, from fibrous capsule formation to systemic sclerosis (Sank et al., 1993; Varga et al., 1989). IL-1ß is a potent cytokine responsible for the recruitment of inflammatory and immune cells to implant sites. IL-1ß stimulates B- and T-cells, contributes to tissue breakdown, causes fibroblast proliferation and induces increased collagen production leading to fibrosis (Dinarello, 1991). Because IL-1ß is soluble, it is not limited to local effects. Macrophages produce IL-1ß in response to lipopolysaccharide (from bacteria), foreign particles, immune complexes, and other stimuli (Nathan, 1987; Oppenheim et al., 1986).

In this study, monocytes were purified from whole human blood. Highly enriched populations of monocytes were isolated using a two-step, density-gradient centrifugation process (Pertoft et al., 1980). The purification scheme produced monocyte populations in excess of 80% purity, with the primary contaminating cells being lymphocytes. Within 2-3 days, the monocytes had differentiated into macrophages, indicated by a dramatic change in morphology. The cells were cultured on polymers for a total of 35 days, removing supernatants at specified times to monitor the production of IL-1ß by the macrophages.

The supernatants were assayed using a commercially-available, enzyme-linked immunosorbent assay (ELISA). Using the methods outlined below, we were able to detect different levels of IL-1ß production by macrophages on the different materials tested.

6.4.3 Materials and Methods

6.4.3.1 Sample Preparation

The materials listed below were used in this study. The mammary and penile prostheses were provided by Mentor Corporation. The abbreviations for each material are given in bold type.

"Silica-free" non-reinforced **RTV** rubber

Penile implant **Bioflex®**, cat. no. 9822I, S/N 116223, B/N 012506

Mammary prosthesis, smooth, cat. no. 350-1850M, lot 70513, **Smooth silicone rubber (SR)**

Mammary prosthesis, textured, cat. no. 354-2835M, lot 71912, **Textured SR**

Cast film of **Nylon® 6**

Tissue-culture treated polystyrene (**TCPS**), with and without lipopolysaccharide (LPS) addition

Polymer samples were punched out in a laminar-flow clean hood with a double solvent-washed (methanol/acetone) paper punch, producing approximately 7 mm diameter discs. The RTV material required hand-cut samples using a solvent-washed scalpel. Every effort was made to minimize contamination of the polymer surfaces. The samples were sterilized per the manufacturer's specifications, ethylene oxide (EtO) for the Bioflex® material, and steam sterilization for the others. After EtO sterilization, the

Bioflex® samples were allowed to degas for 3 weeks before use. Five samples of each polymer group per blood donor were used. The sterile samples are placed in a 96-well tissue culture plate. Prior to the cell seeding, the samples were incubated at 37°C for 8-12 hours in phosphate buffered saline (PBS) containing antibiotics, with one change of buffer during this time period. No protein adsorption was done prior to the addition of purified monocytes.

6.4.3.2 Isolation of Human Monocytes from Blood

A description of the protocol used is found in Chapter 3.4.2.1. Cells were seeded onto the materials in the 96-well plates in culture medium. All plates were incubated at 37°C, 5% CO_2 in air, in a humidified chamber. The plates were enclosed in a plastic box with a loose-fitting lid containing a small amount of water to decrease evaporation from the plates and minimize the chance of contamination. The loose-fitting lid insured adequate gas exchange.

On days 3, 7, 14, 21, 28, and 35 days, 125 μl was removed from each well, placed in labeled Eppendorf tubes, and stored at -20°C until assayed. The volume removed was replaced with fresh culture medium. To the TCPS + LPS wells, one half of the original amount of LPS (25 ng/well) was added after the fresh medium was introduced.

6.4.3.3 Interleukin-1β Enzyme-Linked Immunosorbent Assay (ELISA)

After the completion of the time series, the culture supernatants were assayed using the IL-1ß Quantikine® ELISA from R & D Systems (Minneapolis, MN). The best six preps were chosen to be assayed. One preparation (of nine total) had an incomplete set of culture supernatants due to mold contamination in some of the wells. Another preparation

had a large number of what appeared to be platelets which were carried through with the monocyte population during the purification process, and was not assayed for this reason. The remaining preparation not assayed had cells that failed to thrive. This represents 5 samples for each of the polymer types at 6 time points for 6 donors, for a total of 1257 (3 samples were missing due to contamination in one well of one preparation; this had no effect on neighboring wells). Culture medium was used as the diluent for the ELISAs. Any effect of the serum or other medium components would be the same for the standards as for the culture supernatants.

The standard curves gave very good regressions (data not shown), and there was little plate-to-plate variability. The data are expressed in picograms of human IL-1ß per milliliter. Samples which had been assayed and found to have high levels of activity such that they were over the limit of detection by the ELISA plate reader were re-assayed at greater dilutions.

6.4.4 Results and Discussion

Illustrated in Figures 6.10-6.15 are the results of the IL-1ß production by macrophages on each day. Each data point represents the average of 5 samples (error bars equal 1 standard deviation). Scale changes for each day clearly illustrate the differences between each material as the amount of IL-1ß decreases with time. In Appendix C, the IL-1ß production results are organized by donor covering the total 35 day time course. Graphs in Appendix C are semi-log plots of the IL-1ß concentration in pg/mL.

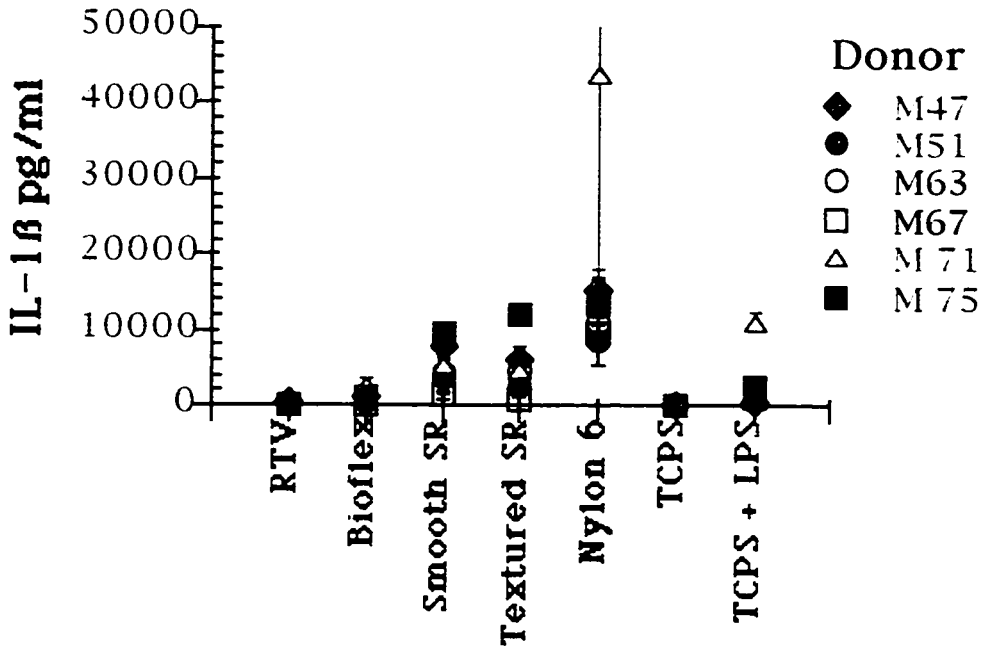

Figure 6.10: IL-1ß production by macrophages after 3 days in culture on materials.

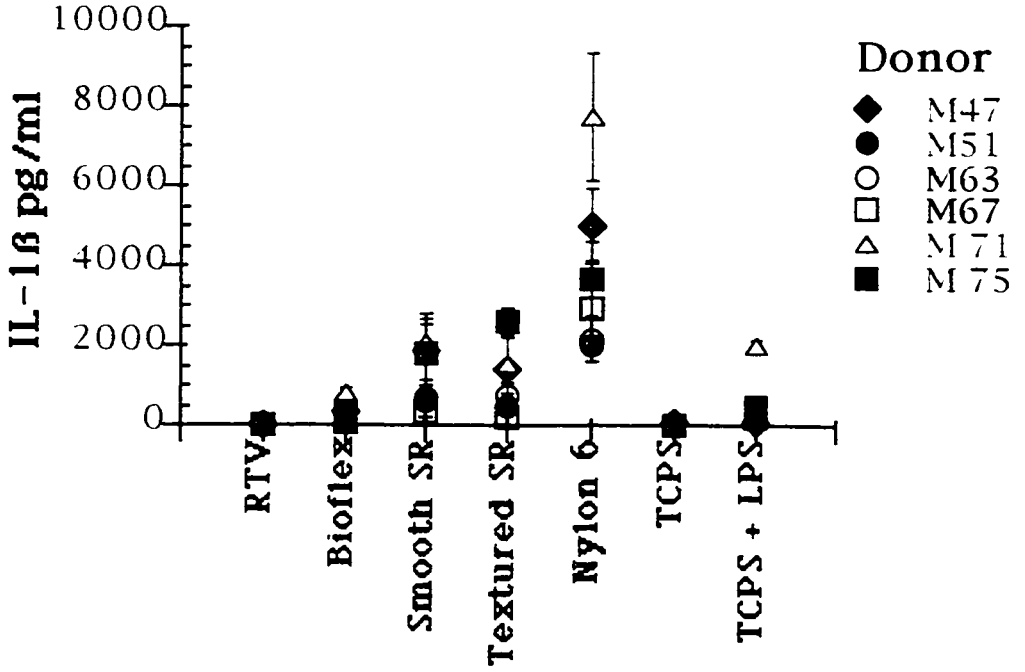

Figure 6.11: IL-1ß production by macrophages after 7 days in culture on materials.

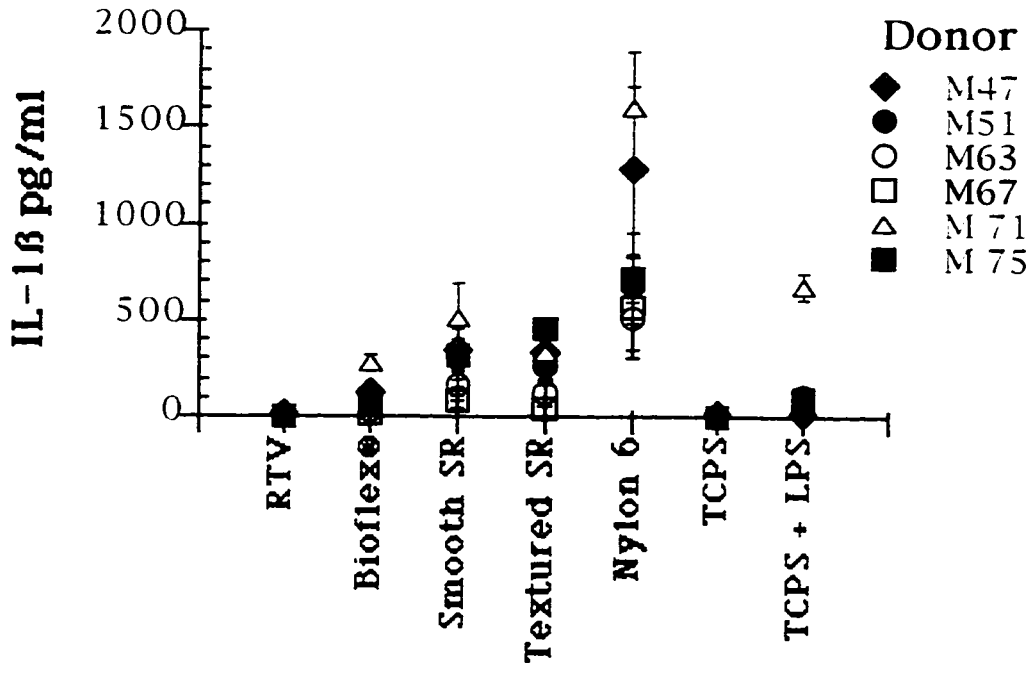

Figure 6.12: IL-1ß production by macrophages after 14 days in culture on materials.

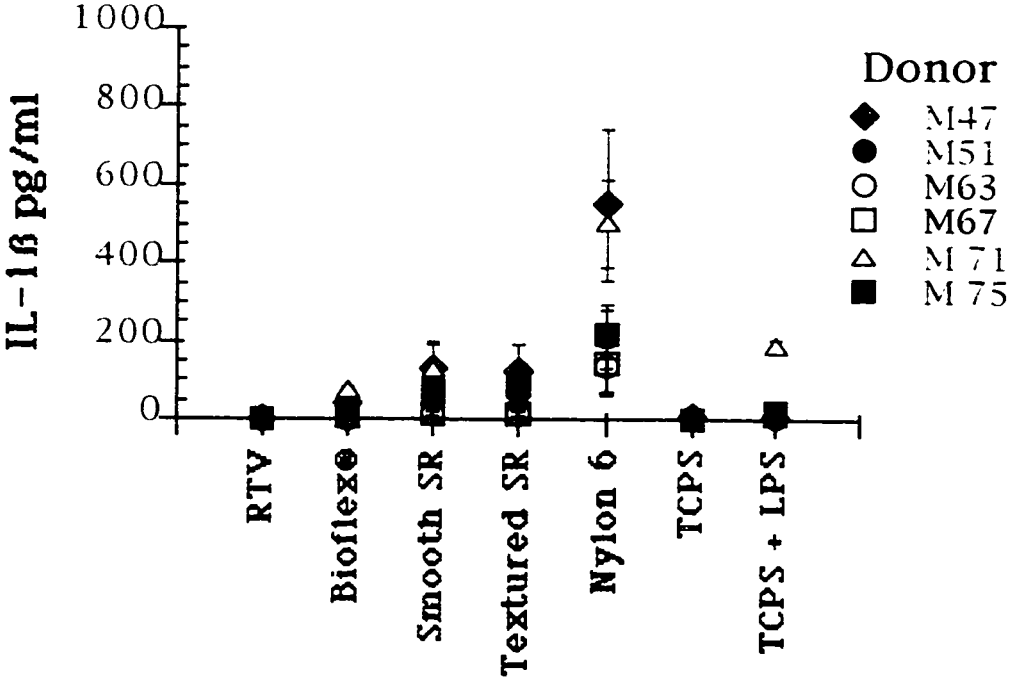

Figure 6.13: IL-1ß production by macrophages after 21 days in culture on materials.

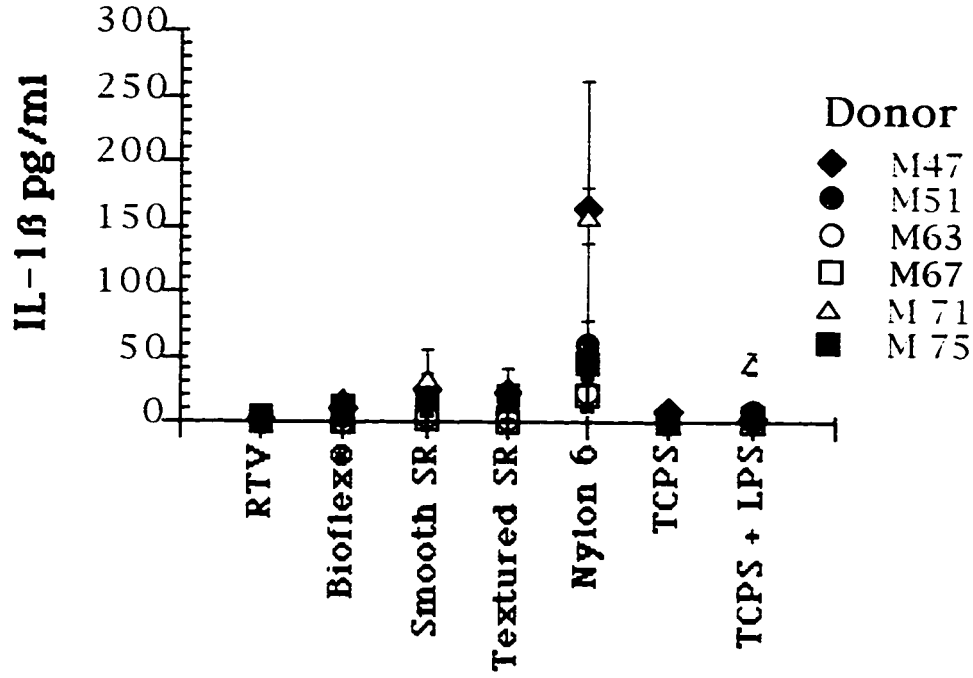

Figure 6.14: IL-1ß production by macrophages after 28 days in culture on materials.

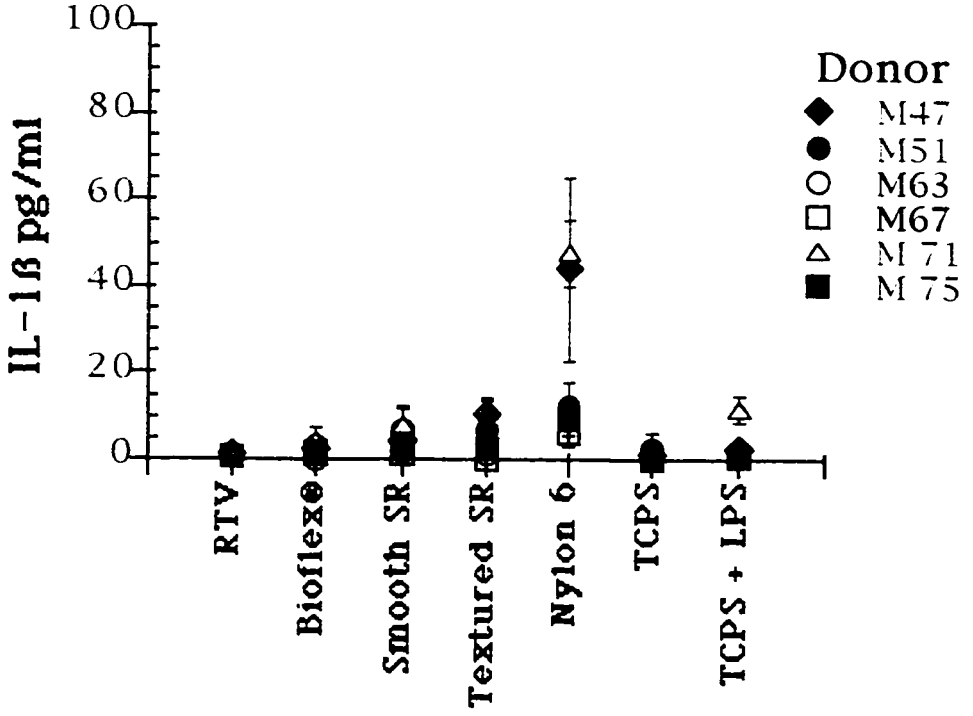

Figure 6.15: IL-1ß production by macrophages after 35 days in culture on materials.

The trends in IL-1ß production by macrophages were the same for all the donors, with the magnitude differing between donors. The reactivity of human macrophages to the polymers is as follows:

"High" IL-1ß **"Low" IL-1ß**

Nylon® 6 >> smooth SR = textured SR > TCPS + LPS > Bioflex > RTV > TCPS

The production of IL-1ß with all of the donors starts out high at day 3 and slowly tapers off (see Appendix C). The smooth and textured SR's were approximately one half of the Nylon® 6 values. By day 28, almost all of the cells in the TCPS + LPS wells appeared dead, presumably due to the high levels of LPS used causing the cells to be over stimulated and ultimately to die. By day 35 there is very little IL-1ß production, probably due to the limited life-span of the cells in culture, which is expected for primary cells. The amount of IL-1ß is about the same for all materials at day 35, even for Nylon® 6, further indicating low cell viability. However, under microscopic evaluation, viable cells were seen even at day 35, with the exception of the TCPS + LPS wells. This indicates that the cells at later time points were senescent or quiescent.

In Figure 6.16, the data per time-point for all donors were pooled. Due to the natural variability in the human population, it was necessary to normalize the data on each day to the Nylon® 6 average. The Nylon® 6 average was chosen because it consistently gave the maximal response on each day tested. The normalized data are expressed as a fraction of the average Nylon® 6 response for each donor on each day. The maximal response for each day is equal to 1, which is equivalent to the average Nylon® 6 IL-1ß production for each day.

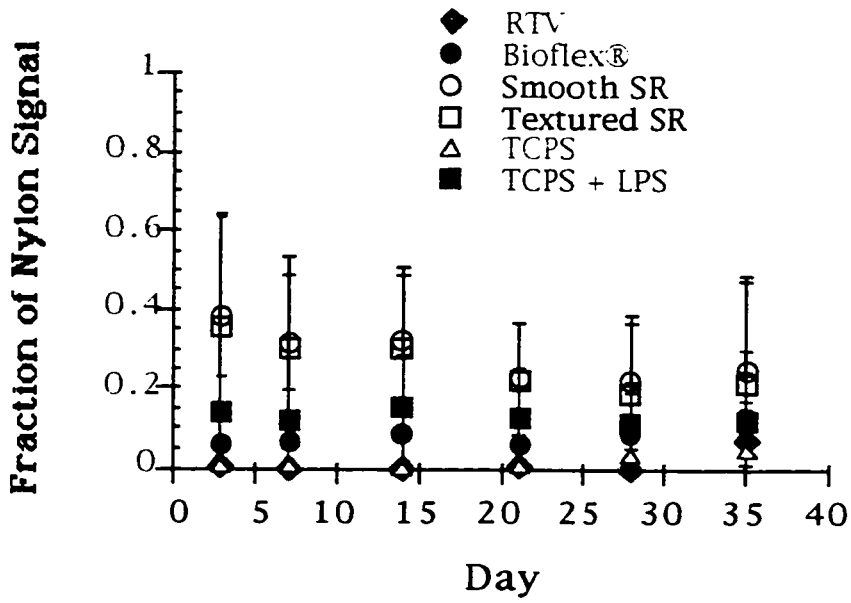

Figure 6.16: Normalized IL-1ß production for all donors.

Most of the materials worked relatively well in this assay system, with the exception of the "silica-free" RTV. This material had a greasy, presumably low-molecular weight film covering its surface which was hydrophobic. It was impossible to keep the RTV samples seated in the bottom of the wells, because they preferred to be at the air-water interface and not submerged in an aqueous environment. As a result, very few cells were seeded on the RTV surface, most fell into the bottom of the well or were killed by exposure to air as the polymer floated to the surface of the medium. Also, the cells in the RTV wells did not have a normal morphology or viability (low) compared to those cells grown on TCPS. The cells exposed to the RTV appeared to be in an inactive or senescent form, remaining apparently undifferentiated and non-functional. The cells retained a monocyte morphology (small, round), and did not phagocytose any cell debris. The cells exposed to the other materials appeared to phagocytose any cell debris in their environment within the first few days of seeding. It was apparent that the cells exposed to RTV were

affected morphologically and functionally by the low molecular weight fraction ("oil") that collected on the material surface and could be transferred to the cell culture well.

None of the materials used were completely sealed on the bottom, allowing some of the cells to be exposed to the other side of the material. Cells on the Nylon® 6 could not be seen because the material was opaque. As a result, all comments on cell morphology and microscopic observations do not necessarily apply to the Nylon® 6 samples.

The cell purification scheme worked well, consistently giving enriched populations of human monocytes in excess of 80% purity. There were, however, always contaminating lymphocytes, and some cell debris and platelets (which were usually removed by the macrophages in the first few days of culture). The lymphocytes persisted throughout the time of the experiment, 35 days, although the number of lymphocytes seemed to vary from material to material, with the highest numbers apparently on Bioflex®. The smooth and textured silicone rubbers also supported lymphocytes, but to a lesser degree. TCPS consistently had low numbers of lymphocytes. One advantage to the presence of the lymphocytes is that more complex sets of interactions are allowed which more closely approximates the events that can occur *in vivo*. It was observed at later time points that a "new" population of cells appeared to be proliferating, particularly evident with donors M71 and M75. These cells had the appearance of mature, antibody-producing B cells, being larger than the other lymphocytes, round, refractive under the microscope, and appeared to be proliferating clonally. IL-1ß is known to promote B-cell maturation and proliferation, so this is a possibility, but without immunohistochemical analysis of these cells this remains purely speculation. The disadvantage of the presence of lymphocytes is their possible consumption of IL-1ß or secretion of other cytokines which affect macrophage IL-1ß production. This is especially true for Bioflex®, since

this material had large numbers of what appeared to be lymphocytes, but low levels of detected IL-1ß in the supernatants.

One donor, M75, answered positively when asked about the presence of a silicone implant. This donor's IL-1ß response was somewhat higher to the silicone rubbers, but not dramatically so (see Appendix C). The M75 data is probably well within the normal distribution in the population, although a greater number of donors would be needed to clearly identify the distribution. It is important to note that the trends remain the same without the inclusion of the M75 data set. Inclusion of M75's data set in no way significantly influences the conclusions.

The IL-1ß data are not normalized to cell number in each well. An equal number of cells was introduced to each well initially, but the cell numbers could have changed with time. Due to the poor optical properties of the SR materials and the opacity of the Nylon® 6, cell number determination using conventional methods of staining and counting was not possible. Bioflex® was an excellent cell growth surface, and appeared to have higher cell numbers of both macrophages and lymphocytes than other materials. The textured SR provided deep clefts for the cells to reside in, making it difficult to assess cell numbers. The materials may impose selection pressures on the initial cell population, thus influencing the cell type and number that persist with time. Also, it is not definitively known if there was any proliferative response to the polymers. However, this appears to be the case for the Bioflex® material.

The surface area of the polymers tested varied widely, from relatively smooth materials such as TCPS, to textured surfaces (textured SR), and a porous material (Nylon® 6). No normalization to surface area was done. The cell density was relatively low on the polymer surfaces (subconfluent), therefore the surface area was not limiting cell exposure to any of the polymers.

None of the polymers used were tested for endotoxin. Endotoxin contamination may occur if the materials were to contact impure water. This probably is not an issue with the commercially available breast and penile implant materials, since these are used clinically and must pass endotoxin testing. These materials needed to be punched into small pieces, but double solvent washed instruments were used and did not contact water. The Nylon 6 used for these studies was cast as a film onto a Teflon sheet, and was washed with water. The level of endotoxin on the Nylon 6 has not been determined.

The study was successful in showing different levels of IL-1ß production by monocytes purified from human blood. This study has a definite advantage over previously published reports in the length of the culture time, 35 days (Cardona et al., 1992; Miller and Anderson, 1988; Miller et al., 1989). The negative control, TCPS, consistently had very low levels of IL-1ß production, demonstrating that background production of IL-1ß is minimal in this system. This also indicates the absence of endotoxin contamination in the culture medium and other reagents used. The cells could be stimulated to produce IL-1ß by the addition of exogenous LPS. Nylon® 6, a material with a history of eliciting an inflammatory response from macrophages, consistently gave the maximal IL-1ß response in all of the assays. It was assumed the half-life of human IL-1ß was less than 3 days at 37°C in culture medium, thus initial "burst" accumulation of IL-1ß (prior to day 3) and dilution with new medium at subsequent time points is not an issue. This is supported by numerous reports in the literature that macrophage production of cytokines is initially high and tapers off with time in culture.

This study indicates human macrophages will respond differently to a variety of materials, in particular, the production of a soluble protein, IL-1ß, involved in acute and chronic inflammation. The silicone rubbers, smooth and textured, showed the highest levels of IL-1ß production from macrophages as with Nylon® 6, and was significantly

higher than the negative control, TCPS. Bioflex® gave an intermediate level of IL-1ß production, but the activation appears to be lower and less persistent on this material. It is not clear which aspects of a material govern the reactivity of cells to implanted materials, although it seems reasonable that a combination of characteristics will dictate the cellular response, including the bulk and surface chemical composition, additives, leachables, protein adsorption, and possibly surface morphology. Also, the degree of change in the polymer with time and exposure to biological fluids, lipids, and enzymes is important.

In the case of the silicone rubbers, silica additives could be a source of inflammation-producing particles, but the IL-1ß production studies do not definitively show silica as the cause of increased IL-1ß production. Indeed, of the non-control materials tested, the silicone rubbers had the highest IL-1ß levels, followed by Bioflex®. Other characteristics of the SR polymer surfaces could be contributing to macrophage activation. As indicated earlier, discussion of the RTV data should not be included due to the degree of cell death and the apparent quiescence of the cells on this material.

The standard deviations of the pooled sets of data were high, even after normalization to Nylon® 6. This is a substantial problem when testing the response of primary human cells, because of the high variability in the human population compared to, for instance, a mouse strain, where the individuals are more genetically identical. However, the use of human cells is far more relevant to clinical considerations. It is probable that monocytes from different individuals would have varying degrees of "sensitivity" to materials (Fisher, 1990; Snow and Kossovsky, 1989). A more thorough investigation would necessitate a larger donor pool, although this may only demonstrate the wide range of sensitivities to polymers in the human population. Using this assay system may be useful for identifying individuals that would be at higher risk for complications related to increased IL-1ß production, such as increased fibrosis.

The possible presence of antibody-producing cells seen in some of the preparations should be investigated further. Increased IL-1ß production may play a role in the development of immunocompetent cells capable of mounting reported auto-immune responses to implants (Kossovsky et al., 1987; Kossovsky et al., 1993). Since macrophages are antigen-presenting cells, the presence of IL-1ß-stimulated lymphocytes may augment the formation of antibodies to antigens from or formed by the implants, such as silicone or denatured protein complexes (Goldblum et al., 1992; Heggers et al., 1983). Testing IL-1ß-neutralizing agents or antagonists currently in clinical trials in this assay system could demonstrate the applicability of therapeutic intervention for complications stemming from high IL-1ß production in response to implants. Also, an immunohistochemical investigation of the cells present at different time points would indicate the selection pressures of different polymers, or proliferative responses of the cells to implant materials.

Comments on the significance of these measurements for the foreign-body reaction are in order. IL-1ß production is only one part of the cytokine communication system that recruits and stimulates cells at an implant site. Many other cytokines are simultaneously released, and may interact (i.e. influence each other's response) in complex ways. Some substances may inhibit cytokine production, or augment it. Since this study was limited to IL-1ß release, other cytokines should be investigated in parallel. The biological activity of IL-1ß can also be suppressed by antibodies, prostaglandins, corticosteroids, and other agents. These substances could potentially affect IL-1ß production or, in the case of anti-IL-1ß antibodies, directly bind to IL-1ß. This action could influence IL-1ß detection in the assay and, *in vivo*, modulate an inflammatory response. This could explain the lower-than-anticipated IL-1ß levels of the LPS-stimulated cells in this study. Thus, although it is interesting and important that the significant differences in IL-1ß were noted between

different materials in this study, the direct consequence of these differences for inflammation and healing *in vivo* are not directly predictable at this time even though chronic production of IL-1ß has been shown to be responsible for or contribute to pathologies such as rheumatoid arthritis (Dinarello, 1991) and silicosis (Hubbard, 1989; Mohr et al., 1991; Struhar et al., 1989).

Within this context, this assay system provides detailed information of human monocyte IL-1ß production in response to contact with different materials. It can be further developed as a method for long-term studies to probe the complex interactions of cells with implant biomaterials *in vitro*, thus reducing the dependence on whole animal studies. Using mixed cell populations *in vitro* provides an easier method for investigating some of the complex interactions which occur *in vivo*. This culture system could be utilized to identify other soluble factors released by a variety of cell types in response to a wide range of polymers, differing in surface chemical composition and topography.

6.5 Interleukin-1ß, Tumor Necrosis Factor α and Interleukin-8 Cytokine Release from Macrophages Contacting Material Surfaces

6.5.1 Background

The experiments conducted in section 6.4 served as preliminary studies which are expanded upon in this section. There are significant modifications in the techniques used here, primarily the method of monocyte isolation and normalization of the cytokine data to cell number. As mentioned in section 6.2, the direct adherence method was used for the studies shown in this section.

A variety of materials were used in these experiments, varying in surface chemistry, surface topography, and adhesive protein coating (with or without FN pre-

coating). The macrophages were sensitive to differences in all of the above surface characteristics, as well as from a soluble activator, lipopolysaccharide. These results support the hypotheses outlined in Chapter 1: surface chemistry, topography and adhesive protein coating will effect macrophage activation and inflammatory cytokine release.

6.5.2 Materials and Methods

The following materials were used for these studies: 0.22μ MEC, 5μ MEC, 8μ MEC, Nylon 6, PTFE, 10μ ePTFE, 30μ ePTFE, and 60μ ePTFE. TCPS and TCPS wells containing glass retaining rings were used as negative controls, and LPS-stimulated monocytes as positive controls. The materials were pre-coated with FN where noted.

Monocytes were isolated using the direct adhesion method described in Chapter 3.4.2.3. Supernatants were harvested at 1, 3, and 7 days in culture, aliquotted and frozen. These supernatants were then assayed for inflammatory cytokines IL-1ß, TNFα, and IL-8 using ELISA kits. All cytokine data is normalized to cell number determined by monocyte-macrophage LDH activity in the wells at each time point. The data generated from individual blood donors was combined for each polymer type tested and organized by cytokine. Polymers pre-coated with FN are included on the same graphs to compare the effect of FN coating on macrophage cytokine production. A negative control, a TCPS well with a glass retaining ring, is included on some graphs for comparison. For the PTFE/ePTFE polymer series, the ePTFEs were compared to PTFE data. Some variability is expected in different monocyte preparations and the human population which is reflected in these results.

6.5.3 IL-1ß ELISA Results

Following are the results of the IL-1ß ELISAs of culture supernatants from macrophages contacting the test materials.

The negative control materials, TCPS and TCPS containing a glass retaining ring, showed very little IL-1ß activity at all time points, as shown in Figure 6.17. In comparison, the LPS-stimulated cells produced large amounts of IL-1ß, in the hundreds to thousands of picograms per milliliter, as expected (data not shown here, refer to Appendix 4). The IL-1ß levels declined with extended culture periods, as has been shown by a number of investigators for monocytes cultured *in vitro*.

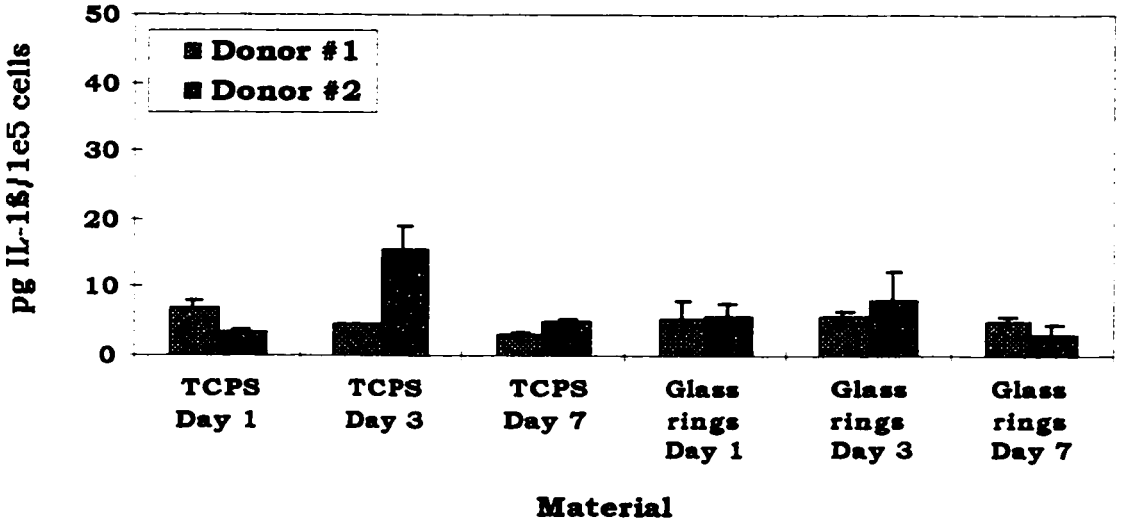

Figure 6.17 Macrophage release of IL-1ß after culture on TCPS or TCPS with a glass ring insert.

Low IL-1ß production from macrophages contacting the hydrophilic MEC polymer series is demonstrated in Figures 6.18-6.20. Values for most donors remained well below 20 ng/mL for all time points. FN-coated materials were tested with only Donors #1 and #6 for the 0.22μ and 5μ MEC polymers. The FN-coated 0.22μ MEC data for Donor #6 has elevated levels compared to the other materials, but is not significantly different due to the large error associated with those samples. Similarly, the results from the 5μ and 8μ MEC data do not indicate significant differences between controls and test materials. FN

showed no effect on IL-1ß production. These materials appear to have little capacity to activate macrophages to produce IL-1ß for the time period tested.

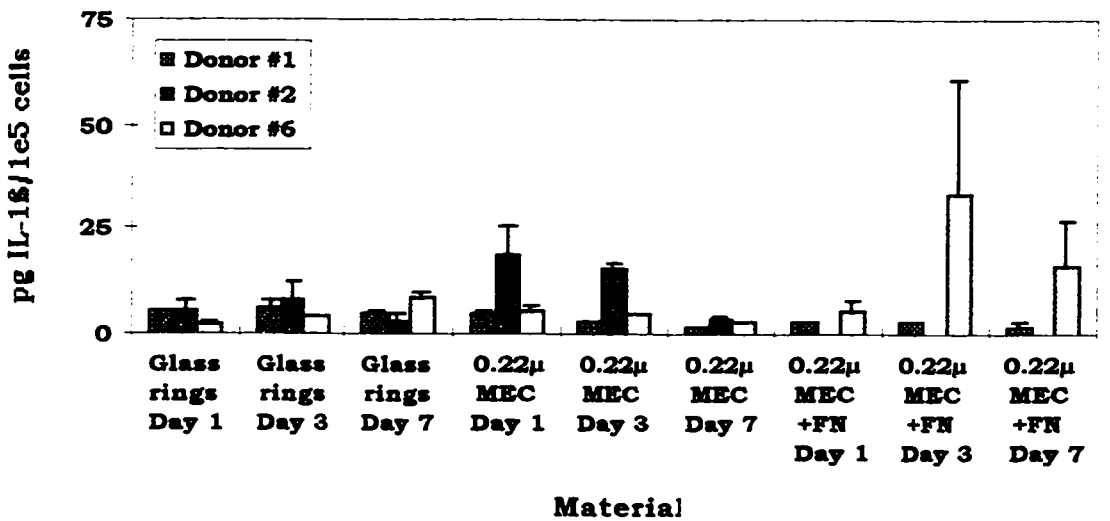

Figure 6.18 IL-1ß production from macrophages contacting 0.22μ MEC

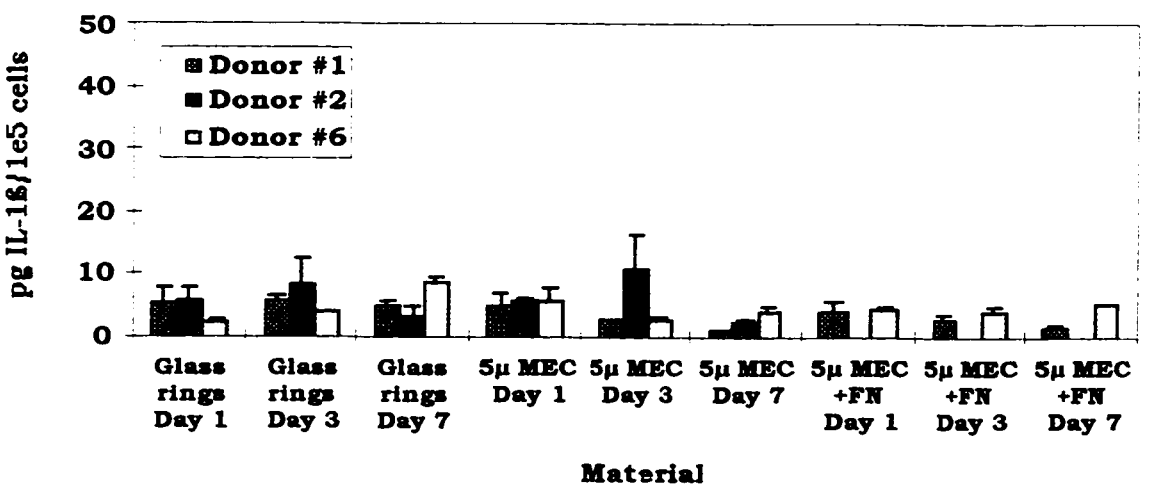

Figure 6.19 IL-1ß production from macrophages contacting 5μ MEC.

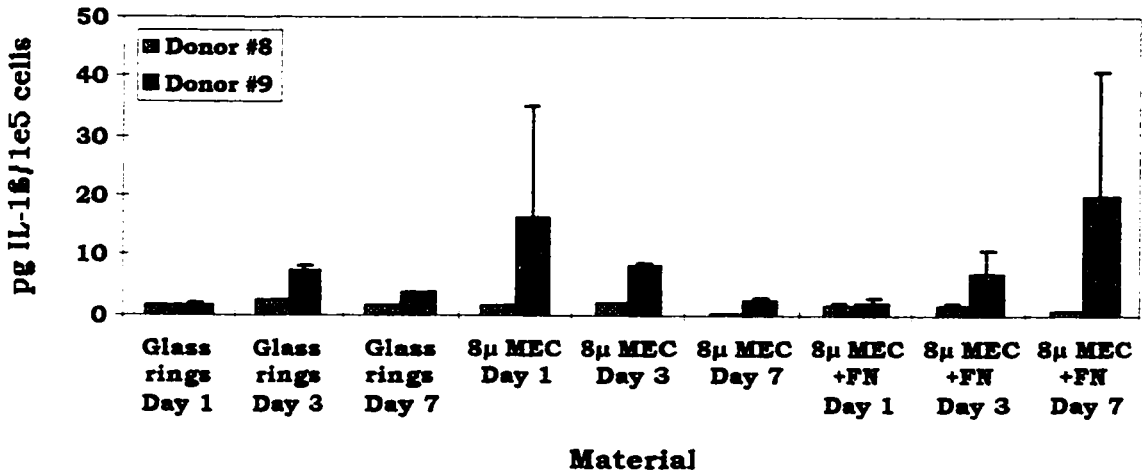

Figure 6.20 IL-1ß production from macrophages contacting 8μ MEC.

Similar to the MEC polymer series results, Nylon 6 had low IL-1ß production from macrophages contacting this material (Figure 6.21). IL-1ß levels remained below 20 ng/mL for most donors and time points. One donor's monocytes, #3, had a significantly higher response to Nylon 6 at days 1 and 3, falling to background levels by day 7. FN-coated Nylon 6 was only tested with Donor #6. FN pre-coating has no apparent effect on IL-1ß production.

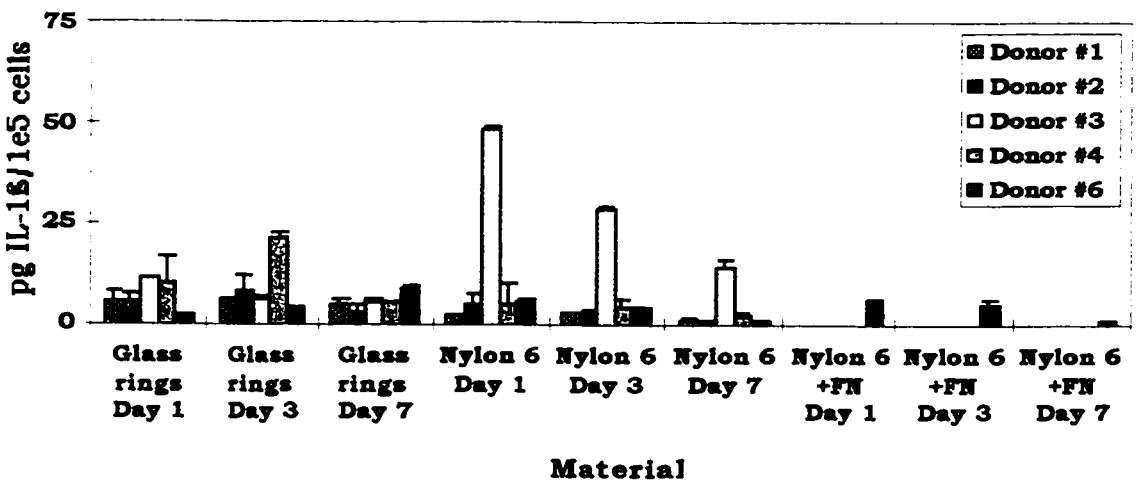

Figure 6.21 IL-1ß production from macrophages contacting Nylon 6.

IL-1ß production from macrophages contacting the hydrophobic polymers showed dramatically different results from the MECs and Nylon 6 hydrophilic polymers. Although there was a fair amount of variability between monocyte preparations/donors for PTFE and 10μ ePTFE, the 30μ and 60μ ePTFE materials were consistently much higher than the controls (Figures 6.22 to 6.25). Please note the differences in scales compared to the MEC and Nylon 6 graphs. These differences will be noted later in the HL-60 adherence assays (Chapter 7) which show a shift in endothelial cell activation and function when exposed to these macrophages supernatants. FN pre-coating of these materials decreased IL-1ß production on PTFE, 10μ ePTFE and 30μ ePTFE, but not for 60μ ePTFE. These data suggest that there is a definite effect of surface topography on IL-1ß production by macrophages contacting these materials. In addition, pre-coating with the adhesive protein FN diminished the inflammatory response for the smaller fibril lengths of ePTFE, but had no effect on the largest fibril length. The effect seen with 60μ ePTFE may be due to macrophages being more activated when adhered to long fibrils, which could over-ride any passivating effects of FN pre-coating. Lower levels of activation seen with the non-porous and shorter fibril lengths suggest that fibrils close to the size of the macrophages will not allow the macrophages to become as activated upon adhesion as on the 60μ ePTFE.

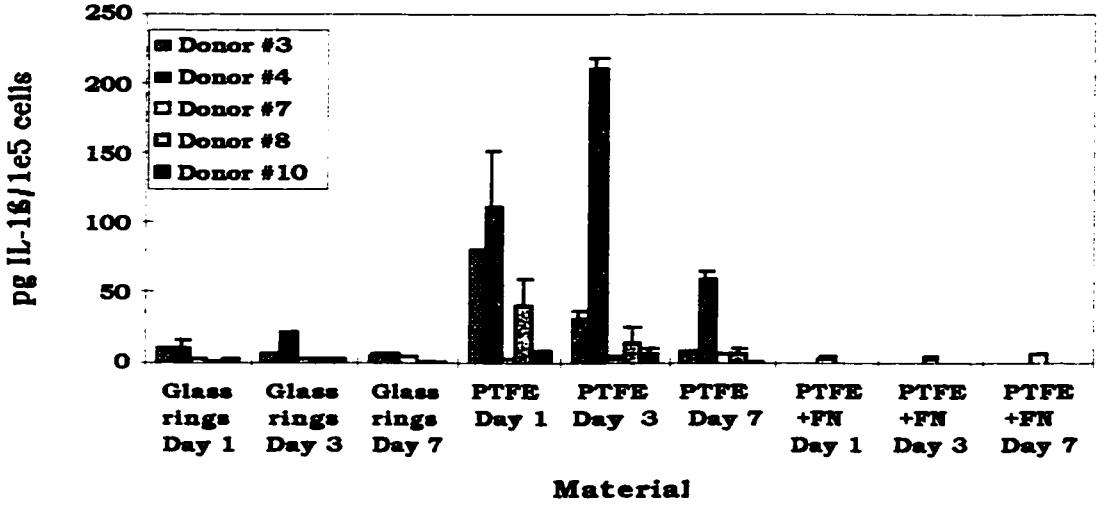

Figure 6.22 IL-1ß production from macrophages contacting PTFE.

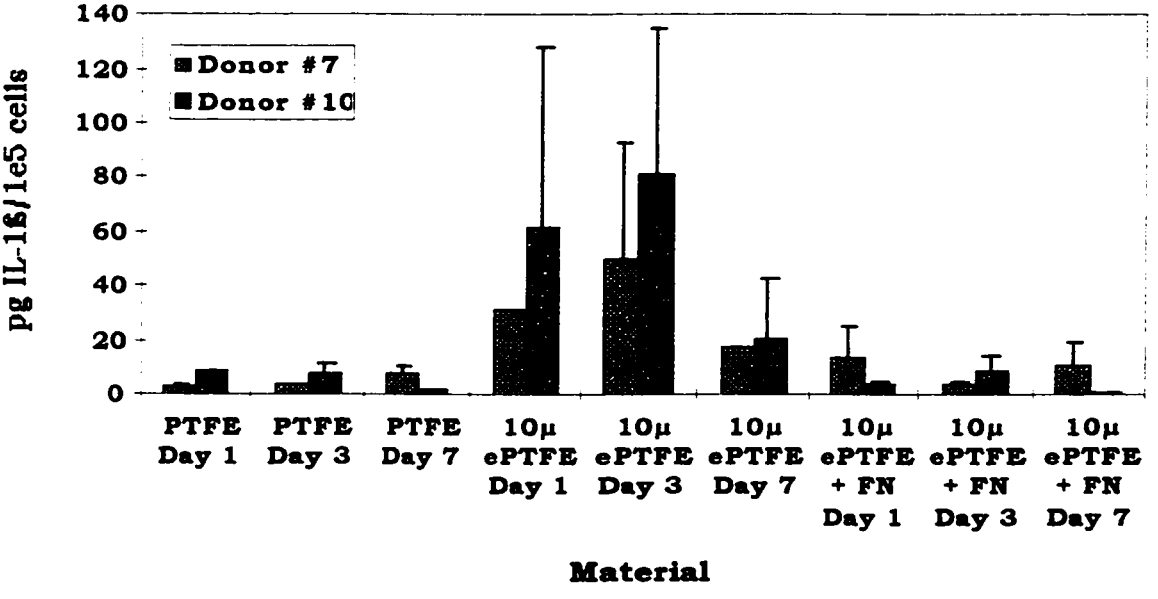

Figure 6.23 IL-1ß production from macrophages contacting 10μ ePTFE.

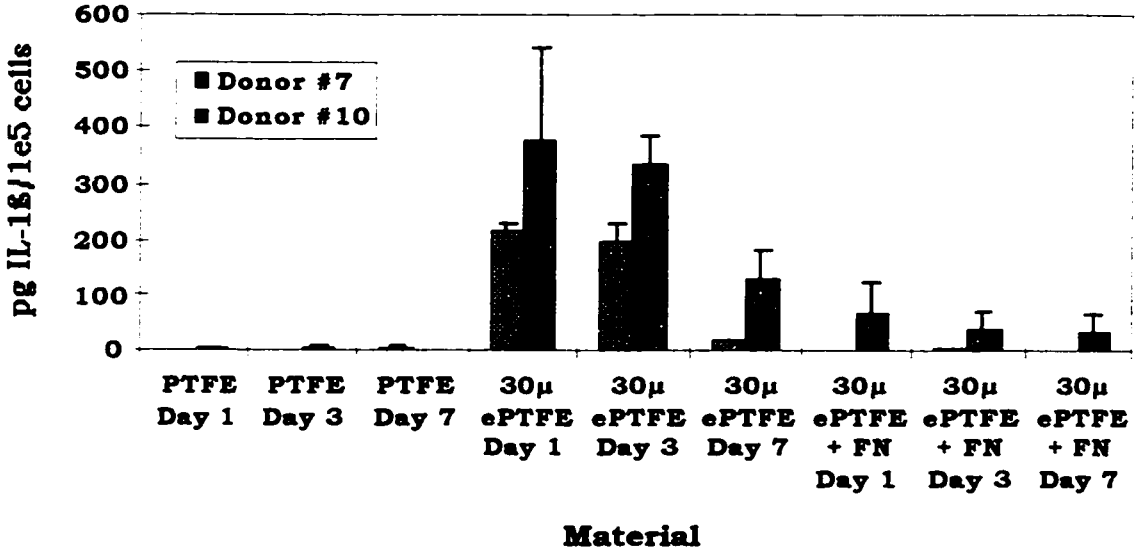

Figure 6.24 IL-1ß production from macrophages contacting 30μ ePTFE.

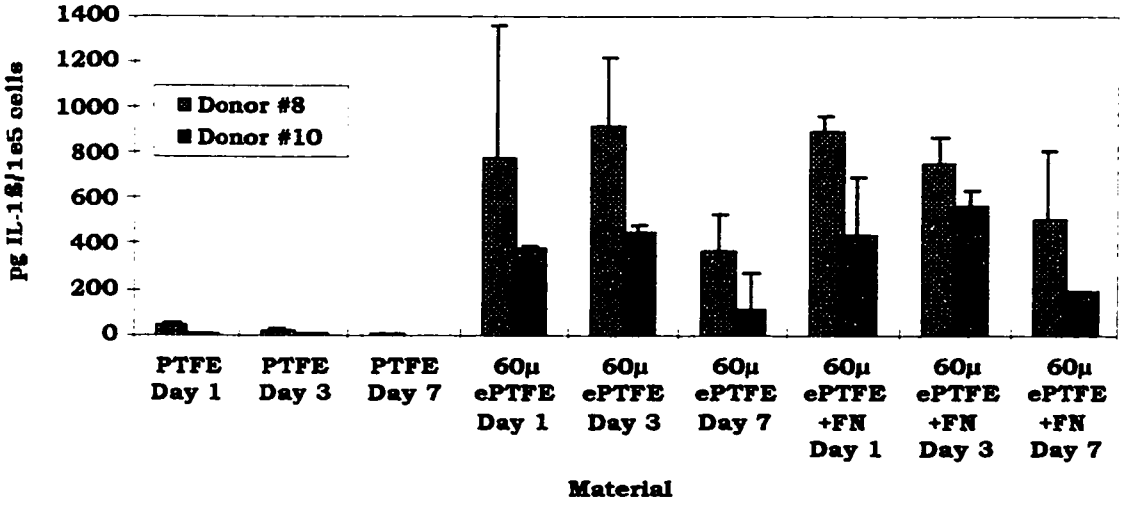

Figure 6.25 IL-1ß production from macrophages contacting 60μ ePTFE.

6.5.4 TNFα ELISA Results

The TNFα results for most polymers mirrored what was seen in the IL-1ß section. Typically, the negative controls showed very low TNFα secretion from macrophages contacting TCPS or glass ring control wells (Figure 6.26). Similarly, the MEC and Nylon 6 materials showed low levels of TNFα, with slightly elevated levels seen at the day 1 time point as shown in Figures 6.27 to 6.30. FN pre-coating appeared to have little or no effect on TNFα secretion from macrophages on these materials.

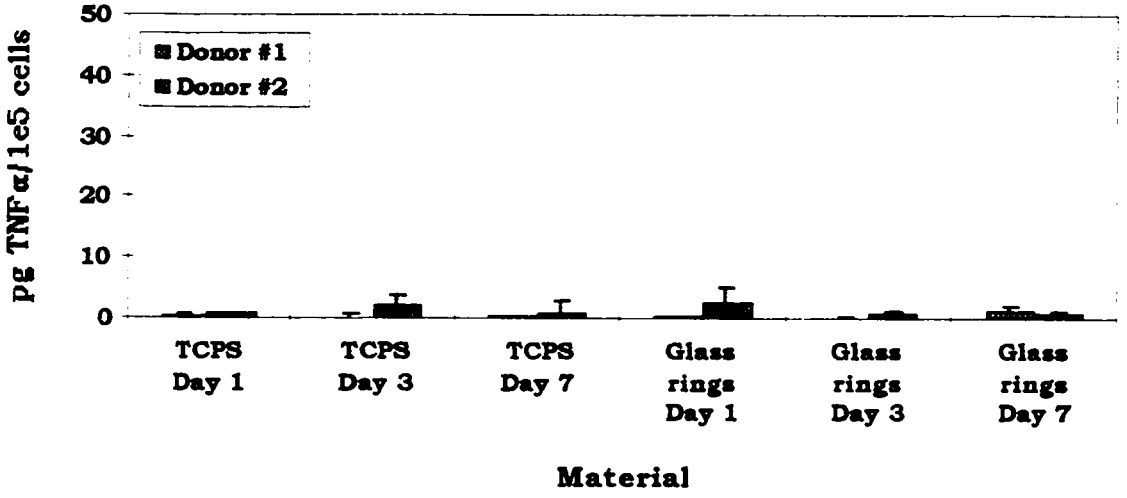

Figure 6.26 TNFα production from macrophages contacting TCPS or TCPS containing a glass retaining ring.

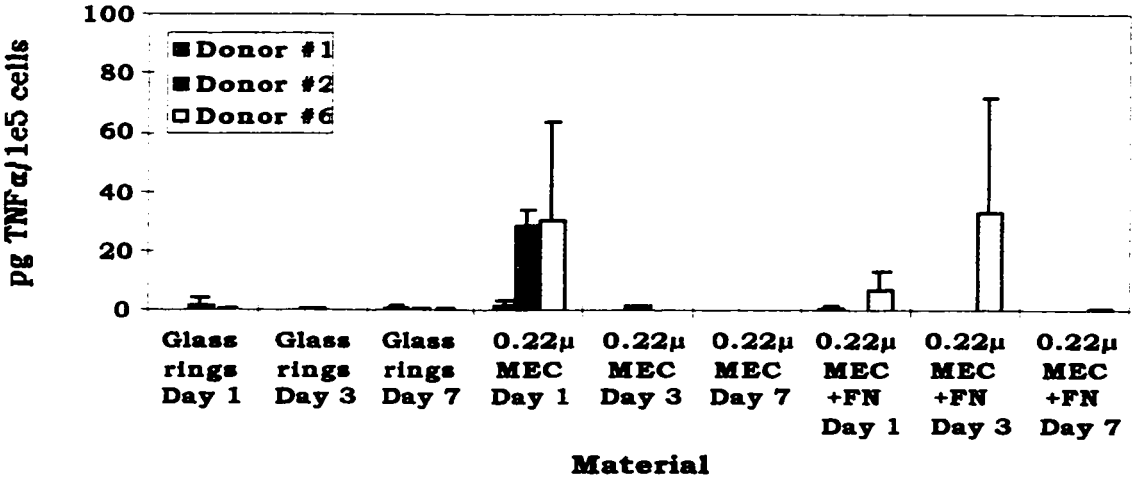

Figure 6.27 TNFα production from macrophages contacting 0.22μ MEC.

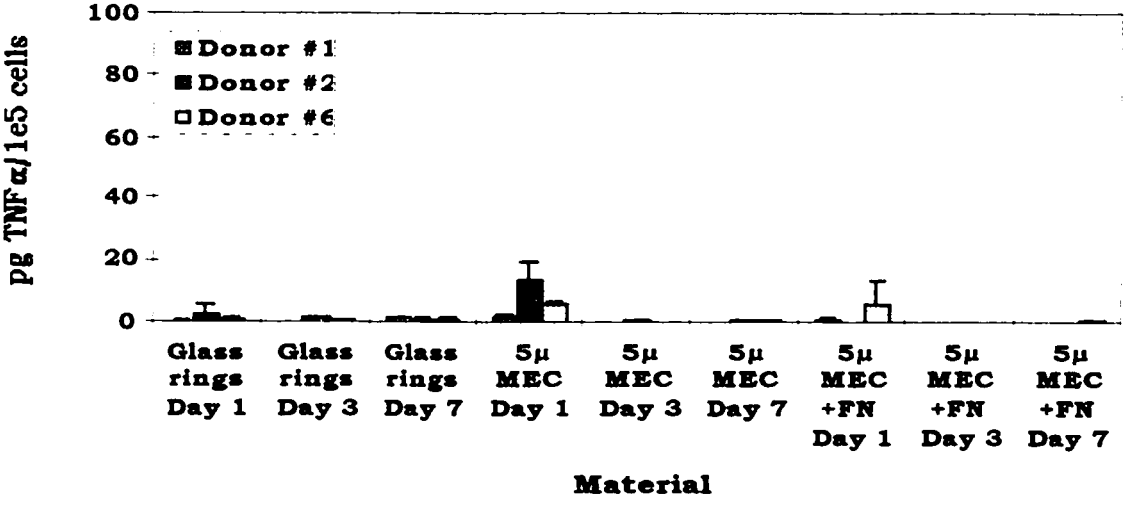

Figure 6.28 TNFα production from macrophages contacting 5μ MEC.

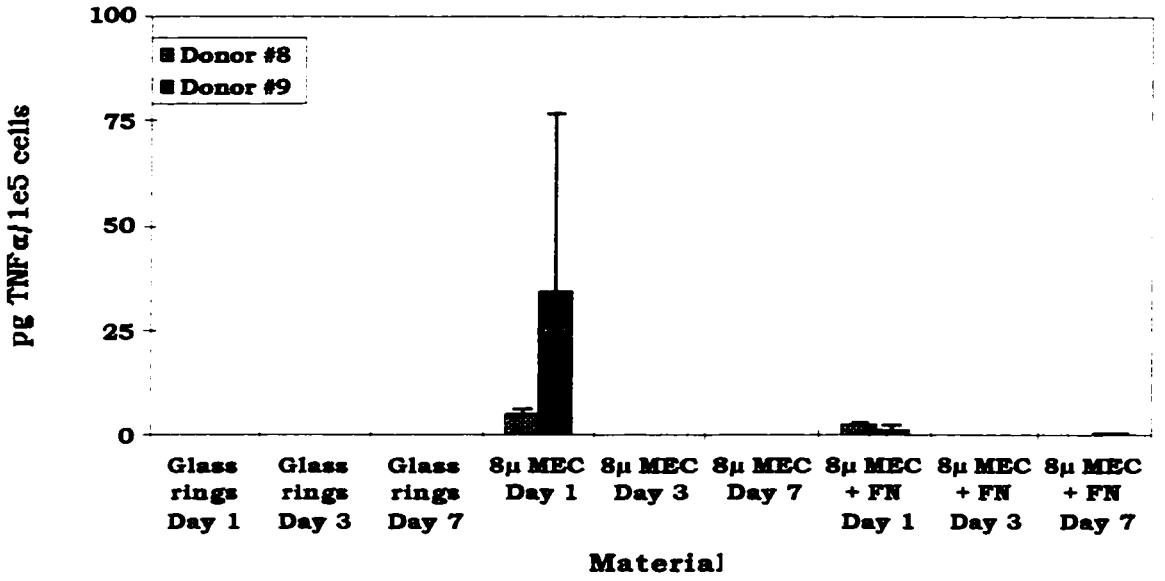

Figure 6.29 TNFα production from macrophages contacting 8μ MEC.

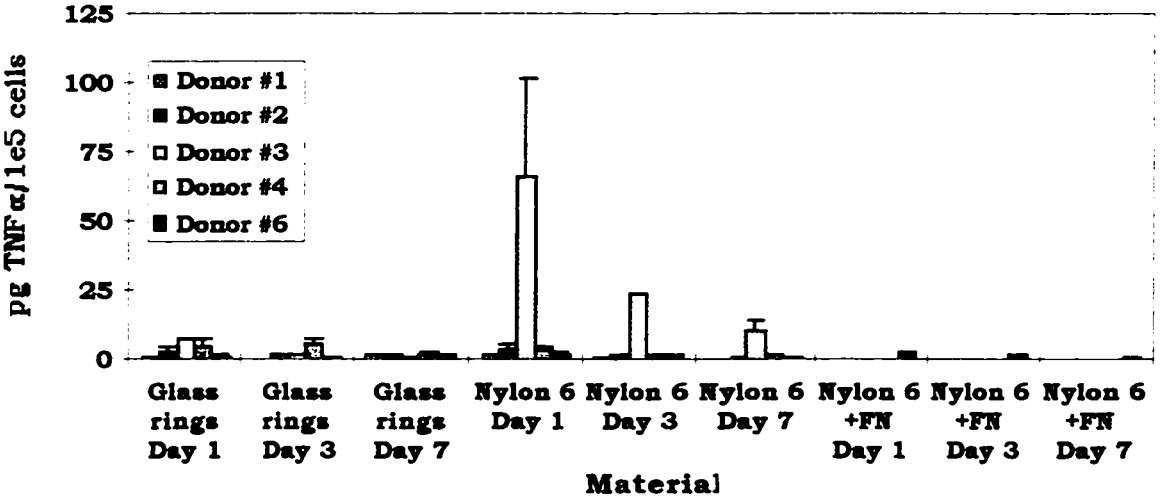

Figure 6.30 TNFα production from macrophages contacting Nylon 6.

Similar to the IL-1ß results, the hydrophobic PTFE/ePTFE polymer series had a dramatic effect on TNFα secretion from macrophages. Once again, the PTFE and 10μ ePTFE showed lower TNFα levels than the 30μ and 60μ ePTFE surfaces as shown in Figures 6.31 to 6.34. The amount of TNFα secretion from the macrophages contacting 60μ ePTFE was dramatically higher than all of the other fibril lengths, again suggesting the role of this parameter on macrophage activation. The same effects were seen with FN pre-coating of the materials as with the IL-1ß data. FN-coated PTFE, 10μ ePTFE, and 30μ ePTFE showed some reduction in TNFα production. The 60μ ePTFE FN-coated materials did not see a reduction in TNFα for macrophages contacting this surface.

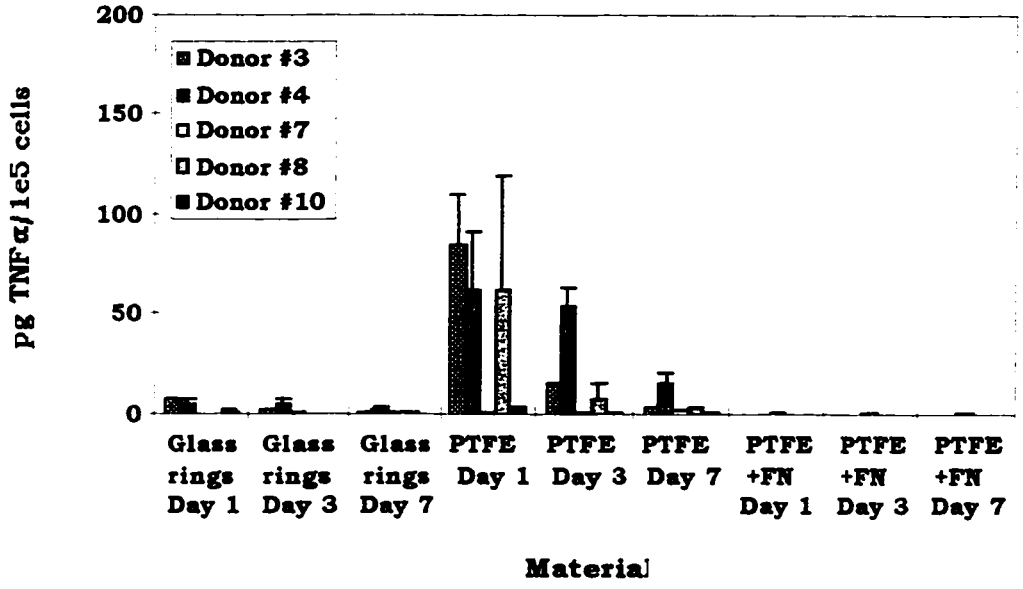

Figure 6.31 TNFα production from macrophages contacting PTFE.

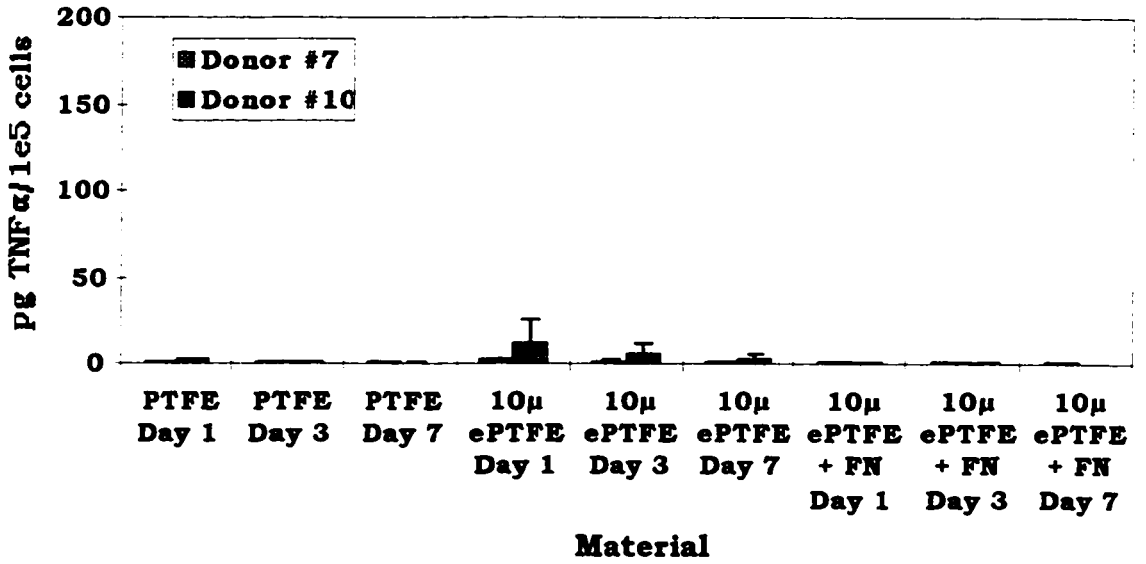

Figure 6.32 TNFα production from macrophages contacting 10μ ePTFE.

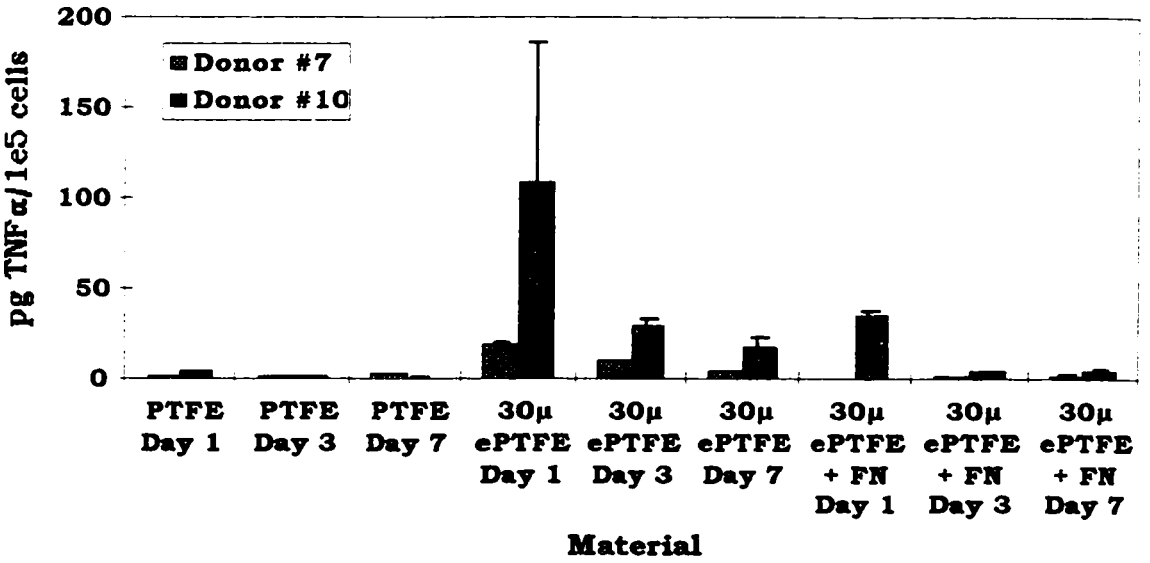

Figure 6.33 TNFα production from macrophages contacting 30μ ePTFE.

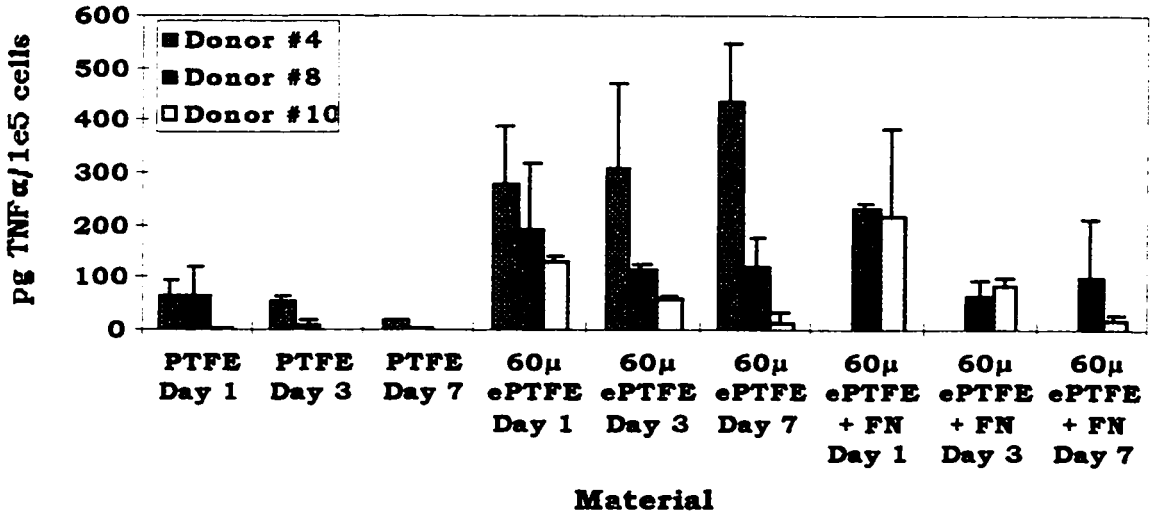

Figure 6.34 TNFα production from macrophages contacting 60μ ePTFE.

6.5.5 IL-8 ELISA Results

IL-8 expression from macrophages contacting all material surfaces were unexpectedly high, even on the negative control materials (Figure 6.35). The results were clearly influenced by monocyte preparation/donor variability. Some donor monocytes were sensitive to the substrate they contacted, while others showed no effect at all. This also holds true for FN pre-coating of materials. This make interpretation of the IL-8 less clear than the other cytokines assayed. The only material that showed definitively higher IL-8 production was for macrophages contacting 60μ ePTFE. This polymer showed dramatically higher levels of IL-8, which may be connected to what is seen with the IL-1ß and TNFα data. It is unclear at this time why such high and variable levels of IL-8 are seen, and what the clinical implications of such high levels of IL-8 would mean in an implant situation. The IL-8 results for the different polymer surfaces are shown in Figures 6.36 to 6.43.

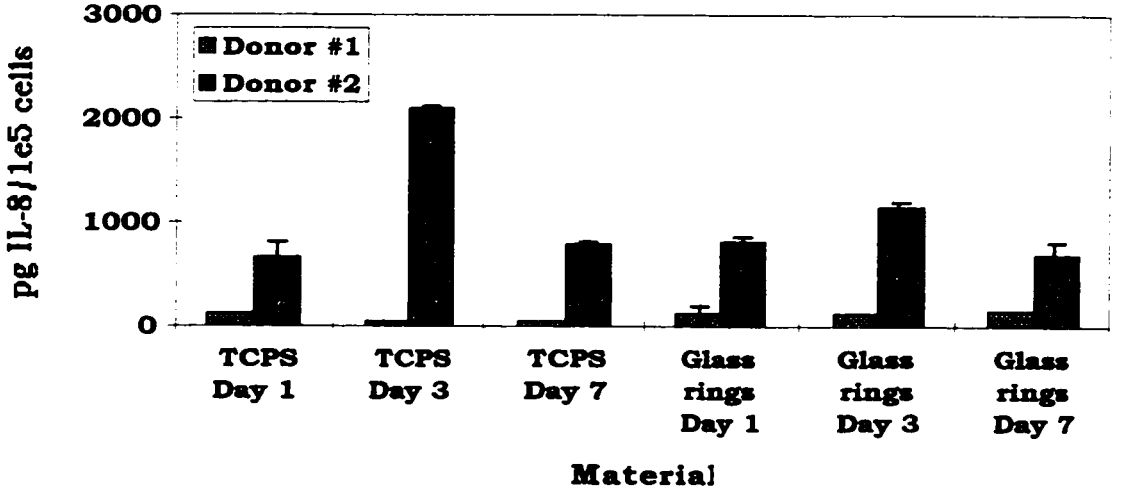

Figure 6.35 IL-8 production from macrophages contacting TCPS or TCPS containing a glass retaining ring.

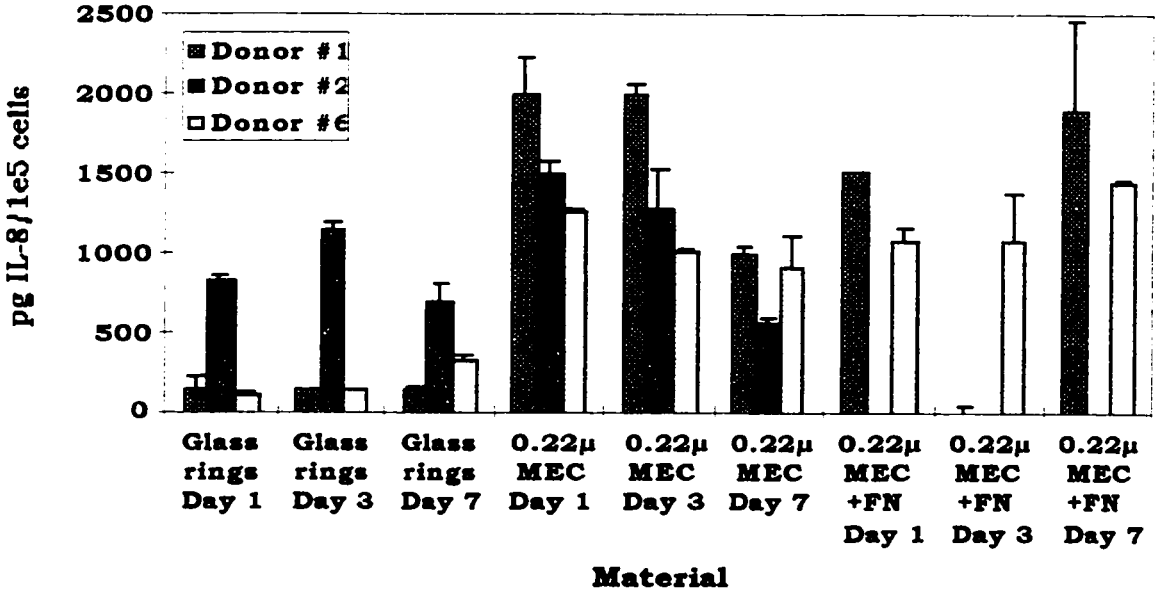

Figure 6.36 IL-8 production from macrophages contacting 0.22μ MEC.

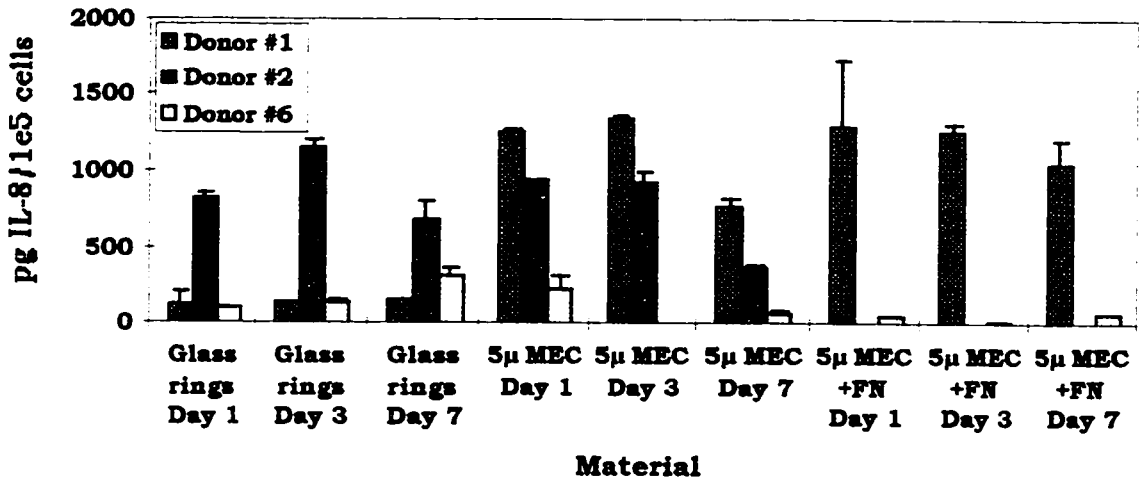

Figure 6.37 IL-8 production from macrophages contacting 5μ MEC.

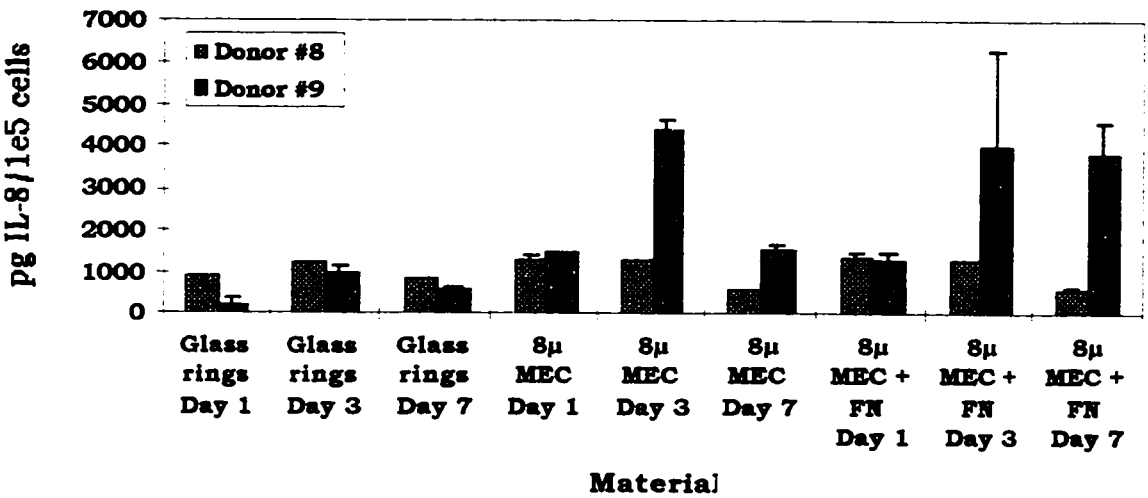

Figure 6.38 IL-8 production from macrophages contacting 8μ MEC.

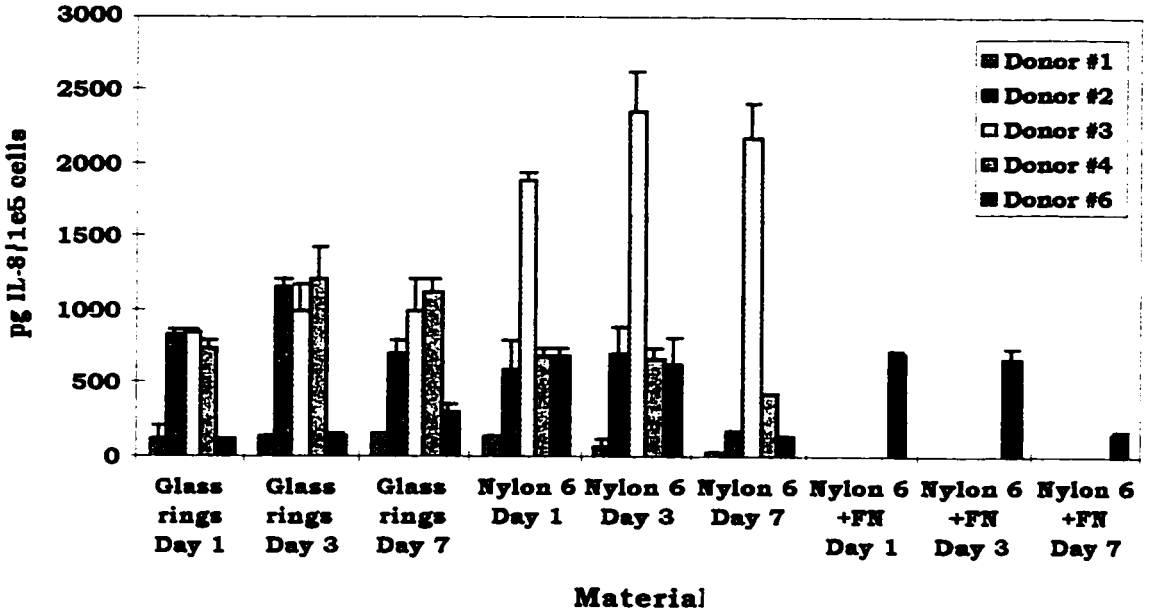

Figure 6.39 IL-8 production from macrophages contacting Nylon 6.

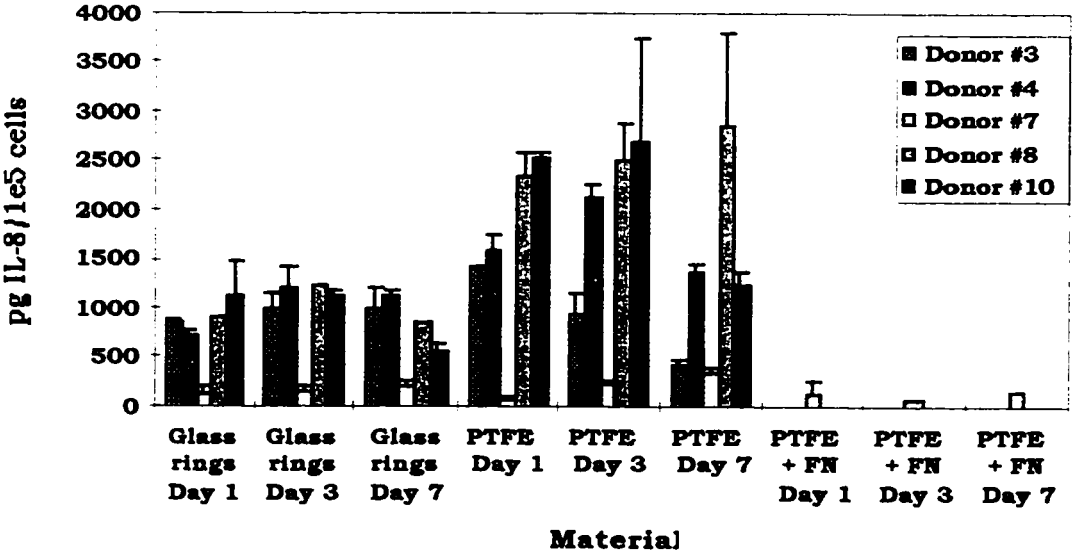

Figure 6.40 IL-8 production from macrophages contacting PTFE.

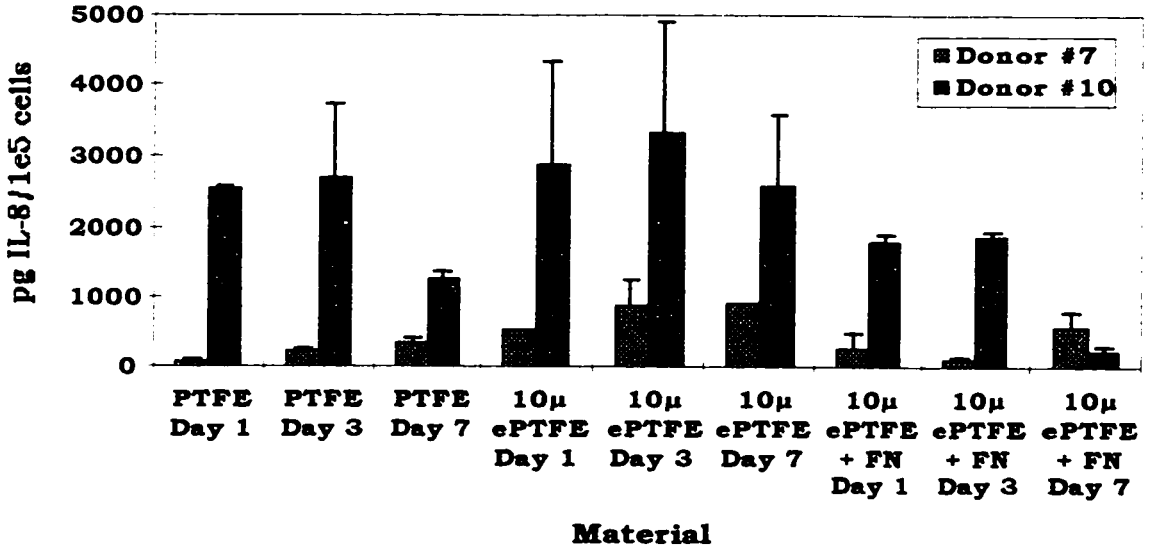

Figure 6.41 IL-8 production from macrophages contacting 10μ ePTFE.

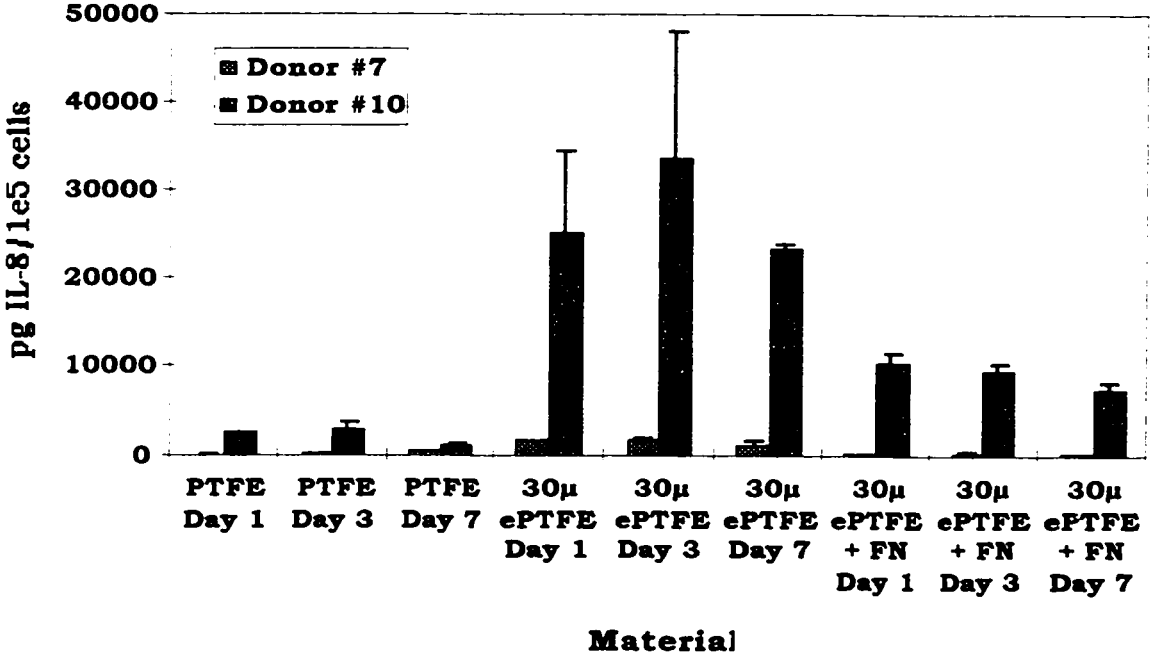

Figure 6.42 IL-8 production from macrophages contacting 30μ ePTFE.

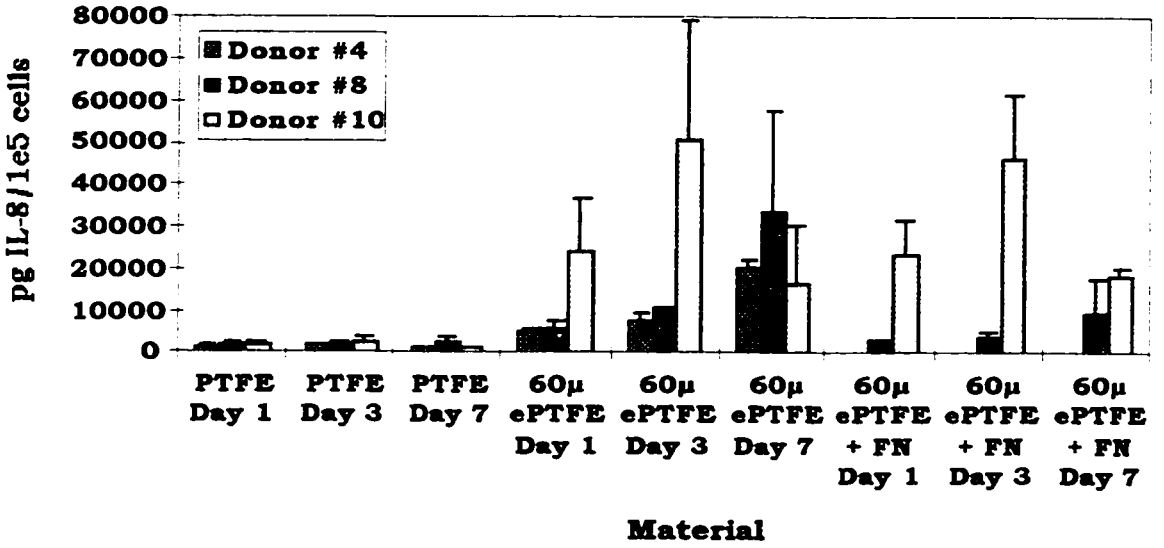

Figure 6.43 IL-8 production from macrophages contacting 60μ ePTFE.

6.5.6 Conclusions

In summary, some obvious trends exist for macrophage inflammatory cytokine release when contacting the different materials tested.

1) IL-1ß and TNFα had similar expression profiles for individual materials.

2) IL-8 expression is not clearly correlated with any surface properties except with 60μ ePTFE, where high levels were seen. IL-8 expression was highly variable depending on the monocyte preparation or donor.

3) IL-1ß and TNFα secretion from monocytes contacting the hydrophilic MEC and Nylon 6 materials were generally very low.

4) Monocytes contacting the hydrophobic PTFE and ePTFE materials showed elevated IL-1ß and TNFα secretion. There appears to be an effect of fibril length on production of these cytokines, with longer fibril lengths producing more of an inflammatory response. This is most marked with the 60μ ePTFE.

5) The effect of pre-coating materials with FN on inflammatory cytokine release from macrophages is dependent upon the material substrate. FN coatings had little or no effect on the hydrophilic MEC and Nylon 6 IL-1ß or TNFα production. In contrast, FN coating diminished the production of these cytokines on PTFE, 10μ ePTFE, and 30μ ePTFE. Pre-coating 60μ ePTFE with FN had no effect in reducing IL-1ß or TNFα secretion from macrophages.

These findings support the hypotheses proposed in Chapter 1. There appears to be an effect of surface chemistry on inflammatory cytokine release from macrophages. This is best demonstrated by comparing the MEC and Nylon 6 hydrophilic materials to the hydrophobic PTFE/ePTFE material series. Also, material topography plays an important part in macrophage activation as seen within the PTFE/ePTFE series, with more IL-1ß and TNFα production on materials with longer fibril lengths. Macrophage reaction to FN adsorption was dependent upon the material substrate. All of these material parameters play an important role in inflammatory cytokine production from macrophages, which will subsequently have effects on other cell types exposed to these cytokines. This will be elegantly illustrated in Chapter 7, where these macrophage supernatants affect endothelial cell activation and function dependent upon the types and amounts of cytokines present.

6.6 Notes for Chapter 6

Cardona, M. A., Simmons, R. L., and Kaplan, S. S. (1992). TNF and IL-1 generation by human monocytes in response to biomaterials. J. Biomed. Mater. Res. *26*, 851-859.

Dinarello, C. A. (1991). Interleukin-1 and Interleukin-1 Antagonism. Blood *77*, 1627-1652.

Fisher, A. A. (1990). Reactions at Silicone-Injected Sites on the Face Associated with Silicone Breast Implant "Inflammation" or "Rejection". CUTIS *45*, 393-395.

Furth, R. v. (1988). Inflammation: Basic Principles and Clinical Correlates, J. I. Gallin, ed. (New York: Raven Press).

Goldblum, R. M., Pelley, R. P., O'Donell, A. A., Pyron, D., and Heggers, J. P. (1992). Antibodies to silicone elastomers and reactions to ventriculoperitoneal shunts. Lancet *340*, 510-513.

Heggers, J. P., Kossovsky, N., Parsons, R. W., Robson, M. C., Pelley, R. P., and Raine, T. J. (1983). Biocompatibility of Silicone Implants. Annals of Plastic Surg. *11*, 38-45.

Hubbard, A. K. (1989). Role for T Lymphocytes in Silica-Induced Pulmonary Inflammation. Laboratory Investigation *61*, 46-52.

Kossovsky, N., Heggers, J. P., and Robson, M. C. (1987). Experimental demonstration of the immunogenicity of silicone-protein complexes. J. Biomedical Materials Research *21*, 1125-1133.

Kossovsky, N., Zeidler, M., Chun, G., Papasian, N., Nguyen, A., Rajguru, S., Stassi, J., Gelman, A., and Sponsler, E. (1993). Patients with Silicone Breast Implants Show Increased IgG Binding Affinity to Extracellular Macromolecules. In The 19th Annual Meeting of the Society for Biomaterials (Birmingham, AL, USA, pp. 231.

Lan, H. Y., Nikolic-Paterson, D. J., Mu, W., and Atkins, R. C. (1995). Local macrophage proliferation in multinucleated giant cell and granuloma formation in experimental Goodpasture's syndrome. Am. J. Pathol. *147*, 1214-1220.

Miller, K. M., and Anderson, J. M. (1988). Human monocyte/macrophage activation and interleukin 1 generation by biomedical polymers. J. Biomedical Materials Research *22*, 713-731.

Miller, K. M., Rose-Caprara, V., and Anderson, J. M. (1989). Generation of IL1-like activity in response to biomedical polymer implants: A comparison of in vitro and in vivo models. J. Biomedical Materials Research *23*, 1007-1026.

Mohr, C., Gemsa, D., Graebner, C., Hemenway, D. R., Leslie, K. O., Absher, P. M., and Davis, G. S. (1991). Systemic Macrophage Stimulation in Rats with Silicosis: Enhanced Release of Tumor Necrosis Factor-alpha from Alveolar and Peritoneal Macrophages. Am. J. Respir. Cell Mol. Biol. *5*, 395-402.

Nathan, C. F. (1987). Secretory Products of Macrophages. J. Clinical Investigation *79*, 319-326.

Oppenheim, J. J., Kovacs, E. J., Matsushima, K., and Durum, S. K. (1986). There is more than one interleukin 1. Immunology Today *7*, 45-56.

Peimer, C. A., Medige, J., Eckert, B. S., Wright, J. R., and Howard, C. S. (1986). Reactive synovitis after silicone arthroplasty. J. Hand Surgery *11A*, 624-638.

Pertoft, H., Johnsson, A., Wärmegård, B., and Seljelid, R. (1980). Separation of Human Monocytes on Density Gradients of Percoll®. J. Immunological Methods *33*, 221-229.

Sank, A., Chalabain-Baliozian, J., Ertl, D., Sherman, R., Nimni, M., and Tuan, T. L. (1993). Cellular Responses to Silicone and Polyurethane Prosthetic Surfaces. J. Surgical Research *54*, 12-20.

Shankar, R., and Greisler, H. P. (1994). Inflammation and Biomaterials. In Implantation Biology: The Host Response and Biomedical Devices, R. S. Greco, ed. (Boca Raton: CRC Press), pp. 67-80.

Snow, R. B., and Kossovsky, N. (1989). Hypersensitivity Reaction Associated with Sterile Ventriculoperitoneal Shunt Malfunction. Surg. Neurol. *31*, 209-214.

Stone, R. (1993). The Case Against Implants. Science *260*, 31.

Struhar, D. J., Harbeck, R. J., Gegen, N., Kawada, H., and Mason, R. J. (1989). Increased expression of class II antigens of the major histocompatibility complex on alveolar macrophages and alveolar type II cells and interleukin-1 (IL-1) secretion from alveolar macrophages in an animal model of silicosis. Clin. Exp. Immunol. *77*, 281-284.

Varga, J., Schumacher, H. R., and Jimenez, S. A. (1989). Systemic Sclerosis after Augmentation Mammoplasty with Silicone Implants. Annals of Internal Medicine *111*, 377-383.

Ziats, N. P., Miller, K. M., and Anderson, J. M. (1988). In vitro and in vivo interaction of cells with biomaterials. Biomaterials *9*, 5-13.

Chapter 7

Activation of Endothelial Cells by Macrophage Interactions with Biomaterial Surfaces

7.1 Introduction

In Chapter 6, evidence was given to support the first three hypotheses stated in Chapter 1: Macrophage activation is affected by differences in material 1) surface chemistry, 2) surface topography, and 3) extracellular matrix coating. In this section, data is presented that will reveal the functional changes that occur in endothelial cells exposed to the macrophage supernatants used in Chapter 6.5. It follows that where inflammatory cytokines are expressed in macrophages contacting different materials, endothelial cells coming in contact with those cytokines will be activated depending upon the levels of cytokines produced. In turn, if endothelial cell activation occurs, a functional change occurs which will promote neutrophil adhesion to the endothelial cell surface.

The pathways of endothelial cell activation are well understood. A vital function of activated endothelium is to recruit inflammatory cells from the bloodstream to sites of inflammation. As discussed in Chapter 2, neutrophil recruitment is initiated by the expression of E-selectin, and subsequent tight binding and diapedesis is accomplished through the interaction of integrin and immunoglobulin superfamily adhesion molecules. Although these activation events can be monitored through Northern blot analysis, it is important to determine whether a functionally active neutrophil adhesion pathway exists. Shown in this chapter, the macrophage/material interactions that caused significant inflammatory cytokine secretion will functionally activate endothelial cells exposed to those supernatants. This will result in the promotion of neutrophil adhesion to activated endothelial monolayers. Neutrophil adhesion is initiated by the up-regulation of a number of cell adhesion molecules, including E-selectin, via cytokine stimulation.

Although the cytokine data would suggest that supernatants which had significant levels of IL-1ß and TNFα would activate endothelial cells, a biological test of endothelial cell activation and the subsequent changes in function (neutrophil adherence) must be tested. Due to the potential for the production of inhibitory as well as inflammatory cytokines, the IL-1ß and TNFα data can not stand alone. A human neutrophil cell line, HL-60, adheres to activated endothelial cells and can be used as a test for activation. By loading HL-60s with Neutral Red dye prior to co-cultivation with endothelial cells, the number of HL-60s attached determines the level of activation of endothelial cell monolayers. When the cells are lysed to release the dye, the amount of dye correlates with the level of endothelial cell activation. The dye content is quatitated by reading each cell lysate on a plate reader.

7.2 Materials and Methods

Macrophage supernatants were generated following the protocols outlined in Chapters 3.4.5 and 6.5. The same macrophage supernatants used for the cytokine data in 6.5 were used to stimulate endothelial cell monolayers seeded in 24-well plates. The level of endothelial cell activation from stimulation was determined using the Neutral Red HL-60 assay as described in Chapter 3.8.2.

In Figure 7.1, HUVEC monolayers were stimulated with varying amounts of IL-1ß. Neutral Red-labeled HL-60s were added and washed after 20 minutes of incubation. The steep slope of the curve indicates that once a critical level of IL-1ß is added to HUVECs, there is a very narrow range where there is an intermediate level of activation. In this way, HUVECs display an "on or off" switch for activation. Once the critical level of IL-1ß is reached, full activation occurs. Maximal activation in this assay was achieved by 100 pg/mL. It is important to note that IL-1ß and TNFα act synergistically, thus lower

concentrations are needed to reach a similar response as that seen with IL-1ß alone (Dinarello, 1988). With the supernatants assayed here, the combinatorial effect of both cytokines will provide maximal activation at levels approximating 100pg/mL seen in Figure 7.1.

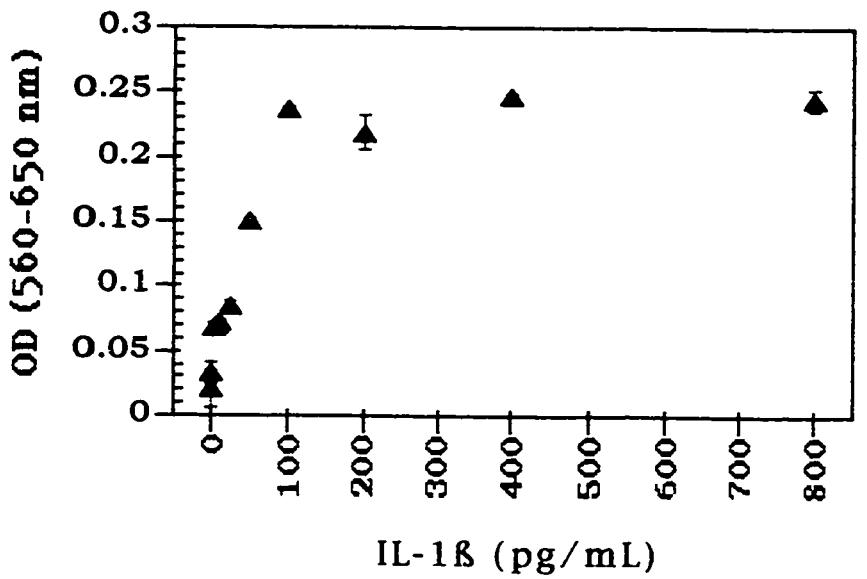

Figure 7.1 HL-60 assay of HUVECs stimulated with varying amounts of IL-1ß.

7.3 Results and Discussion

There is some variation in the HL-60 assays, primarily in the level of HL-60 dye accumulation on any given day. The Neutral Red method is less robust than the ^{51}chromium protocol, but is easier and safer to perform since radioactive materials are not used. There was always some residual unincorporated dye that could not be removed from the HL-60s, which subsequently raised background levels due to endothelial cell incorporation of the dye. This effect was minimized by reducing co-culture incubation times to 15-20 minutes. The combined effect of variable dye loading of HL-60s and short co-culture incubation times reduces the level of sensitivity of this assay compared with the radiolabeled method. This was, however, an adequate method to demonstrate endothelial

cell activation, as shown in the following figures. Also, the rapidity of HL-60 attachment to activated endothelial cells (less than 15 minutes) is dramatic. As soon as the HL-60s settled to the bottom of the well, if activated endothelial cells were present, attachment was immediate.

Monocyte preparation and/or donor variability was apparent, but the HL-60 assay data was consistent with the cytokine data in Chapter 6.5. Due to these variations and to those in individual HL-60 assays, each graph represents the HL-60 assay results from each donor individually.

The HL-60 assay of the MEC and Nylon 6 materials showed low levels of endothelial cell activation that were near or below background levels compared to the glass ring controls, as seen in Figures 7.2-7.4. The 8μ MEC data is shown in Figure 7.4 and later in Figure 7.8. There was some donor variability in the 0.22μ and 8μ MEC cytokine data, which in turn influenced the HL-60 results. An elevation in endothelial cell activation for the Day 1 time points for Donor #2 (0.22μ MEC, Figure 7.3) and Donor #9 (8μ MEC, Figure 7.4). There was no evidence of any effect from FN-coating the 0.22μ and 5μ MEC substrates. FN coating of the 8μ MEC reduced the level of activation, but only significantly for Day 1 for donor #9 (Figure 7.4). As expected, the MEC data correlates well with the low levels of IL-1ß and TNFα cytokine release reported in Chapter 6.5. Nylon 6 also demonstrated low endothelial cell activation (Figures 7.2, 7.3, 7.5-7.7). The hydrophilic polymers generally did not activate HUVECs to any significant degree, especially compared to the PTFE/ePTFE series.

Table 7.1 summarizes the IL-1ß and TNFα cytokine content compared to the measured level of HUVEC activation using the HL-60 assay for the MEC and Nylon materials. The supernatants were diluted 1:3 when added to the HUVECs in the HL-60 assay; the cytokine data reported in Table 7.1 reflects this dilution. Macrophage

supernatants used in these assays were from one macrophage/material well run in duplicate. This was necessary due to the limited amount of macrophage supernatant available to run all of the cytokine and HL-60 assays. The individual normalized cytokine data for these specific wells were used in Table 7.1, and do not represent an average cytokine value. The cytokine data is expressed as pg/mL; the HL-60 data reports the optical density of the Neutral Red found in the HUVEC/HL-60 lysates. The data for the glass ring controls is included to report the background levels observed in the HL-60 assay for each donor set.

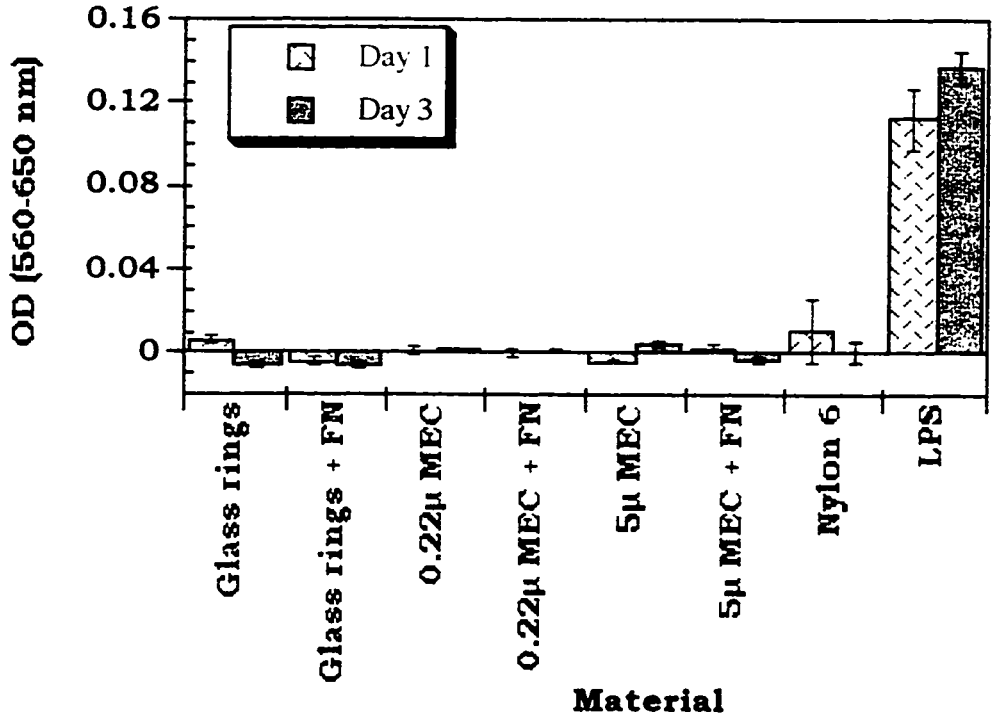

Figure 7.2 HL-60 assay of Donor #1 macrophage supernatants: 0.22μ MEC (+/- FN), 5μ MEC (+/- FN) and Nylon 6.

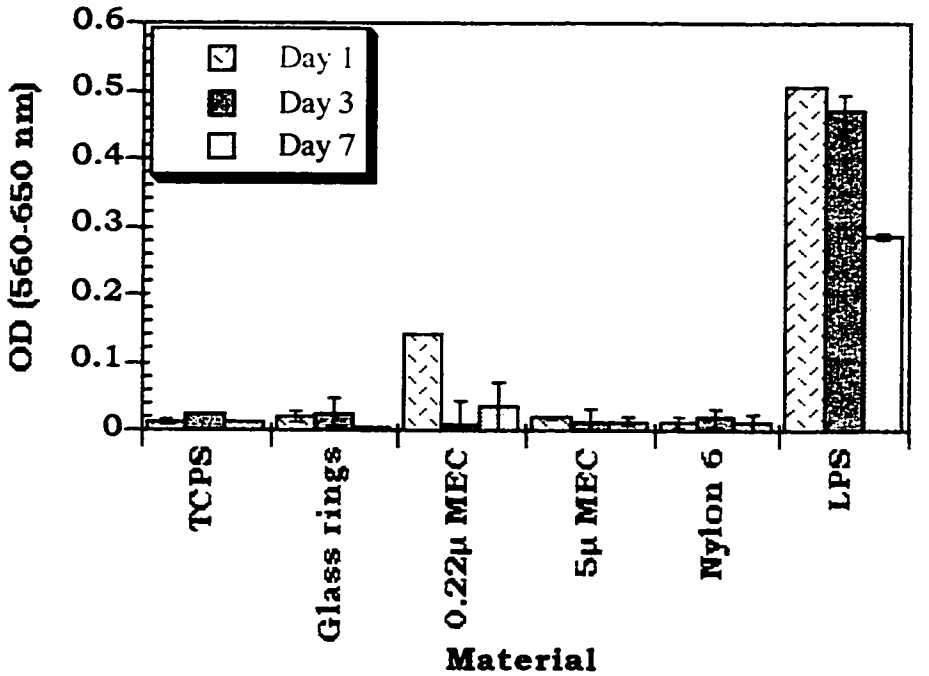

Figure 7.3 HL-60 assay of Donor #2 macrophage supernatants: 0.22μ MEC, 5μ MEC and Nylon 6.

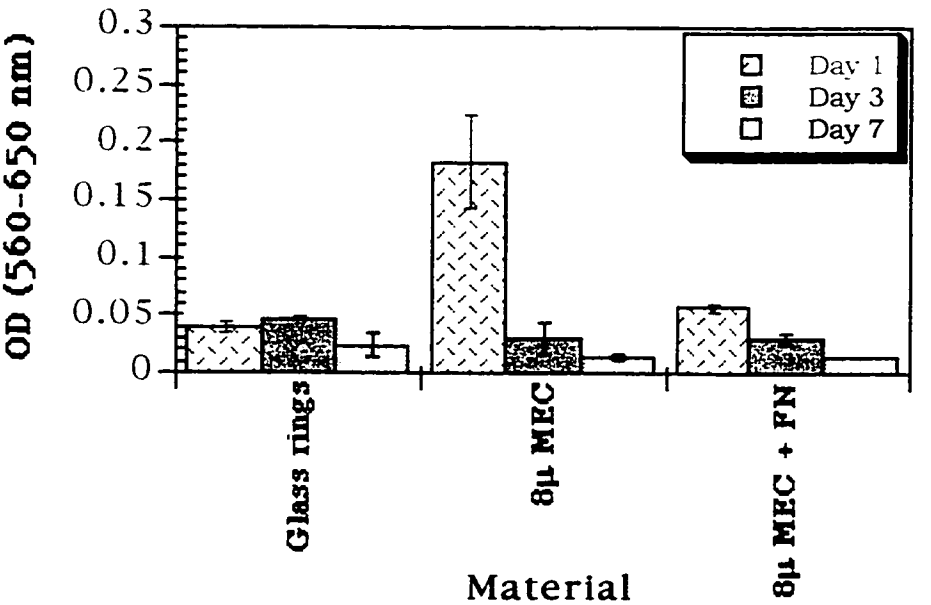

Figure 7.4 HL-60 assay of Donor #9 macrophage supernatants: 8μ MEC (+/- FN).

Table 7.1 HL-60 Adherence Associated with Macrophage IL-1ß and TNFα Production: Hydrophilic Polymers

Material	Donor	Day 1*			Day 3*			Day 7*		
		IL-1ß	TNFα	HL-60	IL-1ß	TNFα	HL-60	IL-1ß	TNFα	HL-60
Glass Rings	1	1.3	0	.006	1.9	0	-0.005	1.5	0.3	---
	2	1.4	0.9	0.019	1.7	0.3	0.025	0.8	0.3	0.006
	3	3.8	2.5	0.007	2.0	0.5	0.006	1.8	0.3	0.013
	4	2.1	1.3	0.023	7.5	1.2	0.023	1.9	0.6	0.010
	7	0.9	0	-0.005	1.1	0.2	0.022	2.1	0.3	0.014
	8	0.6	0.1	0.003	0.9	0	---	0.5	0.2	0.006
	9	0.6	0.1	0.039	2.5	0	0.047	1.4	0	0.024
	10	0.5	0.1	0.001	0.5	0	0.001	0.3	0	0.008
0.22μ MEC	1	1.6	1.1	0.001	1.1	0	0.001	0.4	0	0.001
	2	8.0	9.8	0.141	5.0	0.6	0.007	1.3	0.1	0.034
0.22μ MEC + FN	1	0.9	0.4	0	1.3	0.1	0.001	0.5	0	---
5μ MEC	1	1.3	0.3	-0.004	1.0	0.1	0.005	0.4	0	---
	2	1.9	4.5	0.019	4.9	0.2	0.011	0.8	0.1	0.013
5μ MEC + FN	1	0.9	0.2	0.002	1.1	0	-0.003	0.5	0.1	---
8μ MEC	8	0.7	1.4	0.011	0.7	0.1	0.013	0.3	0	0
	9	5.5	11.5	0.183	2.8	-0.2	0.03	0.9	0.1	0.014
8μ + FN	8	0.7	1.2	0.007	0.7	0	0.010	0.3	0.1	0.005
	9	0.8	0.5	0.057	2.4	0	0.03	6.7	0.2	0.013
Nylon 6	1	0.8	0.5	0.011	0.8	0.2	0.001	0.5	0.1	---
	3	16.2	22.1	0.084	9.6	7.8	0.02	4.8	3.3	0.009
	4	3	0.9	0.039	1.0	0.7	0.005	0.7	0.4	0.009

***IL-1ß and TNFα values are expressed as pg/mL. HL-60 values are expressed as OD (560-650 nm).**

In dramatic contrast to the MEC and Nylon 6 data, the PTFE and ePTFE polymers affected HUVEC activation to a far greater degree (Figures 7.5-7.9). This demonstrates the influence of differing surface chemistries which are translated from macrophage cytokines to endothelial cell activation in this chapter. Higher levels of endothelial cell activation in response to the macrophage supernatants is not unexpected given the results of the cytokine profiles for macrophages contacting these materials as shown in Chapter 6.5.

The donor-to-donor influence was more apparent with these materials, which stemmed from the variable release of cytokines from each donor's macrophages. An example of this is demonstrated by comparing the PTFE data from Figures 7.5-7.7. Despite donor-to-donor variability, the PTFE and ePTFE material supernatants consistently showed higher levels of endothelial cell activation than that seen with the hydrophilic polymers, in agreement with the cytokine data. Also, the HL-60 results were consistent with the cytokine concentration in the supernatants, as shown in Table 7.2.

The trends established with the cytokine data are similar to what is seen in the HL-60 assays. All of the uncoated fluoropolymer supernatants (without FN) showed significant endothelial cell activation. It is apparent that maximal activation was achieved with lower cytokine levels, as shown in the graphs and Table 7.2. For example, similar levels of activation were seen for the PTFE and 10μ ePTFE supernatants compared to the 30μ and 60μ ePTFE supernatants, even though the cytokine levels for the former are much lower than the latter. This may appear to be inconsistent with the macrophage cytokine data, however, if sufficient levels of IL-1ß or TNFα are added, endothelial cell activation is dose dependent only in a very narrow range, as shown by Figure 7.1. IL-1ß and TNFα concentrations in the Day 1 supernatants were sufficient to reach the activation

"plateau." By Day 7, most supernatants returned to near-background levels of activation, with the exception for those supernatants from Donor #4, which remained elevated.

FN pre-coating of the surfaces reduced the amount of activation for only the PTFE, 10μ ePTFE and 30μ ePTFE supernatants (Figures 7.7 and 7.9). The level of activation for the FN-coated 60μ ePTFE supernatants were not influenced by FN preadsorption (Figures 7.8 and 7.9) which is consistent with the cytokine data.

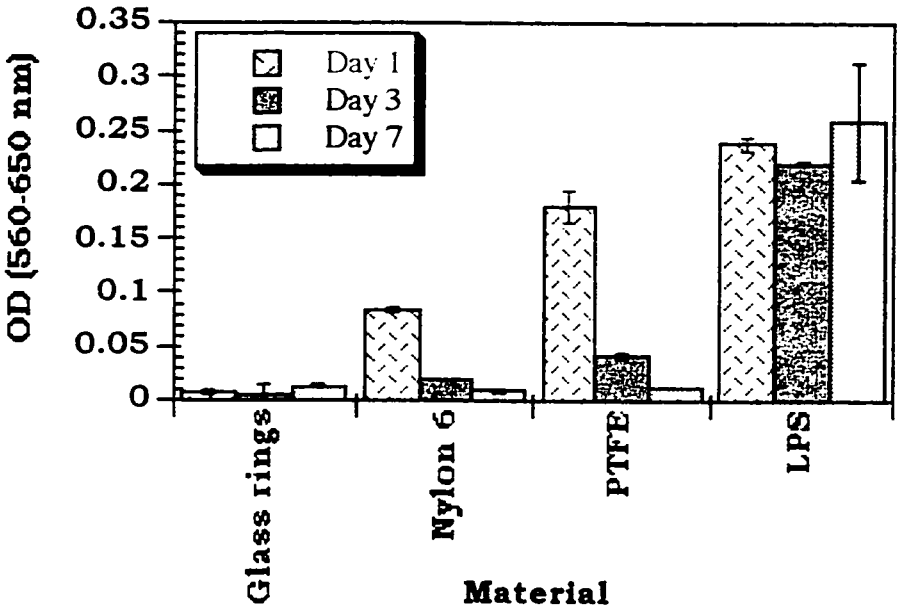

Figure 7.5 HL-60 assay of Donor #3 macrophage supernatants: Nylon 6 and PTFE.

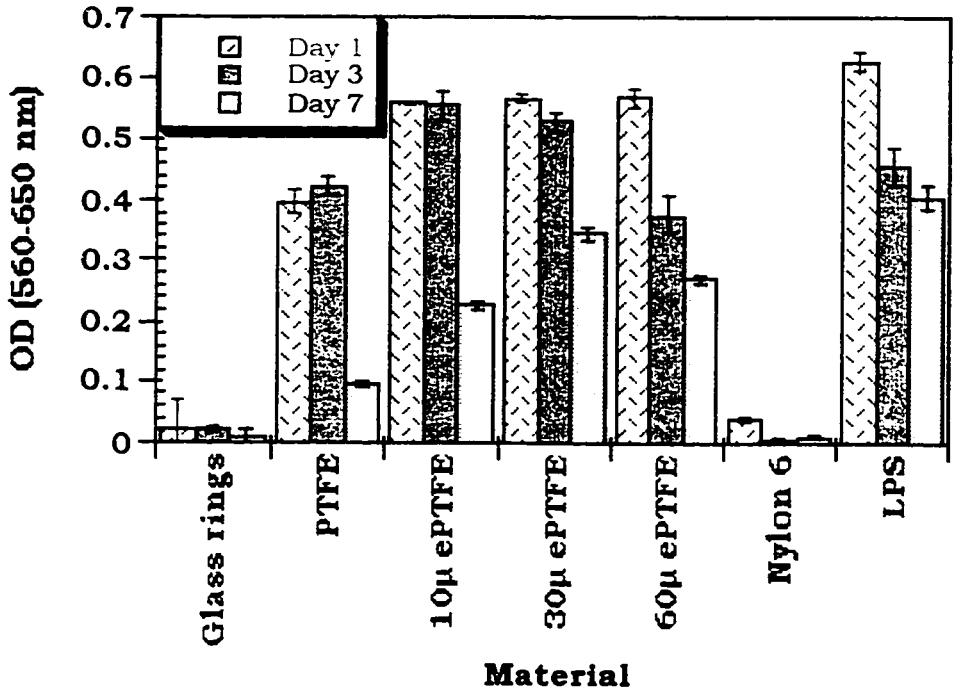

Figure 7.6 HL-60 assay of Donor #4 macrophage supernatants: PTFE, ePTFEs and Nylon 6.

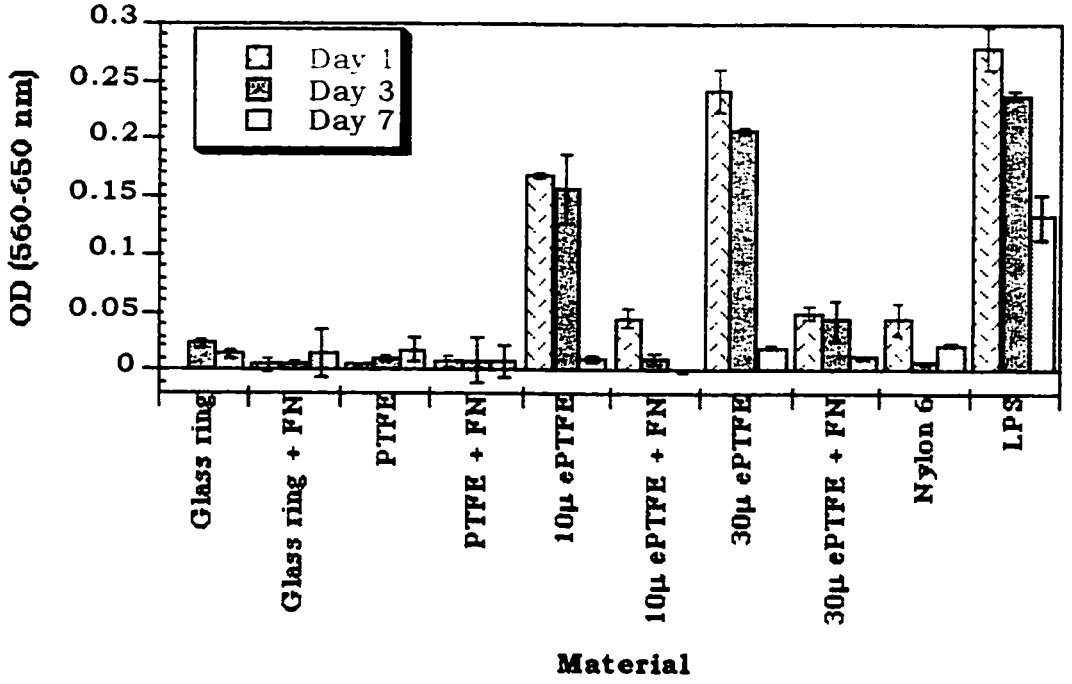

Figure 7.7 HL-60 assay of Donor #7 macrophage supernatants: PTFE, ePTFEs (10μ and 30μ) and Nylon 6.

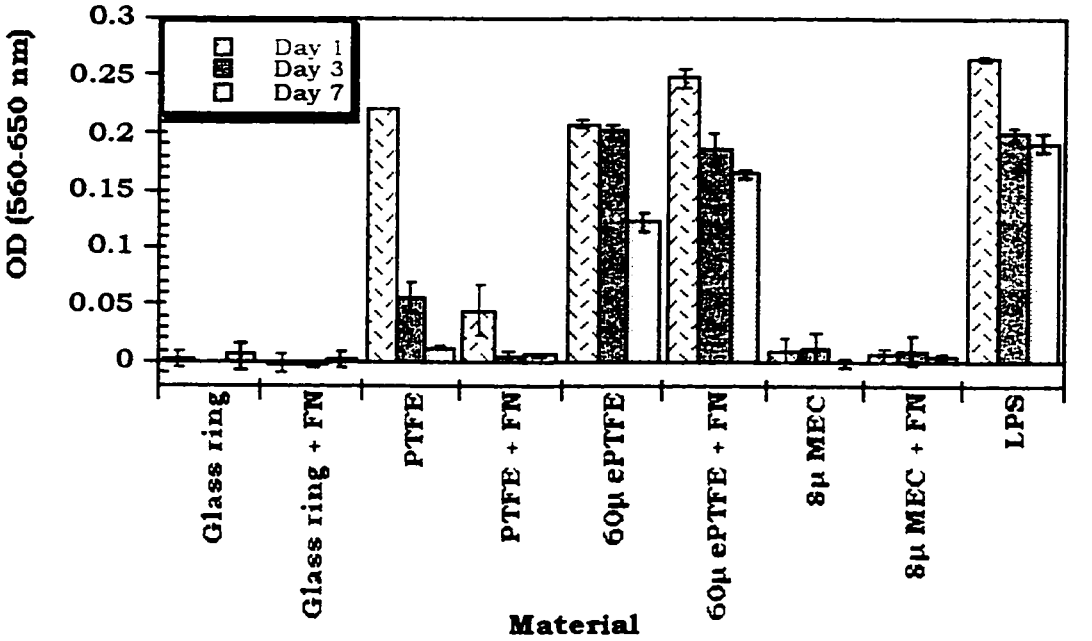

Figure 7.8 HL-60 assay of Donor #8 macrophage supernatants: PTFE, 60μePTFE and 8μ MEC.

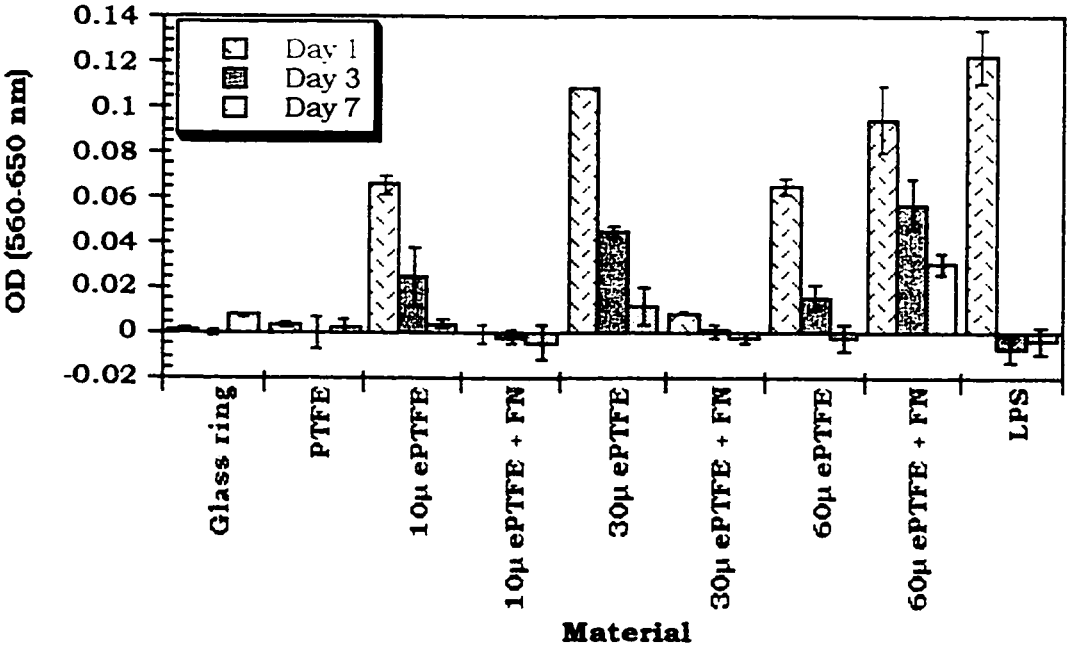

Figure 7.9 HL-60 assay of Donor #10 macrophage supernatants: PTFE, 10μ, 30μ and 60μ ePTFE (+/- FN).

Table 7.2 HL-60 Adherence Associated with Macrophage IL-1ß and TNFα Production: PTFE and ePTFE Polymers

Material	Donor	Day 1			Day 3			Day 7		
		IL-1ß	TNFα	HL-60	IL-1ß	TNFα	HL-60	IL-1ß	TNFα	HL-60
PTFE	3	26.6	28.2	0.181	10.6	4.8	0.041	2.4	0.9	0.013
	4	28.0	13.4	0.397	72.2	20.4	0.423	21.7	4.3	0.096
	7	1.1	0.3	0.004	1.3	0.1	0.010	1.8	0.7	0.017
	8	18.2	34.2	0.221	0.7	4.7	0.057	1.8	1.3	0.013
	10	2.8	0.9	0.004	1.4	0.2	0	0.4	0.1	0.003
PTFE + FN	7	1.1	0.1	0.008	1.4	0.2	0.009	1.7	0.4	0.007
	8	1.9	2.8	0.045	1.3	0.9	0.005	0.7	0.3	0.006
10μ ePTFE	4	138.1	74.1	0.557	159.2	16.0	0.553	30.0	4.6	0.227
	7	10.7	1.4	0.169	27.0	1.1	0.157	6.0	1.1	0.011
	10	36.4	7.5	0.067	39.9	3.5	0.025	12.0	2.0	0.005
10μ ePTFE + FN	7	7.5	0.1	0.045	1.5	0.3	0.010	1.6	0.6	0
	10	1.4	0.4	0.005	4.6	0.6	-0.001	0.2	0.1	-0.003
30μ ePTFE	4	312.8	222.7	0.563	138.4	23.6	0.529	219.5	12.5	0.346
	7	75.0	6.6	0.242	74.1	3.3	0.208	7.5	1.1	0.019
	10	87.8	18.2	0.109	124.2	10.7	0.045	30.9	4.2	0.012
30μ ePTFE + FN	7	0.9	0.1	0.050	2.4	0.4	0.043	0.9	0.4	0.013
	10	10.0	11.6	0.009	6.3	0.6	0.001	1.5	0.2	-0.001
60μ ePTFE	4	556.2	119.8	0.565	400.3	62.7	0.375	964.2	172.1	0.269
	8	394.9	94.0	0.208	376.2	41.2	0.201	161.1	53.2	0.123
	10	124.2	41.2	0.065	158.8	20.9	0.017	2.4	0.5	-0.002
60μ ePTFE + FN	8	283.6	76.2	0.248	224.8	16.4	0.185	242.2	59.6	0.165
	10	86.4	32.6	0.095	175.2	25.1	0.057	58.8	3.6	0.031

***IL-1ß and TNFα values are expressed as pg/mL. HL-60 values are expressed as OD (560-650 nm).**

7.4 Conclusions

In summary, the hypotheses proposed in Chapter 1 are supported by the endothelial cell activation data in this chapter. The material effects, namely those of differing surface chemistry, topography and extracellular matrix coating, were translated from the macrophage supernatants to changes in gene expression in endothelial cells. In addition, where activation in the endothelial cells occurred, an increase in neutrophil adhesiveness is seen.

The trends in endothelial cell activation were similar to those in Chapter 6.5. The donor-to-donor variability was more apparent in the HL-60 assays than the cytokine data.

1) The macrophage supernatants from the MEC and Nylon 6 materials generally had a low capacity to activate endothelial cells in the HL-60 assay. This was in stark contrast to what was observed with the fluoropolymer series. The fluoropolymer supernatants demonstrated near maximal to maximal HUVEC activation for all materials at the Day 1 time point, which significantly decreased by Day 7.

2) The hydrophilic polymers showed little or no effect of FN coating due to the levels of activation being so close to background levels, with the exception of Donor #9 for 8μ MEC. FN pre-coating of materials decreased HUVEC activation for all material in the fluoropolymer series except for the 60μ ePTFE, consistent with the cytokine results. This finding suggests that there is an effect of fibril length on macrophage activation, as was demonstrated with both the cytokine data and endothelial cell activation by those cytokines.

These sets of data elegantly demonstrate how material differences can be propagated to biological effects in a "second party" cell. Even more importantly, endothelial activation by macrophages illustrates how materials with different composition can influence not just cellular interactions, but potentially tissue reactions to implanted materials *in vivo*.

7.5 Notes to Chapter 7

Dinarello, C. A. (1988). Cytokines: Interleukin-1 and Tumor Necrosis Factor (Cachectin). In Inflammation: Basic Principles and Clinical Correlates, J. I. Gallin, I. M. Goldstein and R. Snyderman, eds. (New York: Raven Press), pp. 195-208.

Chapter 8

Material Effects on Macrophage, Endothelial Cell and Smooth Muscle Cell Interactions: Cell Co-cultures with Biomaterials

8.1 Background

The *in vivo* system we are modeling in these experiments is that of vascular grafts. We are concerned that there are cell signals communicated which are inhibitory to endothelial cell growth onto vascular graft materials. The *in vivo* source of these signals is not known at this time, and these experiments are used to investigate the influence of relevant cell types on endothelial cell proliferation or inhibition of growth in an *in vitro* setting. The other cell types of interest are smooth muscle cells that normally are in close apposition to endothelial cells in the normal vessel wall, and monocytes, which arrive at implant sites from the bloodstream, and mature into macrophages. Communication between different cell populations through soluble factors, and the effect that materials have on signalling between cells, is very important to understanding how medical implants are received by the host. Cell proliferation in response to signals generated from another cell type are investigated here.

8.2 Objectives

I investigated the role of soluble factors released from cells on endothelial cell and smooth muscle cell growth through a co-culture system. The role of the material surface was probed to determine its effects on cell proliferation or inhibition of growth. The results of these studies can be used to explore how materials influence cell growth through secretion of growth factors or cytokines. No effort was made at this time to identify the factors that are contributing to growth or inhibition of proliferation. These assays provide

information about cell communication when differing cell types contact biomaterials surfaces.

8.3 Materials and Methods

8.3.1 Materials

The materials used in this study are as follows: tissue culture polystyrene (TCPS), mixed esters of cellulose (MEC) in 3 porosities (0.22μ, 5μ, and 8μ), non-porous polytetrafluoroethylene (PTFE), and expanded PTFE (ePTFE) in 3 fibril lengths (10μ, 30μ, and 60).

8.3.2 Macrophage Purification

The protocol used for purifying macrophages from human blood was developed by Laura Martinson, and is described in Chapter 3.4.2.2. The monocytes were plated at 2 x 10^5 cells/well in 12 well plates with or without materials to be tested.

8.3.3 Cell Number Determination

MTT and MTS tetrazolium compounds were used to determine the number of living cells. These tetrazolium compounds are bioreduced to a colored formazan by viable cells. The bioreduction is dependent on pyridine nucleotides NADH and NADPH and to some extent mitochondrial succinate. The MTT assay produces insoluble formazan crystals that need to be solubilized with acid isopropanol prior to colorimetric analysis by determination of optical density using a plate reader (560-650 nm). The MTS assay produces a soluble formazan salt that does not need further processing prior to colorimetric analysis (490 nm).

The MTS assay is preferred over the MTT assay due to the soluble formazan secreted in culture medium. The solubilization of the insoluble crystals formed in the

MTT assay caused problems due to the adsorption of the crystals into the porous materials. This only created problems when analyzing the cells directly contacting the material surfaces. The data presented here is for those cells that were found in the culture inserts (see illustration below), i.e. for cells not directly contacting the materials tested. Some of the cell insert culture data presented in this report was generated using the MTT assay, and is noted with each data set which assay was used.

8.3.4 Co-culture Studies

Co-cultures of:

- Human umbilical vein endothelial cells (HUVECs) and macrophages (mø)
- HUVECs and smooth muscle cells (SMCs)
- Mø and SMCs

were prepared as illustrated below in Figure 8.1. Materials were fitted into the bottom of 12-well tissue culture plates with glass retaining rings to anchor the materials. One population of cells was seeded in direct contact with the materials. The other (responding) cell type was seeded into cell culture well inserts that are suspended above the bottom of the well. The two cell populations do not directly contact each other, but are able to communicate via soluble growth factors and cytokines through the 0.4μ pores in the culture insert. It was necessary to pre-coat the inserts with gelatin to maintain HUVEC viability. No coating was used for the SMC in the inserts. The number of responding cells in the culture inserts were determined using either the MTT or MTS assays. Several attempts to determine the number of cells on the material surfaces was attempted, but several problems arose and are addressed later in the Discussion.

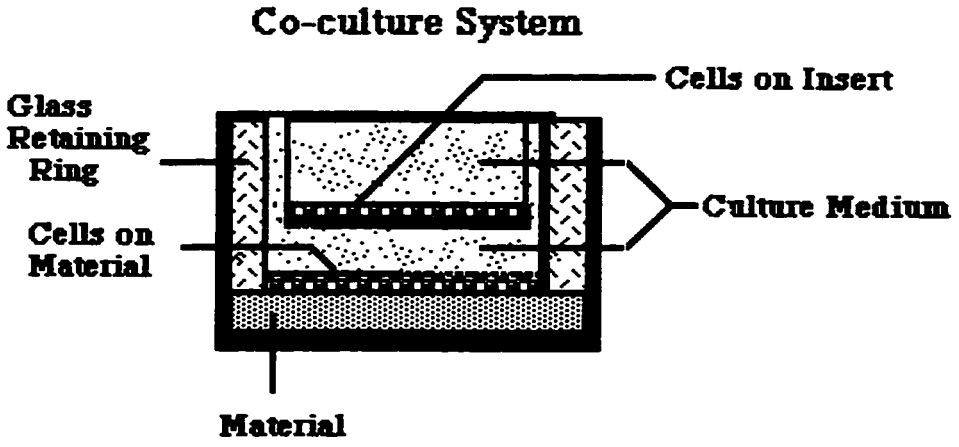

Figure 8.1 Cell Co-culture system.

8.3.5 Cell Supernatant Effect on Responding Cell Growth

Macrophages were grown on the various materials, harvesting supernatants at specified times in culture. The responding cell type, either HUVEC or SMC, were used as proliferation indicators for the collected macrophage supernatants. An MTT or MTS assay was used to determine how each cell type's proliferative response is affected by components secreted into the supernatants. These assays were used as a complement to the co-culture system. I felt it was necessary to verify that both the co-culture and supernatant systems were capable of similar proliferative responses. Also, the supernatants were heat-treated to determine if the substances responsible for the cell proliferation were heat labile, indicating that they would be proteins and not some other non-labile substance such as endotoxin.

8.3.6 Statistical Analysis

Analysis of Variance (ANOVA) was performed using Microsoft Excel 5.1 (ANOVA Tool kit). Significance levels are reported as p values.

8.4 Results and Discussion

8.4.1 HUVEC and Macrophage Co-cultures

The co-culture data presented in this section is for macrophages contacting the different materials and HUVECs seeded in inserts that respond to any secreted macrophage products (refer to Figure 8.1). After 7 days in culture together, the number of HUVECs in the inserts was determined using the MTS assay. The O.D. at 490 nm is proportional to the number of viable HUVECs present in the inserts. Any increases in the O.D. over the control surfaces represents HUVEC proliferation in response to macrophage products.

HUVECs seeded alone in the inserts, shown in the first column in Figure 8.2, were not exposed to any macrophage products, and show a low background level.

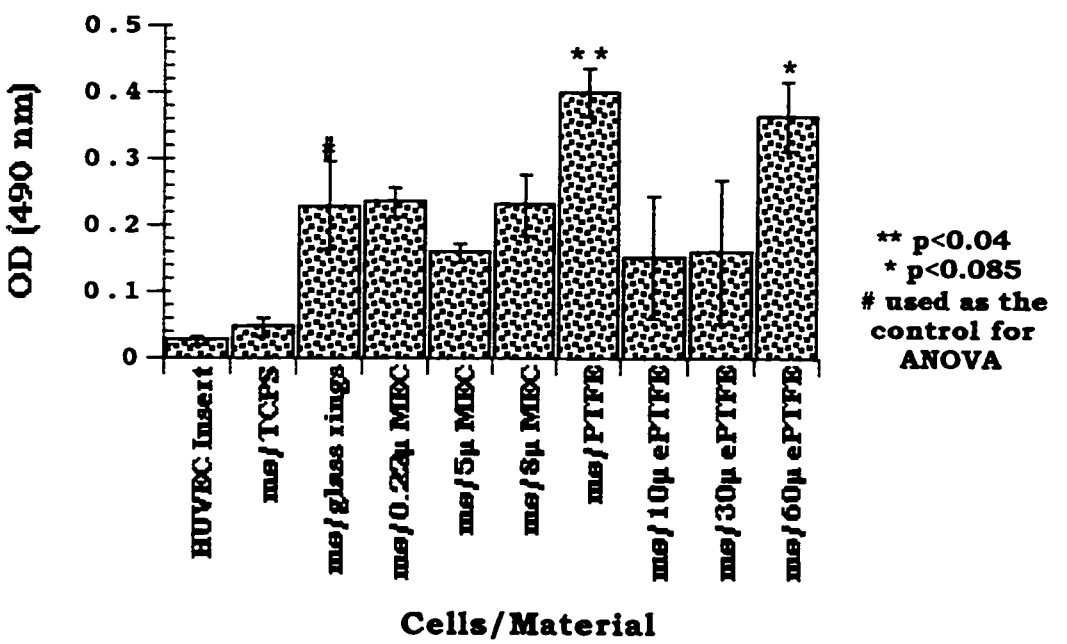

Figure 8.2 HUVEC proliferation in response to co-culture with macrophages (mø) seeded on materials.

Macrophages seeded on TCPS resulted in an insignificant increase in HUVEC cell number shown in the second column. A glass ring control for each experiment was included due to the necessity of anchoring the materials down in the bottom of the cell wells. As seen in Figure 8.2, macrophages contacting the glass retaining rings produce a significantly higher level of HUVEC proliferation ($p=0.013$) compared to HUVECs in the inserts alone. Due to this higher level of proliferation of HUVECs in response to macrophages contacting the glass rings, the glass ring sample is used as the control for the other materials, which all have glass rings anchoring them. When compared to the glass ring control, only macrophages on PTFE showed significantly higher HUVEC proliferation. All of the materials, with the exception of TCPS, 10μ ePTFE, and 30μ ePTFE, increased HUVEC proliferation significantly over the HUVECs in the inserts alone ($p<0.02$).

8.4.2 HUVEC Response to Macrophage Supernatants

In a similar study, macrophages grown on the different materials had supernatants harvested after 7 days in culture. These supernatants were added (half of the total volume) to a constant number of HUVECs seeded in wells of a 24 well plate. After 4 days, the number of HUVECs in each well was determined using the MTS assay. The results are outlined in Figure 8.3. In the first column are HUVECs that were cultured without any exogenous growth factors or macrophage supernatants, and represents the basal cell number level for the assay. Supernatants from macrophages grown on either TCPS or TCPS containing the glass retaining rings gave a slight but significantly higher HUVEC proliferation compared to the HUVECs grown alone ($p<0.005$). All of the macrophage/material supernatants also showed significantly higher proliferation compared to the glass ring control. The HUVEC growth for all of the mø/material supernatants was similar to HUVECs stimulated with endothelial cell growth supplement (ECGS), which is known to stimulate proliferation of HUVECs.

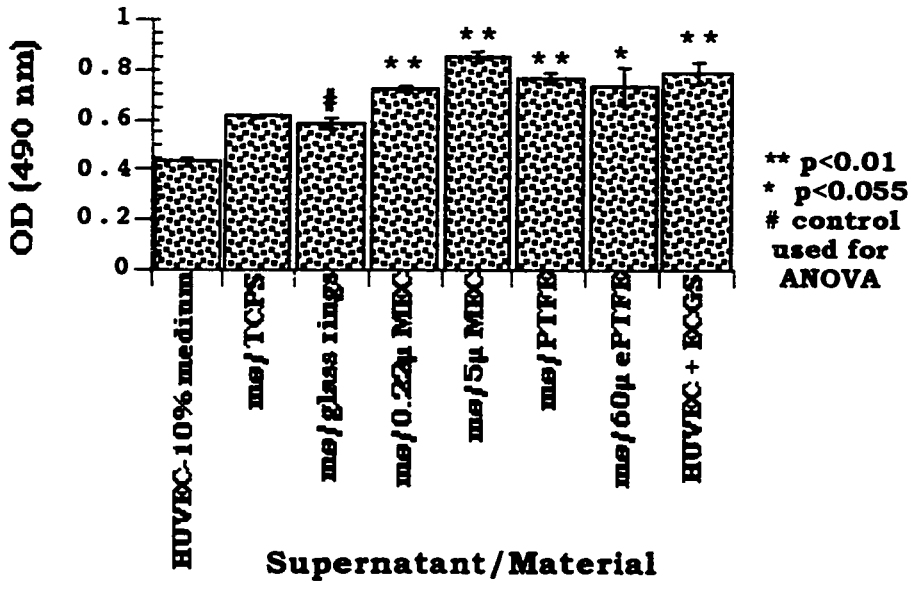

Figure 8.3 HUVEC growth in response to macrophage (mø) supernatants.

These results are slightly different from those outlined in Figure 8.2. Only two materials in the co-culture system, PTFE and 60μ ePTFE, showed any growth over that seen with the glass ring control. In contrast, all of the macrophage/material combinations in the supernatant experiment showed significant increased HUVEC proliferation over the glass ring control. Two explanations for these differences are advanced here. First, in the co-culture system, the two cell populations are communicating with each other, sending stimulating as well as inhibiting cytokine cell signals, which may account for some of the "less proliferative" macrophage/material combinations. Unlike the co-culture system, the macrophage supernatants generated for the experiment in Figure 8.3 were isolated macrophage cultures with no contact or influence from HUVECs. Also, these supernatants were frozen prior to being assayed (-70°C), so it is possible an inhibitory cytokine might be sensitive to the freeze/thaw cycle.

In a separate set of experiments, macrophage supernatants were collected at days 3, 5 and 7 days, and frozen. The supernatants were then thawed and added to a constant

number of HUVECs in a 24-well plate as done previously. On day 4 of culture with the supernatants, the MTS assay was used to determine the number of HUVECs in each well. The results are summarized in Figures 8.4 A, B and C. Figure 8.4 A demonstrated the same HUVEC proliferation trends as seen in the first co-culture experiment (Figure 8.2), with only the macrophage/PTFE supernatant significantly increasing HUVEC proliferation compared to the glass ring control. The macrophage/0.22μ and 8μ MEC supernatants were significantly lower than the glass ring control. This may indicate that these materials have a low "angiogenic" potential due to the low level of HUVEC growth. For the supernatants collected on subsequent days (5 and 7), there was no evidence of induction of HUVEC proliferation by any of the supernatants compared to the glass ring controls. HUVECs stimulated with ECGS showed that the HUVECs were capable of proliferation given the correct stimuli. The data presented in Figure 8.4 demonstrates that there is a burst of cytokine or growth factor release from macrophages contacting the material surfaces, which decreases with time. This "burst effect" has been seen by a number of other investigators, and is a classical response of macrophages activated *in vitro*.

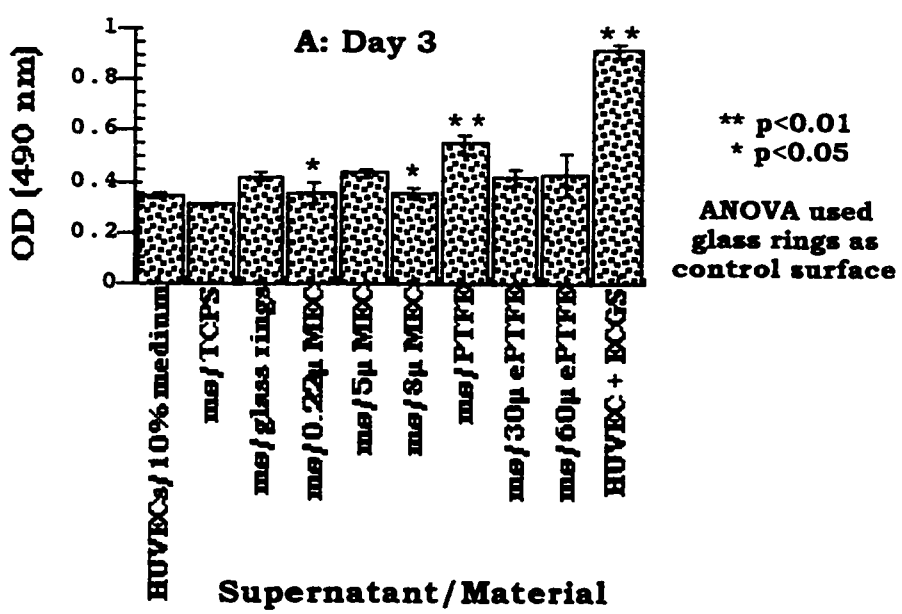

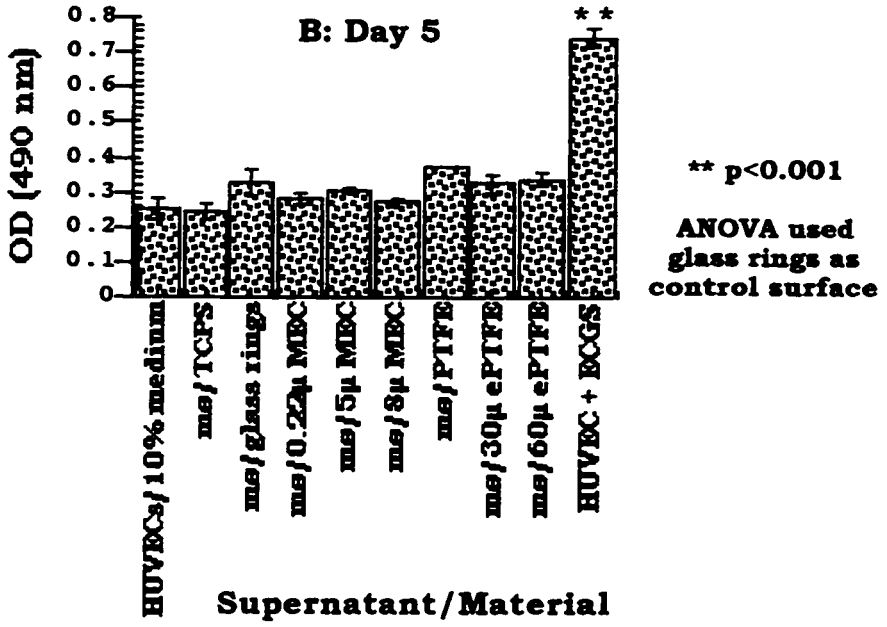

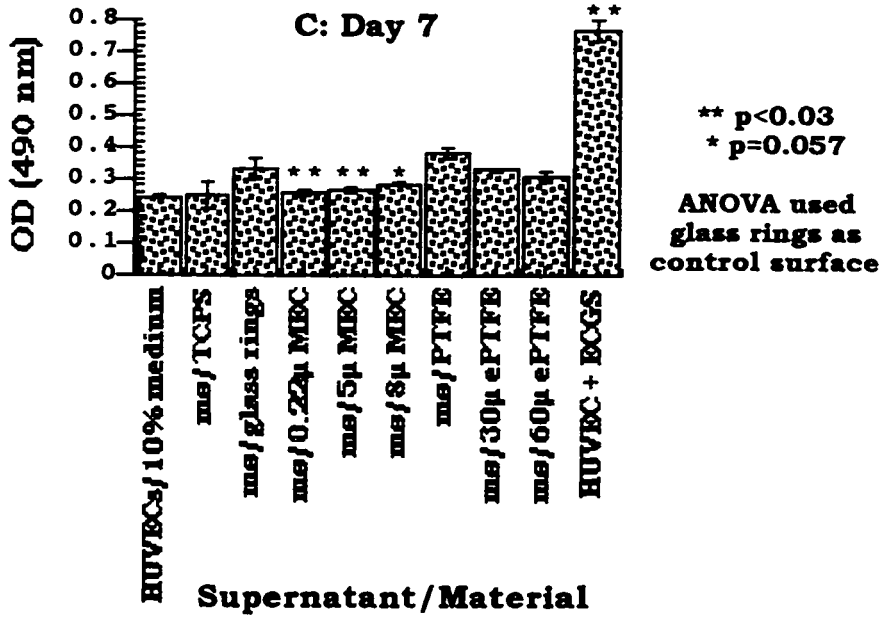

Figures 8.4 A, B, and C HUVEC growth in response to macrophage (mø) supernatants.

8.4.3 Macrophage and SMC Co-cultures

SMCs in culture inserts were co-cultured with macrophages contacting different materials. SMC number was determined using the MTT assay on day 7 of co-culture. As shown in Figure 8.5, all samples were significantly higher than the SMCs in the inserts alone ($p<0.01$). However, the material samples were not significantly different than the glass ring control. It appears that macrophages cultured on these materials do no produce any growth factors for SMCs.

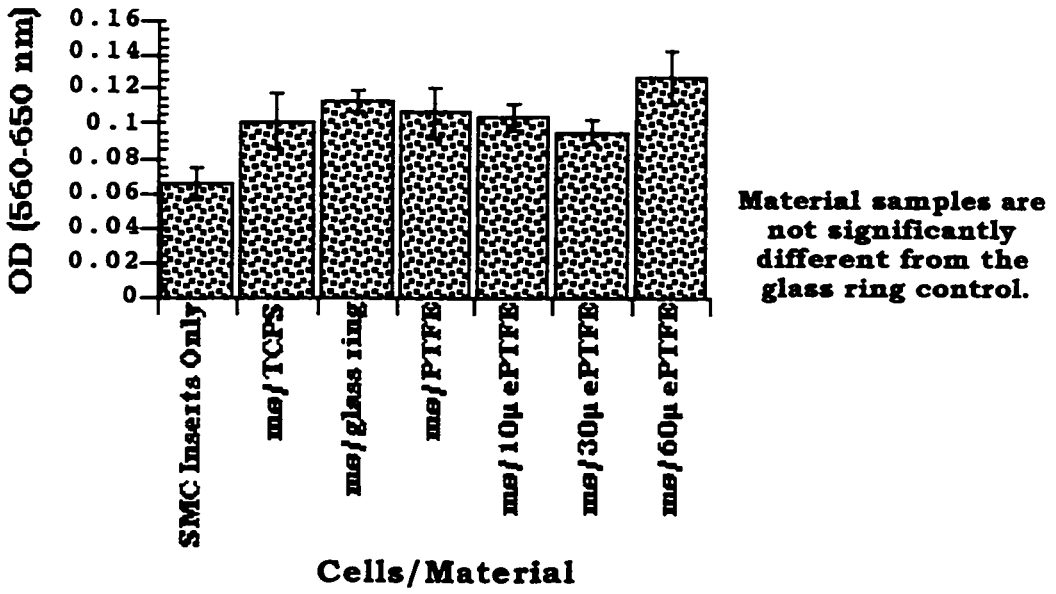

Figure 8.5 Smooth muscle cell (SMC) growth in response to co-culture with macrophages (mø) seeded on different materials.

The supernatants from the previous co-culture experiment were harvested (day 7). These supernatants were added to a constant number of SMCs and cultured for 6 days.

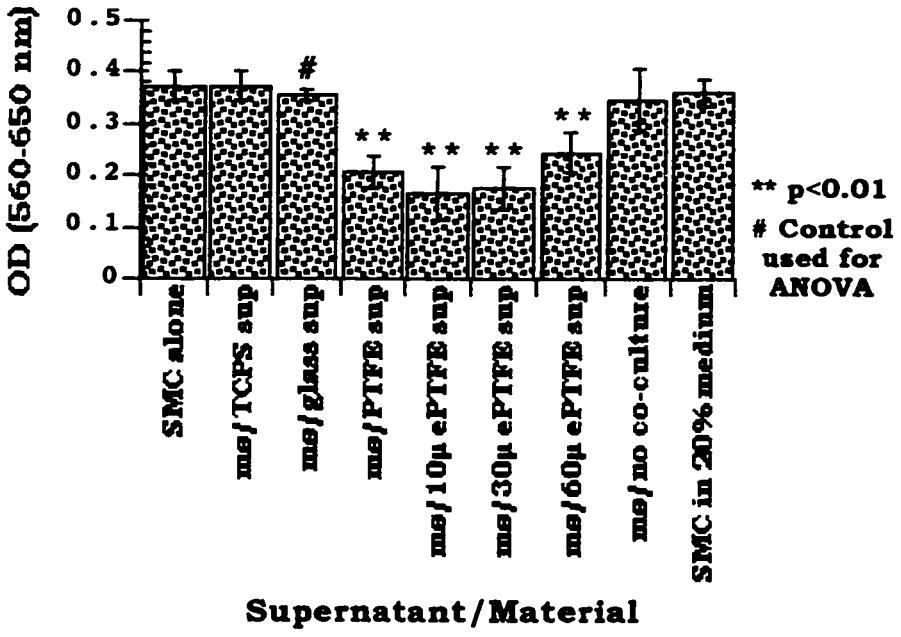

Figure 8.6 SMC growth from SMC/mø co-culture supernatants.

As shown in Figure 8.6, none of the macrophage supernatants induced SMC proliferation, and in fact inhibited SMC growth on all of the PTFE and ePTFE materials. This further supports our findings that macrophages contacting these materials do not appear to produce proliferative factors for SMCs. Cell number was determined using the MTT assay.

8.4.4 HUVEC Growth in Response to SMCs on Materials

HUVECs in inserts were co-cultured with SMCs contacting the materials, and cell number was determined using the MTT assay. In Figure 8.7, the SMC contacting the PTFE and 60μ ePTFE materials significantly increased HUVEC growth compared to the glass ring control.

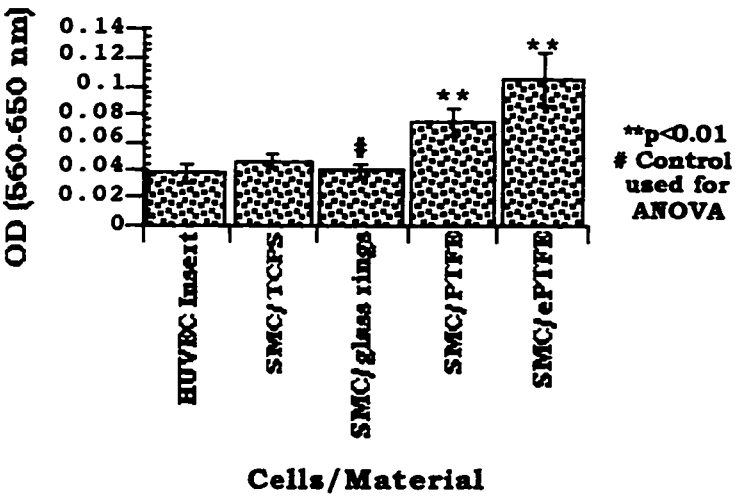

Figure 8.7 HUVEC proliferative response to SMCs seeded on different materials.

This suggests that SMCs are induced to synthesize HUVEC growth factors in response to contact with the materials tested. These data indicate that an intact SMC layer under endothelial cells may be important for endothelial cell growth on materials *in vivo*.

8.4.5 SMC Growth in Response to HUVECs on Materials

Complementary to the data in Figure 8.7, SMCs grown in inserts were co-cultured with HUVECs contacting different materials. Similar to the macrophage/SMC co-cultures, HUVECs contacting the materials did not induce SMC proliferation, and in fact significantly decreased SMC proliferation compared to the TCPS control (Figure 8.8). It appears that HUVECs contacting materials do not promote SMC growth. These data suggest that SMCs in the presence of either macrophages or endothelial cells do not induce SMC growth and may inhibit their growth. Cell number was determined using the MTT assay.

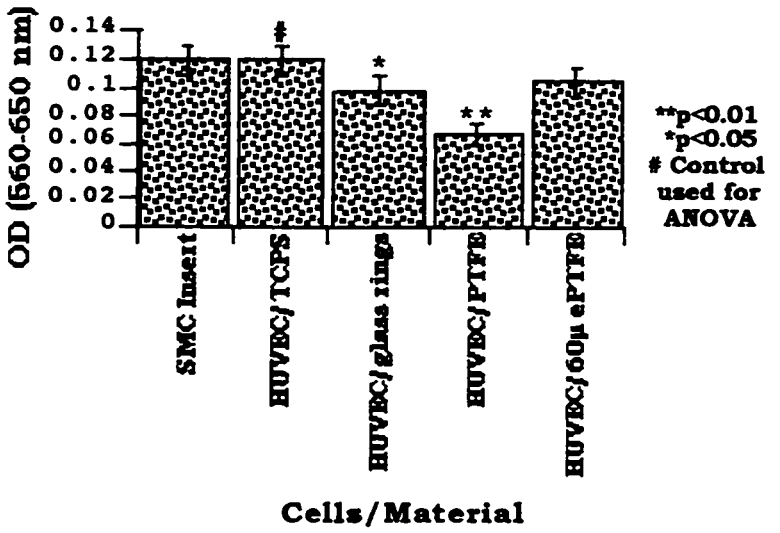

Figure 8.8 SMC proliferation in response to HUVECs seeded on different materials.

8.4.6 Heat-treated Supernatants

In an effort to determine whether the signaling agent(s) responsible for cell proliferation are proteinaceous in nature, we compared native supernatants with supernatants that were heat-treated for their ability to induce cell growth. Macrophage supernatants for each materials group were either left untreated or were boiled for 5 minutes prior to adding to a constant number of HUVECs seeded in 24-well plates. HUVEC cell number was determined using the MTS assay. As seen in Figure 8.9, the ability of heat-treated supernatants to promote growth was significantly reduced, with the exception of the 8μ MEC (p=0.06) and the 60μ ePTFE (p=0.11) samples. These data support our hypothesis that the agents responsible for proliferation are proteins, which are destroyed by the heat treatment. Other proliferative agents, such as endotoxin or lectins, are not destroyed by heat treatment. I saw a consistent reduction in proliferative activity of supernatants that were heat treated for all cell types.

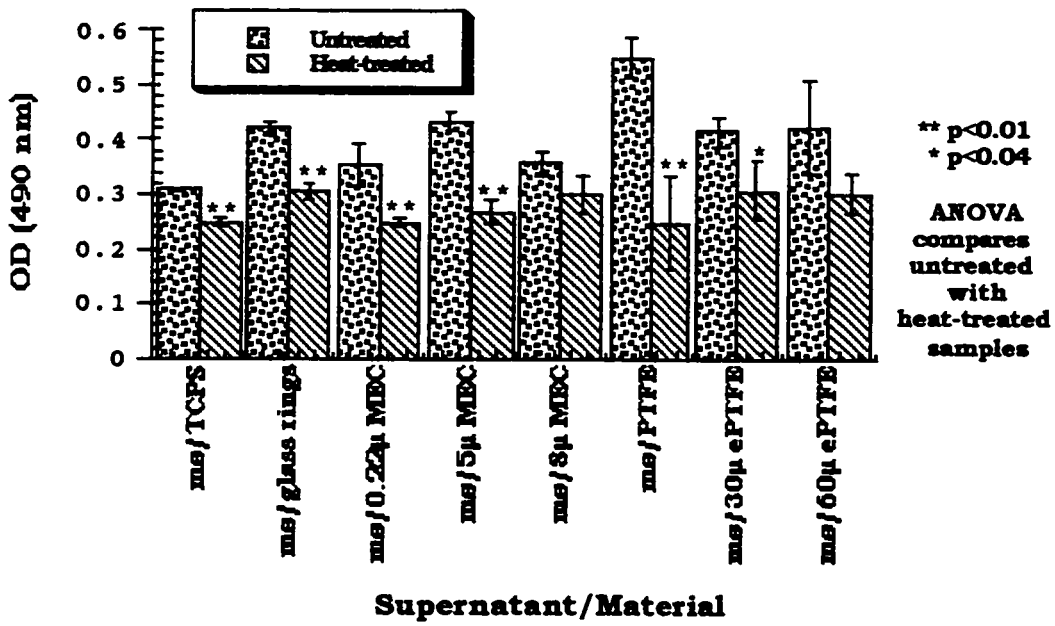

Figure 8.9 Heat treatment of mø supernatants reduces HUVEC proliferation.

8.5 Conclusions

A co-culture system has been developed to study macrophage, endothelial cell, and smooth muscle cell interactions *in vitro*. This assay system has the distinct advantage of looking at a specific outcome, proliferation, in an extremely complex system in which a number of cytokines are suspected to participate. HUVECs have demonstrated proliferative responses to macrophages seeded on different material surfaces. Limited endothelial cell proliferation is also seen with macrophage culture supernatants. HUVECs proliferated in response to SMCs being cultured on materials, but neither macrophage nor endothelial cell supernatants induced SMC growth. Heat treatment of culture supernatants results in a marked reduction in the proliferation of the responding cells, probably due to the destruction of proteinaceous growth factors.

These results highlight the importance of cell-cell signaling in the healing process. We assume that macrophage-derived products are a principal player in orchestrating the

healing process through the production of angiogenic factors. We have shown here that endothelial cells respond to both macrophages and SMCs being cultured on the materials tested. The SMCs used in these experiments do not respond to either macrophages or endothelial cells cultured on materials.

There are some limitations to this assay system that must be noted. None of the insert cell number data was normalized to number of viable cells seeded directly on the materials. The MTT and MTS assays were only useful on certain materials, such as PTFE and ePTFEs, for evaluating cell numbers on the material surfaces. The MEC materials interfered with these assays, apparently by binding the MTT or MTS directly to the material surface, depleting their concentration and availability for reaction with the cells. This resulted in artificially low cell numbers when assayed with these compounds. As a result, the MTT and MTS tetrazolium compounds are not useful due to the interference of the MEC materials with the production of the formazan product. We are currently investigating new methods for determining cell numbers on opaque, porous materials.

A second limitation to using this co-culture system is that these assays were technically difficult to perform. Proliferation results were not always significant from one experiment to the next, thus necessitating the repeat of these assays several times to determine the trends reported here. Part of this may be due to the use of primary cells, which are difficult to culture and often fail to thrive *in vitro*. It has not been determined when using cells from unmatched donors influences the cellular responses, but by using the culture inserts the different cell populations were not allowed to physically contact each other due to the 0.4μ insert pore size.

Another limitation to this culture system is that of identification of the participating cytokines. With all of the stimulatory, inhibitory, and synergistic effects of cytokines that can potentially be produced by the combination of the two cell types raises the level of complexity. We feel that identification of all the cytokines involved would be very

difficult if not impossible, time consuming, and expensive. This culture system has potential use in screening or doing limited evaluation of a material's wound healing potential.

Chapter 9

Endothelial Cell Interactions with Biomaterial Surfaces

9.1 Introduction

Based on preliminary antibody staining experiments of seeded human umbilical vein endothelial cells on a variety of fibronectin-coated materials, we originally hypothesized that certain materials lead to cell surface expression of E-selectin, an inflammatory marker that leads to adhesion of neutrophils to endothelial cells. Through further investigation using multiple techniques such as Northern blot analysis of E-selectin gene expression and a neutrophil adhesion cell assay, this hypothesis has not proven defensible. The early data is explained by an auto-fluorescence artifact for cells seeded on polytetrafluoroethylene (PTFE) sheets and expanded PTFE. The cause of the autofluorescence on these materials has not been identified. These later findings are encouraging for vascular graft materials. This *in vitro* assay system demonstrates that endothelial cells are not induced by materials to express the inflammatory protein E-selectin on their surface. Expression of E-selectin would recruit neutrophils from the bloodstream, which is an unwanted reaction. Some of the techniques described here will be included in later experiments to determine the affect of macrophage cytokine production on endothelial cell activation.

9.2 Objective

My objective was to investigate the role of biomaterials in inducing the expression of an inflammatory marker, E-selectin, on human endothelial cells. This was investigated by cell surface staining with a monoclonal antibody to E-selectin, and by Northern blot analysis to check for the presence of E-selectin messenger RNA as a

measure of E-selectin gene expression. In addition, the function of any expressed E-selectin was tested using a neutrophil adhesion assay.

9.3 Materials

A variety of materials were used in this study, differing in surface chemistry and surface topology. A hydrophobic polymer series consisting of non-porous polytetrafluoroethylene (PTFE) sheeting and expanded polytetrafluoroethylene (ePTFE) varying in fibril length (10μ, 30μ, 60μ and 100μ) were used. A variety of plasma-deposited films were prepared by Winston Ciridon (UW, Bioengineering) with the following plasma-feed compositions: argon-etched polystyrene, acetone-40% O_2, acetone-40% N_2, and tetrafluoroethylene (TFE) plasmas. All ePTFE samples were analyzed using SEM. The fiber lengths were close to the nominal fiber lengths given by the manufacturer. Other materials were Biospan® polyurethane and tissue culture polystyrene (TCPS). See Chapter 3.1 for detail on materials used and cleaning methods. HUVECs were seeded on the materials as discussed in Chapter 3.5 for cell surface staining studies, or as detailed in section 9.4.

9.4 Results and Discussion

9.4.1 Cell Surface Staining for E-selectin

All samples pre-coated with FN and seeded with approximately 2 x 10^4 HUVECs. These cells were stained for the presence of the inflammatory marker E-selectin following the protocol described in section 3.5. A mouse monoclonal antibody recognizing human E-selectin was used in conjunction with a secondary antibody containing a fluorescent tag (FITC-goat-anti-mouse IgG). Cells were photographed under 485 nm light to visualize the fluorescent marker. All slides taken were set at the

same film exposure time so that different samples could be directly compared for their intensity of fluorescence. Details of the staining protocol are found in Chapter 3.5.

Numbers are used to indicate the intensity of fluorescence observed as outlined in Table 9.1. The photographs were interpreted as follows: *a lack of fluorescence indicates no E-selectin antibody binding, fluorescence indicates the binding of E-selectin antibody.* The E-selectin antibody binding results are summarized below in Table 9.2.

Table 9.1: Key to Number Designations for E-selectin Staining

Degree of Fluorescence	**Number Designation**
Background	0
Slight fluorescence	1
Moderate fluorescence	2
Intense fluorescence	3

The two negative controls used were 1) cells seeded on TCPS stained with both primary and secondary antibodies and 2) cells stained with the secondary antibody alone. These are designated "TCPS" and "2nd antibody only". Both negative controls were always at low background levels (0). The positive control was IL-1ß stimulated HUVECs which showed above background levels (1) between 3-8 hours of stimulation, returning to background levels by 12 hours. The data below summarize an experiment 24 hours after seeding cells on the different material surfaces.

Table 9.2: E-selectin Staining Results

Sample	Degree of Fluorescence
TCPS	0
2nd Antibody Only	0
IL-1ß stimulated	1
PTFE	2
10μ Gore	3
30μ Gore	3
60μ Gore	3
100μ Gore	3

In addition to a single 24 hr time point, a time course of expression was performed spanning 36 hours including time points at 4, 8, 12, 18, 24, 30, and 36 hours for the samples listed above. A shorter time course was subsequently run with 1, 2, 3 and 4 hour time points. Data from the two time course studies indicated that E-selectin was being expressed at the earliest time point, 1 hour, continuing at a constant level through the 36 hour time period. This seemed unusual because E-selectin is transcriptionally controlled, and studies done *in vitro* show a peak of expression between 3 and 4 hours when the cells are stimulated with exogenous cytokines such as IL-1ß or TNFα, and no expression past 12 hours. The cell staining results indicated a chronic expression of E-selectin which had not been demonstrated previously *in vitro*. Also, the data showed that E-selectin was being up-regulated at a much faster rate than that found with other reports from the literature. These results were suspicious in light of other published work.

I decided to review the cell staining protocol to determine if a response to something other than the materials was causing activation of the cells on PTFE and ePTFE. The interactions investigated are shown in Table 9.3.

Table 9.3: Troubleshooting the Staining Protocol

Potential Problem Addressed	Reagents Used	Results
Species cross-reactivity with fluorescent second antibody	Replaced FITC-goat-anti-mouse IgG with FITC-rabbit anti-mouse IgG	Fluorescence retained on cells contacting ePTFE
Insufficient blocking	Cell receptors blocked with human IgG	Fluorescence retained on cells contacting ePTFE
Expression of Fc receptors on HUVECs	FITC-goat-anti-mouse-$F(ab)'_2$ second antibody used	Fluorescence retained on cells contacting ePTFE
Expression of C1q on HUVECs	Heat-treat goat serum used as blocking agent to remove complement	Fluorescence retained on cells contacting ePTFE
No E-selectin expression	Cells stained with no primary antibody, only 2nd antibody	Fluorescence retained on cells contacting ePTFE

These experiments determined that the fluorescence was *NOT* due to:

- the binding of the secondary antibody alone,
- expression of Fc receptors on the cell surface,
- insufficient blocking of non-specific binding,
- the cross-reactivity of antibodies of different species,
- or the E-selectin monoclonal antibody binding to the cells.

Upon further inspection, the cells were found to auto-fluoresce on PTFE and ePTFE, *but not on TCPS*. Because the negative controls were run on TCPS only, I had assumed that any fluorescence was due to the binding of the E-selectin antibody to the cell surface. The reasons for this auto-fluorescence are not known; this is an unusual finding. Problems with auto-fluorescence are typically seen with cells that are pigmented (such as melanocytes), or there is a problem with fixing the cells prior to staining. Specific fluorescent probes have narrow excitation and emission spectra, but

most autofluorescent compounds exhibit broad-band spectra (Van-de-Lest et al., 1995). This was noticed with the stained ECs contacting the fluoropolymer surfaces; changing the excitation wavelength did not diminish the autofluorescence. Because the cells were fixed on all materials using the same protocol, the differences seen with TCPS and ePTFE can not be explained as a fixative-induced phenomenon. We do not know if it is due to a material-induced phenomenon, or if the cells produce a fluorescent compound when contacting the PTFE and ePTFE surfaces. This phenomenon has been recently reported in the biomaterials literature (Poole, 1996), and endothelial cells have been reported to produce proteins that fluoresce, namely lipofuscin, primarily in arterial tissue sections (Lal et al., 1994; Monma et al., 1988). Lipofuscin is usually produced in cells undergoing apoptosis, or programmed cell death. We are currently in the process of evaluating if apoptosis is involved as a potential cause of the auto-fluorescence. This phenomenon may be of importance to the field of biomaterials if the cells are responding to materials by initiating apoptosis.

9.4.2 Northern Blot Analysis for the Detection of E-selectin Gene Expression

Concurrently with the cell staining experiments, E-selectin mRNA production was being investigated using Northern blot analysis. This technique detects mRNA in cell lysates and is used to determine if a specific gene is being expressed.

Initially, there was some difficulty in harvesting enough RNA from cells grown on the porous materials. The ePTFEs acted like sponges, resulting in low recovery of cell lysates. A typical experiment now yields 10-30 μg of RNA from 12 ePTFE samples, 18 mm diameter, seeded with approximately 2 x 10^5 cells per sample. This yield was fairly consistent, giving approximately 0.3-1 μg RNA per square centimeter of material or about 4-12 μg RNA per 1 x 10^6 cells. This was much lower than the cells harvested from TCPS which typically yielded 2-3 times that of the porous materials. As

reported in the literature, 10 μg of total RNA from IL-1ß-stimulated HUVECs is sufficient to see on an autoradiograph of a Northern blot (Montgomery et al., 1991). I increased this to 20 μg when the RNA yield permitted to be assured of a sufficient signal. I had no trouble detecting E-selectin mRNA from IL-1ß-stimulated HUVECs, but after repeated experiments none of the RNA harvested from HUVECs grown on the PTFE and ePTFE materials showed significant binding of the radioactive probe for E-selectin. The Northern blot experiments indicated that there was no significant E-selectin expression by the cells grown on the different biomaterial surfaces.

At this point there was a conflict between the cell staining and the Northern blot results. The cell staining showed high levels of expression of E-selectin, whereas no E-selectin gene expression was seen. Thinking that it may be an issue of sensitivity of the blotting technique, I tried in one experiment to dramatically increase the amount of RNA loaded in the gel wells. In this experiment, the following amounts of RNA were loaded in the gel lanes and processed as usual (Table 9.4).

Table 9.4: Amounts of RNA Loaded Per Lane in Agarose Gel

Sample	**Total μg RNA Loaded Per Lane**
TCPS	93
IL-1ß-stimulated HUVECs	110
PTFE	92
10μ Gore ePTFE	87
30μ Gore ePTFE	90
60μ Gore ePTFE	70

After a 5 day exposure of film contacting the Northern blot, *very* faint bands were seen with the RNA harvested from the material samples. A phosphorimage was accumulated from the blot for 5 days and analyzed. Below is a graph summarizing the

results (Figure 9.1). The counts/μg RNA loaded for each sample are found above each bar.

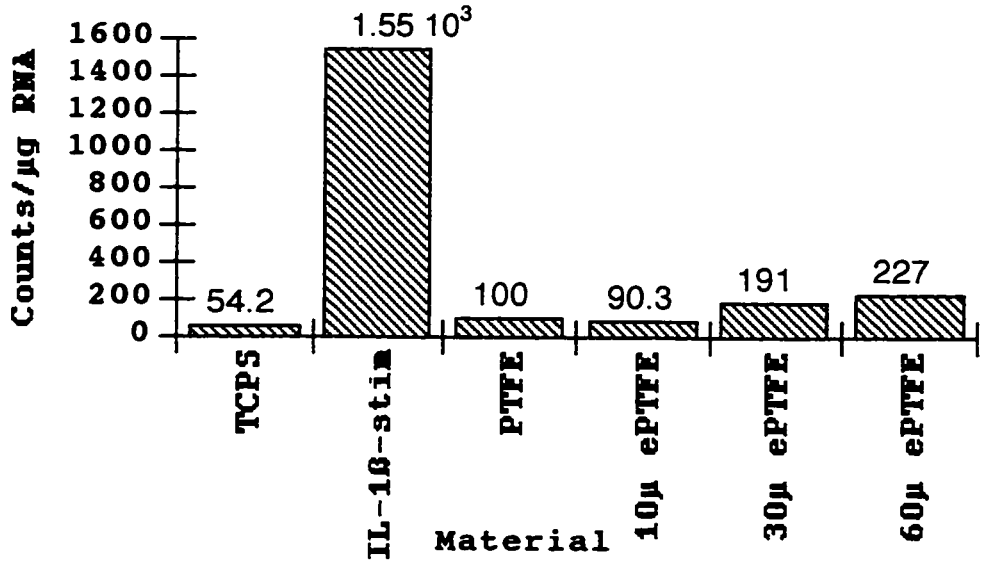

Figure 9.1 Phosphorimage data collected after 5 day exposure of Northern blot to detector.

Although there are slight differences between the materials, they appear not to be significant compared to the IL-1ß positive control. No statistical analysis can be performed with an n=1 for each of the samples. If E-selectin was being expressed at levels indicated in the cell surface staining, the Northern blot analysis was not supporting that conclusion.

9.4.3 Effect of Protein Adsorption on E-selectin Expression

Fibronectin was adsorbed to TCPS under a variety of adsorption conditions to investigate the role of the adsorbed protein layer on E-selectin expression in HUVECs. Fibronectin was adsorbed to polystyrene dishes from buffers differing in ionic strength,

pH, or from urea. Table 9.5 lists of the adsorption conditions used and the Northern blot analysis results:

Table 9.5: Fibronectin Adsorption Conditions and Northern Blot Analysis Results

Adsorption Conditions	Northern Blot Analysis Results
0.1M Phosphate Buffer, pH 7.4	No band
1.0 M Phosphate Buffer, pH 7.4	No band
Phosphate Buffered Saline, pH 2	No band
Phosphate Buffered Saline, pH 7.4	No band
Phosphate Buffered Saline, pH 12	No band
8M Urea	No band
IL-1ß-stimulated	Dark band

As is seen in the table above, changing the adsorption conditions of fibronectin did not affect HUVEC expression of E-selectin. Even when fibronectin is adsorbed in the presence of a known denaturant, urea, there was no effect on how the HUVECs responded to the adsorbed protein.

9.4.4 Effect of Surface Chemistry on E-selectin Expression

To investigate the role of surface chemistry on E-selectin expression, a series of radio-frequency (RF) plasma-deposited films were seeded with HUVECs and analyzed with the Northern blot technique. RF-plasma deposition was done on 60mm polystyrene dishes. Fibronectin coatings on the plasma films were compared to those pre-coated with gelatin to determine the effects of ECM coatings and surface chemistry on E-selectin expression. Table 9.6 lists the RF-plasma depositions used, ECM protein coatings used, and Northern blot analysis results.

Table 9.6: Plasma-deposited Film Coatings and Northern Blot Analysis Results

Material	ECM Coating	Northern Blot Results
Argon-etched polystyrene	Gelatin	No band
Acetone-40% O_2 Plasma	Gelatin	No band
Acetone-40% N_2 Plasma	Gelatin	No band
TFE Plasma	Gelatin	No band
TCPS Control	Gelatin	No band
TCPS/IL-1ß-stimulated cells	Gelatin	Dark band
Argon-etched polystyrene	Fibronectin	No band
Acetone-40% O_2 Plasma	Fibronectin	No band
Acetone-40% N_2 Plasma	Fibronectin	No band
TFE Plasma	Fibronectin	No band
TCPS Control	Fibronectin	No band
TCPS/IL-1ß-stimulated cells	Fibronectin	Dark band

As seen from the results above, no E-selectin was detected on the plasma deposited films or the negative control, TCPS. IL-1ß-stimulated HUVECs produce clear, distinct bands with either ECM coating. Neither surface chemistry nor ECM coating induced E-selectin expression in HUVECs in this system. The surface pre-coatings may mask any effect that surface chemistry has on HUVECs. It was necessary to provide an ECM protein for the cells to attach to--without an attachment protein coating, the cells do not adhere well (even with proteins adsorbed from serum) and eventually die. The surface chemistry did not effect ECM protein adsorption in a manner to promote E-selectin expression in HUVECs.

9.4.5 Neutrophil Adherence Assays

To further support the Northern blot analysis data, HUVECs were grown on 10μ and 30μ ePTFE (in separate experiments), TCPS (negative control), and IL-1ß stimulated HUVECs on TCPS (positive control) and co-cultured with the neutrophil cell line HL-60. If E-selectin is expressed on HUVECs, the HL-60 cells attach to the

HUVECs. The HL-60 cells were loaded with radioactive chromium prior to co-cultivation with the HUVECs. After a short adhesion time (30 min.), the non-adherent HL-60 cells were washed away. The co-cultured cells are lysed and counted on a beta counter to determine the amount of HL-60 attachment to the HUVECs. The percent of attached HL-60s to HUVECs was calculated using the following equation:

% attachment = (mean counts/total HL-60 counts) X 100

The results are summarized in Table 9.7.

Table 9.7: HL-60 Adherence to HUVEC Monolayers

Material	Mean Counts	% Attachment
Experiment 1:		
HUVECs on 30μ Gore ePTFE	917 +/- 196	2.0%
HUVECs on TCPS with Glass Retaining Rings	1089 +/- 291	2.4%
IL-1ß-stimulated HUVECs	4725 +/- 514	10.4%
Labeled HL-60 cells	45323 +/- 1203	---
Experiment 2:		
HUVECs on 10μ Gore ePTFE	342 +/- 109	2.3%
HUVECs on TCPS with Glass Retaining Rings	371 +/- 246	2.4%
10μ Gore ePTFE without HUVECs	301 +/- 146	2.0%
IL-1ß-stimulated HUVECs	1685 +/- 174	11.1%
Labeled HL-60 cells	15148 +/- 142	---

In both experiments, there was no significant attachment to the cells grown on the ePTFE materials compared to the negative control (TCPS), whereas there was significant HL-60 attachment to the IL-1ß-stimulated cells ($p<0.01$) which are known to express E-selectin from the earlier Northern blot analyses. Glass retaining rings were included in the TCPS control to identify any influence the rings have on E-selectin expression, of which there was no effect. An additional control was included in Experiment 2 to determine the level of HL-60 attachment to the material alone without a HUVEC monolayer. The lack of attached HL-60 cells further supports our conclusion that E-selectin is not expressed by HUVECs contacting PTFE and ePTFE materials.

9.5 Conclusions

My investigations did not support the original hypothesis that endothelial cells react to artificial graft materials by eliciting an inflammatory response in the form of E-selectin expression. As shown by the above experiments, E-selectin expression is not indicated in this system. The fluorescence seen with the E-selectin monoclonal antibody staining is regarded as an artifact, the origin of which is unknown at this time. The supporting evidence from the Northern blot analysis and HL-60 leukocyte adherence assays also supports the conclusion that these material surfaces do not induce E-selectin in HUVECs. In addition, changing the surface chemistry and FN adsorption to polystyrene does not affect HUVEC expression of E-selectin.

The fact that E-selectin is not expressed by contacting the materials tested eliminates a potential confounding factor for endothelialization of vascular grafts. It must be noted (focus of Chapter 7) that endothelial cells do no exist without contact with other inflammatory cells such as macrophages *in vivo*. Macrophages, when activated by a number of stimuli (such as biomaterial surfaces), produce cytokines that are known activators of endothelial cells. The cell-cell communication between macrophages and endothelial cells is a vital component to the normal inflammatory response of the body, and is of extreme importance for understanding the foreign body reaction to implanted biomaterials.

9.6 Notes for Chapter 9

Lal, B., Cahan, M. A., Couraud, P. O., Goldstein, G. W., and Laterra, J. (1994). Development of endogenous beta-galactosidase and autofluorescence in rat brain microvessels: implications for cell tracking and gene transfer studies. J. Histochem. Cytochem. *42*, 953-956.

Monma, N., Satodate, R., Suzuki, H., and Ujiie, T. (1988). Ceroid-lipofuscinosis. Report of two autopsy cases. Acta Pathologica Japonica *38*, 1191-1203.

Montgomery, K. F., Osborn, L., Hession, C., Tizard, R., Goff, D., Vassallo, C., Tarr, P. I., Bomsztyk, K., Lobb, R., Harlan, J. M., and Pohlman, T. H. (1991). Activation of endothelial-leukocyte adhesion molecule 1 (ELAM-1) gene transcription. Proc. Natl. Acad. Sci. USA *88*, 6523-6527.

Poole, L. A. (1996). In 5th World Biomaterials Congress (Toronto, pp. Abstract 277.

Van-de-Lest, C. H., Versteeg, E. M., Veerkamp, J. H., and Van-Kuppevelt, T. H. (1995). Elimination of autofluorescence in immunofluorescence microscopy with digital image processing. J. Histochem. Cytochem. *43*, 727-730.

Chapter 10

Conclusions and Future Work

10.1 Conclusions

This research project focused on the development of *in vitro* models to study cell reactions with material surfaces and how materials exert their influence on cell-cell interactions. This model system can be applied to a number of types of implanted materials to study any number of cell interactions. I was able to demonstrate prolonged cytokine release from macrophages in culture, which was normalized to cell number by using the LDH activity of cells. The per cell cytokine release was shown to be sensitive to surface chemistry, topography and extracellular matrix coating. The effects of material characteristics on macrophages contacting a variety of materials were translated to endothelial cells through soluble cytokine signaling, which was manifested in endothelial activation in some cases. The degree of endothelial cell activation depended upon the material that the macrophages contacted. In a related study, endothelial cells directly contacting the materials tested were not activated. The interaction of the two cell types was necessary to observe endothelial cell activation.

Surface chemistry affected the number of human monocytes that initially adhered to the different polymer substrates. The fluoropolymers, especially 60μ ePTFE, had significantly lower monocyte-macrophage adhesion compared to the TCPS or glass retaining ring controls. Adhesion could be improved with FN pre-coating of the materials. There appeared to be significant cell growth on some of the materials, especially the MEC and Nylon substrates, which I found somewhat surprising. Macrophage proliferation has been seen in a variety of pathologies, mainly atherosclerosis and granuloma formation, but may be a new observation for macrophages contacting biomaterials.

Monocytes seeded on the different polymer surfaces were activated to varying degrees determined by measuring inflammatory cytokine release. The hydrophilic polymers, MECs and Nylon 6, showed low levels of IL-1ß and TNFα secreted from macrophages contacting these surfaces. In contrast, the PTFE/ePTFE series showed significantly higher levels of secretion of IL-1ß and TNFα. In particular, the 60μ ePTFE had the highest IL-1ß and TNFα levels of all of the materials tested. These results support the hypothesis that monocyte-macrophage activation can be influenced by different surface chemical properties.

The surface chemistry, determined by ESCA analysis, was shown to be identical for the 3 MEC polymers used. Similarly, all of the fluoropolymers showed the same surface chemistry. Identical surface chemistries within a polymer series allowed for isolation of specific material effects on cells, such as surface topography. The MEC and fluoropolymer groups had very different pore structures: the MECs have a surface similar to an open cell foam, the fluoropolymers consist of long fibrils with intervening solid structures. Due to the dissimilar pore structures between groups, the two polymer types cannot be directly compared on the basis of pore structure since the polymers also differed in surface chemistries. Within each group, however, comparison of pore size or fibril length can be made.

The different MEC pore sizes did not appear to significantly influence macrophage activation. All of the MECs showed similar (low) cytokine production. The MECs had a much narrower range of pore size than the PTFE/ePTFE series, from 0.22μ to 8μ. The fluoropolymer series behaved quite differently. As the fibril length increased from 0 (solid PTFE) to 60μ, there was a rise in the level of IL-1ß and TNFα production. The size of the pores of the MEC materials or fibril lengths of the fluoropolymers is probably very

important. These data suggests that if pore size or fibril length approximates the size of a cell (10-20μ for macrophages), there will be a lower inflammatory response to the material. As the fibrils in the ePTFE series increased, the greater the production of IL-1ß and TNFα. Salzmann et al. recently reported similar observations. The 100μ ePTFE fibril length demonstrated a higher macrophage reaction when implanted in a rat (Salzmann et al., 1997). This makes sense from the stand point of a tissue: cells are more accustomed to having contact in a spherical realm, not a planar one. As macrophages become more elongated, the more likely that "frustrated phagocytosis" will occur. There are years of clinical experience that suggest fibers of specific dimensions produce chronic inflammatory reactions in the lung, resulting in the life-threatening diseases of silicosis and asbestosis. In summary, these data support the hypothesis that the surface topography of a material can affect monocyte-macrophage activation.

Similar to the surface chemistry and topography data, FN pre-coating of the materials showed different effects on the two polymer groups. Due to the low levels of activation on all of the MECs, no significant effect was seen by FN coating these materials. The fluoropolymer series was, however, affected by FN coating. The PTFE, 10μ ePTFE and 30μ ePTFE showed dramatically decreased levels of IL-1ß and TNFα on the surfaces with FN. The macrophage activation on 60μ ePTFE was not influenced by FN, indicating that there may be an additional effect of fibril length that over-rides the "passivating" qualities of FN on these surfaces.

The connection between monocyte adhesion to FN-coated surfaces and cytokine release is not clear at this time. Intuitively, increased adhesion to a material surface would lead to increased macrophage activation, but this was not the case for the 10μ and 30μ materials. More information needs to be gathered on the types of receptors that are engaged on FN-coated and uncoated materials. The differences in total FN adsorption

was not investigated for any of these polymers, primarily due to the difficulties of determining the surface area of very porous materials which is critical to calculating the amount of adsorbed protein. Also, FN conformation was not addressed in this work. These two factors may play a role in the observed data, but they may not. Given the technology available today, these types of investigations would be difficult to perform on porous materials due to their highly variable, and undetermined, surface areas. Although the effects of the amount and conformation of FN could not be determined on the materials tested, FN pre-coating did affect macrophage activation on some of the materials.

The conventional wisdom in the field of biomaterials is that macrophage activation from contact with implanted materials have profound effects on surrounding cells and tissues, although essentially none of these interactions are understood. In this model, we assume that macrophages contacting a material *in vivo* secrete soluble cytokine signals which have significant influence over a number of cell types found at the wound site and surrounding tissues. The specific interaction between macrophages and endothelial cells was investigated here. This influence was demonstrated *in vitro* by the activation of endothelial cells that were exposed to macrophage cytokines generated from contact with the different materials. As summarized above, surface chemistry, topography and FN coating significantly affected macrophage inflammatory cytokine production. When these cytokines were exposed to human endothelial cells, they exhibited a profound effect upon endothelial cell activation. The level of endothelial cell activation directly correlated to the concentrations of IL-1ß and TNFα in the macrophage supernatants. In this fashion, the different surface properties manifest farther reaching effects than just cell-material direct interactions. It will be important to expand these studies to understand the effect of macrophage activation on other cell types important to implanted materials.

The data presented in this dissertation elegantly illustrates the interplay of material properties on macrophage cytokine production and other cells that are found in tissues around medical implants. The assumption made here is that a large and prolonged inflammatory response to an implanted material is not wanted. It is the propagation of cytokine signals that will ultimately dictate how a material is perceived by the body, as "friend" or "foe." The mechanisms of macrophage activation on materials and interactions with other cell types must be elucidated for a number of material types to find the keys to material design that will allow for better integration of medical implants into the body. A few hints for better material design are suggested from this work:

1) The hydrophilic polymers showed the lowest levels of inflammatory cytokine production from macrophages contacting these surfaces. This surface property may prove to be more biocompatible than other materials, such as the hydrophobic fluoropolymers.

2) Logically, porous materials will need to be used to promote tissue integration into or adhesion onto a material.

3) If a porous material contains fibrils, the use of short fibril lengths is suggested. The 10μ ePTFE material showed the lowest inflammatory cytokine production of all of the ePTFE fibril lengths tested. This may be due to the fibril lengths being close to the size of a cell, not allowing the cell to spread or elongate on the fibrils.

4) The use of extracellular matrix protein coatings is suggested for some materials. FN pre-coating showed a decrease in inflammatory cytokine production on the fluoropolymers. This may be important for minimizing the inflammatory response of a material that is ideal for a particular implant application. In this way the material would not need to be re-engineered, merely coated with the extracellular matrix protein of choice.

This research makes a number of contributions to the field of biomaterials. Detailed cytokine data normalized to cell number was generated from macrophages contacting a number of polymer surfaces differing in surface chemistry, topography, and protein coating. A systematic approach to material selection allowed for dissection of the individual surface properties that were to be investigated. Significant differences in cytokine production showed that the macrophages were sensitive to all of the material characteristics of interest, supporting my research hypotheses. Normalization of the cytokine data to cell number provides a distinct advance over other published reports. And finally, macrophage cytokine release was correlated with endothelial cell activation by those macrophage supernatants, demonstrating the potential of macrophage interactions with materials on other cell types. These data, as outlined above, suggest guidelines for improvements in medical implant material design to improve human health.

10.2 Future Work

This research project was a "first stab" at probing into macrophage interactions with materials and how those interactions will influence other cell types. It is the first project in our group that has looked at complex cellular interactions of human cells with material substrates. I feel it provides a solid foundation to build other projects off of. A number of avenues could be pursued:

I think it will be important to determine whether the conclusions made concerning surface chemistry, pore/fibril size and shape, and extracellular matrix coating will transfer to other polymer series. Do other polymers differing in surface topography or chemistry demonstrate any of the hypothesized points? Also, it will be vital to obtain some "in-house" *in vivo* data so that specific material characteristics can be compared to *in vivo*

performance. In other words, is the *in vitro* model developed here adequate for predicting *in vivo* reactions? I stress the generation of this data from within our group to assure the quality and cleanliness of the materials implanted. Implantation results can easily be skewed by improper material handling or surface contamination. Also, it is difficult to obtain detailed histological evaluation from the literature. However, reported findings will be vital to determining the relevance of a particular animal model to human biology.

A large portion of this thesis dealt with the development of different methods of monocyte isolation from blood. There are a number of recent reports which aim at determining the specific macrophage phenotypic subsets that are most important in biomaterials interactions. I think it is important to investigate how specific phenotypes contribute to the inflammatory response of macrophages to materials. Also, are certain phenotypes enriched on specific materials? If so, through what mechanisms (adhesion, proliferation)?

A poorly understood area of biomaterial interactions with all cell types are the mechanisms of cell death and cell proliferation when contacting materials. Part of this has been because of the difficulty of enumerating cells on porous materials, which was overcome in this study by using the LDH protocol developed here. Macrophages were seen to decrease in number on some polymers with time, and increased on others. Is apoptosis involved in the decline in cell numbers, or necrosis? I find it intriguing that monocyte-macrophages are capable of proliferation on certain surfaces. Also, a continued interest of mine is the mystery of why endothelial cells do not readily proliferate from the anastomoses to the center of the graft. What are the cell signaling events that are involved in both cell death and proliferation when contacting materials? Essentially nothing is know about these areas.

One area of my research that I was not able to address was what role IL-8 plays in implant pathology. I was unable to develop an in vitro cell-based assay to try to integrate

the IL-8 release from macrophages contacting the different materials. Possibly a neutrophil maturation assay utilizing flow cytometry, or a neutrophil migration assay using cell culture inserts as was used in Chapter 8 could be used to look at the chemotactic effects of IL-8 secretion from macrophages. Culture insert pore sizes would need to be large enough to allow neutrophils to migrate through the membranes.

An interesting finding from the fluoropolymers was the effect of fibril length on macrophage inflammatory cytokine production. The receptor engagement and signal transduction events that occur for macrophages contacting long fibrils (60μ ePTFE) compared to short fibril lengths (10μ ePTFE) should be investigated.

The role of extracellular matrix (ECM) coatings on materials and their effects on a number of cell types should be expanded upon. Again, the signal transduction in cells contacting ECM protein coatings and how they may reduce inflammatory cytokine release is of importance to the medical implant industry. How other ECM proteins and their conformation on materials influence macrophage response are just a few topics that also need to be addressed.

All of my experiments were done under static conditions. Gimbrone's lab and others have shown how flow can influence gene expression in cells. It would be interesting to conduct similar experiments for cells seeded on materials.

And lastly, studies investigating changes in gene expression for both macrophage and endothelial cell interactions with materials, as well as cell-cell interactions should be expanded upon. Any other actions that macrophage supernatants may have on endothelial cells should be investigated. Two candidates are VEGF and tissue factor. VEGF is an important soluble protein produced by macrophages at wound sites that is responsible for angiogenesis. Tissue factor expression in endothelial cells contacting macrophage supernatants would have implications to potential problems with blood coagulation, an area relevant to vascular grafts. Cell types important to implant pathology, such as

fibroblasts and T-lymphocytes should also be included in these studies. The development of cell-based assays for proliferation, activation, changes in phenotype of cells contacting materials or cell supernatants should be established that directly address biomaterials applications. Incorporation of new and well established techniques, such as subtractive hybridization, *in situ* hybridization, and flow cytometry, into research projects is vital to bringing the field of biomaterials up to speed with the rest of human biology. The technology exists, it just needs to be adapted to the special needs and challenges of working with cells contacting biomaterial surfaces.

10.3 Notes for Chapter 10

Salzmann, D. L., Kleinert, L. B., Berman, S. S., and Williams, S. K. (1997). The effects of porosity on endothelialization of ePTFE implanted in subcutaneous and adipose tissue. J. Biomed. Mater. Res. *34*, 463-476.

BIBLIOGRAPHY

Adamson, A. W. (1982). Physical Chemistry of Surfaces, 4th edition Edition (New York: John Wiley & Sons).

Aggarwal, B. B., and Vilcek, J. (1992). Tumor necrosis factors: structure, function and mechanism of action (New York: M. Dekker).

Albelda, S. M., and Buck, C. A. (1990). Integrins and other cell adhesion molecules. FASEB *4*, 2868-2880.

Baeuerle, P. A., and Baltimore, D. (1988). Activation of DNA-Binding Activity in an Apparent Cytoplasmic Precursor of the NF-kB Transcription Factor. Cell *53*, 211-217.

Baeuerle, P. A., and Baltimore, D. (1988). IkB: A Specific Inhibitor of the NF-kB Transcription Factor. Science *242*, 540-546.

Beamson, G., and Briggs, D. (1992). High Resolution XPS of Organic Polymers (New York: John Wiley & Sons).

Beezhold, D. H., and Personius, C. (1992). Fibronectin fragments stimulate tumor necrosis factor secretion by human monocytes. J. Leukocyte Biol. *51*, 59-64.

Ben-Baruch, A., Michiel, D. F., and Oppenheim, J. J. (1995). Signals and Receptors Involved in Recruitment of Inflammatory Cells. J. Biol. Chem. *270*, 11703-11706.

Benton, L. D., Khan, M., and Greco, R. S. (1993). Integrins, Adhesion Molecules and Surgical Research. Surg. Gyn, Obstet. *177*, 311-327.

Benton, L. D., Purohit, U., Khan, M., and Greco, R. S. (1996). The Biologic Role of B_2 Integrins in the Host Response to Expanded Polytetrafluoroethylene. J. Surg. Res. *64*, 116-119.

Bernatchez, S., Atkinson, M. R., and Parks, P. J. (1997). Expression of intercellular adhesion molecule-1 on macrophages *in vitro* as a marker of activation. Biomaterials *18*, 1371-1378.

Bernatchez, S., Parks, P. J., and Gibbons, D. F. (1996). Interactions of macrophages with fibrous materials *in vitro*. Biomaterials *17*, 2077-2086.

Beutler, B., Greenwald, D., Hulmes, J. D., Chang, M., Pan, Y.-C., Mathison, J., Ulevitch, R., and Cerami, A. (1985). Identity of tumor necrosis factor and the macrophage-secreated factor cachectin. Nature *316*, 552-554.

Bevilacqua, M. P., Stengelin, S., Gimbrone, M. A., and Seed, B. (1989). Endothelial Leukocyte Adhesion Molecule 1: An Inducible Receptor for Neutrophils Related to Complement Regulatory Proteins and Lectins. Science *243*, 1160-1165.

Bhardwaj, R. S., Henze, U., Klein, B., Zwadlo-Klarwasser, G., Klinge, U., Mittermayer, C., and Klosterhalfen, B. (1997). Monocyte-biomaterial interaction inducing phenotypic dynamics of monocytes: a possible role of monocyte subsets in biocompatibility. J. Mater. Sci.: Mater. Med. *8*, 737-742.

Blum, J. L., and Wicha, M. S. (1988). Role of the Cytoskelton in Laminin Induced Mammary Gene
Expression. J. Cell. Physiol. *135*, 13-22.

Bonfield, T. L., and Anderson, J. M. (1993). Functional versus quantitative comparison of IL-1b from monocytes/macrophages on biomedical polymers. J. Biomed. Mat. Res. *27*, 1195-1199.

Bonfield, T. L., Colton, E., and Anderson, J. M. (1992). Protein adsorption of biomedical polymers influences activated monocytes to produce fibroblast stimulating factors. J. Biomedical Materials Research *26*, 457-465.

Bonfield, T. L., Colton, E., Marchant, R. E., and Anderson, J. M. (1992). Cytokine and growth factor production by monocytes/macrophages on protein preadsorbed polymers. J. Biomed. Mater. Res. *26*, 837-850.

Brauker, J. H., Carr-Brendel, V. E., Martinson, L. A., Crudele, J., Johnston, W. D., and Johnson, R. C. (1995). Neovascularization of synthetic membranes directed by membrane architecture. J. Biomed. Mater. Res. *29*, 1517-1524.

Bujan, J., Garcia-Honduvilla, N., Contreras, L., Gimeno, M. J., Escudero, C., Bellon, J. M., and San-Roman, J. (1998). Coating PTFE vascular prostheses with a fibroblastic matrix improves cell retention when subjected to blood flow. J. Biomed. Mater. Res. *39*, 32-39.

Burkel, W. E., Ford, J. W., Vinter, D. W., Kahn, R. H., Graham, L. M., and Stanley, J. C. (1982). Endothelial Seeding of Enzymatically Derived and Cultured Cells on Prosthetic Grafts. In Biologic and Synthetic Vascular Grafts, J. C. Stanley, ed. (New York: Grune & Stratton), pp. 631-651.

Cahalon, L., Hershkoviz, R., Gilat, D., Miller, A., Akiyama, S. K., Yamada, K. M., and Lider, O. (1994). Functional Interactions of Fibronectin and TNFα: A Paradigm of Physiological Linkage Between Cytokines and Extracellualr Matrix Moieties. Cell Adh. Comm. *2*, 269-273.

Callow, A. D. (1988). Problems in the Construction of a Small Diameter Graft. International Angiology *7*, 246-253.

Cardona, M. A., Simmons, R. L., and Kaplan, S. S. (1992). TNF and IL-1 generation by human monocytes in response to biomaterials. J. Biomed. Mater. Res. *26*, 851-859.

Chilkoti, A., Schmierer, A. E., Perez-Luna, V. H., and Ratner, B. D. (1995). Investigating the Relationship between Surface Chemistry and Endothelial Cell Growth: Partial Least-Squares Regression of the Static Secondary Ion Mass Spectra of Oxygen-Containing Plasma Deposited Films. Anal. Chem. *67*, 2883-2891.

Chomczynski, P., and Sacchi, N. (1987). Single-step method of RNA isolation by acid guanidinium thiocyante-phenol-chloroform extraction. Anal. Biochem. *162*, 156-159.

Das, S. K., Johnson, M., Ellsaesser, C., Brantley, S. K., Kanosky, M. G., and Johnson, S. G. (1992). Macrophage Interleukin 1 Response to Injected Silicone in a Rat Model. Ann. Plast. Surg. *28*, 535-537.

Davies, P., Bonney, R. J., Humes, J. L., and F.A. Kuehl, J. (1981). Secretory functions of macrophages participating in inflammatory responses. In Cellular Interactions, J. T. Dingle and J. L. Gordon, eds. (New York: Elsevier), pp. 33-42.

Davis, G. E. (1992). The Mac-1 and p150, 95ß2 integrins bind denatured proteins to mediate leukocyte cell-substrate adhesion. Exp. Cell Res. *200*, 242-252.

DeFife, K. M., Yun, J. K., Azeez, A., Stack, S., Ishihara, K., Nakabayashi, N., Colton, E., and Anderson, J. M. (1995). Adhesion and cytokine production by monocytes on poly(2-methacryloyloxyethyl phosphorylcholine-co-alkyl methacrylate)-coated polymers. J. Biomed. Mater. Res. *29*, 431-439.

Dilks, A. (1981). Electron Spectroscopy: Theory, Techniques and Applications., Volume 4, A. B. Baker and C. R. Brundle, eds. (London: Academic Press).

Dinarello, C. A. (1990). Cytokines and Biocompatibility. Blood Purif. *8*, 208-213.

Dinarello, C. A. (1988). Cytokines: Interleukin-1 and Tumor Necrosis Factor (Cachectin). In Inflammation: Basic Principles and Clinical Correlates, J. I. Gallin, I. M. Goldstein and R. Snyderman, eds. (New York: Raven Press), pp. 195-208.

Dinarello, C. A. (1991). Interleukin-1 and Interleukin-1 Antagonism. Blood *77*, 1627-1652.

Eierman, D. F., Johnson, C. E., and Haskill, J. S. (1989). Human Monocyte Inflammatory Mediator Gene Expression is Selectively Regulated By Adherence Substrates. J. Immunol. *142*, 1970-1976.

Emerick, S., Herring, M., Arnold, M., Baughman, S., Reilly, K., and Glover, J. (1987). Leukocyte depletion enhances cultured endothelial retention on vascular prostheses. J. Vasc. Surg. *5*, 342-347.

Ertel, S. I., Chilkoti, A., Horbett, T. A., and Ratner, B. D. (1991). Endothelial cell growth on oxygen-containing films deposited by radio-frequency plasmas: the role of surface carbonyl groups. J. Biomater. Sci. Polymer Edn. *3*, 163-183.

Ertel, S. I., Ratner, B. D., and Horbett, T. A. (1991). The Adsorption and Elutability of Albumin, IgG, and Fibronectin on Radiofrequency Plasma Deposited Polystyrene. J. Coll. Interface Sci. *147*, 433-442.

Ertel, S. I., Ratner, B. D., and Horbett, T. A. (1990). Radiofrequency plasma deposition of oxygen-containing films on polystyrene and poly(ethylene terephthalate) substrates improves endothelial cell growth. J. Biomed. Mater. Res. *24*, 1637-1659.

Eskin, S. G., Navarro, L. T., Zamora, J. L., Ives, C. L., Anderson, J. M., Weilbaecher, D. G., Gao, Z. R., and Noon, G. P. (1987). Preliminary Studies on Autologous versus Homologous Endothelial Cell Seeding of Ateriovenous Grafts. In Endothelial Seeding in Vascular Surgery, M. Herring and J. L. Glover, eds. (New York: Grune & Stratton), pp. 155-163.

Fasol, R., Zilla, P., Deutsch, M., Grimm, M., and Fischlein, T. (1989). Human endothelial cell seeding: Evaluation of its effectiveness by platelet parameters after one year. J. Vasc. Surg. *9*, 432-436.

Fisher, A. A. (1990). Reactions at Silicone-Injected Sites on the Face Associated with Silicone Breast Implant "Inflammation" or "Rejection". CUTIS *45*, 393-395.

Foxall, C., Watson, S. R., Dowbenko, D., Fennie, C., Lasky, L. A., Kiso, M., Hasegawa, A., Asa, D., and Brandley, B. K. (1992). The three members of the selectin receptor family recognize a common carbohydrate epitope, the sialyl Lewis-x oligosaccharide. J. Cell Biol. *117*, 895-902.

Francese, J. (1989). Application of PLS Modeling to ELISA Measurements of Fibrinogen Adsorption to Untreated and RF Plasma Modified Microtiter Wells. In Chemical Engineering (Seattle: University of Washington), pp. 136.

Frazier, O. H., Kadipasaoglu, K. A., Parnis, S. M., and Radovancevic, B. (1994). Biomaterials Used in Cardiac Surgery. In Implantation Biology: The Host Response and Biomedical Devices, R. S. Greco, ed. (Boca Raton: CRC Press), pp. 165-178.

Fuhlbrigge, R. C., Chaplin, D. D., Kiely, J.-M., and Unanue, E. R. (1987). Regulation of Interleukin 1 Gene Expression by Adherence and Lipopolysaccharide. J. Immunol. *138*, 3799-3802.

Furcht, L. T. (1983). Structure and Function of the Adhesive Glycoprotein Fibronectin. Modern Cell Biol. *1*, 53-117.

Furie, M. B., and Randolph, G. J. (1995). Chemokines and Tissue Injury. Am. J. Path. *146*, 1287-1301.

Furth, R. v. (1988). Inflammation: Basic Principles and Clinical Correlates, J. I. Gallin, ed. (New York: Raven Press).

Ghosh, S., and Baltimore, D. (1990). Activation in vitro of NF-kB by phosphorylation of its inhibitor IkB. Nature *344*, 678-682.

Gimond, C., and Aumailley, M. (1992). Cellular Interactions with the Extracellular Matrix Are Coupled to Diverse Transmembrane Signalling Pathways. Exp. Cell Res. *203*, 365-373.

Goldblum, R. M., Pelley, R. P., O'Donell, A. A., Pyron, D., and Heggers, J. P. (1992). Antibodies to silicone elastomers and reactions to ventriculoperitoneal shunts. Lancet *340*, 510-513.

Graham, L. M., and Bergan, J. J. (1982). Expanded Polytetrafluoroethylene Vascular Grafts: Clinical and Experimental Observations. In Biologic and Synthetic Vascular Grafts, J. C. Stanley, ed. (New York: Grune & Stratton), pp. 563-585.

Graham, L. M., Brothers, T. E., Vincent, C. K., Burkel, W. E., and Stanley, J. C. (1991). The role of an endothelial cell lining in limiting distal anastomotic intimal hyperplasia of 4-mm-I.D. Dacron grafts in a canine model. J. Biomed. Mater. Res. *25*, 525-533.

Greisler, H. P., Endean, E. D., Klosak, J. J., Ellinger, J., Henderson, S. C., Pham, S. M., Durham, S. J., Showalter, D. P., Levine, J., and Borovetz, H. S. (1989). Hemodynamic Effects on Endothelial Cell Monolayer Detachment From Vascular Prostheses. Arch. Surg. *124*, 429-433.

Harlan, J. M., and Liu, D. Y. (1992). Adhesion: Its Role in Inflammatory Disease (New York: W. H. Freeman and Co.).

Hazuda, D. J., Lee, J. C., and Young, P. R. (1988). The Kinetics of Interleukin 1 Secretion from Activated Monocytes. J. Biological Chemistry *263*, 8473-8479.

Heemann, U. W., Tullius, S. G., Azuma, H., Kupiec-Weglinsky, J., and Tilney, N. L. (1994). Adhesion Molecules and Transplantation. Ann. of Surgery *219*, 4-12.

Heggers, J. P., Kossovsky, N., Parsons, R. W., Robson, M. C., Pelley, R. P., and Raine, T. J. (1983). Biocompatibility of Silicone Implants. Annals of Plastic Surg. *11*, 38-45.

Henson, P. M., Webster, R. O., and Henson, J. E. (1981). Neutrophil and monocyte activation and secretion: role of surfaces in inflammatory reactions and *in vitro*. In Cellular Interactions, J. T. Dingle and J. L. Gordon, eds. (New York: Elsevier), pp. 43-56.

Herring, M., Arnold, M., Emerick, S., Ashworth, E., Hoagland, W., and Glover, J. (1987). Suppressing Endothelial Desquamation From Vascular Prostheses. In Endothelial Seeding in Vascular Surgery, M. Herring and J. L. Glover, eds. (New York: Grune & Stratton), pp. 119-138.

Herring, M. B. (1991). Endothelial Cell Seeding. J. Vasc. Surg. *13*, 731-732.

Herring, M. B., Compton, R. S., LeGrand, D. R., Gardner, A. L., Madison, D. L., and Glover, J. L. (1987). Endothelial seeding of polytetrafluoroethylene popliteal bypasses. J. Vasc. Surg. *6*, 114-118.

Herring, M. B., Dilley, R., Gardner, A. L., and Glover, J. (1982). Seeding of Mechanically Derived Endothelium on Arterial Prostheses. In Biologic and Synthetic Vascular Grafts, J. C. Stanley, ed. (New York: Grune & Stratton), pp. 621-629.

Hession, C., Osborn, L., Goff, D., Chi-Rosso, G., Vassallo, C., Pasek, M., Pittack, C., Tizard, R., Goelz, S., McCarthy, K., Hopple, S., and Lobb, R. (1990). Endothelial leukocyte adhesion molecule 1: Direct expression cloning and functional interactions. Proc. Natl. Acad. Sci. USA *87*, 1673-1677.

Horbett, T. A. (1984). Mass Action Effects on Competitive Adsorption of Fibrinogen from Hemoglobin Solutions and from Plasma. Thromb. Haemostas. *51*, 174-181.

Horbett, T. A., Weathersby, P. K., and Hoffman, A. S. (1977). The Preferential Adsorption of Hemoglobin to Polyethylene. J. Bioeng. *1*, 61-78.

Hubbard, A. K. (1989). Role for T Lymphocytes in Silica-Induced Pulmonary Inflammation. Laboratory Investigation *61*, 46-52.

Hunt, J. A., Meijs, G., and Williams, D. F. (1997). Hydrophilicity of polymers and soft tissue responses: A quantitative analysis. J. Biomed. Mater. Res. *36*, 542-549.

Hussain, S., Glover, J. L., Augelli, N., Bendick, P. J., Maupin, D., and McKain, M. (1989). Host response to autologous endothelial seeding. J. Vasc. Surg. *9*, 656-664.

Hynes, R. O. (1992). Integrins: versatility, modulation and signalling in cell adhesion. Cell *69*, 11-25.

Jarrell, B., Williams, S., Park, P., Carter, T., Carabasi, A., and Rose, D. (1988). Human Endothelial Cell Interactions With Vascular Grafts. In Tissue engineering: Proceedings of a workshop, held at Granlibakken, Lake Tahoe, California, February 26-29, 1988, R. Skalak and C. F. Fox, eds. (New York: Liss), pp. 11-15.

Jarrell, B. E., and Williams, S. K. (1991). Microvessel Derived Endothelial Cell Isolation, Adherence, and Monolayer Formation for Vascular Grafts. J. Vasc. Surg. *13*, 733-734.

Jarrell, B. E., Williams, S. K., Carabasi, R. A., and Hubbard, F. A. (1987). Immediate Vascular Graft Monolayers Using Microvessel Endothelial Cells. In Endothelial Seeding in Vascular Surgery, M. Herring and J. L. Glover, eds. (New York: Grune & Stratton), pp. 37-55.

Jones, P. L., Schmidhauser, C., and Bissell, M. J. (1993). Regulation of Gene Expression and Cell Function by Extracellular Matrix. Crit. Rew. Euk. Gene Exp. *3*, 137-154.

Kaplan, S. (1994). Biomaterial-host interactions: consequences, determined by implant retrieval analysis. Medical Progress through Technology *20*, 209-230.

Kempczinski, R. F., Douville, E. C., Ramalanjaona, G., Ogle, J. D., and Silberstein, E. B. (1987). Endothelial Cell Seeding on a Fibronectin-Coated Substrate. In Endothelial Seeding in Vascular Surgery, M. Herring and J. L. Glover, eds. (New York: Grune & Stratton), pp. 57-77.

Kiaei, D., Hoffman, A. S., and Horbett, T. A. (1992). Tight binding of albumin to glow discharge treated polymers. J. Biomater. Sci. Polymer Edn. *4*, 35-44.

Kossovsky, N., Heggers, J. P., and Robson, M. C. (1987). Experimental demonstration of the immunogenicity of silicone-protein complexes. J. Biomedical Materials Research *21*, 1125-1133.

Kossovsky, N., Zeidler, M., Chun, G., Papasian, N., Nguyen, A., Rajguru, S., Stassi, J., Gelman, A., and Sponsler, E. (1993). Patients with Silicone Breast Implants Show Increased IgG Binding Affinity to Extracellular Macromolecules. In The 19th Annual Meeting of the Society for Biomaterials (Birmingham, AL, USA, pp. 231.

Krause, T. J., Robertson, F. M., Liesch, J. B., Wasserman, A. J., and Greco, R. S. (1990). Differential Production of Interleukin 1 on the Surface of Biomaterials. Arch. Surg. *125*, 1158-1160.

Kunkel, S. L., Lukacs, N., and Strieter, R. M. (1995). Expression and biology of neutrophil and endothelial cell-derived chemokines. Cell Biol. *6*, 327-336.

Lafrenie, R. M., and Yamada, K. M. (1996). Integrin-Dependent Signal Transduction. J. Cell. Biochem. *61*, 543-553.

Lal, B., Cahan, M. A., Couraud, P. O., Goldstein, G. W., and Laterra, J. (1994). Development of endogenous beta-galactosidase and autofluorescence in rat brain microvessels: implications for cell tracking and gene transfer studies. J. Histochem. Cytochem. *42*, 953-956.

Lan, H. Y., Nikolic-Paterson, D. J., Mu, W., and Atkins, R. C. (1995). Local macrophage proliferation in multinucleated giant cell and granuloma formation in experimental Goodpasture's syndrome. Am. J. Pathol. *147*, 1214-1220.

Lasky, L. A. (1992). Selectins: Interpreters of Cell-Specific Carbohydrate Information During Inflammation. Science *258*, 964-969.

Lelievre, S., Weaver, V. M., and Bissell, M. J. (1996). Extracellular Matrix Signalling from the Cellular Membrane Skeleton to the Nuclear Skeleton: A Model of Gene Regulation. Recent Prog. Hormone Res. *51*, 417-432.

Li, J., Menconi, M. J., Wheeler, H. B., Rohrer, M. J., Klassen, V. A., Ansell, J. E., and Appel, M. C. (1992). Precoating expanded polytetrafluoroethylene grafts alters production of endothelial cell-derived thrombomodulators. J. Vasc. Surg. *15*, 1010-1017.

Libby, P., Birinyi, L. K., and Callow, A. D. (1987). Functions of Endothelial Cells Related to Seeding of Vascular Prostheses: The Unanswered Questions. In Endothelial Seeding in Vascular Surgery, M. Herring and J. L. Glover, eds. (New York: Grune & Stratton), pp. 17-35.

Limbird, L. E. (1986). Cell Surface Receptors: A Short Course on Theory and Methods (Boston: Martinus Nijhoff Publishing).

López, G. P., and Ratner, B. D. (1991). Substrate Temperature Effects on Film Chemistry in Plasma Deposition of Organics. 1. Nonpolymerizable Precursors. Langmuir *7*, 766-773.

López, G. P., and Ratner, B. D. (1992). Substrate Temperature Effects on Film Chemistry in Plasma Depositions of Organics. II. Polymerizable Precursors. J. Polym. Sci., Polym. Chem. Ed. *30*, 2415-2425.

López, G. P., Ratner, B. D., Rapoza, R. J., and Horbett, T. A. (1993). Plasma Deposition of Ultrathin Films of Poly(2-hydroxyethyl methacrylate): Surface Analysis and Protein Adsorption Measurements. Macromolecules *26*, 3247.

Luna, E. J., and Hitt, A. L. (1992). Cytoskeleton-Plasma Membrane Interactions. Science *258*, 955-964.

Lundahl, J., Sköld, C. M., Halldén, G., Hallgren, M., and Eklund, A. (1996). Monocyte and Neutrophil Adhesion to Matrix Proteins is Selectively Enhanced in the Presence of Inflammatory Mediators. Scand. J. Immunol. *44*, 143-149.

Macchia, D., Almerigogna, F., Parronchi, P., Ravina, A., Maggi, E., and Romagnani, S. (1993). Membrane Tumor Necrosis Factor-a is Involved in the Polyclonal B-Cell Activation Induced by HIV-infected T Cells. Nature *363*, 464-466.

Macey, M. G., McCarthy, D. A., Vordermeier, S., Newland, A. C., and Brown, K. A. (1995). Effects of cell purification methods on CD11b and L-selectin expression as well as the adherence and activation of leukocytes. J. Immunological Meth. *181*, 211-219.

Maniatis, T., Fritsch, E. F., and Sambrook, J. (1982). Molecular Cloning: A Laboratory Manual (Cold Spring Harbor, NY: Cold Spring Harbor Laboratory).

Maniotis, A. J., Chen, C. S., and Ingber, D. E. (1997). Demonstration of mechanical connections between integrins, cytoskeletal filaments, and nucleoplasm that stabilize nuclear structure. Proc. Natl. Acad. Sci. USA *94*, 849-854.

Margiotta, M. S., Robertson, F. S., and Greco, R. S. (1992). The Adherence of Endothelial Cells to Dacron Induces the Expression of the Intercellular Adhesion Molecule (ICAM-1). Ann. Surgery *216*, 600-604.

Massia, S. P., and Hubbell, J. A. (1992). Immobilized Amines and Basic Amino Acids as Mimetic Heparin-binding Domains for Cell Surface Proteoglycan-mediated Adhesion. J. Biol. Chem. *267*, 10133-10141.

Matsuda, T., Kitamura, T., Iwata, H., Takano, H., and Akutsu, T. (1988). A Hybrid Artificial Vascular Graft Based upon an Organ Reconstruction Model. Trans. Am. Soc. Artif. Intern. Organs *34*, 640-643.

Mazzucotelli, J.-P., Klein-Soyer, C., Beretz, A., Brisson, C., Archipoff, G., and Cazenave, J.-P. (1991). Endothelial cell seeding: coating Dacron and expanded polytetrafluoroethylene vascular grafts with a biological glue allows adhesion and growth of human saphenous vein endothelial cells. International J. of Artif. Organs *14*, 482-490.

Menconi, M. J., Owen, T., Dasse, K. A., Stein, G., and Lian, J. B. (1992). Molecular Approaches to the Characterization of Cell and Blood/Biomaterial Interactions. J. Cardiac Surg. *7*, 177-187.

Miller, K. M., and Anderson, J. M. (1988). Human monocyte/macrophage activation and interleukin 1 generation by biomedical polymers. J. Biomedical Materials Research *22*, 713-731.

Miller, K. M., and Anderson, J. M. (1989). *In vitro* stimulation of fibroblast activity by factors generated from human monocytes activated by biomedical polymers. J. Biomed. Mater. Res. *23*, 911-930.

Miller, K. M., Rose-Caprara, V., and Anderson, J. M. (1989). Generation of IL1-like activity in response to biomedical polymer implants: A comparison of in vitro and in vivo models. J. Biomedical Materials Research *23*, 1007-1026.

Mohr, C., Gemsa, D., Graebner, C., Hemenway, D. R., Leslie, K. O., Absher, P. M., and Davis, G. S. (1991). Systemic Macrophage Stimulation in Rats with Silicosis: Enhanced Release of Tumor Necrosis Factor-alpha from Alveolar and Peritoneal Macrophages. Am. J. Respir. Cell Mol. Biol. *5*, 395-402.

Monma, N., Satodate, R., Suzuki, H., and Ujiie, T. (1988). Ceroid-lipofuscinosis. Report of two autopsy cases. Acta Pathologica Japonica *38*, 1191-1203.

Montgomery, K. F., Osborn, L., Hession, C., Tizard, R., Goff, D., Vassallo, C., Tarr, P. I., Bomsztyk, K., Lobb, R., Harlan, J. M., and Pohlman, T. H. (1991). Activation of endothelial-leukocyte adhesion molecule 1 (ELAM-1) gene transcription. Proc. Natl. Acad. Sci. USA *88*, 6523-6527.

Morla, A., and Ruoslahti, E. (1992). A Fibronectin Self-Assembly site Involved in Fibronectin Matrix Assembly: Reconstruction in a Synthetic Peptide. J. Cell Biology *118*, 421-429.

Nathan, C. F. (1987). Secretory Products of Macrophages. J. Clinical Investigation *79*, 319-326.

Nerem, R. M. (1988). Endothelial Cell Responses to Shear Stress: Implications in the Development of Endothelialized Synthetic Vascular Grafts. In Tissue engineering: Proceedings of a workshop, held at Granlibakken, Lake Tahoe, Califonia, February 26-29, 1988, R. Skalak and C. F. Fox, eds. (New York: Liss), pp. 5-10.

Oppenheim, J. J., Kovacs, E. J., Matsushima, K., and Durum, S. K. (1986). There is more than one interleukin 1. Immunology Today *7*, 45-56.

Owen, C. A., Campbell, E. J., and Stockley, R. A. (1992). Monocyte adherence to fibronectin: role of CD11b/CD18 integrins and relationship to other monocyte functions. J. Leukocyte Biol. *51*, 400-408.

Peimer, C. A., Medige, J., Eckert, B. S., Wright, J. R., and Howard, C. S. (1986). Reactive synovitis after silicone arthroplasty. J. Hand Surgery *11A*, 624-638.

Perez, C., Albert, I., DeFay, K., Zachariades, N., Gooding, L., and Kriegler, M. (1990). A nonsecretable cell surface mutant of tumor necrosis factor (TNF) kills by cell-to-cell contact. Cell *63*, 251-258.

Pertoft, H., Johnsson, A., Wärmegård, B., and Seljelid, R. (1980). Separation of Human Monocytes on Density Gradients of Percoll®. J. Immunological Methods *33*, 221-229.

Petillo, O., Peluso, G., Ambrosio, L., Nicolais, L., Kao, W. J., and Anderson, J. M. (1994). *In vivo* induction of macrophage Ia antigen (MHC class II) expression by biomedical polymers in the cage implant system. J. Biomed. Mater. Res. *28*, 635-646.

Pettit, D. K., Horbett, T. A., and Hoffman, A. S. (1992). Influence of the substrate binding characteristics of fibronectin on corneal epithilial cell outgrowth. J. Biomed. Mat. Res. *26*, 1259-1275.

Pober, J. S., and Cotran, R. S. (1990). Cytokines and Endothelial Cell Biology. Physiological Reviews *70*, 427-451.

Pober, J. S., and Cotran, R. S. (1991). What Can Be Learned From the Expression of Endothelial Adhesion Molecules in Tissues? Lab. Invest. *64*, 301-305.

Polley, M. J., Phillips, M. L., Wayner, E., Nudelman, E., Singhal, A. K., Hakomori, S.-I., and Paulson, J. C. (1991). CD62 and endothelial cell-leukocyte adhesion molecule 1 (ELAM-1) recognize the same carbohydrate ligand, sialyl-Lewis x. Proc. Natl. Acad. Sci. USA *88*, 6224-6228.

Poole, L. A., and al., e. (1996). . In 5th World Biomaterials Congress (Toronto, pp. Abstract 277.

Poole, S., Thorpe, R., Meager, A., and Gearing, A. J. H. (1987). Assay of Pyrogenic Contamination in Pharmaceuticals by Cytokine Release From Monocytes. In Developments in Biological Standardization, A. J. H. Gearing and W. Hennessen, eds. (New York: Karger), pp. 121-123.

Pujol-Borrell, R., Todd, I., Doshi, M., Bottazzo, G. F., Sutton, R., Gray, D., Adolf, G. R., and Feldmann, M. (1987). HLA class II induction in human islet cells by interferon-gamma plus tumor necrosis factor of lymphotoxin. Nature *326*, 304-306.

Ratner, B. D., and McElroy, B. J. (1986). Electron Spectroscopy for Chemical Analysis: Application in the Biomedical Sciences, R. M. Gendreau, ed. (Boca Raton, Florida: CRC Press).

Reichle, F. A. (1982). Function and Biologic Fate of Woven Dacron Grafts Compared to Other Materials in Femoropopliteal Arterial Bypass Procedures. In Biologic and Synthetic Vascular Prostheses, J. C. Stanley, ed. (New York: Grune & Stratton), pp. 495-508.

Rhodes, N. P., Hunt, J. A., and Williams, D. F. (1997). Macrophage subpopulation differentiation by stimulation with biomaterials. J. Biomed. Mater. Res. *37*, 481-488.

Rosales, C., and Juliano, R. L. (1995). Signal transduction by cell adhesion receptors in leukocytes. J. Leukocyte Biol. *57*, 189-198.

Salzmann, D. L., Kleinert, L. B., Berman, S. S., and Williams, S. K. (1997). The effects of porosity on endothelialization of ePTFE implanted in subcutaneous and adipose tissue. J. Biomed. Mater. Res. *34*, 463-476.

Sank, A., Chalabain-Baliozian, J., Ertl, D., Sherman, R., Nimni, M., and Tuan, T. L. (1993). Cellular Responses to Silicone and Polyurethane Prosthetic Surfaces. J. Surgical Research *54*, 12-20.

Sastry, S. K., and Horwitz, A. F. (1993). Integrin cytoplasmic domains: mediators of cytoskeletal linkages and extra- and intercellular initiated transmembrane signaling. Current Opinion in Cell Biology *5*, 819-831.

Sauvage, L. R., Walker, M. W., Berger, K., Robel, S. B., Lischko, M. M., Yates, S. G., and Logan, G. A. (1979). Current arterial prostheses: Experimental evaluation by implantation in the carotid and circumflex coronary arteries of the dog. Arch. Surg. *114*, 687-691.

Schleimer, R. P., Sterbinsky, S. A., Kaiser, J., Bickel, C. A., Klunk, D. A., Tomioka, K., Newman, W., Luscinskas, F. W., Michael A. Gimbrone, J., McIntyre, B. W., and Bochner, B. S. (1992). IL-4 Induces Adherence of Human Eosinophils and Basophils but not Neutrophils to Endothelium. J. Immunol. *148*, 1086-1092.

Schneider, A., Chandra, M., Lazarovici, G., Vlodavsky, I., Merin, G., Uretzky, G., Borman, J. B., and Schwalb, H. (1997). Naturally produced extracellular matrix is an excellent substrate for canine endothelial cell proliferation and resistance to shear stress on PTFE vascular grafts. Thromb. Haemost. *78*, 1392-1398.

Schneider, A., Melmed, R. N., Schwalb, H., Karck, M., Vlodavsky, I., and Uretzky, G. (1992). An improved method for endothelial cell seeding on polytetrafluoroethylene small caliber vascular grafts. J. Vasc. Surg. *15*, 649-656.

Shankar, R., and Greisler, H. P. (1994). Inflammation and Biomaterials. In Implantation Biology: The Host Response and Biomedical Devices, R. S. Greco, ed. (Boca Raton: CRC Press), pp. 67-80.

Singhvi, R., Kumar, A., Lopez, G. P., Stephanopoulos, G. N., Wang, D. I. C., Whitesides, G. M., and Ingber, D. E. (1994). Engineering Cell Shape and Function. Science *264*, 696-698.

Smyth, S. S., Joneckis, C. C., and Parise, L. V. (1993). Regulation of Vascular Integrins. Blood *81*, 2827-2843.

Snow, R. B., and Kossovsky, N. (1989). Hypersensitivity Reaction Associated with Sterile Ventriculoperitoneal Shunt Malfunction. Surg. Neurol. *31*, 209-214.

Snyder, R. W., and Botzko, K. M. (1982). Woven, Knitted, and Externally Supported Dacron Vascular Grafts. In Biologic and Synthetic Vascular Prostheses, J. C. Stanley, ed. (New Yord: Grune & Stratton), pp. 485-494.

Stanislawski, L., Serne, H., Stanislawski, M., and Jozefowicz, M. (1993). *Conformational changes in fibronectin induced by polystyrene derivatives with a heparin-like fuction.* J. Biomater. Sci. Polymer Edn. *27*, 619-626.

Steele, J. G., Dalton, B. A., Johnson, G., and Underwood, P. A. (1995). Adsorption of fibronectin and vitronectin onto Primaria and tissue culture polystyrene and relationship to the mechanism of initial attachment of human vein endothelial cells and BHK-21 fibroblasts. Biomaterials *16*.

Steele, J. G., Johnson, G., McFarland, C., Dalton, B. A., Gengenbach, T. R., Chatelier, R. C., Underwood, P. A., and Griesser, H. J. (1994). Roles of serum vitronectin and fibronectin in intial attachment of human vein endothelial cells and dermal fibroblasts on oxygen- and nitrogen-containing surfaces made by radiofrequency plasmas. J. Biomat. Sci. Polym. Edn. *6*, 511-532.

Stone, R. (1993). The Case Against Implants. Science *260*, 31.

Struhar, D. J., Harbeck, R. J., Gegen, N., Kawada, H., and Mason, R. J. (1989). Increased expression of class II antigens of the major histocompatibility complex on alveolar macrophages and alveolar type II cells and interleukin-1 (IL-1) secretion from alveolar macrophages in an animal model of silicosis. Clin. Exp. Immunol. *77*, 281-284.

Swartbol, P., Truedsson, L., Parsson, H., and Norgren, L. (1996). Surface adhesion molecule expression on human blood cells induced by vascular graft materials *in vitro*. J. Biomed. Mater. Res. *32*, 669-676.

Tidwell, C. D., Ertel, S. I., Ratner, B. D., Tarasevich, B. J., Atre, S., and Allara, D. L. (1997). Endothelial Cell Growth and Protein Adsorption on Terminally Functionalized, Self-Assembled Monolayers of Alkanethiolates on Gold. Langmuir *13*, 3404-3413.

Van-de-Lest, C. H., Versteeg, E. M., Veerkamp, J. H., and Van-Kuppevelt, T. H. (1995). Elimination of autofluorescence in immunofluorescence microscopy with digital image processing. J. Histochem. Cytochem. *43*, 727-730.

Varga, J., Schumacher, H. R., and Jimenez, S. A. (1989). Systemic Sclerosis after Augmentation Mammoplasty with Silicone Implants. Annals of Internal Medicine *111*, 377-383.

Wachem, v. (1987). Adhesion of cultured human endothelial cells onto methacrylate polymers with varying surface wettability and charge. Biomaterials *8*, 323-328.

Watson, P. A. (1991). Function follows form: generation of intracellular signals by cell deformation. FASEB *5*, 2013-2019.

Webb, D. S. A., Shimizu, Y., Seventer, G. A. V., Shaw, S., and Gerrard, T. L. (1990). LFA-3, CD44, and CD45: Physiologic Triggers of Human Monocyte TNF and IL-1 Release. Science *249*, 1295-1297.

Weller, P. F., Rand, T. H., Goelz, S. E., Chi-Rosso, G., and Lobb, R. R. (1991). Human eosinophil adherence to vasculr endothelium mediated by binding to vascular cell adhesion molecule 1 and endothelial leukocyte adhesion molecule 1. Proc. Natl. Acad. Sci. USA *88*, 7430-7433.

Williams, S. K., Carter, T., Park, P. K., Rose, D. G., Schneider, T., and Jarrell, B. E. (1992). Formation of a multilayer cellular lining on a polyurethane vascular graft following endothelial cell sodding. J. Biomed. Mater. Res. *26*, 103-117.

Williams, S. K., and Jarrell, B. E. (1996). Tissue-engineered vascular grafts. Nature Medicine *2*, 32-34.

Williams, S. K., Jarrell, B. E., and Kleinert, L. B. (1994). Endothelial cell transplantation onto polymeric ateriovenous grafts evaluated using a canine model. J. Invest. Surg. *7*, 503-517.

Williams, S. K., Jarrell, B. E., Rose, D. G., Pontell, J., Kapelan, B. A., Park, P. K., and Carter, T. L. (1989). Human Microvessel Endothelial Cell Isolation and Vascular Graft Sodding in the Operating Room. Ann. Vasc. Surg. *3*, 146-152.

Williams, S. K., Rose, D. G., and Jarrell, B. E. (1994). Microvascular endothelial cell sodding of ePTFE vascular grafts: Improved patency and stability of the cellular lining. J. Biomed. Mater. Res. *28*, 203-212.

Williams, S. K., Schneider, T., Kapelan, B., and Jarrell, B. E. (1991). Formation of a Functional Endothelium on Vascular Grafts. J. Electron Microscopy Tech. *19*, 439-451.

Winters, H. F. (1980). Elementary Processes at Solid Surfaces Immersed in Low Pressure Plasmas. Top. Curr. Chem. *94*, 69-125.

Winters, H. F., Chang, R. P. H., Mogab, C. J., Evans, J., Thorton, J. A., and Yasuda, H. (1985). Coatings and Surface Modification Using Low Pressure Non-Equilibrium Plasmas. Mater. Sci. and Eng. *70*, 53-77.

Wojciechowski, P. W., and Brash, J. L. (1993). Fibrinogen and albumin adsorption from human blood plasma and from buffer onto chemically functionalized silica substrates. Colloids and Surfaces B: Biointerfaces *1*, 107-117.

Yue, T.-L., Wang, X., Sung, C.-P., Olson, B., McKenna, P. J., Gu, J.-L., and Feuerstein, G. Z. (1994). Interleukin-8: A Mitogen and Chemoattractant for Vascular Smooth Muscle Cells. Circulation Res. *75*, 1-7.

Yun, J. K., DeFife, D., Colton, E., Stack, S., Azeez, A., Cahalan, L., Verhoeven, M., Cahalan, P., and Anderson, J. M. (1995). Human monocyte/macrophage adhesion and cytokine production on surface-modified poly(tetrafluoroethylene/hexafluoropropylene) polymers with and without protein adsorption. J. Biomed. Mater. Res. *29*, 257-268.

Zhao, Q. H., Anderson, J. M., Hiltner, A., Lodoen, G. A., and Payet, C. R. (1992). Theoretical analysis on cell size distribution and kinetics of foreign-body giant cell formation *in vivo* on polyurethane elastomers. J. Biomed. Mater. Res. *26*, 1019-1038.

Ziats, N. P., Miller, K. M., and Anderson, J. M. (1988). In vitro and in vivo interaction of cells with biomaterials. Biomaterials *9*, 5-13.

Appendix A: Cell Culture Materials and Reagents

Materials

Tubes: Corning 15 ml (#25310-15) and 50 ml (#25339-50)
Vacutainer tubes: 10 and 15 ml sodium heparin
(Becton Dickinson #6498 and #16938)
15ml "red top" Vacutainer tubes for serum collection (#6432)
T25 and T75 tissue culture flasks (Corning)
Welled plates:
12-well: Falcon 3043
24-well: Falcon 3047
96-well: Falcon 3072

Reagents

All reagents are sterile unless indicated.

Buffers

Phosphate buffered saline (Dulbecco's) w/o Ca^{+2}, Mg^{+2} (PBS);
Sigma #D-577
EDTA: (disodium EDTA) 100mM (100x); Fisher #7376
Sodium Heparin: diluted to 6000U/ml in PBS (100x); Gibco/BRL#15077-019
HEPES Buffer Solution (1M): Gibco/BRL #15630-080

Media

RPMI 1640 + l-glutamine + 25 mM HEPES; Gibco/BRL #22400-055
Iscove's Modified Dulbecco's Medium (IMDM), Gibco/BRL #12440-053
Fetal Bovine Serum (FBS): heat- inactivated; qualified; USA source; Gibco/BRL #16140-071
MEM Sodium Pyruvate 100mM (100x); Gibco BRL #11360-070
MEM Non-essential Amino Acids 10mM (100x);Gibco BRL #11140-050
Penicillin/Streptomycin (100x); Gibco/BRL #15140-122

Misc. Reagents

Endothelial Cell Growth Supplement (ECGS): Collaborative Biomedical Products #40006
Gelatin (2% solution): Sigma #G-1393
Trypsin/EDTA: Gibco/BRL #25300-054
Histopaque-1077: Sigma #H-8889

Stains

Trypan Blue Stain, 0.4%: Gibco/BRL, #15250-061. Diluted to 0.2% in PBS + 0.01% sodium azide added and 0.2μ filtered before use.
Turks Stain:
10mg Crystal Violet; Baker #F906-3
1.5 ml glacial acetic acid
48.5 ml dIH_2O.
Dissolve crystal violet in dIH_2O, add acetic acid, mix, 0.45um filter before use.

Appendix B: Messenger RNA Isolation from Whole Cell Lysates

Provided by Prof. Timothy Pohlman's Lab, 1993

Protocol

Solutions Needed (for details see (Chomczynski and Sacchi, 1987))

RNase-free water

Ice cold PBS

Solution D: 4 M guanidinium thiocyanate; 25 mM sodium citrate, pH 7; 0.5% sarcosyl; 0.1M 2-mercaptoethanol.

Sodium Acetate (NaAcO): 0.2 M in RNase-free water

Chloroform/Isoamyl Alcohol (49:1)

Isopropanol (2-propanol)

Phenol (nucleic acid grade), water saturated

70% Ethanol (EtOH)

Day 1

1) Place dish on ice, wash samples in wells with ice cold PBS, aspirate.
2) Sample is held on inside of a 15 mL polypropylene tube; 300 μl of Solution D is used to cover the sample. The sample is scraped on the side of the tube using a cell scraper trimmed to fit into the tube. Six samples are pooled for a total volume of 1.8 mL.
3) Add 180 μl 0.2 M Na acetate, mix by inverting.
4) Add 1.8 mL phenol, mix by inverting.
5) Add 360 μl chloroform/isoamyl alcohol solution.
6) Shake vigorously for 15 seconds, and place on ice for 15 minutes.

7) Centrifuge at 10K x g for 20 minutes at 4°C.

8) Transfer upper aqueous phase to a clean 15 mL tube, avoid collecting material at the interface (RNase-rich fraction is at the interface).

9) Add equal volume of isopropanol (2-propanol), mix gently.

10) Place in -20°C freezer overnight, or over the weekend if necessary.

Day 2

11) Centrifuge at 10K x g for 20 minutes at 4°C.

12) Carefully aspirate liquid away from pellet.

13) Dissolve RNA pellet in 300 μl Solution D, transfer to microfuge tube.

14) Add 300 μl isopropanol, and place in -20°C freezer for 1 hour.

15) Microcentrifuge at 10K x g for 15 minutes at 4°C.

16) Aspirate, wash pellet with 1 mL ice cold 70% ethanol. Vortex lightly to loosen pellet.

17) Microcentrifuge at 10K x g for 15 minutes at 4°C.

18) Optional washing step here: Aspirate, add 1 mL ice cold 95% EtOH. Microcentrifuge as in 17.

19) Aspirate all liquid from pellet, allow pellet to air dry.

20) Resuspend pellets in 20 μl H_2O. Add 2 μl of RNA to 1 mL H_2O for each sample to measure O.D. (260/280 nm) of solution for determination of RNA concentration as follows:

1 O.D. unit of ss RNA = 40 μg/mL
Purity: 260/280 = 2.0 for RNA, 1.8 for DNA.

(Maniatis et al., 1982)

Appendix C: IL-1ß Production by Human Monocytes Cultured on Silicone Implant Materials

Results from Chapter 6.4

The following graphs summarize the IL-1ß response of each donor over the 35 day period. Please note that these are semi-log plots.

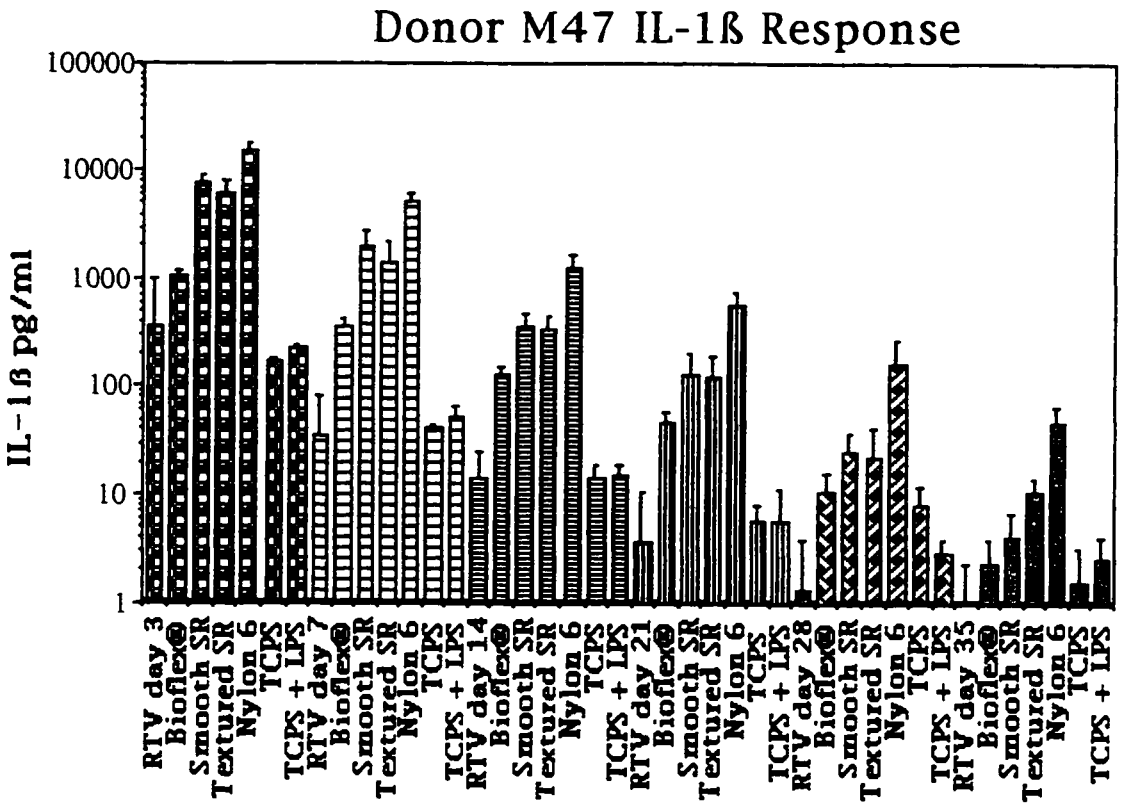

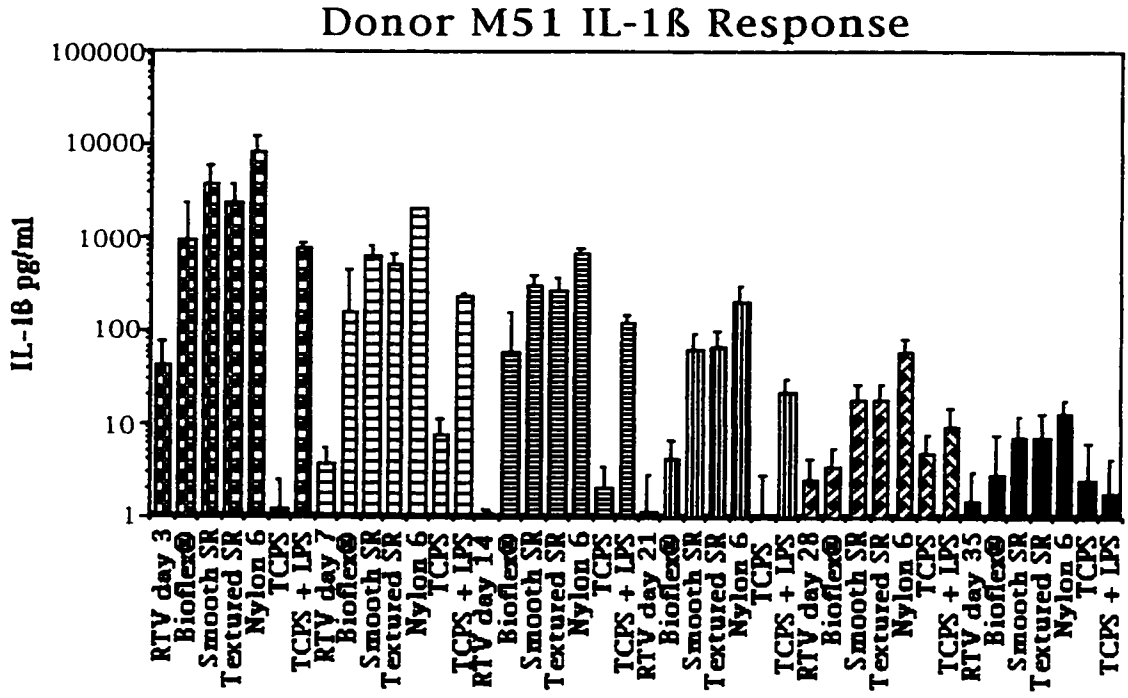
Donor M51 IL-1ß Response
IL-1ß pg/ml
100000
10000
1000
100
10
1
RTV day 3
Bioflex®
Smooth SR
Textured SR
Nylon 6
TCPS
TCPS + LPS
RTV day 7
Bioflex®
Smooth SR
Textured SR
Nylon 6
TCPS
TCPS + LPS
RTV day 14
Bioflex®
Smooth SR
Textured SR
Nylon 6
TCPS
TCPS + LPS
RTV day 21
Bioflex®
Smooth SR
Textured SR
Nylon 6
TCPS
TCPS + LPS
RTV day 28
Bioflex®
Smooth SR
Textured SR
Nylon 6
TCPS
TCPS + LPS
RTV day 35
Bioflex®
Smooth SR
Textured SR
Nylon 6
TCPS
TCPS + LPS

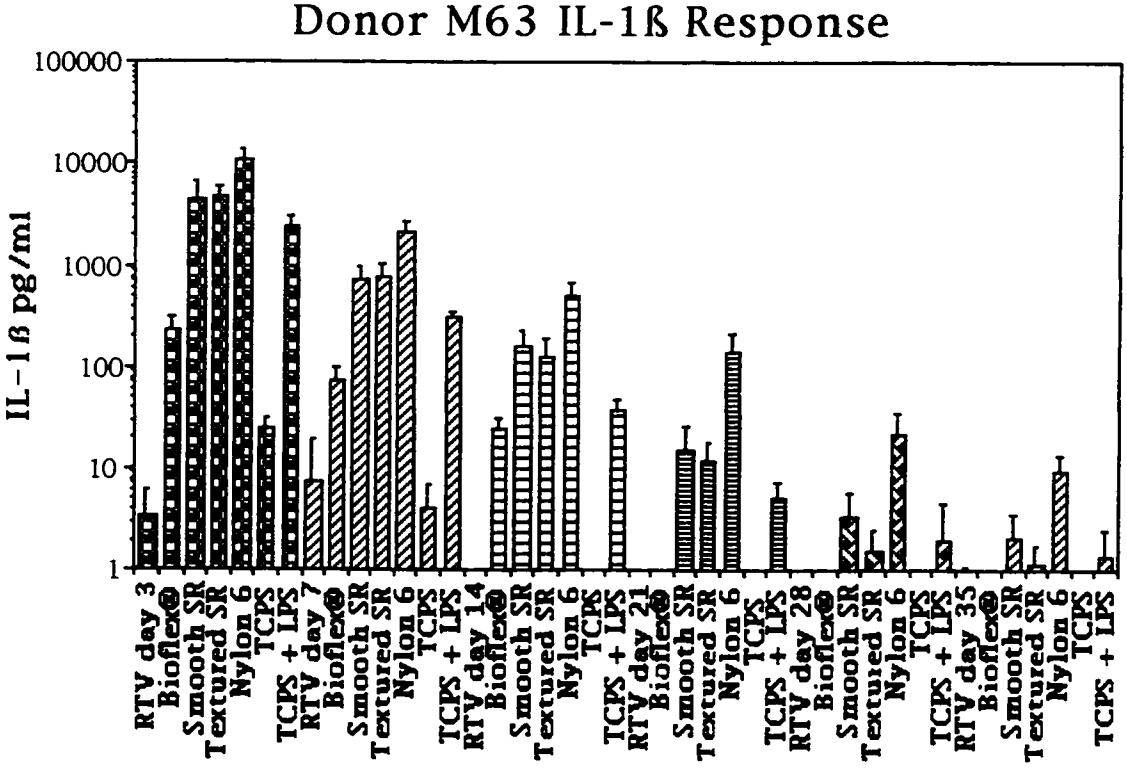
Donor M63 IL-1ß Response
IL-1ß pg/ml
100000
10000
1000
100
10
1
RTV day 3
Bioflex®
Smooth SR
Textured SR
Nylon 6
TCPS
TCPS + LPS
RTV day 7
Bioflex®
Smooth SR
Textured SR
Nylon 6
TCPS
TCPS + LPS
RTV day 14
Bioflex®
Smooth SR
Textured SR
Nylon 6
TCPS
TCPS + LPS
RTV day 21
Bioflex®
Smooth SR
Textured SR
Nylon 6
TCPS
TCPS + LPS
RTV day 28
Bioflex®
Smooth SR
Textured SR
Nylon 6
TCPS
TCPS + LPS
RTV day 35
Bioflex®
Smooth SR
Textured SR
Nylon 6
TCPS
TCPS + LPS

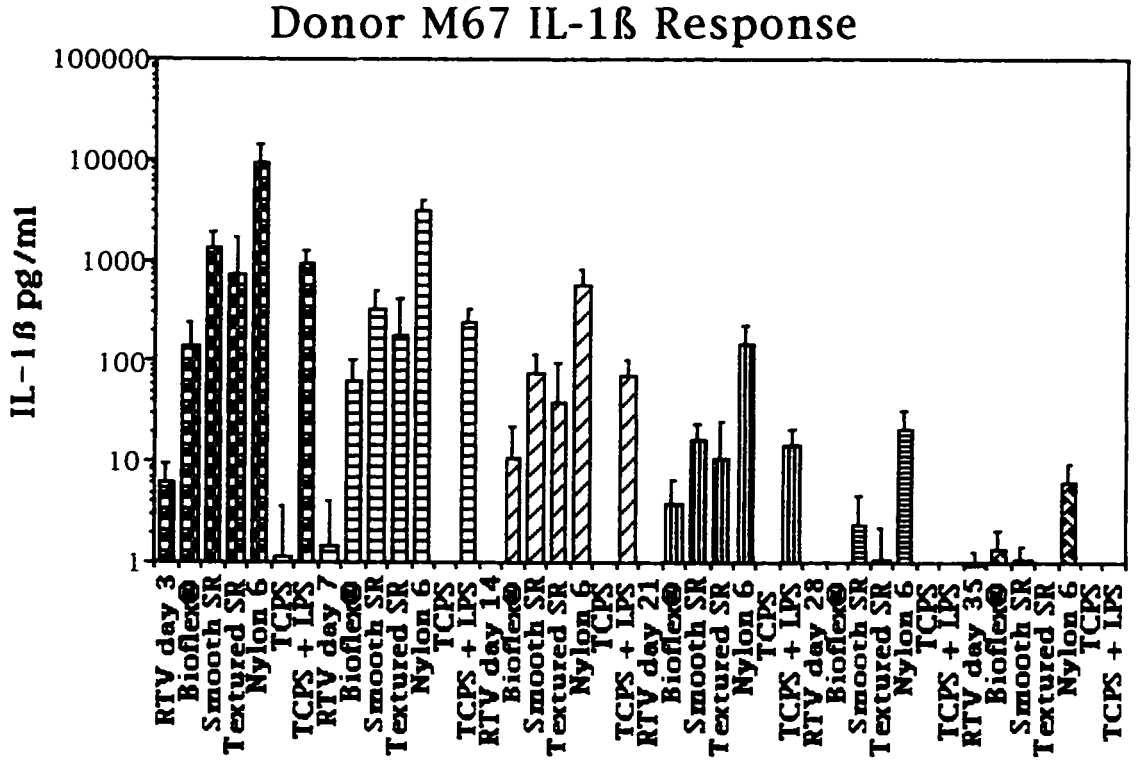
Donor M67 IL-1ß Response
IL-1ß pg/ml
100000
10000
1000
100
10
1
RTV day 3
Bioflex®
Smooth SR
Textured SR
Nylon 6
TCPS
TCPS + LPS
RTV day 7
Bioflex®
Smooth SR
Textured SR
Nylon 6
TCPS
TCPS + LPS
RTV day 14
Bioflex®
Smooth SR
Textured SR
Nylon 6
TCPS
TCPS + LPS
RTV day 21
Bioflex®
Smooth SR
Textured SR
Nylon 6
TCPS
TCPS + LPS
RTV day 28
Bioflex®
Smooth SR
Textured SR
Nylon 6
TCPS
TCPS + LPS
RTV day 35
Bioflex®
Smooth SR
Textured SR
Nylon 6
TCPS
TCPS + LPS

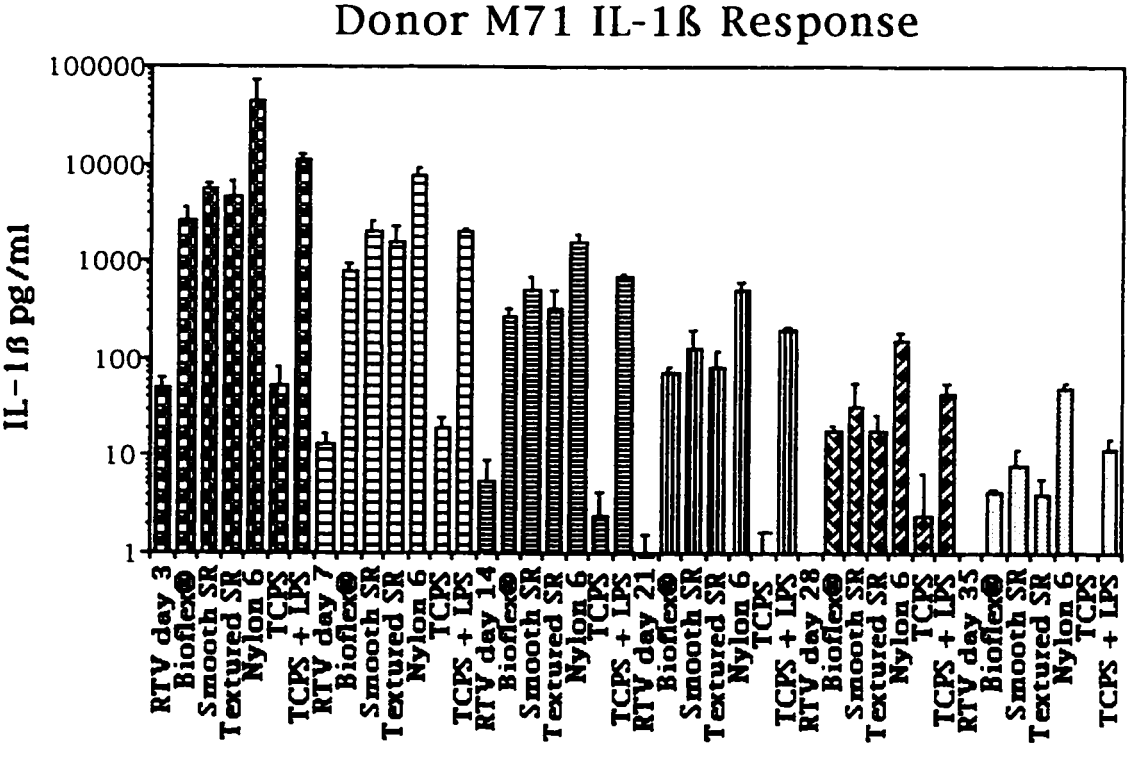
Donor M71 IL-1ß Response
IL-1ß pg/ml
100000
10000
1000
100
10
1
RTV day 3
Bioflex®
Smooth SR
Textured SR
Nylon 6
TCPS
TCPS + LPS
RTV day 7
Bioflex®
Smooth SR
Textured SR
Nylon 6
TCPS
TCPS + LPS
RTV day 14
Bioflex®
Smooth SR
Textured SR
Nylon 6
TCPS
TCPS + LPS
RTV day 21
Bioflex®
Smooth SR
Textured SR
Nylon 6
TCPS
TCPS + LPS
RTV day 28
Bioflex®
Smooth SR
Textured SR
Nylon 6
TCPS
TCPS + LPS
RTV day 35
Bioflex®
Smooth SR
Textured SR
Nylon 6
TCPS
TCPS + LPS

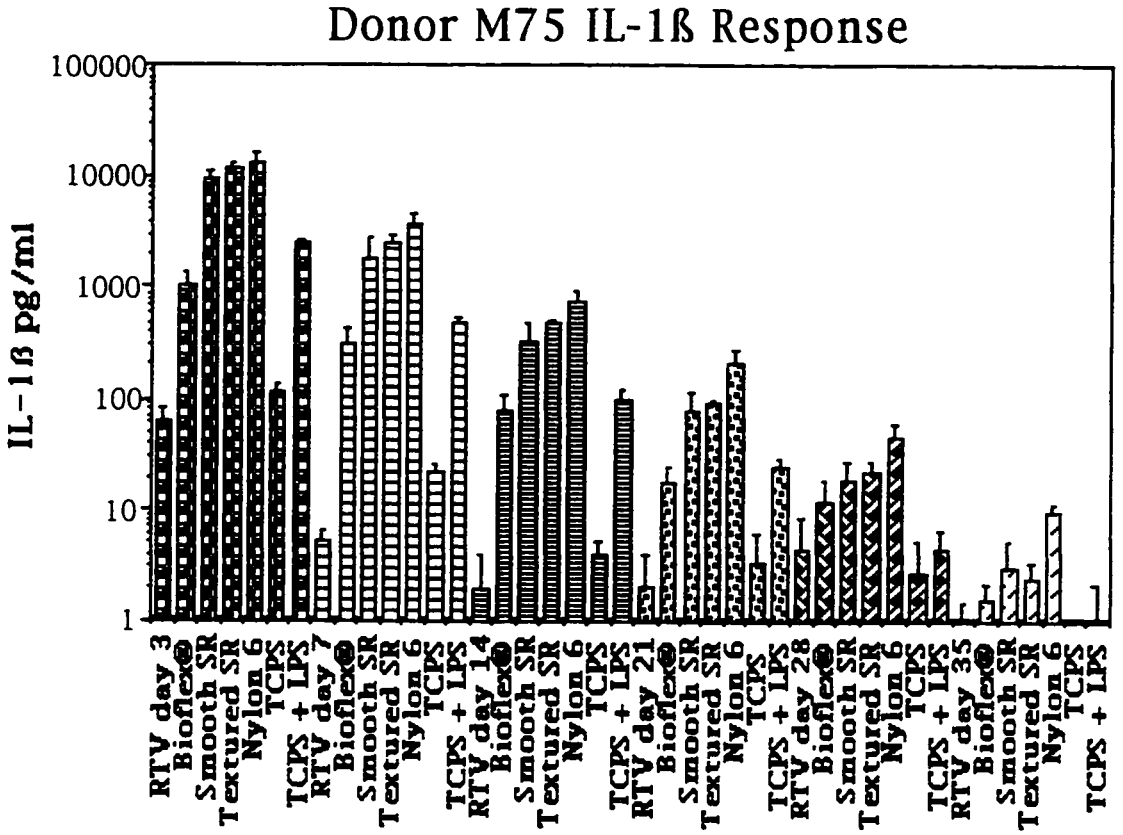
Donor M75 IL-1ß Response
IL-1ß pg/ml
100000
10000
1000
100
10
1
RTV day 3
Bioflex®
Smooth SR
Textured SR
Nylon 6
TCPS
TCPS + LPS
RTV day 7
Bioflex®
Smooth SR
Textured SR
Nylon 6
TCPS
TCPS + LPS
RTV day 14
Bioflex®
Smooth SR
Textured SR
Nylon 6
TCPS
TCPS + LPS
RTV day 21
Bioflex®
Smooth SR
Textured SR
Nylon 6
TCPS
TCPS + LPS
RTV day 28
Bioflex®
Smooth SR
Textured SR
Nylon 6
TCPS
TCPS + LPS
RTV day 35
Bioflex®
Smooth SR
Textured SR
Nylon 6
TCPS
TCPS + LPS

Appendix D

Macrophage IL-1ß, TNFα, and IL-8 Production: By Donor

Donor #1

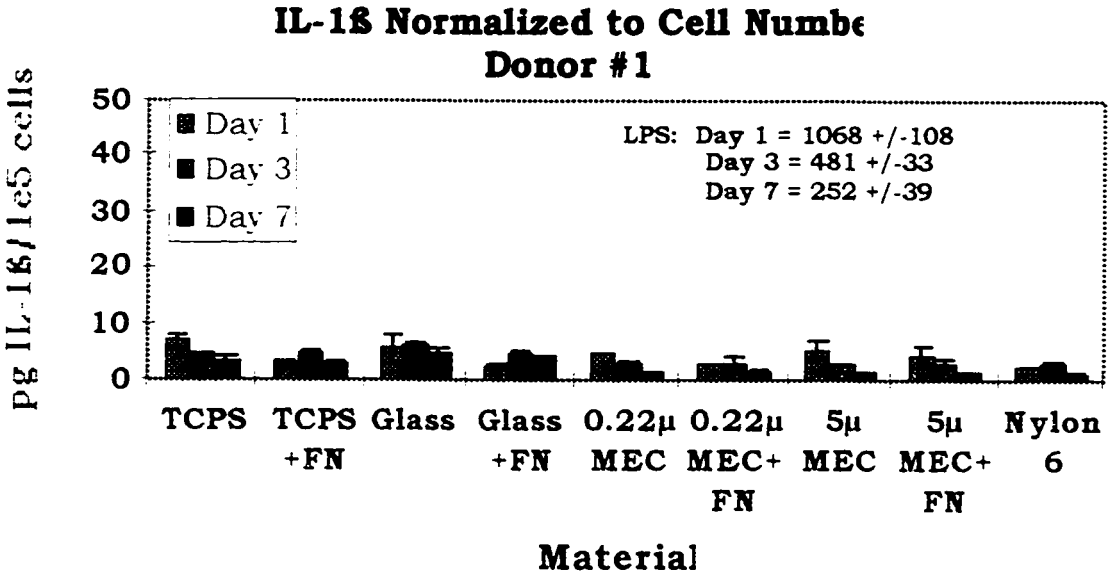

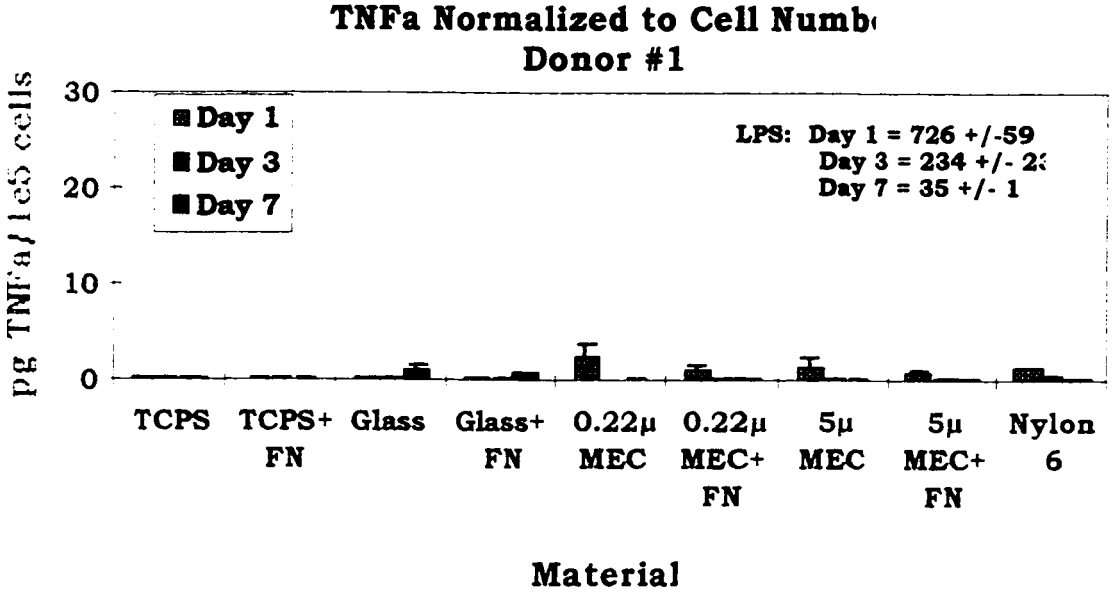

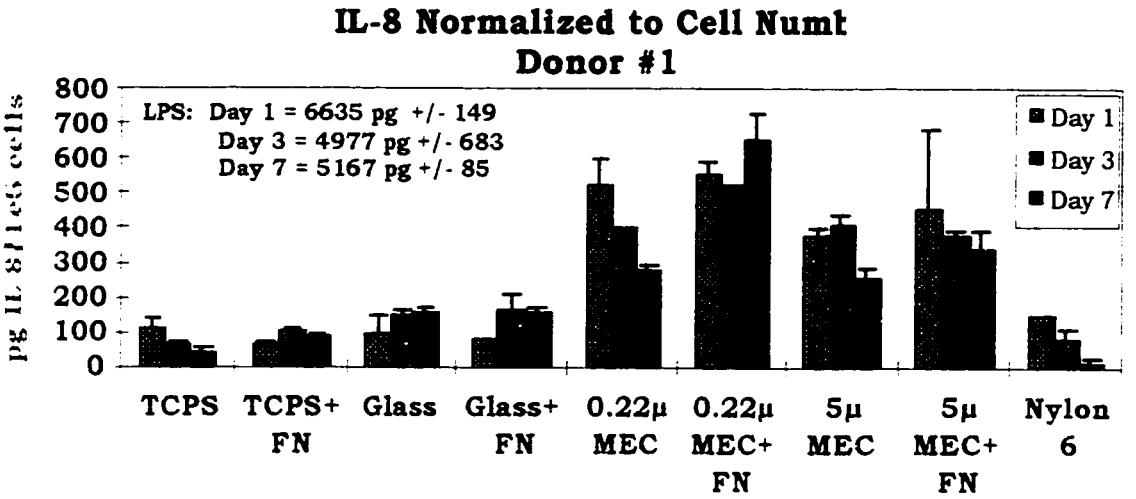
IL-8 Normalized to Cell Numt
Donor #1
pg IL-8/1e5 cells
800
700
600
500
400
300
200
100
0
LPS: Day 1 = 6635 pg +/- 149
Day 3 = 4977 pg +/- 683
Day 7 = 5167 pg +/- 85
Day 1
Day 3
Day 7
TCPS
TCPS+ FN
Glass
Glass+ FN
0.22µ MEC
0.22µ MEC+ FN
5µ MEC
5µ MEC+ FN
Nylon 6

Donor #2

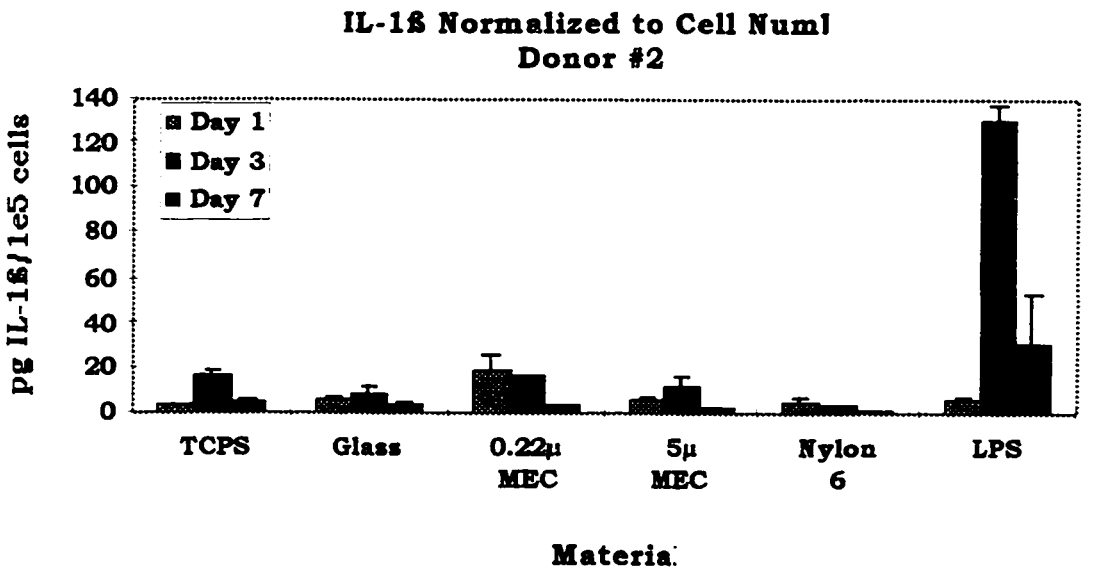
IL-1ß Normalized to Cell Numl
Donor #2
pg IL-1ß/1e5 cells
140
120
100
80
60
40
20
0
Day 1
Day 3
Day 7
TCPS
Glass
0.22µ MEC
5µ MEC
Nylon 6
LPS
Materia

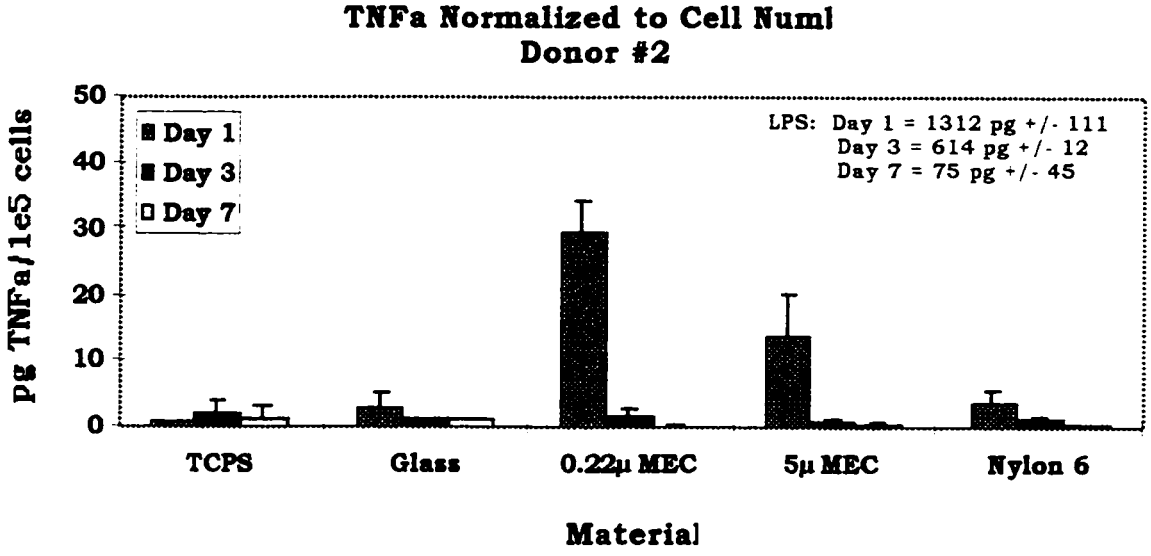
TNFa Normalized to Cell Numl
Donor #2
pg TNFa/1e5 cells
50
40
30
20
10
0
Day 1
Day 3
Day 7
LPS: Day 1 = 1312 pg +/- 111
Day 3 = 614 pg +/- 12
Day 7 = 75 pg +/- 45
TCPS
Glass
0.22μ MEC
5μ MEC
Nylon 6
Material

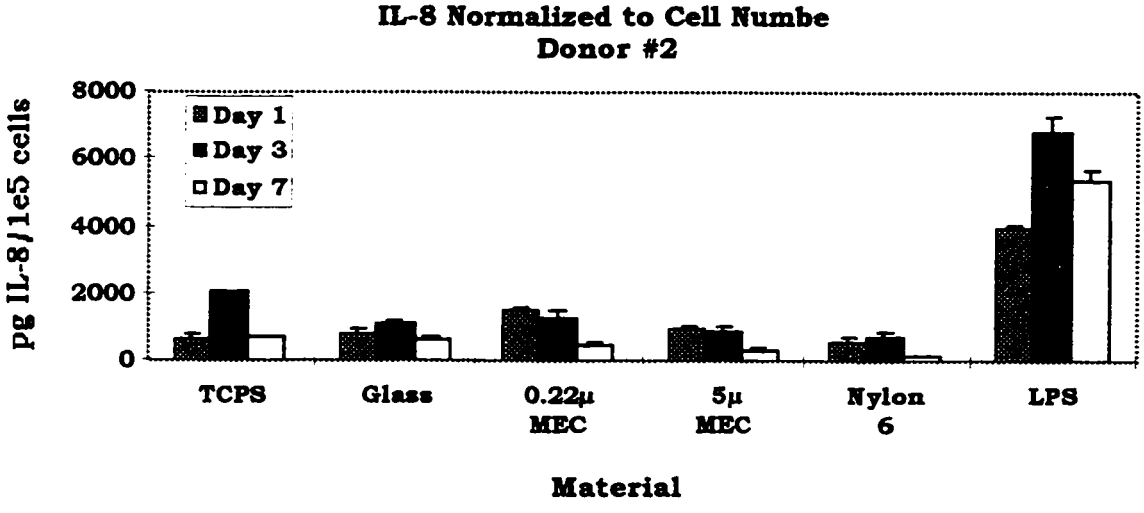
IL-8 Normalized to Cell Numbe
Donor #2
pg IL-8/1e5 cells
8000
6000
4000
2000
0
Day 1
Day 3
Day 7
TCPS
Glass
0.22μ MEC
5μ MEC
Nylon 6
LPS
Material

Donor #3

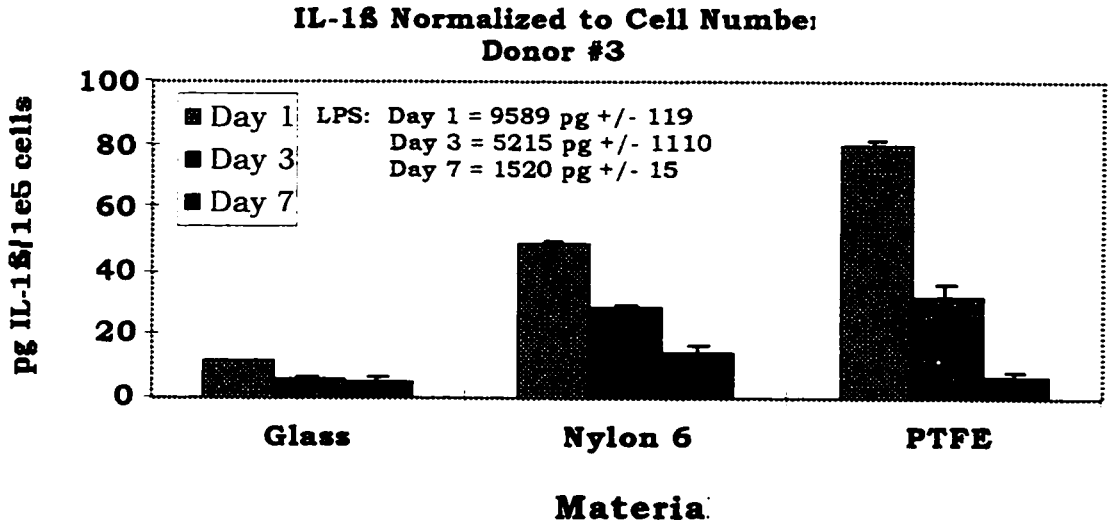
IL-1ß Normalized to Cell Numbe
Donor #3
pg IL-1ß/1e5 cells
100
80
60
40
20
0
Day 1
Day 3
Day 7
LPS: Day 1 = 9589 pg +/- 119
Day 3 = 5215 pg +/- 1110
Day 7 = 1520 pg +/- 15
Glass
Nylon 6
PTFE
Materia

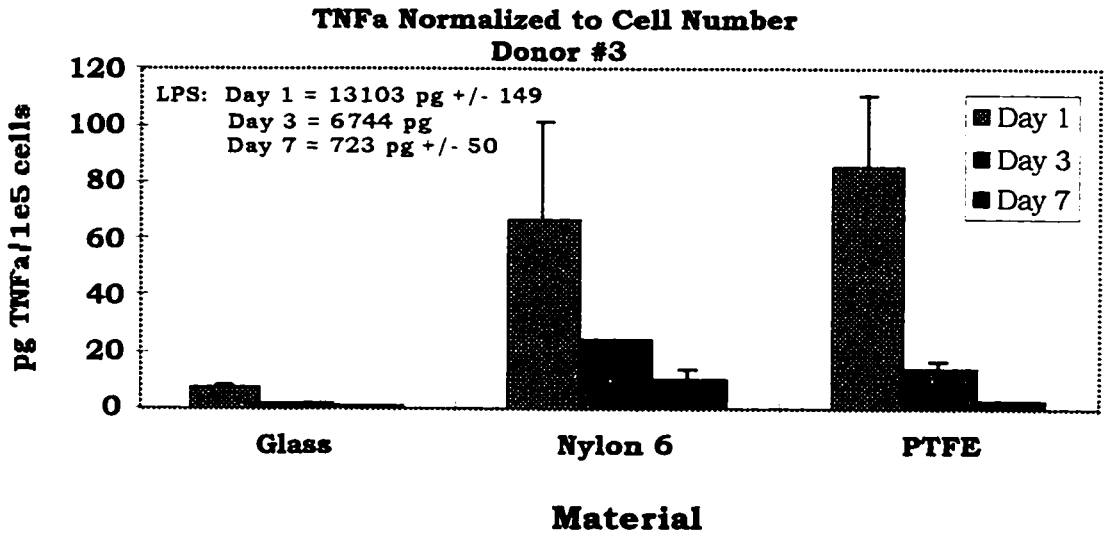
TNFa Normalized to Cell Number
Donor #3
pg TNFa/1e5 cells
120
100
80
60
40
20
0
LPS: Day 1 = 13103 pg +/- 149
Day 3 = 6744 pg
Day 7 = 723 pg +/- 50
Day 1
Day 3
Day 7
Glass
Nylon 6
PTFE
Material

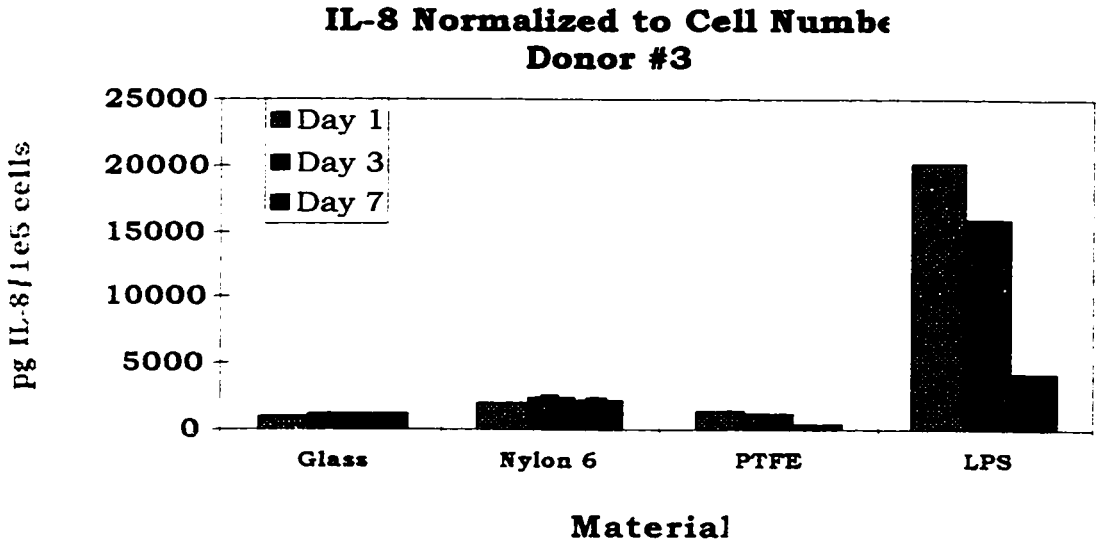
IL-8 Normalized to Cell Numbe
Donor #3
pg IL-8/1e5 cells
25000
20000
15000
10000
5000
0
Day 1
Day 3
Day 7
Glass
Nylon 6
PTFE
LPS
Material

Donor #4

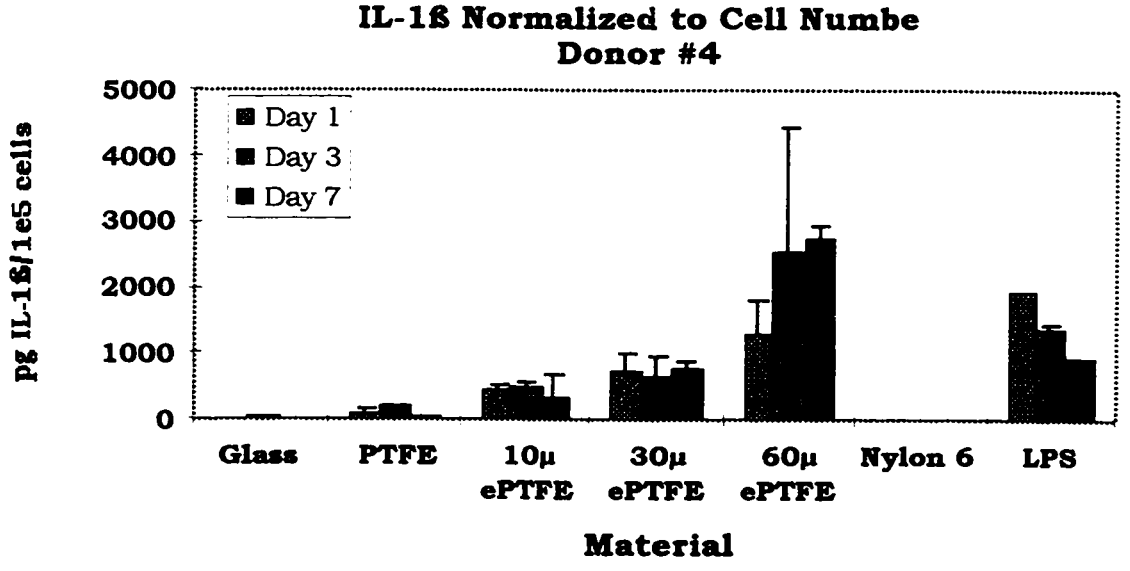
IL-1ß Normalized to Cell Numbe
Donor #4
pg IL-1ß/1e5 cells
5000
4000
3000
2000
1000
0
Day 1
Day 3
Day 7
Glass
PTFE
10µ ePTFE
30µ ePTFE
60µ ePTFE
Nylon 6
LPS
Material

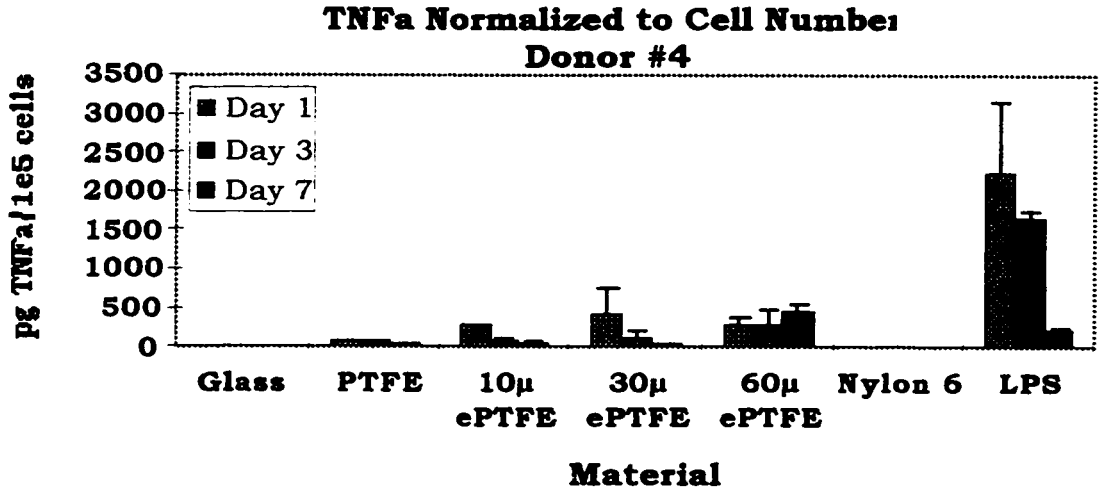
TNFa Normalized to Cell Numbe:
Donor #4
pg TNFa/1e5 cells
3500
3000
2500
2000
1500
1000
500
0
Day 1
Day 3
Day 7
Glass
PTFE
10µ ePTFE
30µ ePTFE
60µ ePTFE
Nylon 6
LPS
Material

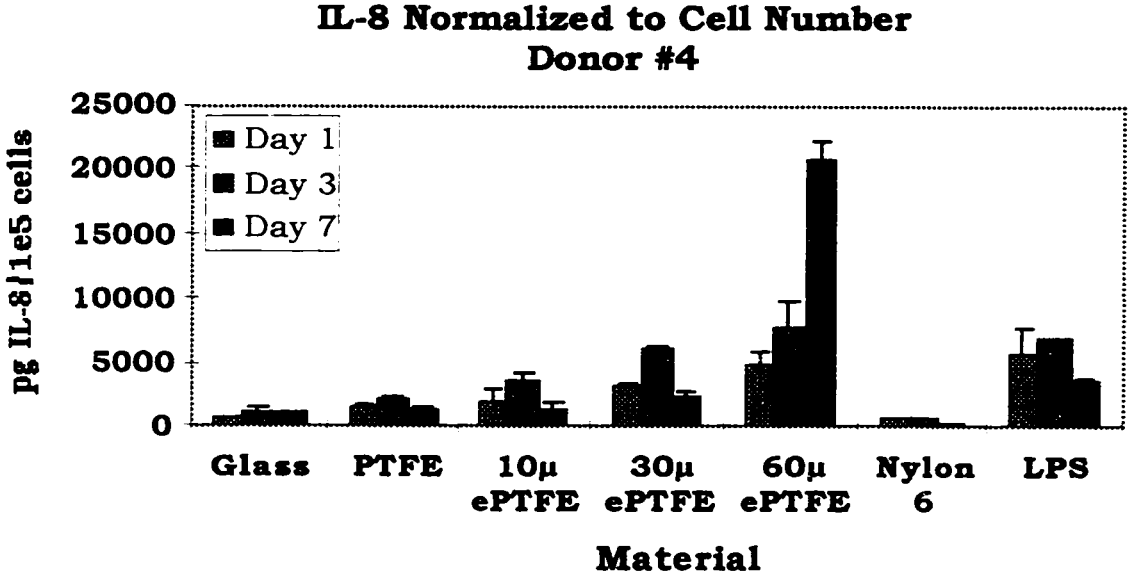
IL-8 Normalized to Cell Number
Donor #4
pg IL-8/1e5 cells
25000
20000
15000
10000
5000
0
Day 1
Day 3
Day 7
Glass
PTFE
10µ ePTFE
30µ ePTFE
60µ ePTFE
Nylon 6
LPS
Material

Donor #6

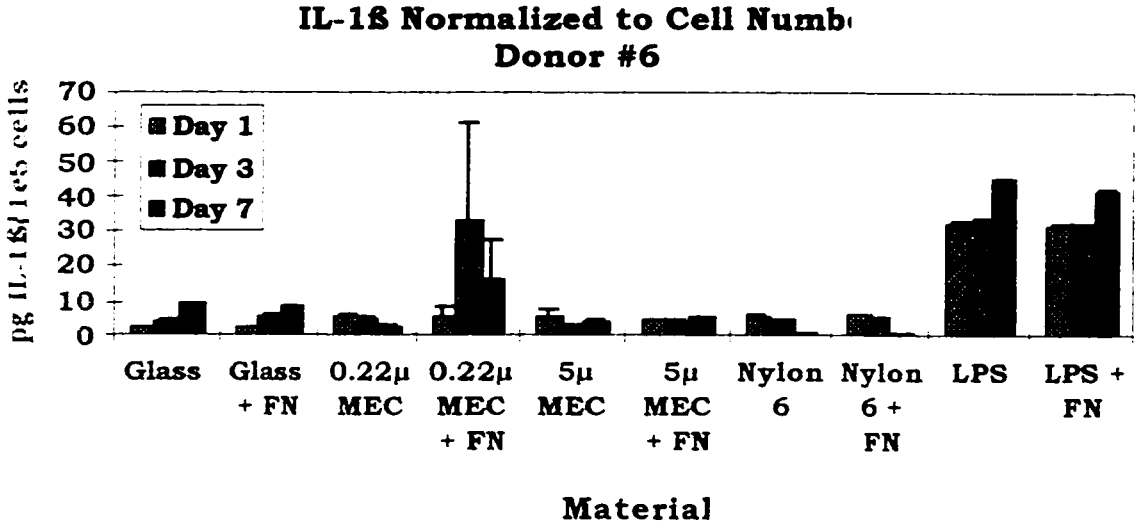
IL-1ß Normalized to Cell Numb
Donor #6
pg IL-1ß/1e5 cells
70
60
50
40
30
20
10
0
Day 1
Day 3
Day 7
Glass
Glass + FN
0.22µ MEC
0.22µ MEC + FN
5µ MEC
5µ MEC + FN
Nylon 6
Nylon 6 + FN
LPS
LPS + FN
Material

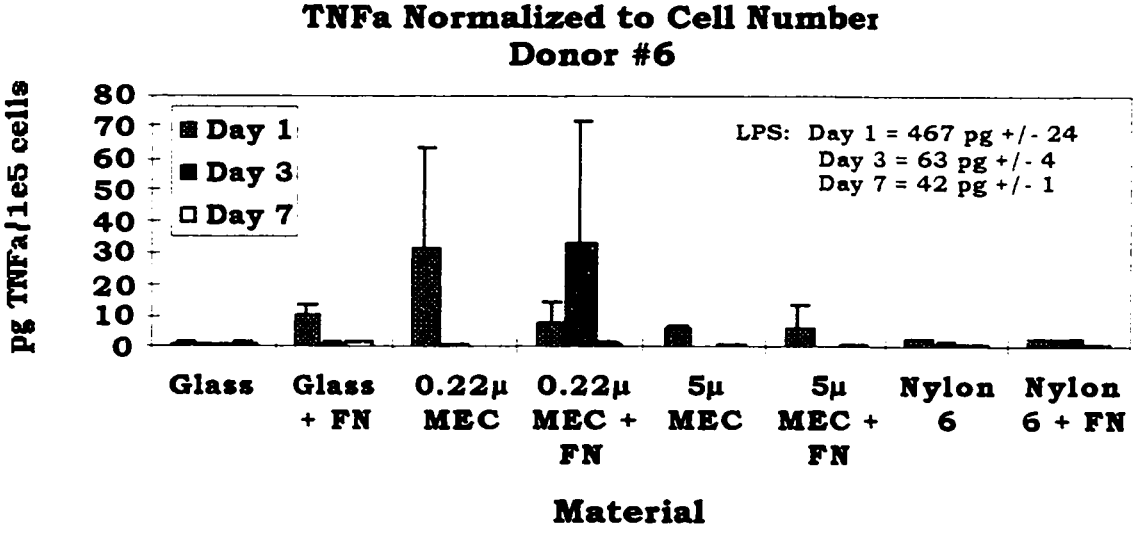
TNFa Normalized to Cell Number
Donor #6
pg TNFa/1e5 cells
80
70
60
50
40
30
20
10
0
Day 1
Day 3
Day 7
LPS: Day 1 = 467 pg +/- 24
Day 3 = 63 pg +/- 4
Day 7 = 42 pg +/- 1
Glass
Glass + FN
0.22µ MEC
0.22µ MEC + FN
5µ MEC
5µ MEC + FN
Nylon 6
Nylon 6 + FN
Material

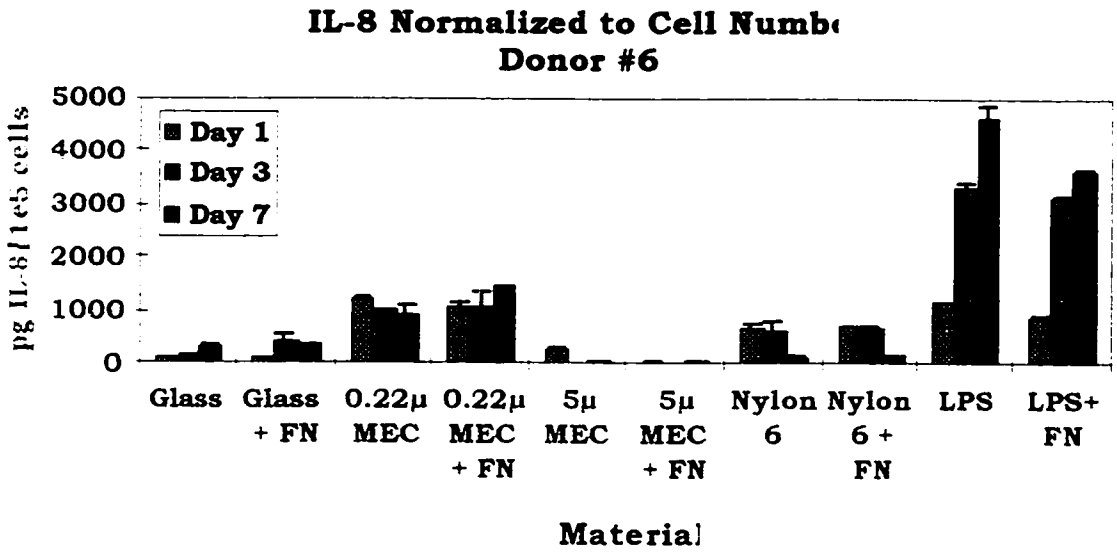
IL-8 Normalized to Cell Numbe
Donor #6
pg IL-8/1e5 cells
5000
4000
3000
2000
1000
0
Day 1
Day 3
Day 7
Glass
Glass + FN
0.22µ MEC
0.22µ MEC + FN
5µ MEC
5µ MEC + FN
Nylon 6
Nylon 6 + FN
LPS
LPS+ FN
Material

Donor #7

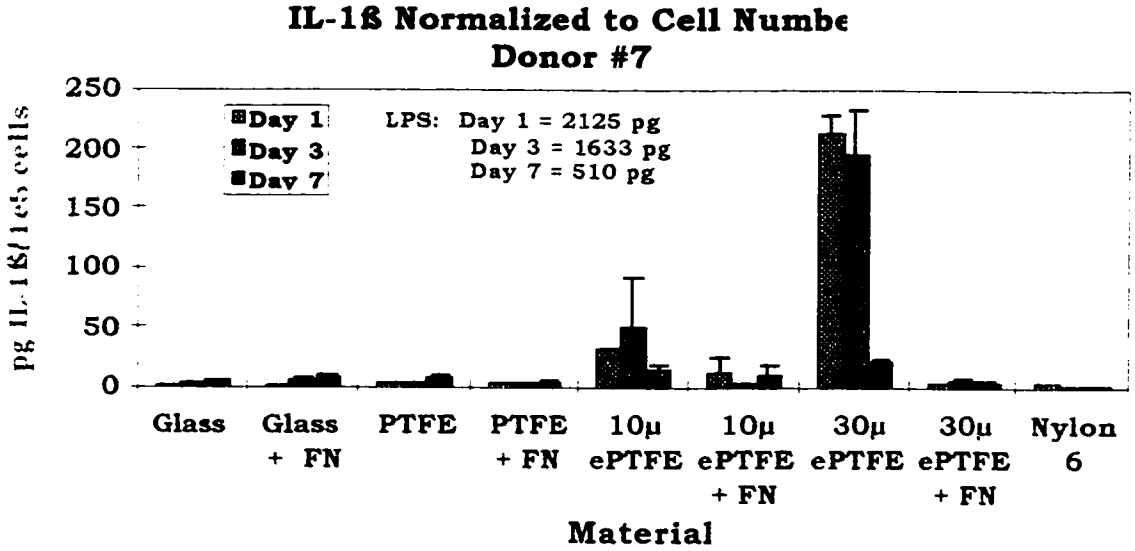
IL-1ß Normalized to Cell Numbe
Donor #7
pg IL-1ß/1e5 cells
250
200
150
100
50
0
Day 1
Day 3
Day 7
LPS: Day 1 = 2125 pg
Day 3 = 1633 pg
Day 7 = 510 pg
Glass
Glass + FN
PTFE
PTFE + FN
10µ ePTFE
10µ ePTFE + FN
30µ ePTFE
30µ ePTFE + FN
Nylon 6
Material

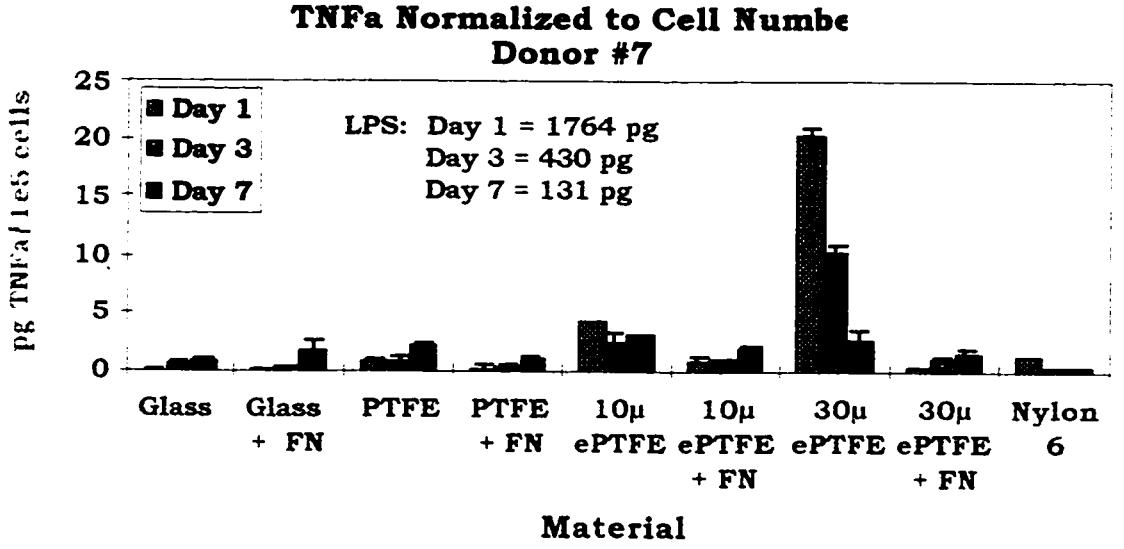
TNFa Normalized to Cell Numbe
Donor #7
pg TNFa/1e5 cells
25
20
15
10
5
0
Day 1
Day 3
Day 7
LPS: Day 1 = 1764 pg
Day 3 = 430 pg
Day 7 = 131 pg
Glass
Glass + FN
PTFE
PTFE + FN
10µ ePTFE
10µ ePTFE + FN
30µ ePTFE
30µ ePTFE + FN
Nylon 6
Material

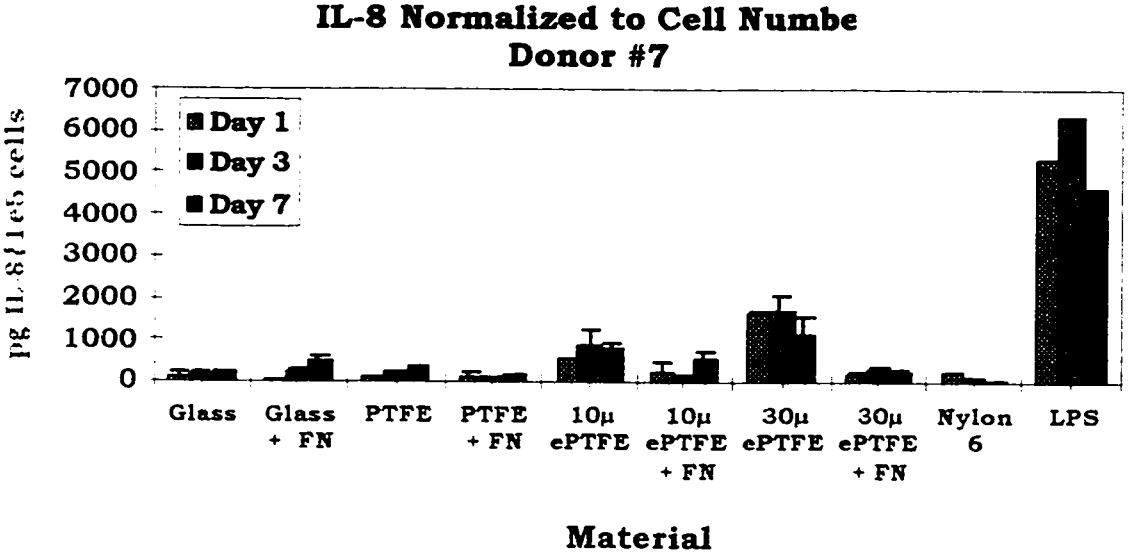
IL-8 Normalized to Cell Numbe
Donor #7
pg IL-8/1e5 cells
7000
6000
5000
4000
3000
2000
1000
0
Day 1
Day 3
Day 7
Glass
Glass + FN
PTFE
PTFE + FN
10µ ePTFE
10µ ePTFE + FN
30µ ePTFE
30µ ePTFE + FN
Nylon 6
LPS
Material

Donor #8

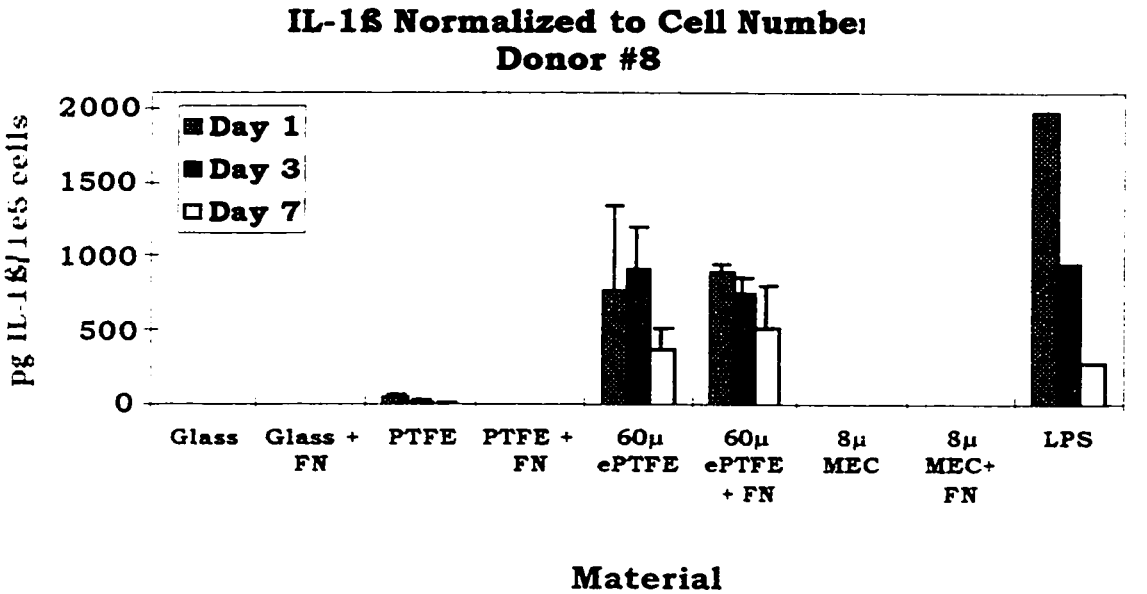
IL-1ß Normalized to Cell Numbe
Donor #8
pg IL-1ß/1e5 cells
2000
1500
1000
500
0
Day 1
Day 3
Day 7
Glass
Glass + FN
PTFE
PTFE + FN
60µ ePTFE
60µ ePTFE + FN
8µ MEC
8µ MEC+ FN
LPS
Material

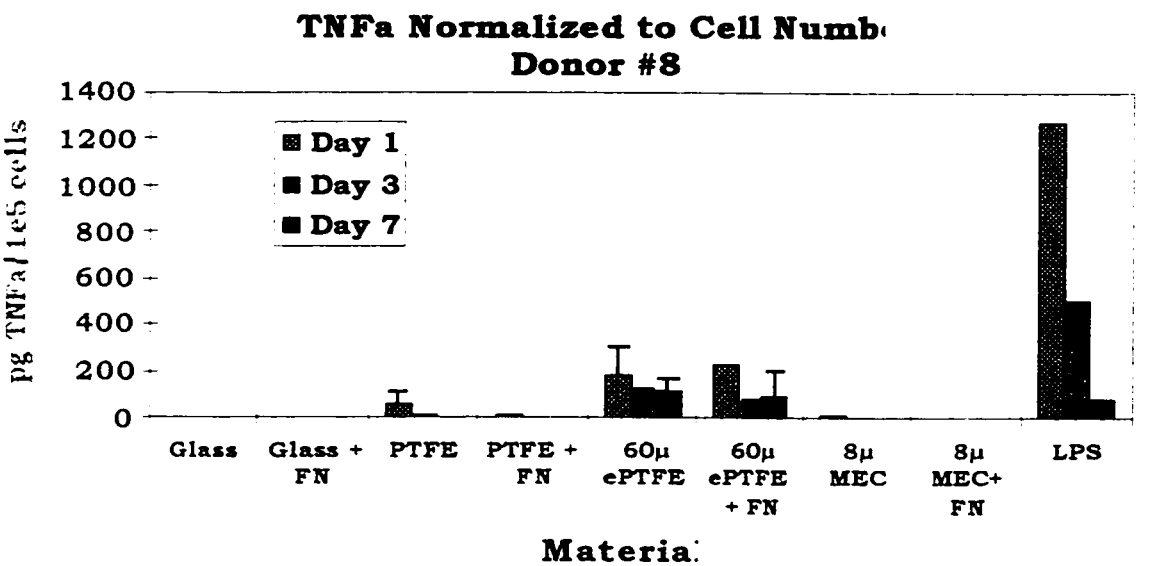
TNFa Normalized to Cell Numb
Donor #8
pg TNFa/1e5 cells
1400
1200
1000
800
600
400
200
0
Day 1
Day 3
Day 7
Glass
Glass + FN
PTFE
PTFE + FN
60µ ePTFE
60µ ePTFE + FN
8µ MEC
8µ MEC+ FN
LPS
Materia

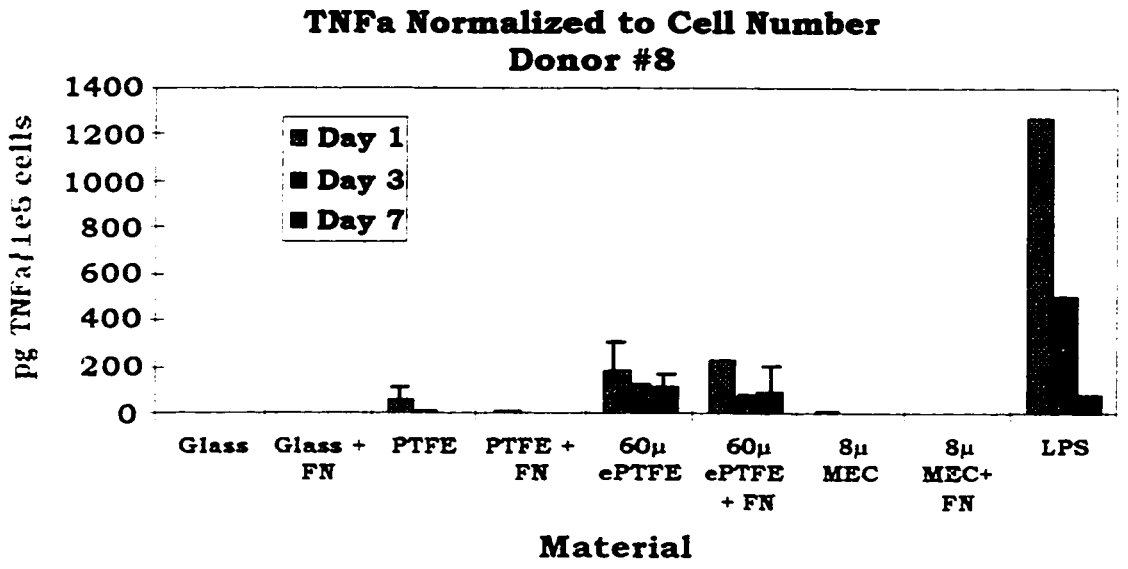
TNFa Normalized to Cell Number
Donor #8
pg TNFa/1e5 cells
1400
1200
1000
800
600
400
200
0
Day 1
Day 3
Day 7
Glass
Glass + FN
PTFE
PTFE + FN
60µ ePTFE
60µ ePTFE + FN
8µ MEC
8µ MEC+ FN
LPS
Material

Donor #9

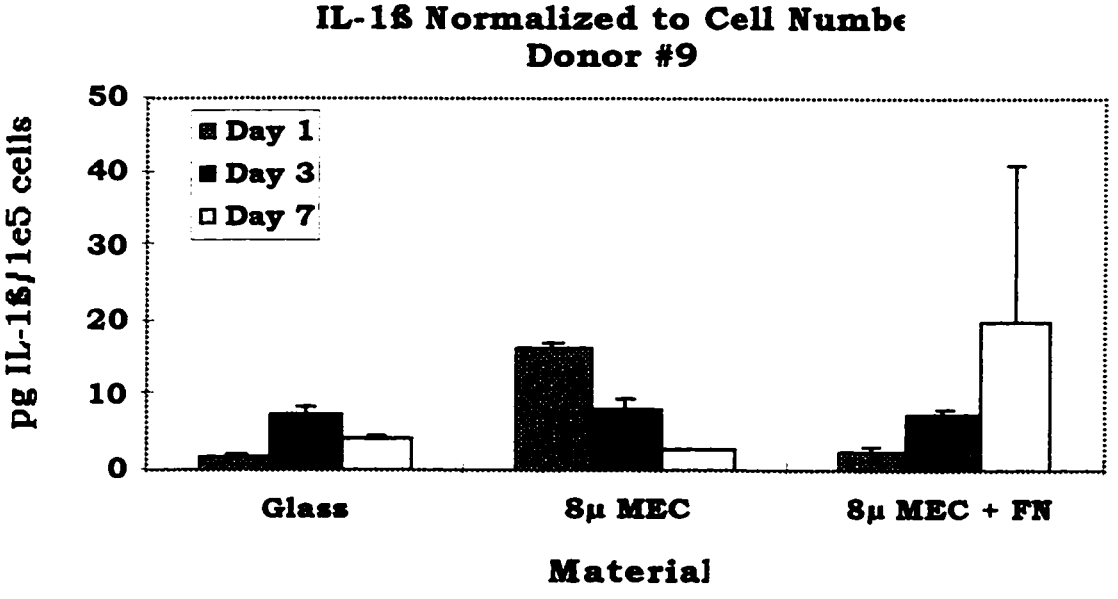
IL-1ß Normalized to Cell Numbe
Donor #9
pg IL-1ß/1e5 cells
50
40
30
20
10
0
Day 1
Day 3
Day 7
Glass
8µ MEC
8µ MEC + FN
Material

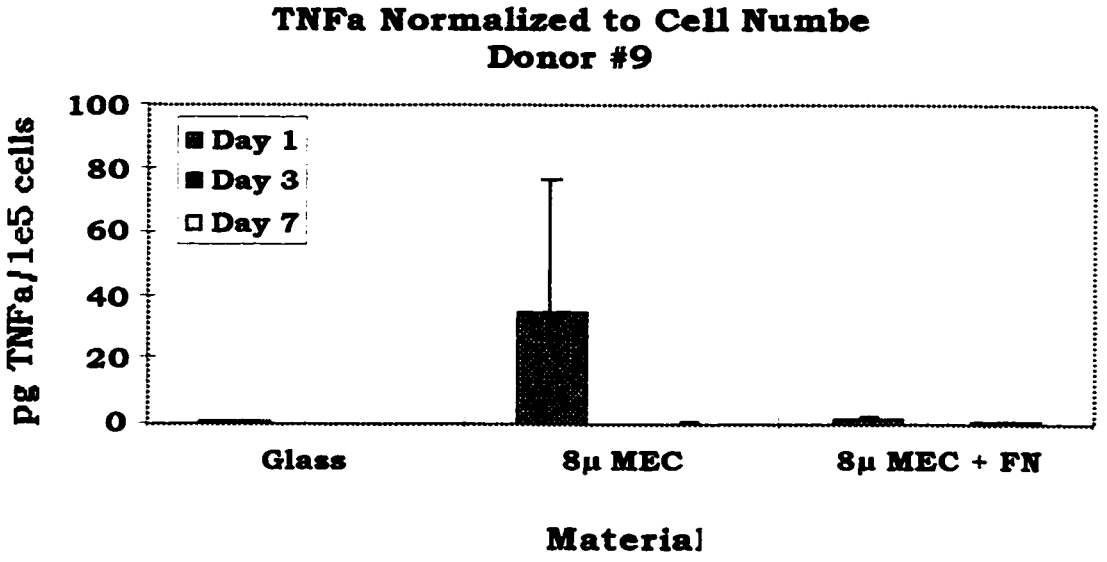
TNFa Normalized to Cell Numbe
Donor #9
pg TNFa/1e5 cells
100
80
60
40
20
0
Day 1
Day 3
Day 7
Glass
8μ MEC
8μ MEC + FN
Material

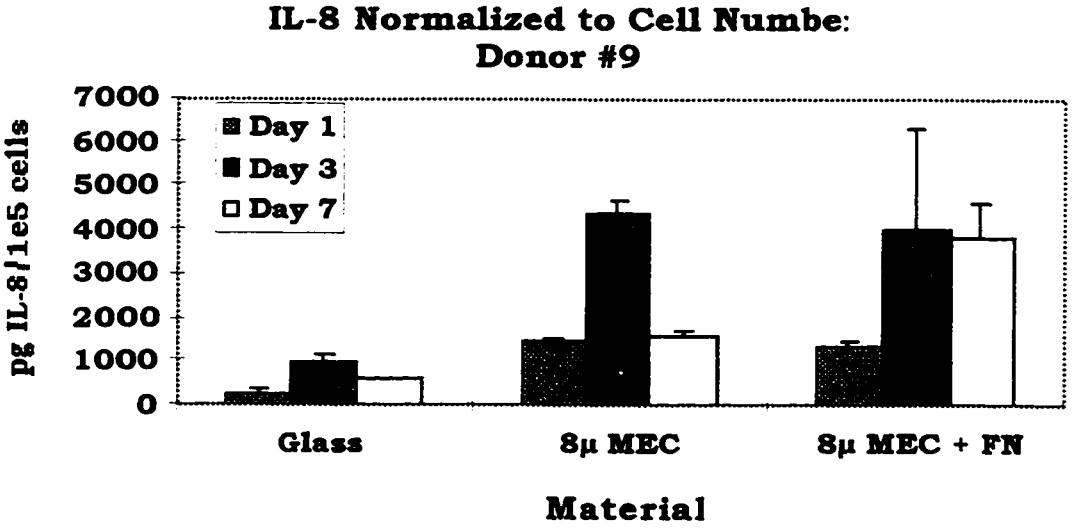
IL-8 Normalized to Cell Numbe:
Donor #9
pg IL-8/1e5 cells
7000
6000
5000
4000
3000
2000
1000
0
Day 1
Day 3
Day 7
Glass
8μ MEC
8μ MEC + FN
Material

Donor #10

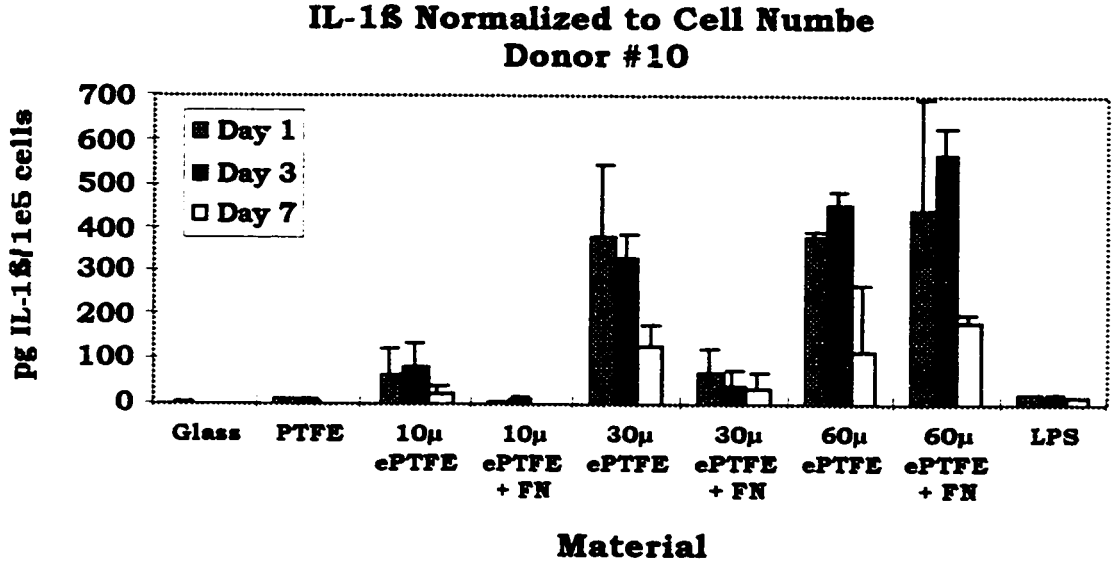
IL-1ß Normalized to Cell Numbe
Donor #10
pg IL-1ß/1e5 cells
700
600
500
400
300
200
100
0
Day 1
Day 3
Day 7
Glass
PTFE
10µ ePTFE
10µ ePTFE + FN
30µ ePTFE
30µ ePTFE + FN
60µ ePTFE
60µ ePTFE + FN
LPS
Material

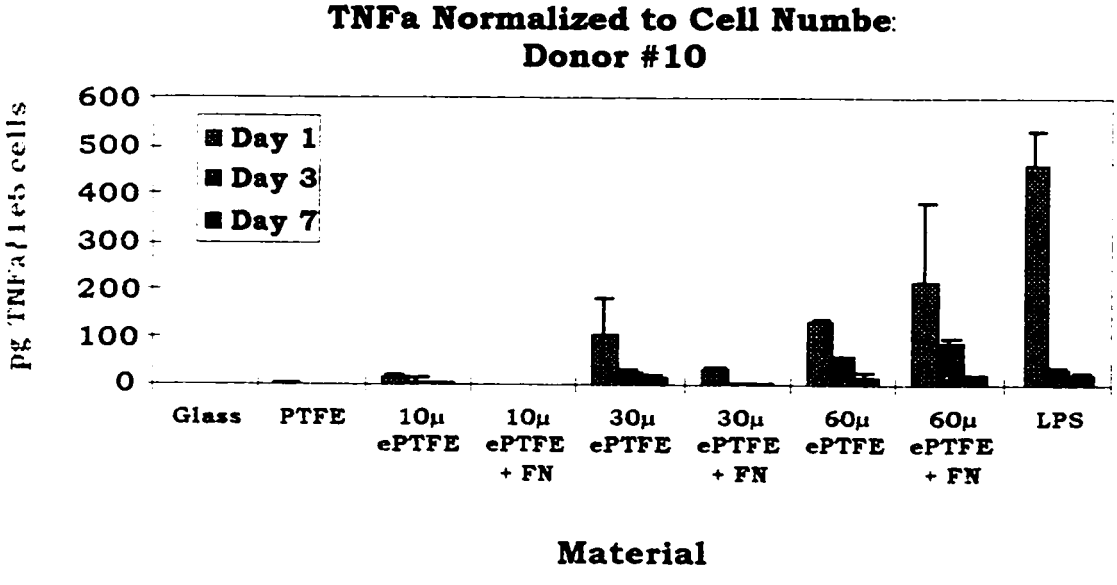
TNFa Normalized to Cell Numbe:
Donor #10
pg TNFa/1e5 cells
600
500
400
300
200
100
0
Day 1
Day 3
Day 7
Glass
PTFE
10µ ePTFE
10µ ePTFE + FN
30µ ePTFE
30µ ePTFE + FN
60µ ePTFE
60µ ePTFE + FN
LPS
Material

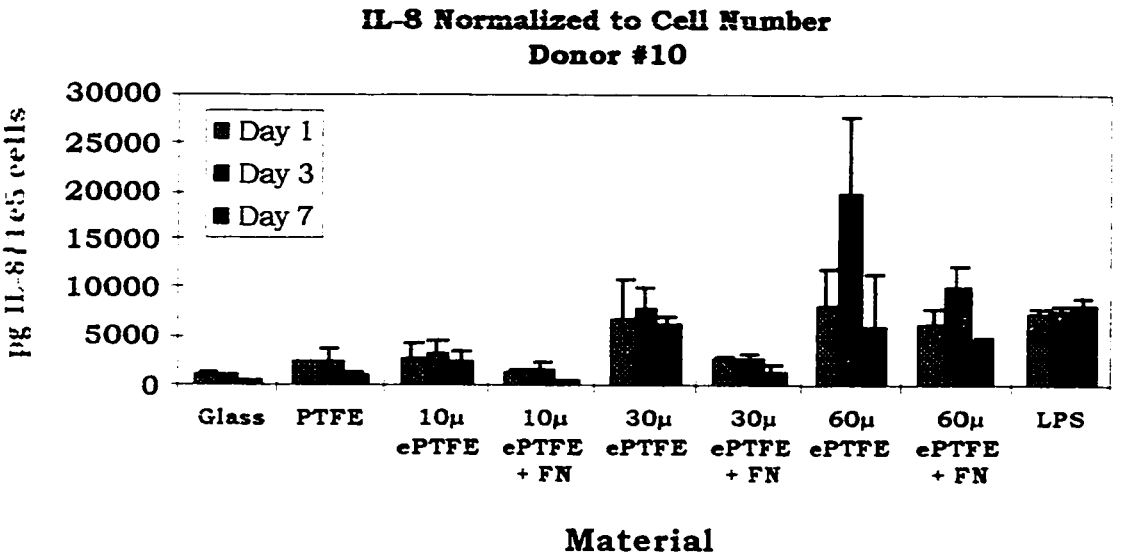
IL-8 Normalized to Cell Number
Donor #10
pg IL-8/1e5 cells
30000
25000
20000
15000
10000
5000
0
Day 1
Day 3
Day 7
Glass
PTFE
10µ ePTFE
10µ ePTFE + FN
30µ ePTFE
30µ ePTFE + FN
60µ ePTFE
60µ ePTFE + FN
LPS
Material

VITA

Ann E. Schmierer
University of Washington
1998

Date and Place of Birth:

April 22, 1960, Everett, Washington

Education:

1998: Doctor of Philosophy, Department of Bioengineering, University of Washington, Seattle, Washington

1983: Bachelor of Science Degree, Combined Major in Chemistry and Biology, Western Washington University, Bellingham, Washington

1981: Associate Arts and Sciences Degree, Edmonds Community College, Lynnwood, Washington

1978: High School Diploma, Cascade High School, Everett, Washington

Work Experience:

1984-1990: Senior Research Assistant, Experimental Hematology, Immunex Corporation, Seattle, Washington

Invention Disclosure:

A Synthetic Polymer that Permits Cell Growth, 1993, Buddy D. Ratner and Ann Schmierer, University of Washington.

Abstracts:

AE Schmierer, TH Pohlman, and BD Ratner, Endothelial Cell Activation on Biomaterials: Expression of the Inflammatory Marker E-Selectin. Fifth World Biomaterials Congress, May 29-June 2, 1996.

Ann E. Schmierer, Buddy D. Ratner, and Marcel Jozefowicz, Protein Adsorption to Plasma-Deposited Films: Scatchard Analysis and Cell Growth. Society for Biomaterials, Boston, MA, April 5-9, 1994

Ann E. Schmierer, Buddy D. Ratner, Endothelial Cell Activation on Biomaterials. Keystone Symposia on Molecular and Cellular Biology: Tissue Engineering, Taos, NM, Feb. 20-26, 1994. Published in J. Cell. Biochem., Supplement 18C, 1994.

AE Schmierer, A Chilkoti, and BD Ratner. Correlation of cell growth with surface properties, Future Perspectives in Biomedical Polymers, Maui, HI, Dec. 4-6, 1992.

Buddy D. Ratner and Ann E. Schmierer, Surface Analysis in Tissue Engineering: Material Surfaces and Cell Surfaces. Bionic Design Workshop, Tsukuba, Japan, Feb. 21-23, 1994.

Buddy D. Ratner, Ann E. Schmierer, Ashutosh Chilkoti, Ellen Davis, and Winston Ciridon. Exploring the Nature of Cell Growth Surfaces. AIChE Annual Meeting, 1992.

Buddy D. Ratner, Sylvie I. Ertel, Ashutosh Chilkoti, and Ann Schmierer, Cells and Surfaces. Surfaces in Biomaterials Symposium, Minneapolis MN, October 14-16, 1992.

Ashutosh Chilkoti, Buddy D. Ratner, Ann Schmierer, Sylvie I. Ertel, and Thomas A. Horbett. An Investigation of the Relationship Between Surface Chemistry and Endothelial Cell Growth on Oxygen-Containing Plasma Deposited Films. AIChE Annual Meeting, Los Angeles, CA, November 17-22, 1991.

List of Publications:

Chilkoti, A., Schmierer A. E., Perez-Luna, V. H., and Ratner, B. D. (1995). Investigating the Relationship between Surface Chemistry and Endothelial Cell Growth: Partial Least-Squares Regression of the Static Secondary Ion Mass Spectra of Oxygen-Containing Plasma-Deposited Films. Analytical Chemistry, 67:2883-2891.

Overell, R. W., Clark, L., Lynch, D., Jerzy, R., Schmierer, A., Weisser, K., Namen, A., Goodwin, R. (1991). Interleukin-7 retroviruses transform pre-B cells by an autocrine mechanism not evident in Abelson murine. Molecular and Cellular Biology, 11:1590-1597.

Park, L. S., Friend, D. J., Schmierer, A. E., Dower, S. K., Namen, A. E. (1990). Murine interleukin 7 (IL-7) receptor. Characterization on an IL-7-dependent cell line. J. Experimental Medicine, 171:1073-1089.

Cosman, D., Namen, A. E., Lupton, S., Wignall, J., Hjerrild, K. J., Jerzy, R., Schmierer, A., and Goodwin, R. G. (1989). Lymphokine Receptor Interactions, 179:229-236.

Goodwin, R. G., Lupton, S., Schmierer, A. E., Hjerrild, K. J., Jerzy, R., Clevenger, W., Gillis, S., Cosman, D., Namen, A. E. (1989). Human interleukin 7: molecular cloning and growth factor activity on human and murine B-lineage cells. Proc. Natl. Acad. Sci. U.S.A., 86:302-306.

Namen, A. E., Lupton, S., Hjerrild, K., Wignall, J., Mochizuki, D., Schmierer, A., Mosely, B., March, C., Urdal, D., Gillis, S. (1988). Stimulation of B-cell progenitors by cloned murine interleukin-7. Nature, 333:571-573.

Namen, A. E., Schmierer, A. E., March, C. J., Overell, R. W., Park, L. S., Urdal, D. L., Mochizuki, D. Y. (1988). B cell precursor growth-promoting activity. Purification and characterization of a growth factor active on lymphocyte precursors. J. Experimental Medicine, 167:988-1002.

Awards and Fellowships:

Whitaker Fellowship Recipient 1990-92.

French Chateaubriand Research Fellowship, research conducted at Université Paris Nord, Villetaneuse, France, March-August 1993.

NIH Biotechnology Fellowship, 1993-1995.

Student Poster Award, Tissue Engineering Keystone Symposium, Taos, NM, 1994.

IMAGE EVALUATION TEST TARGET (QA-3)

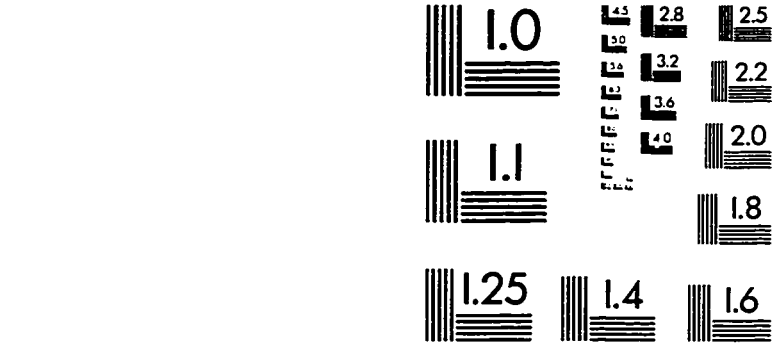

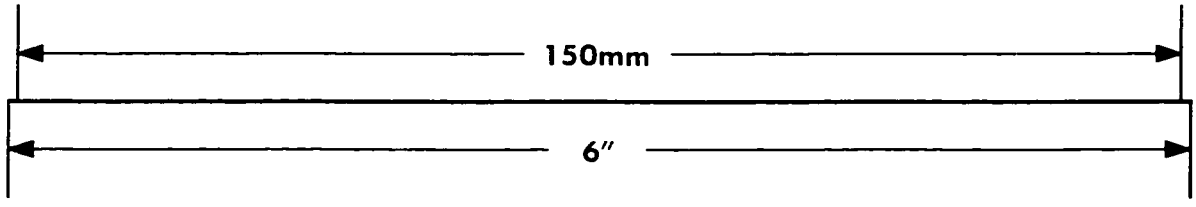

APPLIED IMAGE, Inc
1653 East Main Street
Rochester, NY 14609 USA
Phone: 716/482-0300
Fax: 716/288-5989

© 1993, Applied Image, Inc., All Rights Reserved